Optimisation of Water Treatment Works using Monte-Carlo Methods and Genetic Algorithms

by

Roger William Swan

A thesis submitted to the

University of Birmingham

for the degree of

DOCTOR OF PHILOSOPHY

College of Engineering and Physical Sciences

School of Civil Engineering

University of Birmingham

January 2015

ABSTRACT

Optimisation of potable water treatment could result in substantial cost savings for water companies and their customers. To address this issue, computational modelling of water treatment works using static and dynamic models was examined alongside the application of optimisation techniques including genetic algorithms and operational zone identification. These methods were explored with the assistance of case study data from an operational works.

It was found that dynamic models were more accurate than static models at predicting the water quality of an operational site but that the root mean square error of the models was within 5% of each other for key performance criteria. Using these models, a range of abstraction rates, for which a water treatment works was predicted to operate sufficiently, were identified, dependent on raw water temperature and total organic carbon concentration. Genetic algorithms were also applied to the water treatment works models to identify near optimal design and operating regimes. Static models were identified as being more suitable for whole works optimisation than dynamic models based on their relative accuracy, simplicity and computational demands.

ACKNOWLEDGEMENTS

This thesis would not have been possible without the help of many other people. Firstly I would like to thank Jai for being ever supportive and understanding. I also thank Hamish and Lyra for always keeping the challenge of completing this project in perspective. Many thanks Mum and Dad for agreeing to proof read thousands and thousands of words. Thanks to my supervisors John and Mark for your professionalism and to John in particular for his many motivational speeches along the way. The help I received from many employees of Severn Trent Water was also appreciated. Finally would like to thank all my fellow research students for sharing the experience and answering the many, many questions I had.

TABLE OF CONTENTS

LIST OF ILLUSTRATIONS

LIST OF TABLES

LIST OF ABBREVIATIONS

CSTR	Continuous stirred tank reactor
CT	Disinfectant concentration times contact time
DAF	Dissolved air flotation
DBP	Disinfection by-product
eSCADA	Electronic supervisory control and data acquisition
GA	Genetic algorithm
HAA	Haloacetic acid
HBC	Hopper bottomed clarifier
NOM	Natural organic matter
NTU	Nephelometric turbidity unit
R^2	Coefficient of determination
RGF	Rapid gravity filter
t_{10}	Time taken for 10% of tracer chemical to be detected in tracer test
THM	Trihalomethane
TSS	Total suspended solids
TTHM	Specifically THMs: chloroform; bromoform; bromodichloromethane and dibromochloromethane
WQP	Water quality parameter
WTW	Water treatment works

1 INTRODUCTION

This thesis investigates the modelling of potable water treatment and the application of optimisation techniques including genetic algorithms. These methods are explored through the use of case study data from an operational works.

1.1 Water treatment

By continual and costly control of water quality, it has been possible to drastically reduce the harm caused by waterborne diseases (Tebbutt, 1992). Focusing on this goal, water supply up until the second half of the twentieth century was relatively simple (Binnie et al., 2006). Water abstracted from a reservoir supplied by a protected catchment or well was distributed after minimal treatment. River water sources received slightly greater treatment, whilst water from poor quality lowland rivers underwent extensive storage, to allow self-purification, before being slow sand filtered (Binnie et al., 2006). Up until 1958, when the World Health Organisation published its first drinking water standards, water quality in the UK was assessed on the basis of "wholesomeness" (Purcell, 2005). This in practice meant that there was a requirement for sampling and analysis of final water microbiological content and chlorine concentration (Binnie et al., 2006).

In the late twentieth century, water treatment in developed countries began to focus on reducing exposure to man-made chemicals, including disinfection by-products (DBPs) such as trihalomethanes (THMs) and Haloacetic acids (HAAs).

This change in focus occurred in the UK due to:

- improved analytical techniques allowing the identification of hundreds of trace chemicals produced by industrial processes and water/wastewater treatment;
- heightened public concern about the consequences of man-made chemicals;
- the application of water quality standards derived from the 1980 European Drinking Water Directive; and
- additional regulations prompted by the privatisation of the water industry (Binnie et al., 2006).

Alongside this change in focus, the risks posed by viruses and zoonotic pathogens (capable of transferring disease between species) were also identified. Some of the organisms of concern proved to be difficult to remove or inactivate, resulting in additional treatment being required (Crittenden et al., 2005). Due to these findings, the trade-off between achieving sufficient disinfection and minimising DBP formation became paramount. Increased removal of solids and inorganic compounds prior to disinfection, reducing free chlorine demand, became desirable at some WTWs in order to help achieve these conflicting disinfection goals.

In the twenty first century, the removal of man-made and microbiological contaminants remain priorities along with the development of risk assessment methods to assess the impacts of trace quantities of harmful substances (Crittenden et al., 2005). Water provided to customers must be safe for consumption but must also be palatable and suitable for other domestic and industrial uses such as washing. To achieve these goals, the water must meet certain criteria to ensure acceptable levels of visible suspended matter, colour, taste, odour, harmful dissolved matter,

aggressive constituents, harmful man-made chemicals and bacteria indicative of faecal pollution (Tebbutt, 1992).

1.2 Water treatment modelling

Numerical modelling of water treatment works (WTWs) offers a means by which designers and operators can assess the likely impact of raw water quality or process modifications on treated water quality. This helps to provide an indication of the likelihood of failure to meet water quality standards under different scenarios. A variety of different programs have been written to model whole WTWs including OTTER (WRc), WATPRO (Hydromantis), Stimela (DHV), Metrex (University of Duisburg) and WTP (USEPA). However, there has been little use of these programs in comparison with wastewater programs (Dudley et al., 2008). Commonly used wastewater programs include GPS-X and BioWin (Phillips et al., 2009). Potable water modelling (developed in the 1990s) is thought to be less developed and applied than wastewater modelling (developed in the 1970s) due to the amount of time they have existed (Dudley et al., 2008). Some existing water treatment modelling programs, such as OTTER, model whole works comprehensively and have been generally successful when used in several studies, but have required relatively extensive calibration data (Rietveld and Dudley, 2006, Dudley et al., 2008). Other programs are more suitable for modelling specific water quality parameters, such as WATPRO, which has been found to be effective at predicting disinfection by-product formation but is otherwise a poor example of the state of the art in water treatment modelling (Rietveld and Dudley, 2006). The majority of the mathematical models available within these programs are empirical, but some of the models are based on fundamental scientific principles

and rate-type partial differential equations to perform mass balances. The mechanistic models are less dependent on arbitrary constants than the empirical models and they also attempt to model mechanisms that are prevalent in the processes.

1.3 Optimisation of water treatment works using computational methods

It has been estimated that 15% to 20% of the cost of supplying potable water is incurred at the treatment stage (Mhaisalkar et al., 1993). Significant cost savings can therefore be made to water companies and their customers if treatment is optimised. These optimisations will strive to achieve acceptable water quality whilst minimising capital, operational or whole life costs.

Optimisation of water treatment is complex, as the performance of each individual process affects subsequent processes. For example, reducing the concentration of organic matter at the clarification stage results in reduced chlorine demand (Vasconcelos and Boulos, 1996) and trihalomethane production (Brown et al., 2011a) at the disinfection stage. Due to this inter-dependency, it is advantageous to identify suitable designs or operating regimes that take into account the interactions between the processes. Optimising WTW involves multiple, non-linear relationships between solution parameters that are often constrained and multiple objectives that are often conflicting. Evolutionary algorithms (EAs) are a practical tool with which to approach these problems. The applicability of EAs is, however, limited by their potentially considerable computational demands and uncertainty in the quality of the solutions they identify (Nicklow et al., 2010).

There have been previous attempts to optimise WTW performance using computational models, including the work of Mhaisalkar et al. (1993), Dharmappa et al. (1994a) and Gupta

and Shrivastava (2006, 2008, 2010). This previous work has primarily focused on suspended solids removal using static models. Mhaisalkar et al. (1993) applied deterministic conditions with dynamic programming to simulate the optimisation of operational WTW and identified potential cost savings of approximately 5%. Particle size distribution data were used with non-linear programming by Dharmappa et al. (1994a) to identify a correlation between the proportion of fine particles in raw water and treatment costs. Most recently, Gupta and Shrivastava (2006, 2008, 2010) applied stochastic conditions to a pseudo-constrained WTW design problem using a genetic algorithm to successfully identify near-optimal solutions. Although WTW modelling has the potential to offer interesting insights into potentially effective treatment options and rough design parameters, computational modelling has not historically been accurate enough to replace laboratory or pilot plant testing for operational purposes (Gupta and Shrivastava, 2006, Dharmappa et al., 1994b).

1.4 Aims and objectives

The primary aim of the work proposed here is to draw upon previous work undertaken at the University of Birmingham and elsewhere to develop a methodology and software tool to:

A1. Compare the accuracy of static and dynamic models to predict the performance of an operational water treatment works (WTW) over multiple seasons, using data historically recorded for quality control purposes;

A2. Identify operating conditions under which the WTW is expected to produce water of an acceptable water quality; and to

A3. Optimise the design and operational regime of the WTW taking into account operating conditions and risk acceptance, using genetic algorithms and Monte Carlo techniques.

Specifically, the objectives of the project are to:

O1. Develop overall static and dynamic, generic water treatment process models which could be applied to planned or existing water treatment works;

O2. Calibrate and verify the accuracy of these models using case study data.

O3. Specify performance criteria for acceptable WTW operation;

O4. Identify operating conditions for which an operational WTW is expected to meet specified performance criteria;

O5. Identify the probability distributions of key operational parameters;

O6. Assess the accuracy of applying Monte-Carlo techniques to WTW models to predict WTW reliability; and

O7. Compare the optimised designs and operational regimes identified for an examined WTW using static and dynamic models along with genetic algorithms.

1.5 Thesis layout

This thesis aims to investigate how the comparative performance of WTWs could be assessed, what the most suitable methods of modelling entire WTWs are and what methods of optimisation could be applied successfully. Specifically, the chapters comprising this thesis are presented as follows:

Chapter two provides the founding principles of water treatment modelling and genetic algorithm application. Water quality parameters and measurement techniques, conventional water treatment processes and previous water treatment modelling programs are described. This is followed by a description of the essential knowledge required for the implementation of genetic algorithms (GAs). The information in this chapter identifies the key water quality parameters relevant to the modelling processes and enables the development of a coherent method for optimising the performance of computationally modelled WTWs. This chapter closes with a summary of the knowledge gaps identified in the existing literature.

Chapter three is dedicated to describing the generic water treatment models used in this work. The WTW modelling approaches and the programming methods used in this research are defined, along with a description of the modelling techniques used.

Chapter four illustrates the performance and accuracy of the WTW process models when used to simulate an operational site using observed time series and Monte-Carlo operating conditions. This chapter describes the WTW modelled, the methods used to adapt the general models to the specific site, the data used to calibrate and verify the models and the verification results.

Chapter five covers the application of optimisation techniques along with the WTW process models calibrated to represent the conditions at an operational site. Three optimisation processes are investigated: the identification of operational conditions for which acceptable final water quality would be expected, the application of the models along with a genetic algorithm to identify solutions for minimising footprint area and unacceptable performance and the application of the models along with a genetic algorithm to identify solutions for minimising operating costs and unacceptable performance. The methods, results, analysis and conclusions of these optimisations are described.

Chapter six discusses the findings of the modelling and optimisation work completed and examines their relevance and implications in a broader context. Chapter seven summarises the key findings and conclusions and chapter eight provides recommendations for future research.

2 FOUNDING PRINCIPLES

This chapter provides the founding principles of water treatment modelling (section 2.1) and genetic algorithm application (section 2.2) used as the basis for the research in this thesis.

2.1 Potable water treatment & modelling

This section provides a description of how water quality is described and measured along with an overview of conventional water treatment processes. The research described in this section is vital in identifying the key water quality parameters modelled within this study.*Water quality*

Because water has a high dielectric constant and low conductivity, many substances dissolve in it (Binnie et al., 2006). Water chemistry is therefore complex. This section gives an overview of the different groups of substances found in raw water sources followed by a description of common physical, chemical and biological parameters used to describe water's characteristics.

2.1.1.1 *Water's impurities*

The different types of impurities in water, as described by Binnie et al. (2006), are summarised here:

Suspended solids: Solid particles transported in running water. Higher velocities result in greater numbers and larger particles being transported.

Colloids: Fine particles fail to coalesce into larger particles due to electrostatic repulsion. The self-repulsion is due to colloids having similar, usually negative, charges. Colloids are too small to be seen individually with the human eye but contribute to colour and turbidity.

Dissolved solids: A variety of chemicals dissolved into water as it passes through or over land. Naturally occurring dissolved solids are rarely harmful in low concentrations.

Micro-organisms: Pollution from organic matter, particularly faecal, is of concern due to the risk of disease transmission. Most surface water sources will contain substantial amounts of coliform bacteria, including those that are faecal, but ground waters usually have greater biological purity. It is possible to identify individual disease causing organisms through analysis but this can be difficult, risky and for viruses, impractical. Instead, easily identifiable bacteria that are known to be present in human faeces are tested for and if they are not present the water is considered microbiologically safe. Viruses present in the water can be effectively inactivated by disinfection and there is little evidence of viral transmission by adequately treated water.

Micro-pollutants: Some substances, although usually occurring in very low concentrations of µg/l or ng/l, may have significant adverse environment and human health effects (Jiang et al., 2013). Examples of micro-pollutants include: some metal, metalloids, radioactive elements, pesticides, hydrocarbons, solvents, detergents, hormones, pharmaceuticals and endocrine disrupting chemicals.

Natural organic matter: Some organic compounds are toxic, some are suspected of being carcinogenic and some can lead to taste and odour issues (Crittenden et al., 2005). These compounds can be formed from either natural or anthropogenic sources. Natural sources of organic matter can come from the chemical or biological degradation of vegetable and soil derived material, along with secretions from micro-organisms and excretions from aquatic organisms. Anthropogenic organic matter sources include landfills, chemical spills and effluents from manufacturing and water/wastewater treatment.

Organic matter comprises a complex matrix of organic chemicals which tend to give water an unappealing yellowish tinge. Historically, this discolouration has been an aesthetic concern, but more worryingly, organic matter is now also known to be a precursor for possibly carcinogenic disinfection by-products. Organic matter is also of concern as it: reacts with coagulants and disinfectants; adsorbs onto activated carbon, reducing its capacity for its target compounds; and can biodegrade in the distribution network, providing a food source for biological growth. Organic matter can form soluble complexes with metal and hydrophobic organic chemicals, including pesticides. Once these substances are dissolved they can be transported more easily and can be difficult to remove by conventional treatment processes.

2.1.1.2 *Physical water parameters*

These properties are relatively easy to measure or observe. Some of these properties define the water quality but others are of interest as they will influence the effectiveness of water treatment processes.

Solids content: Solids content can be either organic or inorganic in nature and can be either dissolved or suspended. Suspended solids can further be classified using a standard settling procedure to determine what proportion is settleable.

Turbidity: Turbidity measures the cloudiness of water due to the presence of colloids, clay/silt particles and micro-organisms. A high degree of turbidity is aesthetically unappealing and a potential indicator of poor water quality. Turbidity has been and will continue to be a valuable tool in guiding and monitoring performance of water treatment and distribution systems. It is considered to be an effective method for assessing particulate matter concentrations in treated water and can be used as a relative measure of reliable treatment (Burlingame et al., 1998).

2.1.1.3 *Chemical quality parameters*

Alkalinity: Alkalinity represents the acid neutralising capacity of an aqueous system (Stumm and Morgan, 1970). If it is assumed that the aqueous carbonate system is dominant, making the influence of other hydrogen ion transferring substances in the water insignificant, then the alkalinity can be quantified as the additional concentration of hydrogen ions that can be added before the solution reaches an equivalence point where all of the carbonate exists as carbonic acid. Alkalinity can be measured as a molar concentration [Alk] but it is more commonly measured in units equivalent to a concentration of calcium carbonate ($CaCO_3$) that would have the same acid neutralising capacity.

The carbonic acid system's equilibrium equations are shown in Equation 2-1 and Equation 2-2 (Crittenden et al., 2005). The consequences of these equilibrium equations are that the carbonate species act as a pH buffer and the concentration of the carbonate species depends on the pH of the solution.

$$H_2CO_3^* \Leftrightarrow H^+ + HCO_3^- \qquad \text{Equation 2-1}$$

$$HCO_3^- \Leftrightarrow H^+ + CO_3^{2-} \qquad \text{Equation 2-2}$$

If enough hydrogen ions (H^+) are introduced to the solution then the equilibrium moves towards an equivalence point where all of the carbonate exists as carbonic acid or dissolved CO_2 ($H_2CO_3^*$). If additional hydrogen ions are added to a pure carbonic acid system solution no buffering will occur and there will be a relatively large decrease in pH.

Organic matter parameters: The complex nature of organic matter makes it impractical to measure all its individual components. Instead, bulk parameters are used to describe its composition and concentration including organic carbon concentration, ultraviolet absorbency and fluorescence. Organic carbon is often measured as total (TOC) or dissolved (DOC) concentrations. Both of these measurements are based on completely oxidising the organic matter present and then measuring the concentration of carbon (DOC samples are first passed through a 0.45 µm filter). If treatment does not change the composition of the organic matter too considerably, organic carbon can be used a surrogate parameter for estimating the efficiency of organic matter removal. TOC is a suitable surrogate parameter for organic matter as it is relatively easy to analyse, includes all organic components and correlates well with trihalomethane formation potential (Chen et al., 1996, Wang et al., 2013).

Ultraviolet absorbency is usually measured for light with a wavelength of 254 nm (UV_{254}) in pre-filtered samples. Organic matter with specific molecular structures absorbs light, and if these structures are removed proportionally then UV_{254} can be used as a surrogate for organic matter removal. An additional assessment of the composition of organic matter can be made by using the specific ultraviolet absorbency (SUVA) which is the ratio of UV_{254} to organic carbon. SUVA is of interest because it has been found to be proportional to the adsorbable, hydrophobic fraction of organic matter (Edwards, 1997).

Disinfection by-products (DBPs): Disinfectants which are strong oxidising agents do not only interact with pathogens but also with many other chemicals in the water. The products of these reactions, including those suspected of being harmful, are known as disinfection by-products (DBPs). DBPs are created by disinfectants including chlorine, chlorine dioxide, hydrogen peroxide, potassium permanganate and ozone. Perhaps the most commonly formed DBPs are

those produced by chlorine, particularly with humic and fulvic acids found in peaty soils, to form organochlorine compounds including: trihalomethanes (THMs) and haloacetic acids (HAAs). Commercial chlorine gas may also contain some bromine and this will also form THMs and HAAs. Although these substances have been identified as being carcinogenic to animals at high doses (Tebbutt, 1992) there is no conclusive evidence that these substances are harmful at the concentrations found in drinking water. It is, however, prudent to limit concentrations of these substances to reduce the consumption that individuals are exposed to during their lifetime.

THMs have a chemical structure similar to methane (CH_4) with one or more of the hydrogen atoms replaced with halogens (fluoride, chlorine, bromine or iodine). The four compounds that are commonly identified to represent total trihalomethane (TTHM) concentration are chloroform, bromoform, bromodichloromethane and dibromochloromethane, as defined in both the regulations of England, Wales and the US. The regulatory limit at consumers' taps in England and Wales is 100 µg/l (DWI, 2010).

2.1.1.4 *Biological quality parameters*

Historically water treatment has focused on controlling faecal-oral route diseases, which are spread by pathogens such as bacteria, protozoa and viruses. The risks posed by pathogens which can spread disease from other animals and opportunistic pathogens which reside in aquatic environments are now also of concern (Crittenden et al., 2005).

Coliform bacteria: Coliform bacteria are an indicator of possible faecal contamination but they may also arise from other sources. *Escherichia coli* are a member of the coliform group but are almost exclusively from faecal sources and are of particular concern. Due to the relative concern

of these two groups of pathogens the regulatory limit for final water from a WTW in England and Wales is zero coliform bacteria per 100 ml sample with 95% compliance and zero *Escherichia coli* (*E. coli*) per 100 ml sample at all times from service reservoirs (DWI, 2010).

Protozoa: Certain protozoa, including *Cryptosporidium parvum* and *Giardia lamblia*, can cause gastroenteritis. These protozoa have a complex reproductive cycle that includes the formation of oocysts which are thick walled, resistant to chemical attack and able to remain dormant for many months. Due to increasing concern over the presence of these organisms, all UK companies are required to carry out risk assessments for *Cryptosporidium*, produce water "wholesome" with regard to *Cryptosporidium* and reported any oocysts found in final water to the DWI so they can investigate if any regulations have been contravened (Foundation for Water Research, 2011).

Viruses: Viruses are parasitic organisms which cannot grow outside of other living organisms. Human viral diseases include small pox, yellow fever and a range of gastroenteritis infections (Tebbutt, 1992). Viruses are present in most surface waters that are subject to pollution and due to their small size (less than 0.3µm) they are difficult to remove by conventional water treatment processes. Although they are difficult to remove, viruses are effectively inactivated by disinfection.

Turbidity as a surrogate for microbiological quality: Past experience and data have shown that pathogen monitoring does not confirm absolute presence or absence of micro-organisms (Allen et al., 2000). The best method of ensuring microbiological quality of water is to protect the catchment, optimise the treatment process and maintain the infrastructure integrity. To help optimise the process, measurements should be made of parameters which effectively assess the efficiency of the treatment processes (Allen et al., 2000). No single parameter can be relied

upon to individually assess the efficiency of treatment (Nieminski et al., 2000). However, turbidity is often used as a key indicator of general works performance.

CT as a measure of disinfection: The product of residual disinfectant concentration and contact time (CT) is used as an indicative measure of the disinfection performance of a contact tank. The contact time is usually taken as being $t_{10,}$ the time taken for 10% of the concentration of a tracer chemical to be detected at the outlet of the tank after being added at the inlet (Teixeira and Siqueira, 2008). The concentration of the disinfectant used is usually its residual value at the outlet of the contact tank. Under most conditions, a sufficient degree of inactivation can be defined by a target CT value. The use of CT values to define expected disinfection is consistent with other first order models such as Chick, Chick-Watson, Rennecker-Mariñas, Collins-Selleck and under certain circumstances Hom-Haas (Crittenden et al., 2005). These models are based on the assumption that the inactivation of microbiological organisms is proportional to the concentration of the organisms (Chick, 1908) and the concentration of disinfectant (Watson, 1908).

The range of substances found in water and their influences on the quality of the water distributed are broad and it is important that they are all considered for a supplied water. For whole works optimisation purposes it may, however, be necessary that a reduced number of water quality considerations are investigated.

2.1.2 Water Treatment

2.1.2.1 *Overview*

Water treatment processes are physical, chemical or biological. The performance of physical treatment processes such as screening, clarification and filtration are predominantly influenced

by physical properties such as the size and density of suspended solids to be removed and the viscosity of the water. Chemical processes such as coagulation or liming are dependent on the interaction between the chemical properties of the impurities and the chemical reagents added. Finally, biological processes depend on creating conditions suitable for organisms which have a beneficial influence on water quality. Although some source waters could achieve the required improvement in water quality through the application of a single treatment process, it is more common that several complementary processes are applied. The information in this section was used to identify what treatment processes and mechanisms were likely to require modelling.

The treatment applied to each individual source water is dependent on its unique water quality, the existing infrastructure, social, environmental and economic conditions, the strategic goals of the operator and the knowledge and preferences of the engineering decision makers. As there are many factors that influence what treatment is appropriate, a wide variety of approaches have been applied in the past. One of the most important factors in determining what treatment is suitable is the water source. Some ground waters will only require disinfection to achieve the desired degree of water quality. However, additional treatment to reduce the iron and nitrate concentration, soften or stabilise the water may also be necessary. Water abstracted from a protected upland catchment is likely to require greater additional treatment, including some form of screening to remove floating or suspended matter and possibly filtration or colour removal. Waters from lowland river extractions will usually require the greatest degree of treatment as they are more likely to be polluted by agricultural or urban runoff and point source pollution from wastewater discharges. Water abstracted from these lowland river sources is likely to require coagulation, clarification, filtration and disinfection and may require additional storage, adsorption or nitrate removal (Tebbutt, 1992).

There are a wide selection of traditional processes that have historically been applied to achieve the goal of preventing waterborne disease. However, with the more recent focus on reducing the presence of anthropogenic organic chemicals in water (see section 1.1), new treatment process have been developed to meet the fresh challenges. These traditional and modern treatment processes are listed in Table 2-1 (Binnie et al., 2006).

Table 2-1 Surface water treatments (adapted from Binnie et al, 2006)

Traditional	**Modern**
Storage	Enhanced coagulation
Screening	Dissolved air flotation (DAF)
Sedimentation	Lamella separators
Aeration	Sludge blanket clarifiers
Coagulation	Ozonation
Flocculation	Activated carbon (granular and powdered)
Filtration (slow, rapid gravity or pressure)	Membranes
Chlorination (contact tank and residual)	Air Stripping
Sludge dewatering and disposal	Alternative disinfection (i.e. ultraviolet, ozonation or chlorine dioxide)

The following sections give an overview of the theory and practical application of a selection of widely used surface water treatments.

2.1.2.2 *Coagulation*

Larger suspended solids are more efficiently removed by physical removal processes such as clarification and filtration. In order to improve the solids removal it is necessary to target colloids (see section 2.1.1.1), which do not readily settle or coalesce. Their similar charge and small size results in them having a large surface area where surface phenomena predominate and gravitational effects are unimportant (Binnie et al., 2006). The coagulation and flocculation

processes bring about the agglomeration of colloids into larger particles called flocs which are more easily removed by physical treatment processes. Coagulation, which is the action of adding chemical coagulants to the water to increase attachment affinity between suspended substances, has the additional advantage that the coagulants also adsorb dissolved natural organic matter (NOM). The removal of NOM is of importance because it is formed of some precursors to disinfection by-products, including trihalomethanes. The coagulation process requires high energy mixing of the coagulant with the water to promote uniform distribution before stable complexes are formed (Binnie et al., 2006). The mixing during coagulation is achieved by turbines, propellers, static mixers or weirs (Binnie et al., 2006).

Colloids can be destabilised by a variety of mechanisms including charge neutralisation; entrapment, bridging and double layer compression as described in Table 2-2 (Binnie et al., 2006). A variety of these destabilisation mechanisms are exploited by coagulants, however, deliberate alteration of the ionic strength (increasing double layer compression) is not commonly practiced in water treatment (Crittenden et al., 2005).

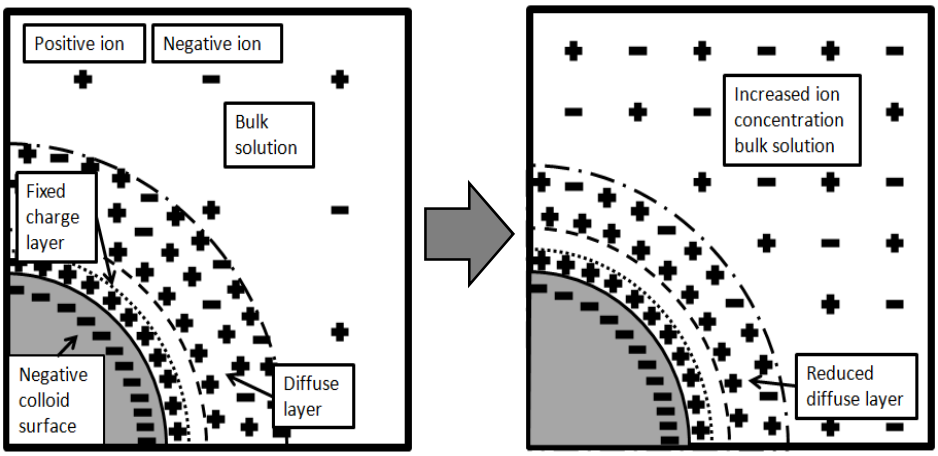

Figure 2-1 Double layer compression, adapted from Crittenden et al.(2005)

Table 2-2 Coagulation destabilisation mechanisms, adapted from Binnie et al. (2006)

Destabilisation mechanism	**Description of mechanism**	**Dosing considerations**
Charge neutralisation	Ions with opposite charge to colloids are added and adsorbed onto the surface of colloid. This reduces the overall surface charge, reducing colloid repulsion.	Dose required is proportional to colloidal concentration.
		Overdosing can result colloids polarity reversing.
Entrapment in a precipitate	Soluble salt is added to water and hydroxide flocs form around the colloids. Other colloids can also be captured as salts forms.	Inverse relationship between concentration of colloid and coagulant dose required.
		Optimum pH for coagulant required to maximise precipitation (minimise solubility). This is obtained by jar tests.
		pH control hampered by acidity of some coagulants used and the low alkalinity of some waters.
		Minimum alkalinity is needed to react with some coagulants, if not present in sufficient concentration then addition required.
Particle bridging	Polymers are believed to work by bridging between colloids. High energy mixing is not needed in this process.	Anionic and cationic polymers capable of use with negatively charged colloids.
		Often used during flocculation to aid agglomeration.
Double layer compression	Electrolyte is added to the water, increasing the number of ions. This reduces the thickness of the colloidal double layer, making it easier to get colloids close together for other forces to overcome double layer repulsion (see Figure 2-1).	Effective whilst coagulant is in ionic form and no additional effect is seen once any resulting insoluble compounds are formed.
		The effectiveness of the process is independent of colloidal concentration.
		Effectiveness is proportional to the change in ionic concentration.

The type and dose of coagulant applied to water depends on the characteristics of the water to be treated. An overview of common coagulants is given in Table 2-3, which also includes additional chemicals used at this stage of treatment.

Table 2-3 Coagulant aids

Coagulant aid	Dosing considerations
Aluminium sulphate (alum) $Al_2(SO_4)_3.14H_2O$ (commercial composition)	Risk of exceeding aluminium standards if raw water concentrations are high.
	Reacts with natural alkalinity
Ferric sulphate $Fe_2(SO_4)_3$	More pH tolerant than alum and effective for decolourisation and clarification at low pH and removing Mn at high pH
	Reacts with natural alkalinity
Ferric chloride $FeCl_3$	Relatively corrosive
	Reacts with natural alkalinity
Polymerised aluminium and iron salts (polymers)	More expensive than traditional salts
	Better performance at low temperatures; faster floc formation; lower dosage rates and less pH adjustment costs
Lime $Ca(OH)_2$	Enables precipitation of aluminium and iron salts whilst stabilising pH
Weighters	Fine material that increases the solids concentration enabling entrapment to occur at lower coagulant doses

The dose of coagulant was traditionally determined using jar tests to assess the degree of turbidity removal achieved by different coagulation concentrations. From these jar tests optimal doses were identified by trying to ensure that the incremental benefit of any additional coagulant was greater than the additional cost. Due to the concerns of disinfection by-products, of which natural organic matter (NOM) is a precursor, many WTWs now use 'enhanced coagulation' where a higher concentration of coagulant is used. The required concentration of coagulant is again identified using jar tests but with NOM removal as the performance indicator rather than turbidity.

2.1.2.3 *Flocculation*

Coagulated particles that have been destabilised by coagulation agglomerate into large particles, known as flocs, when agitated. This process is known as flocculation. Some long chain hydrophilic colloids with multiple charges can also be flocculated by entanglement even though they have not been coagulated. Flocculation can be achieved by either mixing, differential settling or Brownian motion (Binnie et al., 2006). Where mixing is applied, either by mechanical mixers, static mixers or a weir, the energy input to the water needs to be controlled so that floc accumulation and breakup are optimised to form floc of an acceptable size and strength. WTWs are generally designed to minimise floc breakage but high shear zones still exist, so flocs need to be strong to prevent fracturing as fragmented flocs are harder to remove (Jarvis et al., 2005a). The intensity of mixing is usually reduced as the flocculation process progresses to reduce the degree of floc breakage that occurs. The effectiveness of the flocculation process is usually considered to be dependent on the retention time and the mean velocity gradient (Binnie et al., 2006). Optimal values for these parameters are difficult to predict from water quality, so jar tests are often carried out to identify suitable values (Binnie et al., 2006).

2.1.2.4 *Clarification*

Traditionally, settlement tanks were used to remove the majority of suspended solids but it is more common now to use sludge blanket or dissolved air flotation (DAF) clarifiers (Binnie et al., 2006). These clarification processes are commonly used to remove previously flocculated particles. When identifying a suitable clarification treatment, laboratory tests can be used to give an indication of suitable process, coagulant dose and surface loading but as it is difficult

to accurately predict the range of different conditions that will be experienced, generous safety factors are applied (Binnie et al., 2006).

The settlement, or buoyancy in the case of DAF clarifiers, of suspended solids is inversely proportional to both the viscosity and temperature of water. The removal rate of clarifiers is approximately twice as great at 33°C as at 0°C. It is useful that the efficiency of clarification is greater during warmer weather as this is when water consumption tends to be greater.

2.1.2.4.1 Hopper bottomed clarification (HBC)

Water is passed up through these clarifiers whilst suspended solids settle. The buoyancy of these solids within the HBC is determined by the velocity of the water passing upwards through the clarifier and the settling velocity of the solids. Due to the hopper design, the velocity of the water is greater towards the bottom. The suspended solids in the HBC form a blanket of sludge at a height where their settling velocity is equivalent to the upwards velocity of the water. This sludge blanket acts to entrap smaller floc than would otherwise be removed by settling alone (Tebbutt, 1992). The sludge blanket has a variable solids concentration which helps to stabilise its height. As the blanket settles, it compresses and its solids concentration increases. The greater particle hindrance of the increased solids concentration of the blanket reduces its settling velocity and helps stabilise the blanket height. The hopper bottomed design also increases flocculation in the blanket. Surface loading rates typically vary from between 0.8 m/h to 5 m/h dependent on the type of water being treated and whether coagulant aids are used (Binnie et al., 2006).

One of the advantages of HBCs over other clarification processes is that its sludge can be easily removed using the available hydraulic head and without the need for mechanical scrapers. If

the discharge of a HBC is too great or increased too rapidly then it is possible that the sludge blanket can be lost, resulting in drastically reduced water quality and operational problems downstream, particularly at filtration. In the longer term, the solids removal efficiency of the HBC will be substantially reduced until a new sludge blanket is formed. The drawbacks to sludge blanket clarifiers are their limited ability to treat higher turbidity waters; the risk of the blanket overtopping, overturning or contaminating the clarified water and high construction costs for larger sites.

2.1.2.4.2 Dissolved air flotation (DAF) clarification

Dissolved air flotation (DAF) works on the principle of joining flocs with air bubbles to form buoyant aggregates which float to the surface, where they are scraped to waste. A diagram of the process is provided in Figure 2-2.

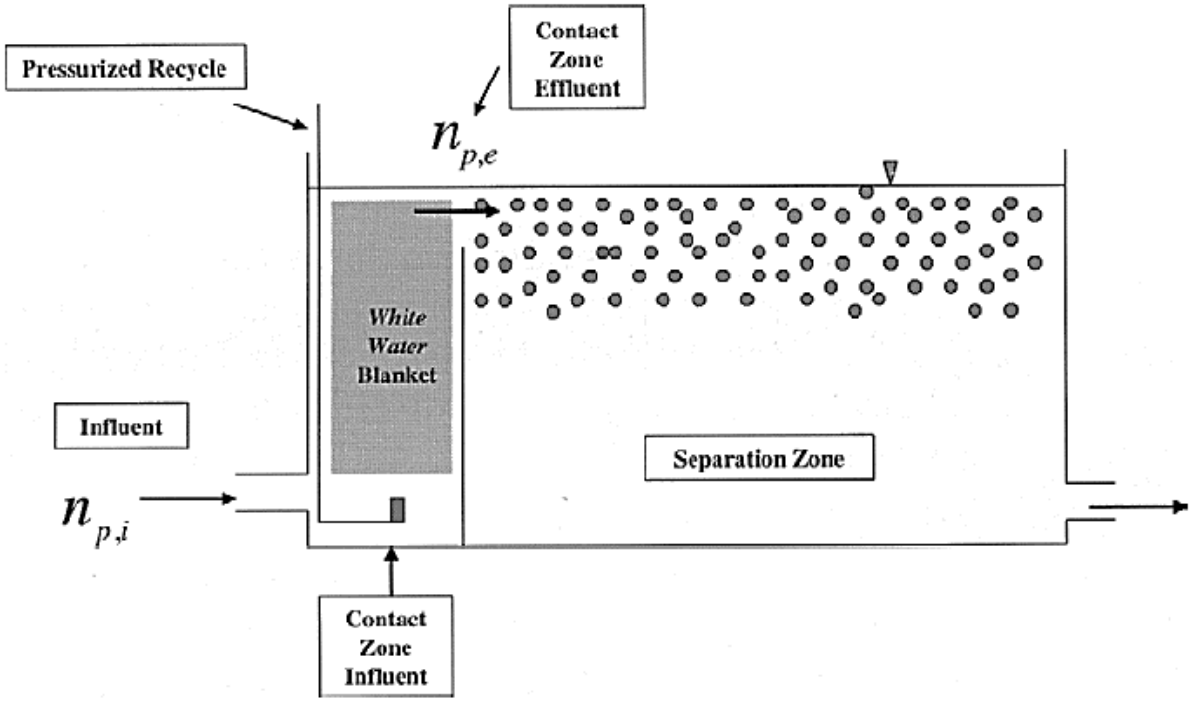

Figure 2-2 Schematic diagram of DAF tank (Edzwald, 2006)

A proportion of the treated water, usually between 8-12%, has air injected into it at high pressures of typically between 400 – 600 kPa using a saturator (Crittenden et al., 2005). This water is then returned to the inlet of the DAF tank where the sudden reduction in pressure supersaturates the water with air, releasing a cloud of fine air bubbles. These bubbles attach to flocs primarily in the contact zone before the floc-air aggregates rise to the surface in the separation zone where they are scraped to waste. Baffle walls are usually placed between the contact and separation zones to help ensure sufficient contact time between the flocs and air bubbles. The clarified water is finally drawn off from the bottom of the tank at the end of the separation zone.

DAF clarification is suitable for waters that contain significant amounts of low density solids, including some algae which have densities lower than water. The process is also effective at removing colour, iron and manganese (Binnie et al., 2006). Suitable coagulation and flocculation are essential before DAF treatment as small, high relative surface area, destabilised flocs with low net charge and hydrophobic natures are required to achieve good attachment with air bubbles. Smaller flocs are also more capable of withstanding the high shear forces of the turbulent flow within DAF tanks (Crittenden et al., 2005). The bubbles used should be small (10 - 100μm) in order to achieve high relative surface area and to ensure laminar conditions. The presence of laminar conditions reduces detachment caused by shear forces.

The DAF process is capable of high surface loading rates and so its footprint size is usually smaller than that of alternative treatments. Other advantages of the process include its potential to produce low turbidity clarified water, short start up times, high solids content sludge and lower capital costs. The process has high operational costs due to the energy requirements of pumping and air-saturating the recycle water (Tebbutt, 1992).

2.1.2.5 *Filtration*

Arguably the most important process in water treatment, filtration involves passing water through suitable media at relatively low speeds. The media retains the majority of the solid matter and a low solids content filtrate is produced. Except for very high quality ground waters, filtration is usually required after clarification. Filtered water's solids content is therefore usually dependent on the performance of both of these processes.

There are three main types of filter used in water treatment: rapid gravity, pressure and slow sand. This work will concentrate on the more common rapid gravity filtration (RGF). Rapid gravity filtration uses relatively coarse, permeable media at high filtration rates, usually downwards through the filter, to achieve purely physical removal. These filters are cleaned by reversing the direction of flow to wash out accumulated solids in a process known as backwashing.

2.1.2.5.1 Filtration mechanisms

Suspended solids do not tend to be removed by the straining process of RGFs. This is fortunate, as if straining was the dominant removal process, filters would quickly become clogged with particles and require frequent backwashing. To prevent the filter becoming quickly fouled, it is desirable for the vast majority of particles entering the filter to be less than 20% of the diameter of the filter media (Binnie et al., 2006). This can be achieved by effective clarification, or for low solids content raw water, direct filtration can be applied without prior clarification.

The removal of solids by filtration can be explained by five transportation mechanisms (interception, sedimentation, diffusion, hydrodynamic motion and inertia) along with

attachment (Binnie et al., 2006). The transportation mechanisms bring the suspended solids into contact with the filter media under the laminar conditions typical in filtration.

Once the solids have come into contact with the filter media it is desirable that they are retained. Sufficient charge neutralisation needs to be achieved in order to prevent repulsion between similarly charged particles and filter media. Otherwise, attachment will not occur. If charge neutralisation has been achieved then inter-particle attractions such as van der Waals forces will be the dominant mechanism responsible for retention, particularly for smaller particles. Generally particles substantially smaller than a micron are removed by diffusion and particles substantially larger than a micron are removed by straining. Particles of approximately a micron in size are removed less effectively by a combination of interception and sedimentation (Binnie et al., 2006). It is therefore desirable to try to ensure that particles entering the filter are substantially smaller than a micron for effective treatment to take place.

2.1.2.5.2 Backwashing

Once filters have accumulated so much solid material that they can no longer remove suspended solids effectively the quality of filtrate deteriorates rapidly and filters are said to have reached breakthrough. Filters can be thought of as containing a working layer which moves through the filter finally resulting in the breakthrough curve having an S shape. When this occurs, and preferably before, the filter needs to be backwashed in order to remove some of the solids that have been retained. Backwashes are either triggered by a schedule or due to filtered turbidity or head loss exceeding set values. Ideally, filters would reach their design limits for filtrate quality, head loss and maximum filtration run time simultaneously. If a filter is backwashed before turbidity or head loss increase substantially then this suggests that the filter's capacity is

not being fully utilised. However, if backwashes are triggered by turbidity or head loss frequently then a filter would spend too much time backwashing, reducing its effective treatment capacity. For operational simplicity and in order to reduce the likelihood of multiple filters backwashing at the same time, backwashes are usually triggered according to a conservative schedule.

After backwashing has been completed the filter is brought back into service gradually and run to waste until any remaining disturbed solids have been washed away and a sufficient amount of solids have attached themselves to the filter media to create an efficient collector surface. The initial period of instability in the performance of the filter is known as the ripening period and it has been suggested that its cause is due to differing removal mechanisms at the surface to within the filter (Saatci and Halilsoy, 1987) or because previously retained particles serve as additional collectors for suspended particles (Darby and Lawler, 1990).

2.1.2.5.3 Operation

When treating waters with a turbidity of less than 5 NTU, RGFs are capable of producing filtered waters with a turbidity of around 0.1 NTU. Due to outbreaks of cryptosporidiosis in the 1980s and 1990s, the Badenoch (Packham, 1990) and Bouchier reports (Bouchier, 1998, Cunningham, 1999) were commissioned and made the following recommendations: turbidity should be monitored for individual filters with backwashing being triggered if breakthrough is observed; filters should brought back into service gradually after backwashing and run to waste after backwashing; sudden changes in filtration rate should be avoided and turbidity should also be monitored at the coagulation and clarification stages (Binnie et al., 2006).

2.1.2.6 *Adsorption*

Adsorption is the process of accumulating a dissolved substance onto the surface of a material. Once the adsorbate has made contact with adsorbent material, it is held in position by a mixture of physical, chemical and ionic forces (Tebbutt, 1992). The kinetics of adsorption is controlled by two mechanisms, the mass transfer between the water to the solid and intra-particle transport within the particle. The water to solid transfer rate is controlled by the surrounding laminar water film and the intra-particle transport within the particle by surface and pore diffusion (Rietveld and de Vet, 2009).

Synthetic and natural organic substances in small concentrations can cause taste and odour issues and health concerns. As analytical processes have improved, it is now possible to detect specific organic compounds in very small concentrations. Recent concerns about long term exposure to these compounds has resulted in an increased focus on limiting their concentrations in drinking water. Adsorption has been identified as a suitable method to remove soluble organic compounds, including pesticides, as unlike many chemical oxidation processes it does not form potentially harmful by-products (Tebbutt, 1992).

2.1.2.6.1 Granular and powdered activated carbon

As adsorption is a surface mechanism, adsorbents should have a high surface area to volume ratio to maximise their effectiveness. A suitable media for this purpose is activated carbon. Activated carbon, in comparison with other adsorbents, has a wide range of pore sizes which make it suitable for removing a multitude of different dissolved organic compounds.

Activated carbon can be produced either as powder or granules. Granular activated carbon (GAC) is usually applied in contact beds for continual treatment whilst powdered activated

carbon (PAC) is usually dosed for intermittent treatment issues or as a temporary measure until a fixed bed contactor can be installed.

Where adsorption occurs in a fixed continuous flow bed, the majority of the removal of the adsorbate occurs in a segment of the bed known as the adsorption zone. This zone starts initially at the surface of the bed but as the upper levels reach equilibrium with the incoming water, the zone progresses downwards through the bed. When the adsorption zone reaches the outlet of the adsorption bed, the concentration of adsorbate is seen to increase rapidly and breakthrough is observed. The depth of the adsorption zone is dependent on the rate of removal and the velocity of the water through the bed.

When the media needs replacing, as the risk of breakthrough occurring has become unacceptable, the GAC is usually removed and replaced as slurries (Binnie et al., 2006). The removed GAC can be regenerated either onsite or more often taken away to be processed by a specialist supplier (Tebbutt, 1992). The cost and environmental impact of GAC operation is dependent on the frequency of regeneration of the carbon. The frequency of the regeneration is in practice triggered when an effluent limit is exceeded. Measurements of individual micro pollutants which could be of concern for individual sites are measured infrequently due to relatively high costs (Rietveld and de Vet, 2009).

Adsorption beds can require occasional backwashing to wash away accumulated solids. This backwashing can result in mixing of the media, with saturated media being distributed throughout the bed. This can result in the saturated media releasing contaminants back into the water, resulting in a reduction of the time to breakthrough. This issue can be reduced by fully fluidising the bed on backwash, encouraging the media to stay more localised, with finer graded

media near the surface and coarser media at the bottom. Another solution is to use multiple adsorbent beds in series.

2.1.2.7 *Disinfection*

Physical removal of microbiological contaminants occurs before the disinfection stage. Any microbiological pathogens remaining are exposed to a disinfectant such as chlorine, which inactivates the majority of them. A residual concentration of disinfectant is then usually applied to maintain the microbiological quality of the water in the distribution system.

Disinfection is applied in order to inactivate as many pathogenic bacteria, protozoa or viruses as possible. The inactivation of bacteria by oxidants is achieved by rupturing their cell membranes and destroying their enzymes. Although this is an effective way of inactivating many pathogens, certain protozoa oocysts such as *Cryptosporidium parvum* will have to be physically removed. *E. coli* is also relatively resistant to disinfection hence it is commonly used as an indicator organism (Binnie et al., 2006). Disinfection can be achieved through the application of chlorine gas, hypochlorite, on-site electrolyte chlorination (OSEC), chloramination, chlorine dioxide, ozone or ultraviolet radiation.

2.1.2.7.1 Chlorination

The most common method of disinfection is chlorination, which used to be commonly applied as a pre-treatment, but is now, due to concerns about disinfection by-product formation, usually applied to otherwise fully treated water or very high quality ground waters. Chlorine, despite being a poisonous gas and being responsible for some taste and odour issues, is a popular disinfectant because it is readily available, cheap, highly stable, able to leave a residual and very toxic to most micro-organisms (Tebbutt, 1992). Chlorine is commonly applied using super

chlorination and residual dosing. Super chlorination is the process of adding a sufficient dose that the chlorine demand of the water is met, leaving a residual. This process usually occurs in a dedicated contact tank where sufficient time is provided for full disinfection to be achieved. These contact tanks are designed to have a consistent volume, independent of discharge, and have baffles to prevent the formation of short circuits and dead zones. The super chlorinated water requires dechlorination after it leaves the control tank, usually using sulphur dioxide, to achieve a residual dose for distribution of approximately 0.5 mg/l, which is low enough to minimise taste and odour issues.

The rate of disinfection is dependent on the concentration of the active disinfectant present. The active disinfectants measured (molecular chlorine (Cl_2), hypochlorous acid (HOCl), and hypochlorite ions (OCl^-)) are reported as the free available chlorine concentration. When gaseous chlorine is added to water, it reacts to form hypochlorous acid and dissolved hydrochloric acid, as shown in Equation 2-3. Hypochlorous acid can go on to dissociate, as shown in Equation 2-4. The proportions of the substances in solution are heavily dependent on pH, with the addition of chlorine gas reducing pH and hypochlorite increasing pH. The equilibrium points of these reactions are of importance as hypochlorous acid is a more effective disinfectant than the chlorite ion (Tebbutt, 1992).

$$Cl_2 + H_2O \Leftrightarrow HClO + H^+ + Cl^- \qquad \text{Equation 2-3}$$

$$HClO \Leftrightarrow H^+ + OCl^- \qquad \text{Equation 2-4}$$

2.1.3 Existing WTW modelling programs

Many commercial software programs able to model the performance of WTWs have been produced. These programs are similar in their modular approach, allowing different processes to be easily combined. Some key differences between the models are discussed below.

Stimela (stimela.nl): Stimela was developed by Delft University of Technology, Kiwa and DHV (Stimela). It uses dynamic models made from partial differential equations that are numerically integrated, allowing water quality parameters to be traced temporally and spatially (Rietveld et al., 2010). The models are constructed in MATLAB/Simulink and within Stimela, the source code is accessible to allow development by competent users (Rietveld et al., 2004).

The models have a standard modular format with a standardised handling of the models' input and output. They can run online, allowing collaborative model building and development by different user groups (researchers, engineers and operators). The models are built to a consistent structure, which allows them to be connected in series or sequentially, enabling complete treatment works to be modelled (Rietveld et al., 2004). The model, however, is specialised for Dutch processes, and has a lack of coagulation/flocculation modules (Dudley et al., 2008), limiting its usefulness for UK WTW design.

Metrex (www.uni-due.de/il/metrex): Metrex was developed as a research tool by Duisberg University of Technology (Dudley et al., 2008). It focuses on particle size distribution and requires the collection of a higher than average amount of data (Dudley et al., 2008). Like Stimela, Metrex is programmed in MATLAB/Simulink and has a standardised treatment design requiring all parameters to be passed through the model. This allows the user to take a modular approach to works design (Mälzer and Ding, 2006). It, unlike Stimela, does not expose the

MATLAB/Simulink environment, simplifying its interface but making it less flexible (Dudley et al., 2008). The models used are theoretical and in cases qualitative knowledge exists about the parameters' range of values and their dependence on other variables. This enables the user to more reliably estimate suitable parameter values (Dudley et al., 2008). Two types of simulation are possible: whole WTW and single process. Whole WTW mode simulates the whole treatment process in operation mode whereas single process modelling gives guidance for designing and dimensioning single process steps. The major disadvantages of the model for UK works design are its specialisation as a research tool, its lack of critical review or use, its difficulty to use and its lack of current development (Dudley et al., 2008).

Water treatment plant (WTP) simulation program (www.epa.gov): WTP was developed by the United States Environmental Protection Agency (USEPA) to model disinfection and disinfection by-products in support of the Disinfectant/Disinfection By-products Rule (Dudley et al., 2008). It models the general case rather than site specific conditions and is not designed to replace site-specific studies. It is mainly used for the evaluation of design rather than for optimisation and is designed for experienced engineers (Rietveld et al., 2010, Lemont, 2010). The WTP model uses empirical relations obtained from regression analysis. Its predictions reflect typical average performance values, and it is focused on the removal of NOM, the formation of DBPs and disinfection effectiveness. The major disadvantages of the model for UK works design include its focus on disinfection only and the significant reliance on the original database used to verify its predictions (although it was updated in 2000 (Dudley et al., 2008)).

WATPRO (www.hydromantis.com/WatPro.html): Using USEPA correlations, WATPRO is effective at modelling chlorination by-product formation. Other aspects of water treatment

are modelled by user specified removal rates or flow (Hydromantis, 2009). Due to its limitations of modelling aspects of treatment other than by-product formation it was considered a poor example of the state of the art in water treatment modelling by Rietveld and Dudley (2006).

SimEau (www.techneau.org): Developed by the European Commission integrated project Techneau, SimEau hopes to build on the strengths of OTTER and Stimela. It plans to have improved performance over OTTER and Stimela by improving the existing models of processes (particularly coagulation/flocculation), simplifying the calibration process by focusing on the use of routine data improved validation of the models outside of their calibration zones (Dudley et al., 2008). The aims of the program are to model: the overall mass balance; the inactivation of microbiological organisms; the change in water chemistry and downstream dependence on upstream processes (Dudley et al., 2008). If the approach of using particle size distribution is found to be superior, it is believed that UK companies would invest in required online particle size monitors (Dudley et al., 2008). In order to ensure uptake of the new model by European users, the models will be verified using data from five works across Europe, this will ensure it is not only suitable for small regions of Europe. The program will be freely distributed via the internet and calibration support will be provided.

2.1.4 Water treatment and modelling summary

This section investigated how water quality is described and measured, gave an overview of conventional water treatment practices and reviewed the performance of existing water treatment programs. This research influenced the subsequent choice of water quality parameters and modelling processes described in the proceeding chapters.

Although all of the water quality parameters discussed in this chapter should be considered for a drinking water supply, for whole works modelling, it may be practical to model a reduced number of site specific water quality parameters and treatment processes due to either a lack of suitable treatment models or to limit model complexity. Through a study of water treatment quality parameters, turbidity, THM and organic compounds concentrations along with CT were identified as key parameters. Turbidity was identified as a useful indicator of solids removal efficiency that can be used as a potential surrogate parameter for total suspended solids content. The degree of disinfection required was found to be sufficiently specified by the CT value. THMs were identified as important as they are potentially carcinogenic and are currently legislated against in the UK. Finally, organic concentrations should be considered due to their influence on the production of DBPs and their interaction with coagulants, activated carbon, disinfectants and distribution systems.

The degree of water treatment required is dependent on the source but often multiple complimentary processes are applied such as: coagulants to help colloids coalesce and to reduce organic compounds concentrations; flocculation to control the size and strength of floc; clarification and filtration to remove the majority of suspended matter; activated carbon to reduce the concentration of target organic compounds and disinfection to inactivate any

remaining pathogens. General models for these processes are described in detail in chapter three.

The existing software was found to have varying availability and documentation. Processes modelled were also skewed towards those prevalent in the country where each program was produced. The existing software all model treatment processes as modules which could be organised to represent different sequential or parallel treatment streams and often use the MATLAB/Simulink modelling environment.

2.2 Genetic algorithms

A conceptual view of evolutionary computation and the main different types of algorithms that exist are described in this section. A description of how current genetic algorithms function, the advantages and drawbacks to using genetic algorithms and the different approaches that are applied are then discussed. The final part of this section looks at how GAs can be applied to solve multi-objective problems to optimise the design and operating regimes of water treatment works. In this last section WTW optimisation, multi-objective problems, the Pareto concept, multi-objective evolutionary algorithms (MOEA) and the Non-Dominated Sorting Algorithm II (NSGAII) are described. The use of the NSGAII algorithm to identify potential optimal designs and operating regimes for a case study site is described in chapter five.

2.2.1 Overview of genetic algorithms

Optimisation is the method of comparing alternatives using a standard measure of performance and iteratively improving performance by selecting better solutions over time (Fogel, 1994). Evolutionary algorithms (EAs) have proved to be a particularly robust method of achieving this goal. These programs, which were first developed in the 1960s, are based on the principles of

Darwinian evolution, applying the processes of variation and selection to solve problems which traditional methods could not resolve.

Some alternatives to EAs exploit the best known solutions for further improvement without exploring for alternative solutions, whilst other random search techniques explore but do not take advantage of the best known solutions. What makes EAs such a powerful search technique is its capability of both exploring new solutions whilst simultaneously taking advantage of the known best solutions (Michalewicz, 1996).

2.2.2 Evolutionary algorithms

Evolutionary algorithms follow a common procedure of:

1. Initialising a population of candidate individuals;
2. Evaluating their fitness based on performance;
3. Selecting which individuals get the chance to reproduce;
4. Replacing individuals with the lowest fitness with offspring created using cross-over and/or mutation operators; and
5. Repeating the process from stage two until the procedure is terminated.

The amount of offspring insertion that occurs each generation can vary between complete replacement of parents to regimes where offspring only replace the worst, the oldest or their own parents (Fonseca and Fleming, 1998).

Evolutionary Algorithms (EA) are broadly split into three groups of programs: Genetic Algorithms (GAs), Evolutionary Strategies (ESs) and Evolutionary Programs (EPs) (see Figure 2-3). Each of these programs operates on a different scale of evolutionary unit. Genetic algorithms operate at the level of chromosomes, evolutionary strategies operate at the level of

individuals and evolutionary programming at the level of species. Evolutionary strategies are further differentiated from evolutionary programming by their reliance on deterministic selection and the presence of sexual communication between individuals in their populations (Fogel, 1994).

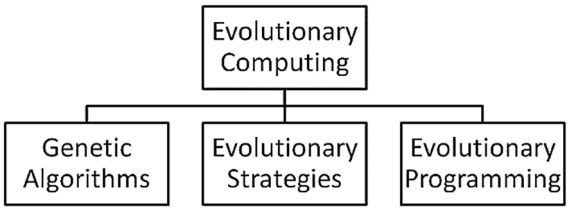

Figure 2-3 Evolutionary computing hierarchy

EAs have been used to solve a variety of problems where other techniques have performed unsatisfactorily (Fogel, 1994). However, like other search and optimisation techniques, EAs do have limitations, including an inability to ensure true randomness, difficulty in identifying suitable EA parameters and high computational demands. These problems can be addressed in a number of ways. Random number generator algorithms are used to produce, as closely as possible, random numbers. In order to maximise the efficiency of the optimisation process, the parameters of EAs for population size and likelihood of cross-over and mutation should be selected appropriately. It is especially important to ensure the efficiency of the process as due to the lack of problem knowledge used within EAs, they can require substantial computational resources.

2.2.3 Genetic algorithms

Genetic algorithms (GAs) are the most popular application of evolutionary algorithms, which apply the theory of natural selection to identify near optimal solutions. In genetic algorithms, a random group of initial parent and offspring solutions are produced by applying crossover and mutation functions. Together these parent and offspring solutions make up the first generation

of solutions, which have their performance assessed before a second generation of parent solutions is identified. As the number of generations increases, the performance of the population should improve (see Figure 2-4).

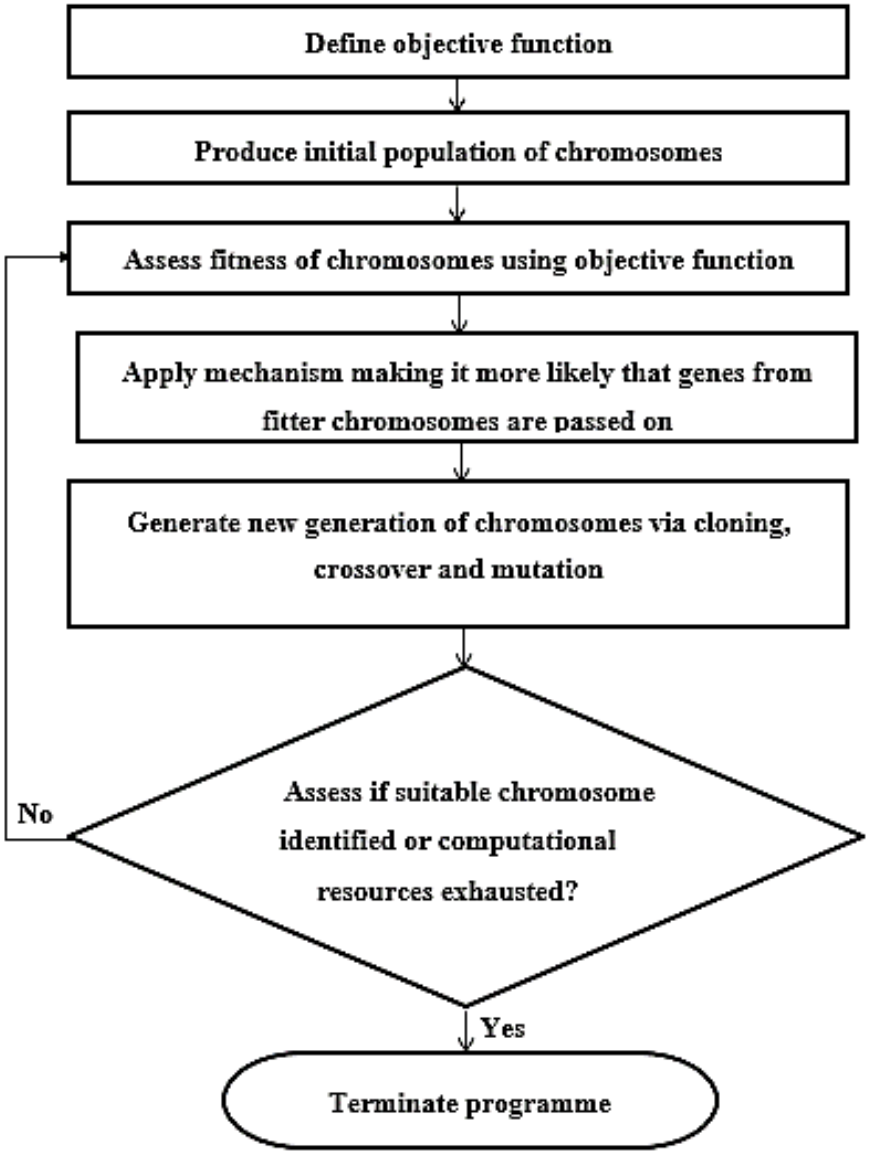

Figure 2-4 Flowchart of genetic algorithm process

2.2.3.1 *Advantages and previous application of GAs*

GAs were chosen to optimise WTWs in this work for a number of reasons: they are based on the widely known theory of evolution; they can be applied to existing models; they contain all of the genetics-based processes present in more complex evolutionary algorithms; they can

search spaces with many local optima; they are able to estimate parameters that interact non-linearly; they can handle non-continuous search spaces; they are usually insensitive to initial conditions; they can be used effectively to locate global peaks (Coley, 1999) and they present the opportunity to apply problem constraints directly by limiting chromosome values or indirectly by applying penalty functions to form pseudo-constraints.

Genetic algorithms have been used to solve multi-objective problems, as well as problems involving chaos, chance, temporality and non-linearity (Fogel, 1994). GAs have been used to optimise a wide range of engineering problems in diverse fields such as parameter and signal identification, control, robotics, pattern and speech recognition, planning and scheduling, classification and engineering design problems (Man et al., 1996). GAs have been used in water sector applications, including the optimisation of regional wastewater pipelines and treatment (Brand and Ostfeld, 2011), agricultural management practices (Kaini et al., 2012), regional water use and water treatment processes (Tudor and Lavric, 2010), potable water distribution (Kadu et al., 2008) and potable water treatment works design (Gupta and Shrivastava, 2006, 2008, 2010).

2.2.3.2 *Limitations of GAs*

Genetic algorithms do have limitations. These limitations can be grouped into three main areas of concern: that non-optimal solutions may be identified, that large computational resource may be required and that solution quality can be uncertain. The causes of these limitations are provided here and some common approaches to limiting their influence are discussed later in this section.

GAs are not guaranteed to identify optimal solutions due to their stochastic nature and many generations may be needed to achieve even near-optimal solutions (Izquierdo et al., 2004). Poor

optimisation performance is more likely if a low degree of population diversity occurs due to premature convergence to sub-optimal solutions in the early generations. Premature convergence is caused when there are many possible optimal solutions but only a limited population. Under these conditions the population tends to settle on a single or a few "good" solutions (Fonseca and Fleming, 1998). A symptom of premature convergence is that offspring cease to reliably outperform their non-optimal parents. Under these conditions, offspring represent their parents too closely and further optimisation becomes dependent on mutation, which tends to be slower (Fogel, 1994). A common cause of premature convergence is the selection of too low a population size (Man et al., 1996).

Even if appropriate GA parameters are applied, there is no guarantee that optimal solutions will be identified. Some problems are just difficult to optimise using GAs. This is because poor performing offspring are sometimes prone to be generated through the combination of genes from successful parent solutions. These problems are said to contain GA-deceptive objective functions. Various approaches have been applied to try and treat these functions successfully, including code modification, chromosome inversion and messy GAs. These techniques themselves have drawbacks, including necessary prior knowledge of the objective function performance, additional complexity and in the case of chromosome inversion, lack of evidence of its effectiveness (Man et al., 1996).

The last limitation outlined here is simple in nature. As GAs are random, it is sometimes difficult to decide whether the solutions identified are optimal or even near optimal. This is because only certain areas of the search space may have been explored and until all possible solutions have been evaluated it is impossible to know that no better solutions exist. As this could take an excessive amount of computational resources (and negate the purpose of the GA),

it is necessary to assess the solutions in other ways to decide when the solutions identified are good enough.

2.2.3.3 *Solution evaluation*

Before the best solutions can be identified for a problem a method must be found to measure the fitness of different solutions. The evaluation of the solutions' fitness is achieved using objective functions. These functions calculate values that describe how well each solution achieves certain goals. The form that the objective functions take is dependent on the problem being optimised and the desired characteristics of the final solution. Good objective functions will result in a fine graded differentiation between different solutions, enabling effective optimisation. Examples of objective functions include cost, failure rate or error. Single or multiple objectives can be applied; multiple objective problems are discussed further in section 2.2.4.1.

Objective functions can also be used to implicitly set solution constraints by applying penalty functions if constraints are not met. If these penalties are significant enough, chromosomes which do not meet the constraints should be efficiently removed from the population. The advantage of applying pseudo-constraints is that chromosomes can be limited to meet objective targets even if the relationship between chromosome and objective functions are complex or unknown. If the magnitudes of penalty functions are too great then premature convergence can occur. This is because intermediate solutions, which may be necessary to achieve alternative solutions, are unable to pass on their genes in the early stages of evolution if they do not meet the constraint conditions (Michalewicz, 1996). Conversely, if the penalty functions applied are too small then optimal solutions may be identified which do not meet the desired constraints.

2.2.3.4 *Selection*

Identifying those chromosomes which are going to pass on their genes to the following generation is usually determined using two groups of techniques: those where the probability of selection is proportional to the performance of solutions and those where only solutions identified as being the fittest are selected. Using the proportional method, a chromosome with an objective functional score twice as great another has double the likelihood of passing on its genes. There are some drawbacks to this method, including the possibility of losing the best chromosomes from the population, the necessity for objective scores to be proportional to performance and the fact that to operate efficiently, objective scores need to vary significantly between chromosomes (Fogel, 1994). If the objective scores do not vary significantly then the selection process becomes akin to a random process. Some solutions have been proposed to these issues such as elitist selection (keeping the best chromosomes in a secondary population), scaling the objective function relative to the lowest scoring chromosome or ranking to determine the likelihood of selection (Fogel, 1994). In the alternative method, where only the fittest solutions are able to reproduce, tournament selection compares a limited number of solutions and selects the best solutions. This process is repeated until a sufficient number of solutions have been identified.

As has already been mentioned, one of the biggest challenges to a GA is ensuring that solutions do not converge too quickly before the objective space has been sufficiently searched. Many of the methods which are used to prevent premature convergence take place during the selection phase of the genetic algorithm, including pre-selection and niching. Pre-selection ensures that each new generation of chromosomes contains a proportion of the previous generation's chromosomes. Niching is achieved using crowding or fitness sharing functions which cause similar chromosomes to have their fitness reduced irrespective of how well they achieve the

primary objective functions. These methods result in isolated individuals being given a greater chance of survival. Fitness sharing imitates competition for finite resources in an environment by sharing a fitness value between all solutions inhabiting the same region of the search space (Fonseca and Fleming, 1998). Crowding operators measure the variation between different genes or objective functions and identify diverse solutions as being more desirable.

2.2.3.5 *Reproduction*

Those chromosomes which have been selected for passing on their genes to the next generation can do so by either cloning themselves (asexual reproduction) or by mixing their genes with another chromosome (sexual reproduction). The offspring's genes can then undergo possible mutation. It is argued by Fogel (1994) that, based on the probabilities of these processes occurring in historical studies (see Table 2-4), cross-over is the dominant feature of a genetic algorithm, with mutation existing purely to ensure that every possible solution can potentially enter the population. The literature emphasises the importance of avoiding premature convergence, which also highlights the significance of cross-over (Fogel, 1994, Man et al., 1996, Fonseca and Fleming, 1998).

2.2.3.6 *Cross-over*

Cross-over imitates sexual reproduction, with the genes of parents influencing the genes of their offspring. The proportion of offspring which are created by cross-over is defined by the cross-over probability. The cross-over probability can influence the efficiency of the search procedure, with greater amounts of cross-over reducing the risk of premature convergence but increasing the likelihood that unpromising regions of the search space are explored. Cross-over can be achieved by swapping a single, random length of binary code between two

chromosomes. This method was identified as being preferable by Holland (1975, cited by Fogel, 1994) to the random cross-over of individual genes, as it was thought that co-operative genes could be swapped together. This assumption was contradicted by Syswerda (1989, cited by Fogel, 1994), who found that uniform cross-over was able to identify generally better, faster solutions than both single and double point cross-over.

Intermediate recombination performs an operation similar to that of cross-over by blending the values of genes using a range of statistical averaging techniques. Simulated binary cross-over (SBX) is one example of an averaging technique which has been shown to have the potential to outperform traditional binary cross-over in a direct comparison (Deb and Agrawal, 1995 cited in Nicklow, 2010).

2.2.3.7 *Mutation*

Mutation increases the diversity of the population by altering randomly selected genes of offspring. This ensures that all possible solutions could be examined, if the genetic algorithm were allowed to run indefinitely. The proportion of offspring genes which are altered in this way is defined by the mutation probability. If this is set too high then the evolutionary progress becomes more akin to a random search but if it is set too low then the ability of the GA to explore the search space is diminished.

2.2.3.8 *GA internal parameters*

There are few clear conclusions, in the existing literature, about identifying appropriate genetic algorithm parameters and due to complex interactions between the parameters, fine tuning them is a difficult and time consuming process (Davis, 1991). It has been found that mutation probability should be kept below 5% to be effective (De Jong, 1975, Grefenstette, 1986), but a

complete lack of mutation is also associated with poorer performance (Grefenstette, 1986). Grefenstette's (1986) work on identifying optimal GA parameters, also identified the benefits of higher proportions of the solution population being replaced each generation and the use of elitist selection policies. For smaller populations (approximately thirty), Grefenstette identified that higher cross-over probability (approximately 90%) was an important factor in the prevention of premature convergence. Optimal GA parameter settings have been found to: vary from problem to problem; be sensitive to alterations in genetic algorithm implementation (Davis, 1991) and be more influential for problems with a greater number of decision variables (Siriwardene and Perera, 2006). Despite the benefits of optimising GA parameters, it has been found that very good performance can also be obtained using a range of settings (Grefenstette, 1986). For some problems, robust general GA parameters identified the same optimal solutions as optimised values (Franchini and Galeati, 1997).

Table 2-4 Genetic algorithm parameterization sets used in previous work, where L is number of design parameters being optimised

GA parameter	**Sharifi (2009)**	**Jain et al. (2007)**	**Nazemi et al. (2006)**	**Sarkar and Modak (2006)**	**Tang et al. (2006)**	**Kapelan et al. (2005)**	**Deb et al. (2004)**	**Inamdar et al (2004)**	**Deb et al. (2002)**
Population	200	(15-25)*L	50	500	10	200	200	50	100
Probability of cross-over	0.70	0.90	0.80	0.90	1.00	0.70	0.90	0.98	0.9
Cross-over distribution index	10	2-10	n/a	20	n/a	n/a	n/a	n/a	20
Probability of mutation	0.05	1/L	0.01	0.05 - 0.08	1/L	0.90	0.20	0.01 - 0.05	1/L
Mutation distribution index	20	10-50	n/a	20	n/a	n/a	n/a	n/a	20
Generations	500	100	100	1000	n/a	500	500 - 800	100	250

2.2.3.9 *Efficient use of genetic algorithms*

In order that the objective space is thoroughly searched in a reasonable time period, it is possible to apply GAs over multiple processors, either as independent synchronous runs or as a method to distribute objective performance calculations for a single optimisation process. The advantage of multiple independent runs includes the reduced influence of any possible premature convergence to localised areas of the solution space.

Due to the stochastic nature of GAs, it is possible that some optimal solutions may be lost before the final population is assessed. In order to avoid this, Van Veldhuizen and Lamont (2000) and

Horn (1997) recommend the collation of a secondary population, made up of all of the Pareto optimal chromosomes identified throughout the optimisation.

2.2.4 Application of genetic algorithms to multi-objective problems

2.2.4.1 *Multi-objective problems (MOPs)*

A multi-objective problem may arise, for example, during a manufacturing process, with the cost and quality of produced goods conflicting with each other. An optimisation of this problem would result in a selection of trade-offs between the two objectives and it would be necessary for a decision maker (DM) to select an appropriate solution. Different DMs could select different solutions to be applied based on their individual preferences.

MOPs can be difficult to solve as they often have complex conflicting objective functions and require extensive computational resources (Van Veldhuizen and Lamont, 2000). Single objective problems often have a unique optimal solution but MOPs can potentially have an infinite number of optimal solutions, each of which represents a different trade-off between the different objectives. If the objectives were never conflicting then a single aggregated objective function could be used and the problem could be simplified to a single objective problem (Horn, 1997).

The greater the number of objective functions that are assessed in determining the fitness of chromosomes, the greater the number of chromosomes which could be determined as optimal (Van Veldhuizen and Lamont, 2000). In order to keep the number of optimal solutions manageable, the number of primary objective functions should be limited. It has been found that two or three primary objectives are sufficient to describe the performance of chromosomes.

Other additional secondary fitness functions can then be used to assist the optimisation process (Van Veldhuizen and Lamont, 2000).

There are three main types of methods to identify the most desirable chromosomes based on their separate objective scores: those that make comparisons between the values of the individual objectives, those which consider the objectives separately and those which consider the objectives simultaneously but do not compare them. Those which compare the value of the separate objectives are aggregative and calculate a single summative objective score for each chromosome using either scalar-aggregative or order-aggregative approaches. The scalar approach uses either a linear combination of weighted objective scores or a non-linear approach where chromosomes are assigned penalty functions for any objectives not met (therefore possibly acting as a pseudo-constraint). The order-aggregative, also known as lexicographic, method orders the chromosomes by considering each objective in turn, only moving to secondary objectives when primary objective scores are tied (Horn, 1997). The method which considers the separate objective functions to be incomparable is known as the Pareto concept. To identify MOP solutions which represent the different trade-offs between the objectives, many researchers use this method, as described in the next section (Van Veldhuizen and Lamont, 2000).

2.2.4.2 *The Pareto concept*

Multi-objective problems rarely have a unique solution, but rather a set of alternative trade-offs which are not dominated by each other. The Pareto concept allows these non-dominated solutions to be identified when it is not possible to directly compare different objective functions. The Pareto criterion defines a solution as dominating another only if is at least as good in all attributes and better in at least one (Horn, 1997). Solutions which are dominated are

clearly not optimal but the non-dominated solutions will potentially be incomparable with each other, being better in one regard but worse in another. The blue markers in Figure 2-5 represent the non-dominated solutions to a problem where both objective functions A and B are to be minimised. This set of solutions is known as the Pareto set and the interpolated line between them is known as the Pareto front. The solutions in the second Pareto front are dominated by the first front and dominate those in the third front. A decision maker can choose a suitable solution by using the Pareto set to identify whether a single optimal solution exists or if certain solutions stand out. Some solutions may stand out, for example, if they are optimal in one of the objectives or they reside at a "knee" in the front, where a large sacrifice in one objective yields a small improvement in another. The accuracy of the decision maker's choice of an appropriate solution depends on the identified Pareto set being close to the true Pareto set (Van Veldhuizen and Lamont, 2000). The Pareto concept gives an indication of how the objectives interact, allowing the nature of the observed trade-offs to be investigated and not just the solutions (Horn, 1997).

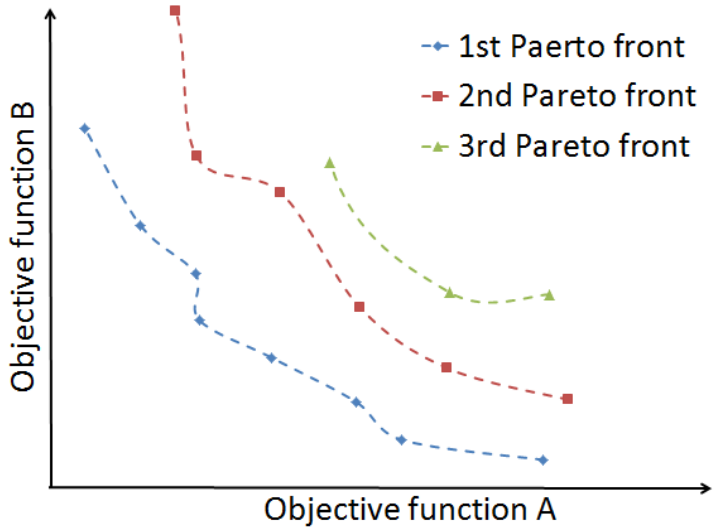

Figure 2-5 Pareto front in objective space

To order the fitness of chromosomes systematically, they can be ranked based on how close to being in the Pareto set they are. Two methods are primarily used to achieve this ranking. Both

methods operate by assigning the Pareto set to an elite rank and the other solutions to less desirable ranks. In a method proposed by Goldberg (1989, cited by Van Veldhuizen and Lamont, 2000), the Pareto set of solutions are assigned to the first Pareto rank and then removed from the selection population. Solutions non-dominated by the remaining solutions are then assigned to the second Pareto rank. This process is continued until all chromosomes have been assigned a Pareto ranking. The other ranking method outlined in Fonseca and Fleming (1998) ranks the Pareto set as belonging to a zeroth order rank and the other chromosomes are ranked on the basis of how many chromosomes dominate them. Fonseca and Fleming's method enables finer grading of the chromosomes but there is no definitive evidence of either of these ranking systems being superior to the other (Van Veldhuizen and Lamont, 2000).

2.2.4.3 *Multi-objective evolutionary algorithms*

Multi-objective evolutionary algorithms (MOEAs) were developed to solve complex problems with frequently conflicting multiple objectives in acceptable time frames (Van Veldhuizen and Lamont, 2000, Man et al., 1996). MOEAs are well placed to solve problems which cannot be easily solved by alternative methods (Horn, 1997), such as those which have complex Pareto fronts, possibly containing multiple peaks or discontinuities. MOEAs try to achieve two goals: to move the population towards the Pareto front and to maintain diversity in the population (Deb et al., 2002). There are many different MOEAs detailed in the literature but two in particular are prevalent (Hirschen and Schafer, 2006): the Improved Strength Pareto Evolutionary Algorithm (SPEA2) (Eckart et al., 2001) and the Non-Dominated Sorting Algorithm II (NSGAII) (Deb et al., 2002). It is the second of these two algorithms which is applied in this work.

2.2.4.4 *Non-dominated sorting genetic algorithm II (NSGAII)*

The Non-dominated sorting genetic algorithm II (NSGAII) (Deb et al., 2002) is a type of second generation multi objective evolutionary algorithm (MOEA). NSGAII finds and preserves the best solutions through the use of an elite preserving operator, the application of a fast algorithm to sort non-dominated fronts and the use of a two level ranking method to assign effective fitness to solutions. Solutions are first ranked by Pareto set and then by crowding, so that dissimilar solutions are favoured. NSGAII has been shown to exhibit good diversity preservation in comparison with other GAs (Deb et al., 2002, Laumanns et al., 2002) and to be able to identify Pareto fronts in both constrained and non-constrained problems. In comparisons performed by Deb et al. (Deb et al., 2002) against two other contemporary algorithms, Pareto-archived evolution strategy (PAES) and Strength Pareto Evolutionary Algorithm (SPEA), and a binary coded version of NSGAII, a real-value coded version of NSGAII was found to perform best in nine test problems identified from past studies. This evaluation was based on the assessment of convergence to known optimal solutions and the degree of diversity achieved. A drawback to the NSGAII is that it allows non dominated solutions to replace each other, which over time can result in the deterioration of the population's performance and therefore not guarantee convergence to the Pareto set. Further details of how the NSGAII algorithm is applied can be found in Appendix A).

2.2.5 Genetic algorithms summary

This section examined how GAs are applied to solve MOPs. The research of GAs is used to apply NSGAII algorithms to solve design and operating regime optimisation problems, which is described in chapter five.

The operation, advantages and limitations of GAs were investigated with the intention of using them to optimise the design and operating regime of a modelled WTW. GAs were found to be appropriate as they use variation and selection to solve MOPs by exploring within solution spaces whilst taking advantage of currently best known solutions. The use of the Pareto concept was considered appropriate where objectives are considered to be incomparable. The NSGAII was selected as an effective, widely used GA which uses the Pareto concept. This algorithm attempts to move the solution population towards the best possible solution population whilst maintaining solution diversity. A secondary population, made up of all of the Pareto optimal chromosomes identified throughout the optimisation can be compiled to avoid losing some non-dominated solutions before the final population is assessed.

2.3 Knowledge gap

Based on the review of water treatment quality, treatment, existing programs and genetic algorithm optimisation covered in this chapter the following gaps in current knowledge are identified.

- Historically poor uptake of water treatment modelling has been previously attributed to the quantity of non-standard calibration data required (Dudley et al., 2008). The performance of WTW models using only conventionally collected data is unknown.
- The accuracy of water treatment solids removal models has typically been assessed using bench scale or pilot plants for periods of time of less than a week (Edzwald et al., 1992, Adin and Rebhun, 1977, Saatci and Oulman, 1980) and occasionally using operational works for periods of time less than a month (Head et al., 1997). The accuracy of water treatment works models calibrated and verified over annual periods has not

been investigated. Assessing models over longer periods with greater diversity in operating conditions would allow influences such as seasonality to be investigated.

- Previous water treatment modelling programs have taken either a static or dynamic approach to modelling processes (i.e. WRc's dynamic OTTER and Hydromantis's static WATPRO programs). A comparison of the relative accuracy of using both types of models for whole works modelling purposes has not been completed.
- Water quality variance at operational sites has been described broadly by mean and standard deviation values (Clark et al., 2011). The variance of key water quality parameters have not been more fully defined by appropriate probability distributions. Distributions for key parameters have not been defined in detail from an operational site, along with an assessment of how accurately they approximate to standard distributions (such as normal, exponential or log-normal).
- Due to multiple water quality parameters, being dependent on multifaceted operating conditions, it is problematic to gain simple guidance from a WTW model that can be applied by operational staff in real time. Simple methods of providing this guidance are presently missing.
- Existing genetic algorithm optimisation studies of water treatment works have focused on solids removal, using static models for theoretical water treatment works (Gupta and Shrivastava, 2006, Gupta and Shrivastava, 2008, Gupta and Shrivastava, 2010). The concurrent optimisation of solids removal and disinfection processes using both static and dynamic models along with data from operational sites has not previously been examined.

3 GENERIC WTW MODELS

To achieve the aims and objectives for this study (see section 1.4), computational models of common treatment processes for lowland surface waters in the UK are required. In order to develop and test these models, case study data from Trimpley, an operational WTW (see chapter four), is used. The processes modelled include: coagulation; dissolved air flotation (DAF) and hopper bottomed clarification (HBC); rapid gravity filtration (RGF); granular activated carbon (GAC) and super chlorination. The models described in this chapter are used to predict the performance of Trimpley WTW (see chapter four). The models are also used to theoretically optimise the design and operation of Trimpley WTW (see chapter five).

3.1 Model overview

The models are programmed using Simulink, an extension of MATLAB that provides an interactive graphical environment for modelling time varying systems. Process models are built as modules that can be grouped together to represent whole WTWs. This allowed the effect of operational changes in proceeding treatment processes to be evaluated throughout the works. As MATLAB/Simulink is used, the models are easily accessible, the structure is open and flexible (van der Helm and Rietveld, 2002) and all routines, toolboxes and visualisation techniques of MATLAB/Simulink can be used. The ODE45 solver is used with a variable time step for all of the models in this work with a minimum time step of fifteen minutes, which is commonly the eSCADA data time step observed in the case study works.

3.2 General models

This section describes water characteristics, inter-relationships and processes that apply to WTWs as a whole and therefore cannot be assigned to single process models.

3.2.1 Water density

Water density is determined using an empirical relationship with temperature as developed by Civan (2007) (Equation 3-1). The accuracy of this relationship was tested by Civan using the experimental data of Weast & Astle (1982). Weast & Astle reported 104 densities of water from -30 °C to 89 °C at 1 atm. The density / temperature relationship has a coefficient of determination (R^2) of approximately 1.0, and an average relative deviation from the data of 10^{-4} °C (Civan, 2007). The R^2 value is a measure of the degree of variation in the response variable that is accounted for by the independent variables of a mathematical relationship (Nelson et al., 2003).

$$\rho_w = 1065 * \left\{1 - e^{\left[1.2538 - \frac{1.4496\times10^3}{(T+175)} + \frac{1.2971\times10^5}{(T+175)^2}\right]}\right\} \qquad \text{Equation 3-1}$$

Where: ρ_w = density of water (kg/m^3) and T = temperature (°C).

3.2.2 Dynamic viscosity

Dynamic viscosity is calculated using Equation 3-2 from Kestin et al. (1978) for water at atmospheric pressure and temperature between 0 °C and 40 °C. The relationship is based on four independent data sets (Korson et al., 1969; Eicher & Zwolinski, 1971; Hardy and Cottington 1949 and Korosi and Fabuss, 1968), which were the most precise over particular temperature ranges at the time of Kestin et al's analysis. The relationship has a reported error in reference viscosity of 0.1% and the temperature relationship has a standard deviation of 0.1%.

$$\mu = 1.002 \times 10^{-3} * 10^{\langle\left\{\frac{[20-T]}{[T+96]}\right\} * \{1.2364 - [1.37\times10^{-3} * (20-T)] + [5.7\times10^{-8} * (20-T)^2]\}\rangle}$$ Equation 3-2

Where: μ = dynamic viscosity (Ns/m2) and T = temperature (°C).

3.2.3 Mixed flow within dynamic models

Continuous stirred tank reactors (CSTRs) are used to model the degree of mixing that occurs within processes. A single CSTR models perfect mixing. The more tanks there are, the more the tanks act like a plug flow system. To model complete mixing within a CSTR where mass is conserved, the instantaneous change in the concentration of the reactor is calculated using an ordinary differential equation (ODE) as shown in Equation 3-3. A modified ODE can model non-conservative mechanisms by having additional terms added, for instance first order decay can be modelled as shown in Equation 3-4.

$$\frac{dC}{dt} = \frac{Q(C-C_0)}{V}$$ Equation 3-3

$$\frac{dC}{dt} = \frac{Q(C-C_0)}{V} - kC$$ Equation 3-4

Where: C = outlet concentration, C_0 = inlet concentration, t = time, Q = flow, V = volume and k = first order decay rate (h^{-1}).

3.2.4 Relationship between turbidity and suspended solids

Many water treatment solids removal models use suspended solids (SS) as a performance parameter, i.e. Head et al. HBC model (1997); Edzwald DAF model (2006) and Adin and

Rebhun rapid gravity filtration model (1977). Most WTWs however, routinely measure turbidity as a surrogate parameter for SS concentration. In order to accurately gauge SS concentrations either continual SS sampling can be implemented or a correlation between turbidity and SS can be determined based on a period of sampling data. This relationship is usually expressed as a directly proportional relationship, as shown in Equation 3-5. This relationship may require continual adjustment to take into account seasonal and episodic events.

$$SS = b \times NTU \qquad \text{Equation 3-5}$$

Where: b = empirical parameter (mg/l.NTU).

The value of the empirical parameter b in Equation 3-5 was found to vary between 0.7 to 2.2, for low colour water that predominantly required turbidity removal treatment by Cornwell et al. (1987) cited by AWWA (1999).

Turbidity, when used as a surrogate for SS concentration, has some further limitations. Most importantly, turbidity and suspended solids do not measure the same constituents of the water, as shown in Figure 3-1. Turbidity measures the effects of conventional suspended solids as well as effects of other smaller and larger solids and dissolved compounds. For this reason it is possible that a high turbidity reading does not necessarily mean a high suspended solids concentration (Bilotta and Brazier, 2008).

The turbidity of water, which relates to its propensity to scatter light, is also not solely dependent on the concentration of solids present. The size, shape and refractive index of the suspended solids also affect turbidity readings (Mhaisalkar et al., 1993, Bilotta and Brazier,

2008), and these properties change during treatment (Mhaisalkar et al., 1993). For these reasons it is challenging to correlate accurately turbidity to SS (Mhaisalkar et al., 1993).

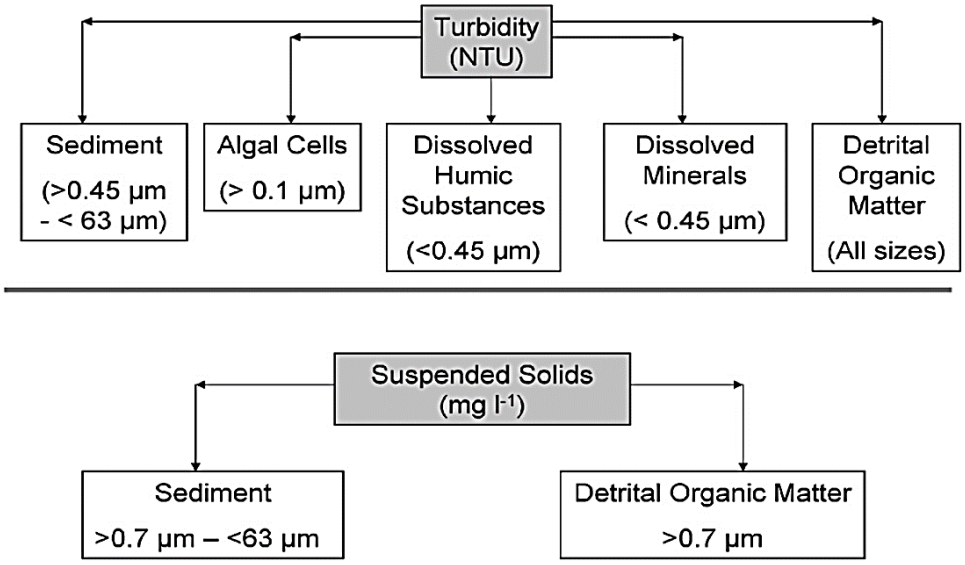

Figure 3-1 Turbidity and suspended solids constituents (Bilotta and Brazier, 2008)

Despite the limitations of correlating suspended solids concentrations to turbidity measurements, it is frequently done by environmental bodies such as the Australian and New Zealand Environment Conservation Council (ANZECC) and the United States Environmental Protection Agency (USEPA) due to its ease of application (Bilotta and Brazier, 2008).

In the work reported here, the ratio between suspended solids (mg/l SS) and turbidity (NTU) is set at 2:1, as used as a default value in the OTTER program (WRc, 2002) and as suggested by Binnie et al. (2006), where sufficient data are not available to define it accurately. This is done so that the accuracy of the WTW models, which only use conventionally collected measurements, can be assessed. This ratio is likely to vary temporally and spatially in practice but is likely to range from approximately 0.5 to 3:1.

3.3 Coagulation and flocculation

The coagulation module for both the dynamic and static models is identical and static in nature. It is assumed that either conventional ferric or aluminium salt based coagulants are applied. The pH and alkalinity both reduce due to the addition of acidic coagulant and the suspended solids concentration increases due to the formation of metal hydroxides. The total organic carbon (a surrogate parameter for NOM) that is removed during the clarification process is modelled as being dependent on the coagulant dose and as such is modelled as a coagulation process.

3.3.1 Suspended solids adjustment

Assuming that all of the metal ions in the ferric or aluminium based coagulants form metal hydroxides, which precipitate out of solution, then by stoichiometric analysis, the amount of suspended solids added by ferric sulphate is 1.9 g/g Fe^{3+} and by alum 2.9 g/g Al^{3+}. This assumption is expected to be approximately true if: (i) reactions between TOC and coagulant formations are negligible; (ii) doses of coagulant are greater than 2 mg/l as Fe^{3+} and (iii) pH is such that iron has a low solubility (i.e. $4.0 < pH < 11.0$) (Tseng and Edwards, 1999). It is likely that operating conditions at a WTW will be within these criteria. This method of calculating additional solids loading agrees with that reported by Warden (1983) as reported by Binnie et al.(2006). Any additional solids loading caused by the precipitation of metal-NOM complexes or adsorption of TOC on to the surface of the metal hydroxides formed is not calculated and is a limitation of the method.

3.3.2 TOC Modelling

Edwards' (1997) model, based on the Langmuir equation, is used to model dissolved organic carbon (TOC) removal due to coagulation. The extent of TOC removal is predicted by the raw

water's TOC concentration, ultraviolet absorption at 254 nm and the coagulated water's pH. In the Edwards (1997) model, organic matter is assumed to be adsorbed onto the surface of metal hydroxide flocs that are formed by ferric or alum coagulants. The metal hydroxide ions Fe^{3+} and Al^{3+} are considered to be almost completely insoluble over the operational pH range (3.0-8.0 for ferric coagulants and 5.5-8.0 for alum coagulants) and so the available sorbent surface is considered to be proportional to the dose of coagulant (Edwards, 1997). Some of the organic matter is assumed to be non-adsorbable and the rest exists in equilibrium, between solution and adsorption, which is described by a Langmuir isotherm. A Langmuir isotherm was used by Edwards to describe the adsorption equilibrium in preference to Freundlich or diffuse layer modelling, due to superior agreement of 50 preliminary trials of each approach to experimental data (Edwards, 1997). A full description of this model is provided in Edwards (1997) and Tseng & Edwards (1999).

The 'general low DOC' parameters are used to model TOC in this work. The application of these parameters for TOC application is considered to be appropriate as TOC typically approximates to DOC to within 2-17% for low turbidity water sources (Owen et al., 1995). The accuracy of the low DOC model for TOC use, for a selection of jar, pilot and full scale tests is shown in Table 3-1, based on the reported analysis in Edwards (1997) and Tseng & Edwards (1999). A meta-analysis of these results indicates that the low DOC model for TOC use, has an accuracy described by a coefficient of determination (R^2) between 0.76 – 0 .96 and a maximum standard error of 0.6 mg/l. Taking the results from Table 3-1 as a whole, the standard error of the model can be estimated as being approximately ± 20% or 0.5 mg/l. It is worth noting that the regulatory limit for bias and precision from Analytical Quality Control (AQC)

measurements is currently 5% (Mills, 2013), which is a significant fraction of the predicted model error.

Table 3-1 Edwards' TOC model accuracy (data from Edwards, 1997 unless otherwise stated)

Data description	**n**	**Number of tests**	**Number of locations**	**R^2**	**RMSE**
Randke et al.	858	60	n/a	0.96	n/a
TOC jar tests from AWWA survey	1804	219	n/a	0.88	n/a
Full scale and pilot scale multiple sampling events from NECSD	n/a	n/a	7 WTWs across 5 states of USA	0.89	0.3 mg/l
Full scale and pilot scale single raw and coagulated water grab samples	n/a	n/a	17 WTWs across 14 states of USA	0.87	0.6 mg/l
All jar test, full scale and pilot scale data applied to TOC model	n/a	n/a	n/a	n/a	12%
Ferric, alum and poly aluminium chloride (treated as alum) coagulants full scale and pilot scale, grab and continuous data sets, cited in Tseng and Edwards (1999)	n/a	n/a	31 WTWs	n/a	Alum 0.51 mg/l 21% Ferric 0.32 mg/l 11%

Where: n = number of data points; R^2 = coefficient of determination; RMSE = route mean squared error; AWWA = American Water Works Association and NECSD = National Enhanced Coagulation and Softening Database.

3.3.2.1 *Coagulant dosing model*

Based on the Edwards model, it is possible to calculate a coagulant dose to achieve a desired clarified total organic carbon (TOC) concentration. Based on the TOC and ultraviolet adsorption at 254 nm (UV_{254}) of the initial water, the fraction of non-sorbable TOC can be calculated using Edwards' model. This can be combined with a target TOC concentration to calculate a target equilibrium concentration of adsorbate in solution (C_{eq}) using Equation 3-6

$$C_{eq} = TOC_{target} - TOC_{non}$$ Equation 3-6

The coagulant dose is calculated using Equation 3-7 with a maximum limit specified for how much coagulant a works can dose.

$$M = \frac{(1 + bC_{eq})(TOC_0 - TOC_{non} - C_{eq})}{abC_{eq}}$$ Equation 3-7

Where: C_{eq} = equilibrium concentration of adsorbate in solution (mg/l); TOC_{target} = target TOC (mg/l); TOC_{non} = non-sorbable TOC (mg/l); M = dose of coagulant (mMol Me^{3+}) b = Langmuir adsorption equilibrium parameter (l/mg adsorbate); TOC_0 = initial TOC (mg/l); a = maximum adsorbent-phase concentration of adsorbate at saturation (mg/l adsorbate/mMol/l adsorbent).

In order to accurately predict the extent of organic matter removal using the Edwards (1997) model, it is necessary to predict the pH of the coagulated water. The coagulated water will have a lower pH than the source water due to the acidic nature of ferric and alum coagulants. The pH at which this coagulation occurs is fed back from the carbonate model (section 3.3.3). Applying this feedback mechanism resulted in a marginal increase in model run times (<5%) compared to when a coagulation pH was set at a representative value of 6.1.

3.3.3 Carbonate system

The model used to represent the influence of chemical addition on pH is based on the carbonate chemistry described in Stumm and Morgan (1970) and Snoeyink and Jenkins (1980a, Snoeyink and Jenkins, 1980b) and is similar to the method described in Najm (2001) which was independently developed. The coagulation process is treated as a closed system and ionic strength effects are assumed to be negligible due to the low concentrations of chemicals found

in water treatment. Instabilities in this carbonate model are limited through the application of the Newton-Raphson method to iteratively calculate representative pH values. Full details of the carbonate chemistry model are provided in Appendix B. Daly et al. (2007) compared the carbonate chemistry approach to an empirical method which was calibrated to evaluate the buffering capacity of a source. The carbonate chemistry approach was found to be more accurate when tested using jar tests and pH titrations and of a similar accuracy for pilot plant tests.

3.4 Hopper bottomed clarification (HBC)

3.4.1 Dynamic HBC model

Floc blanket clarifiers are modelled using a similar method to that presented in Head et al. (1997). Head et al's model was found to give good predictions of plant performance based on it predicting blanket concentration to ±5% and clarified turbidity to ±0.5 NTU. The predicted clarified turbidity identified trends in turbidity (over days) but not shorter term fluctuations (over hours), this was partly attributed by Head et al. to the nature of on line measurements. HBCs are represented by a series of homogeneous CSTR sections. Within a CSTR, solids either pass through or are absorbed into a sludge blanket. The model is based on the assumption that the flocs are bimodal, with smaller initial flocs and larger flocs within the blanket. All initial flocs are also assumed to be equally well removed by the sludge blanket. Figure 3-2 illustrates how the different aspects of the Head et al. (1997) HBC model interact. It should be noted that there are more links between the mechanisms than are shown in the diagram and that only the key relationships have been shown.

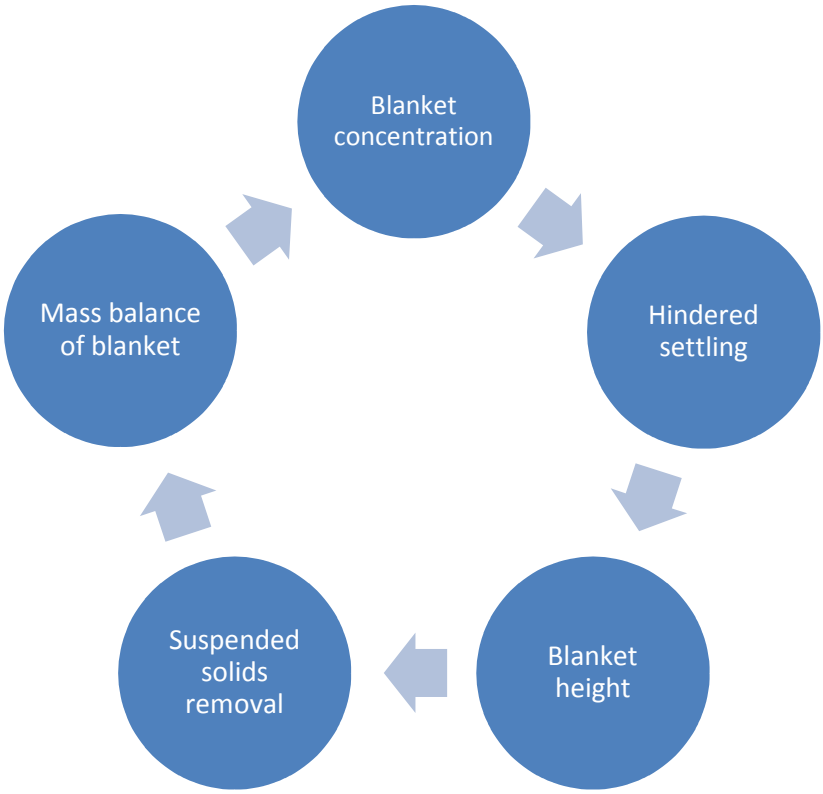

Figure 3-2 Illustration of key links between mechanisms within HBC clarifier model

A full description of the HBC model's mechanisms can be found in Head et al. (1997) and the OTTER manual (WRc, 2002); only deviations for the model's standard application are noted here. The calibration parameters of the Barnea and Mizrahi (1973) equation can be identified for a specific works, but in this model, values from Head et al. (1997) were used to see how effectively modelling of a works could be achieved using only existing data collected from a WTW. The parameters used from Head et al (1997) are works specific and therefore if not representative of other works could be a substantial source of error.

The settlement of flocs is also not modelled in this work. Removal due to settlement is not included due to the relative dominance of blanket removal (approximately 1% of solids removed were found to be due to settlement under conditions observed). Removal due to settlement is only significant at low flow rates, and in these conditions, removal due to blanket

formation would be effective. For this reason, modelling settlement would not significantly influence the likelihood of unacceptable HBC clarified turbidity being predicted, and so would not be of use in assessing the reliability of the process.

3.4.2 Static HBC model

Using the solids removal equation from the dynamic HBC model and making the assumptions that the blanket concentration and height remain consistent and the flow through the clarifier is plug flow, then the removal of solids can be approximated by Equation 3-8. Although turbulence at the inlet to the process is substantial, the degree of mixing within the majority of the clarifier is minimal and so plug flow is an appropriate approximation. The clarification efficiency parameter is found by optimising its value to reduce the summative error squared between predicted and actual clarified turbidity.

$$SS = SS_0 \times exp^{-kt} \qquad \text{Equation 3-8}$$

Where: SS = clarified suspended solids (mg/l); SS_0 = flocculated suspended solids (mg/l); t = contact time (h) and k = clarification efficiency parameter (h^{-1}).

3.5 Dissolved air flotation (DAF) clarification

The dynamic and static models described in this section are based on the static models developed by Edzwald (2006) and by their application for dynamic systems described in the OTTER WTW modelling program (WRc, 2002).

3.5.1 Dynamic DAF model

The attachment efficiency of bubbles onto suspended solids by dissolved air flotation is based on Equation 3-9 and Equation 3-10 (Edzwald, 2006). These are based on the plug flow assumption of flow through the contact zone which was found to be approximately true (Haarhoff and Edzwald, 2004, reported in Edzwald, 2006). In order to make the Edzwald model dynamic, complete mixing is applied through the use of a representative number of CSTRs, and the entire tank is modelled as a contact zone. This is represented by Equation 3-11 as used in the OTTER program (WRc, 2002). In this model no flocculation occurs within the DAF tank and the removal performance is unaffected by the accumulation of floating sludge.

$$\text{Efficiency} = 1 - exp^{-k*t} \qquad \text{Equation 3-9}$$

$$k = \frac{-\frac{3}{2}\alpha\eta_T\phi_b\upsilon_b}{d_b} \qquad \text{Equation 3-10}$$

$$\frac{dSS}{dt} = \frac{QSS_0}{V} - \left(\frac{Q}{V} + k\right)SS \qquad \text{Equation 3-11}$$

Where: SS = clarified suspended solids (mg/l), SS_0 = raw water suspended solids (mg/l), t = time (h), Q = flowrate (m^3/h), V = volume of flotation tank (m^3), k = floc flotation parameter (h^{-1}), α = attachment coefficient (dimensionless), η_T = individual bubble collision efficiency (dimensionless), ϕ_b = bubble volume concentration (dimensionless), v_b = bubble rise rate (m/h), d_b = bubble diameter (m).

A full description of the HBC model's mechanisms can be found in Edzwald (2006) and the OTTER manual (WRc, 2002). Only a description of the calculation of the individual bubble collision efficiency (η_T) is provided here, as it required further specification than was provided in Edzwald (2006) and WRc (2002).

3.5.1.1 *Individual bubble collision efficiency (η_T)*

Three factors contribute to the frequency of collisions between bubbles and flocs: Brownian diffusion, interception of the flocs by the bubbles and settling of the flocs onto the bubbles. At floc sizes larger than a micron, interception dominates and so only this mechanism, determined by bubble and floc size, is modelled. Equation 3-12 is used to calculate η_T as recommended by Edzwald (2006).

$$\eta_T = \left(\frac{d_{fl}}{d_b} + 1\right)^2 - \frac{3}{2}\left(\frac{d_{fl}}{d_b} + 1\right) + \frac{1}{2}\left(\frac{d_{fl}}{d_b} + 1\right)^{-1} \qquad \text{Equation 3-12}$$

Where: η_T = individual bubble collision efficiency (dimensionless), d_{fl} = diameter of floc (m), d_b = diameter of bubble (m).

Edzwald et al. (1992) found that DAF clarification using mean floc diameters of 30 microns (on a volume basis) was effective, producing clarified water with turbidity below 0.5 NTU. Adlan (1998), citing Klute et al. (1995) and Bunker et al (1995), reported effective sizes to be between 30 – 45 microns. Effective flocculation is assumed to occur with floc diameters of 30 µm. Hence, that value has been adopted in this thesis.

The bubble size formed in a DAF tank depends on the saturator pressure, the method of injection and the recycle rate (Edzwald, 2006). At some WTWs, the saturator pressure or recycle rate is automatically adjusted in order to stabilise the bubble volume concentration. This adjustment will alter the bubble size. However as the effect of the saturator pressure and recycle rate adjustment on bubble size is unknown, a consistent size is used here. The diameter of the bubbles are assumed to be 40 microns as given as a typical value in Edzwald et al. (1992). This fits below an upper estimate of 64 microns reported by Sebau (1997) as reported by Adlan (1998) for bubbles produced in the laboratory.

3.5.2 Static DAF Model

A static model is produced based on Equation 3-9 and Equation 3-10. In fitting with Edzwald's theory, attachment is assumed to occur only in the initial contact zone. All of the other parameters are defined in the same way as the dynamic model.

3.6 Rapid gravity filtration (RGF)

The dynamic and static RGF models described in this section are based on the Bohart and Adams Equation (1920). The filtration head loss in the dynamic model is described using the solids accumulation relationship identified by Adin and Rebhun (1977).

3.6.1 Dynamic RGF model

The removal of solids by filtration is modelled using the Bohart & Adams model (1920) as shown in Equation 3-13 (the derivation of this equation from first principles can be found in Appendix C). The Bohart & Adams model (1920) was originally developed for the adsorption of chlorine and is based on the following assumptions:

- The capacity of a media to remove substances reduces in proportion to the media capacity and the initial concentration of the substance being removed; and
- The rate of media capacity reduction is equal to the rate of substance removal.

These assumptions are in agreement with the experimental findings for filters that the rate of particle removal is dependent on the concentration of particles similar to a first rate equation (Iwasaki, 1937 referenced in Crittenden et al, 2005).

The original work of Bohart & Adams defined the velocity in Equation 3-13 as the rate that the adsorbing material became saturated. For removal of solids by filters this velocity has been

redefined as the superficial velocity of the water through the media in Saatci and Oulman (1980), Saatci and Halilsoy (1987), Saatci (1989, 1990) and WRc (2002). The filter capacity is defined as the accumulated suspended solids concentration at which the rate of solids attachment and detachment is assumed to be equivalent and the media ceases to overall reduce the overall suspended solids concentration.

$$\frac{SS}{SS_0} = \frac{1}{e^{\mathrm{xka_0/v - tkSS_0}} + 1} \qquad \text{Equation 3-13}$$

Where: SS_0 = flocculated SS (mg/l); SS = clarified SS (mg/l); x = depth of filter media (m); k = attachment coefficient (h-1); a_0 = filter capacity (mg/l); v = superficial velocity of water through filter media (m/h) and t = time since last backwash (h).

The Bohart & Adams model is static in nature and so assumes consistent operating conditions. In order to account for dynamic conditions, the input suspended solids concentration and the superficial velocity are taken as running means over a filtration run. This acts to dampen the response of the output turbidity to fluctuating water quality. Another dynamic aspect which was added to the model, is that backwashes can be triggered by head loss or filtered turbidity exceeding maximum limits.

3.6.1.1 *Calibrating parameters for Bohart and Adams (1920) model*

The calibration of this filter model can be completed using representative pilot filters of differing length as described in Saatci and Oulman (1980). Saatci and Oulman (1980) also describe an alternative method for calibrating from operational initial breakthrough data, when pilot filter data are unavailable. Where insufficient breakthrough is observed from the operational data, it may be necessary to use a conservative estimate of the filter capacity (a_0).

Based on the values reported in Table 3-2, a value of approximately 1000 (mg/l) is appropriate as for the majority of operational conditions it should result in a conservative estimate of the time until filter breakthrough.

Table 3-2 Comparison of filter capacities estimated in previous research

Source	**Conditions**	**Filter capacity (mg/l)**
Saatci and Oulman (1980) using data from Cleasby's doctoral dissertation, run 23, 1960.	Filtration of iron by sand filter 76 cm sand, effective diameter 1.05 mm 14.4 m/h Initial iron concentration 7-9 mg/l	8140
Adin and Rebhun (1977)	Filtration of 20 mg/l kaolinite suspension 100 cm sand ,effective diameter 0.7 – 1.4 mm 5 – 25 m/h Theoretical capacities Maximum observed capacities	 9700 – 81540 2800 - 35500
OTTER WTW program manual (WRc, 2002)	Initial concentration of solids 4 mg/l 60 cm filter 10.5 m/h 10% non-filterable solids	950

3.6.1.2 *Filter ripening model*

As discussed in section 2.1.2.5.2, after backwashing, the effectiveness of filters to remove suspended solids is temporarily reduced until the filter has gone through a ripening process. It is necessary to model this process in order to account for the temporary reduction in water quality that backwashing causes.

Filter ripening is modelled by adjusting the attachment coefficient (k) using an empirical relationship (Equation 3-14) which WRc (2002) found gave a good fit to operational data.

$$k_t = k\left(1 - \alpha e^{-t/t_r}\right)$$ Equation 3-14

Where: k_t = attachment coefficient at time t; k = attachment coefficient; α = initial attachment factor (dimensionless) t_r = ripening period (h); t = time since last backwash (h).

Using turbidity and discharge eSCADA data from January 2012 the dynamic filter model is run with varying values of α and t_r and the predicted and observed filtered turbidity against time since last assumed backwash is compared using lines of best fit produced using the two-term exponential fitting tool within MATLAB. As can be seen in Table 3-3, the maximum value of initial attachment factor (assuming an initial attachment coefficient of zero) and a ripening time of one hour is found to result in the smallest RMSE.

Table 3-3 RMSE observed for combinations of α and t_r

Ripening period (t_r)	**Initial attachment factor (α)**		
	0.1	**0.5**	**1.0**
0.1	0.0442	0.0425	0.0403
1.0	0.0427	0.0332	0.0243
10	0.0412	0.0372	0.0970

Using a filter capacity of 1000 mg/l and an attachment coefficient at 0.005 hr^{-1}, predicted filtered turbidity for the initial six hours after assumed backwashes is compared to that observed and found to have a RMSE of 0.025 NTU and a similar profile and distribution of results (see Figure 3-3).

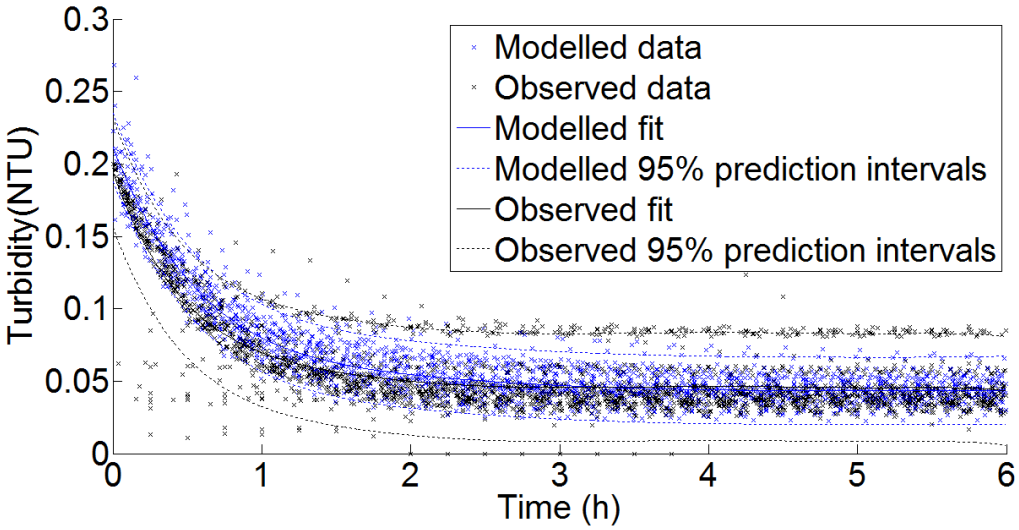

Figure 3-3 Modelled vs. observed filter ripening

3.6.1.3 *Clean bed head loss modelling*

The flow regime for rapid gravity filters is typically in the region of Darcy flow (Re < 1) and Forchheimer flow (1 < Re < 100) (Crittenden et al., 2005). Head loss estimated on the assumption of Darcy flow (using the Kozeny-Carman equation) or Forchheimer flow (using the Ergun equation) gradually deviates for Reynolds numbers greater than one (Crittenden et al., 2005). Little difference (less than 1 cm) is observed between estimates made of clean bed head loss for typical operating conditions using the two methods. Due to its dependence on fewer empirical parameters the Kozeny-Carman method is used (Equation 3-15).

$$h_L = \frac{\kappa_k \mu \left[\frac{6(1-\varepsilon)}{\psi d}\right]^2 vL}{\rho_w g \varepsilon^3}$$ Equation 3-15

Where: h_L = clean filter head loss (m); K_k = Kozeny coefficient (dimensionless); μ = water dynamic viscosity (Ns/m^2); ε = voidage (dimensionless); ψ= sphericity of filtration media (dimensionless); d = media diameter (m); v = filtration rate (m/h); L = filter bed depth (m) and ρ_w = water density (kg/m^3).

The filter length, media effective diameter, porosity and sphericity need to be specified, however, if porosity or sphericity data are not available then the values used in Table 3-4 can be applied as general values. As supplied media is made up of grains of varying diameter, it is necessary to take this into account when defining the size of media required. A commonly used method for characterising the media size distribution is by effective size (Crittenden et al., 2005). The effective size is defined as being the diameter of media for which 10%, by mass, of the media is smaller.

Table 3-4 General values of granular bed porosity and sphericity

Media	**Granular bed porosity**	**Sphericity**
Anthracite	0.5 Typical value to 1 significant figure for use with effective sized media (Crittenden et al., 2005)	0.6 Typical value to 1 significant figure for UK anthracite (Dharmarajah and Cleasby, 1986)*
Sand	0.4 Midpoint of the range to 1 significant figure for use with effective sized media (Crittenden et al., 2005)	0.8 Typical value to 1 significant figure for UK sand of sizes between 0.5 mm to 2 mm (Dharmarajah and Cleasby, 1986)*

*These sphericities were calculated by Cleasby & Fan using the Ergun equation, which correlates pressure drop in a fixed bed with particle diameter, voidage, Reynolds number and sphericity. These values were modified by Dharmarajah and Cleasby to consider loose packaging of particles instead of tightly packed arrangements as were considered by Cleasby & Fan.

3.6.1.4 *Head loss due to solids accumulation*

Adin & Rebhun (1977) provided experimental data for head loss due to solids accumulation from which they derived Equation 3-16 (see Appendix D for derivation).

$$H = \frac{H_0}{\left(1 - \beta\sqrt{\sigma}\right)^3}$$ Equation 3-16

Where: H = head loss (m); H_0 = clean bed head loss (m); σ = accumulated solids concentration (mg/l) and β = rate of head loss coefficient (√l/√mg).

The rate of head loss coefficient can be found empirically from plotting a graph of $[(H/H_0)^{1/3}-1]$ against √ σ and taking the gradient as β. The accumulated solids in the filter can be calculated based on the mass of suspended solids removed from treated water. If this method does not result in a clear linear relationship, then a best fit value of β can be identified.

3.6.2 Static RGF model

The Bohart & Adams equation, described in Equation 3-13, is used to statically model filter solids removal. The dynamic components which are not present in the static model are the use of running means of influent suspended solids concentration and superficial velocity, the calculation of predicted head loss and the use of non-scheduled backwashes.

3.7 Granular activated carbon (GAC) adsorption

The GAC model used here, predicts the removal of TOC, as a surrogate for natural organic matter. Although GAC is usually applied to target a specific organic compounds such as pesticides, only TOC removal is modelled in order to keep the number of water quality parameters investigated manageable and also because TOC was identified as a good indicator of adsorption performance by Lykins et al. (1988) as it is: easy to analyse, includes all organic components, and it correlated well with THM formation potentials.

At Trimpley WTW, TOC is recorded monthly in the reservoir water and final water, but not before and after GAC adsorption. This frequency of TOC measurement is typical of other WTWs operated by Severn Trent Water. As TOC removal will be influenced by processes other than GAC adsorption, in particular coagulation and filtration, it will not be possible to directly measure the influence of the GAC on TOC concentration. Collection of pre and post adsorption TOC concentrations are not measured as the potential for modelling WTWs using only historically collected data is examined. Due to the lack of appropriate data, TOC removal due to GAC adsorption and filtration is modelled as a fractional reduction as described in the next section.

3.7.1 Combined TOC removal due to RGF and GAC

It has been found that the TOC removal at WTWs predominantly occurs at the clarification stage. Brown et al. (2011b) reported TOC removal data for six large WTWs, in the West Midlands of the UK, for the summers of 2006 and 2007, with varying source waters and treatment processes. These data are reported in Table 3-5 and Figure 3-4.

Table 3-5 Comparison of removal due to different treatment processes, adapted from Brown et al. (2011b)

WTW processes	Removal due to process (%)								
	1	2	3	4	5	6	Mean	Min	Max
Coagulation, Flocculation & Clarification	25	30	16	40	24	21	26.0	16.0	40.0
Filtration	8	2	5	2	4	7	4.7	2.0	8.0
GAC adsorption	13	8	10	15	18	16	13.3	8.0	18.0
Disinfection and final water treatments	3	5	2	1	6	-4	2.2	-4.0	6.0

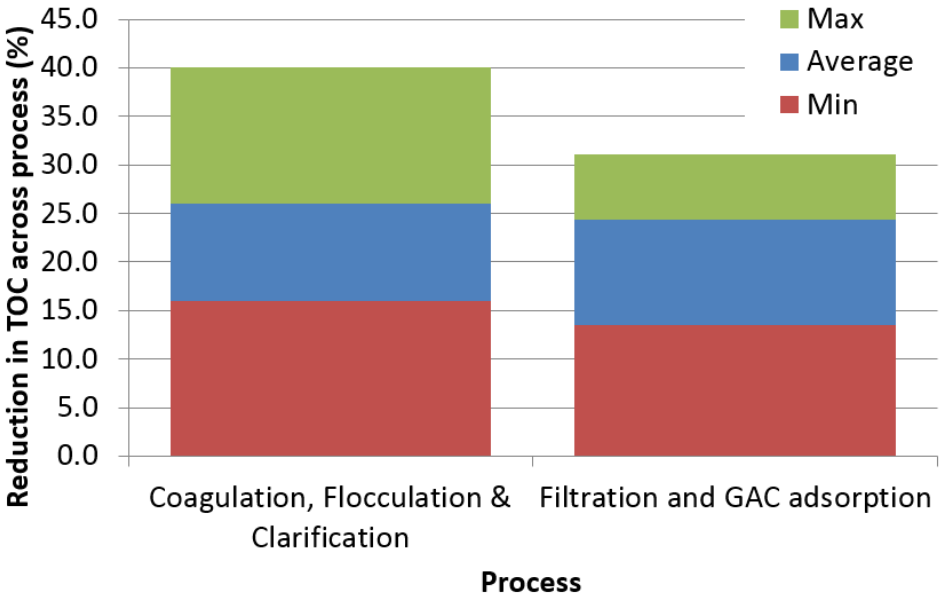

Figure 3-4 Comparison of removal across clarification vs. removal across filtration and GAC adsorption, adapted from Brown et al. (2011b)

It can be seen in Table 3-5 that the largest amount of removal (~25%) occurred across the clarification process, which is in agreement with other studies of Severn Trent WTWs (Hua et al., 1999, Courtis, 2003). Considerable TOC removal also occurred across the filtration (~5%) and GAC adsorption processes (~20%). From Brown et al.'s data (2011b) a typical reduction from filtration and GAC adsorption is of the magnitude of 25% although for one site examined the reduction was more in the region of 15%. A reduction of 25% of clarified TOC due to

filtration and GAC adsorption can be assumed as typical. The inaccuracy of this assumption will have to be considered in any analysis made using it.

3.7.2 GAC suspended solids removal

Suspended solids (SS) removal by GAC is not be modelled, as although it has been shown to be at least as affective as conventional filtration media at removing SS from water (Love and Symons, 1978) this is not the process's principal purpose at works where it is conventionally used as a tertiary treatment. Increased SS removal by the GAC process will lead to an increased need to backwash the activated carbon, which disrupts the mass transfer zone and causes premature breakthrough (Crittenden et al., 2005). This premature breakthrough along with the increased activated carbon loss, due to backwashing will result in more frequent reactivations of the carbon. Since regeneration contributes a "major part" of the total cost of the GAC system (Clements and Haarhoff, 2004) and production costs rise exponentially which decreased periods between regeneration (Gumerman et al., 1979a), all SS removal modelling is accounted for by clarification and filtration here.

3.8 Chlorination

3.8.1 Initial chlorine concentration

Due to the action of control systems which respond to changes in water quality, the concentration of chlorine dosed at WTWs fluctuates. To assess whether the chlorine dose can be modelled as a consistent value over continuous periods, a case study is completed using 2011 eSCADA data for Trimpley WTW (Severn Trent, 2012a). At Trimpley the chlorine dosing point is approximately ten metres upstream from the entrance of the contact tank and so some chlorine decay and mixing occurs before the water reaches the contact tank. Both the dynamic and static models, described in this section, are run using contact tank inlet chlorine concentrations from either quarter hourly eSCADA data or from monthly mean values calculated from the same eSCADA data. The predicted residual chlorine concentrations using both models and methods of estimating the initial chlorine concentration are shown in Figure 3-5 and Figure 3-6 along with the observed residual for the same period.

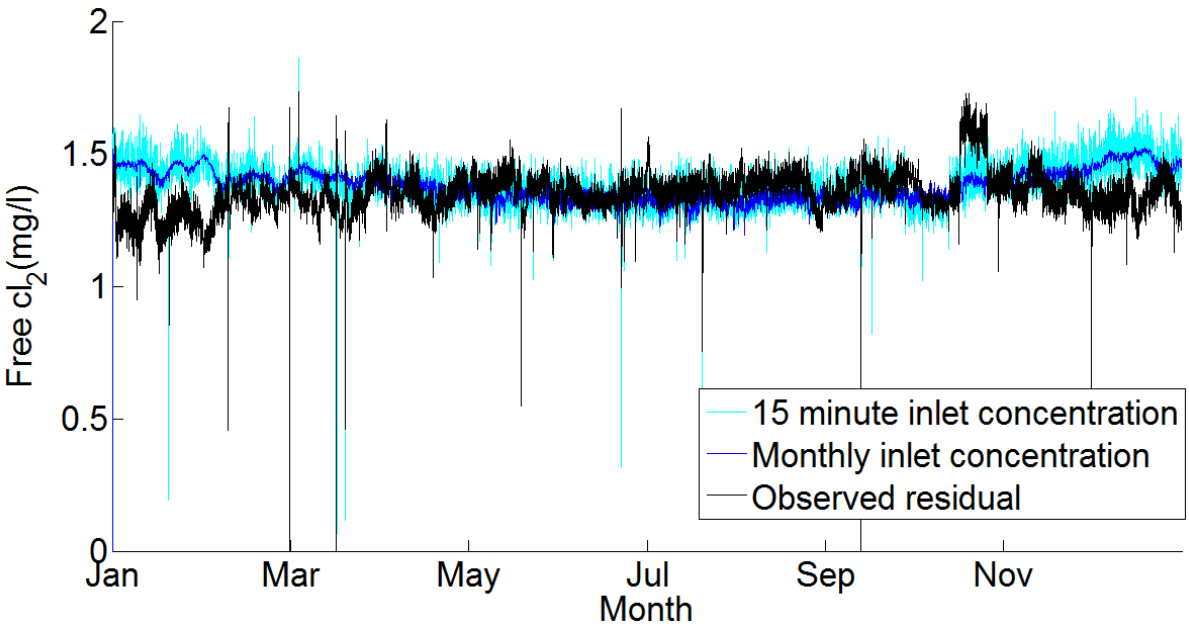

Figure 3-5 Residual free chlorine concentrations from static model

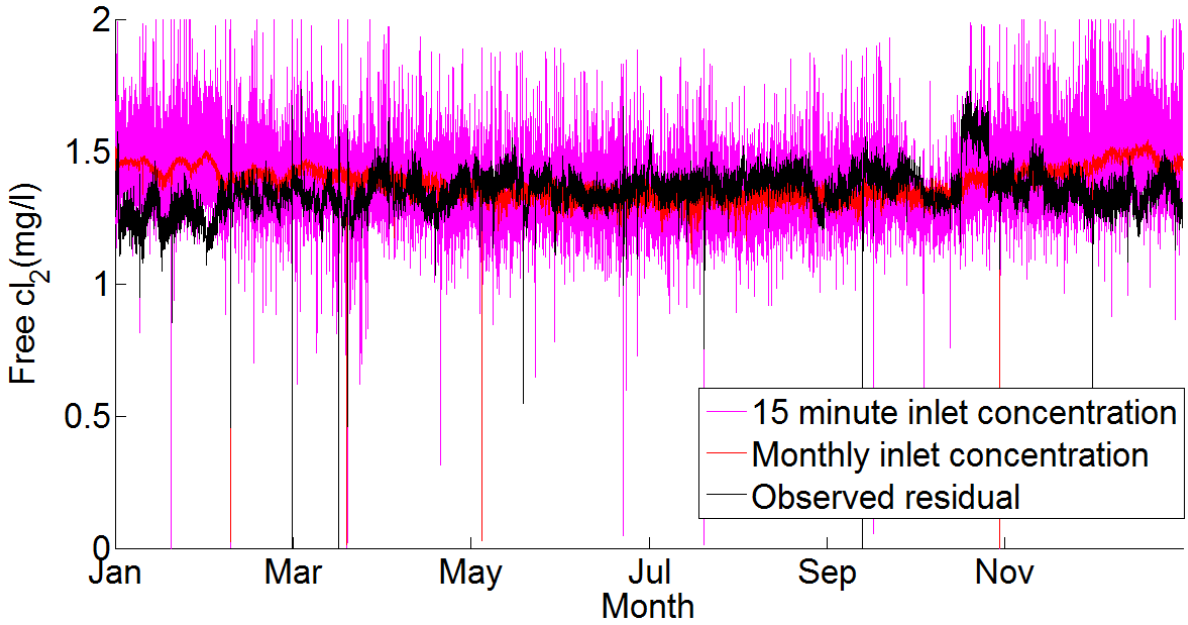

Figure 3-6 Residual free chlorine concentrations from dynamic model

Figure 3-5 and Figure 3-6 show that considering the chlorine dose to be consistent over monthly periods does not reduce the accuracy of the model substantially and also makes the variation in residual free chlorine concentration more representative of that observed. The static model in particular benefits from this approximation. Figure 3-5 and Figure 3-6 also suggest that the chlorine consumption is over-predicted for colder winter periods.

3.8.2 Contact tank hydraulic efficiency

Flow within contact tanks resembles plug flow with a degree of dispersion that can be accounted for by different modelling techniques. The flow regime of the contact tank is defined by the tanks hydraulic efficiency (t_{10}:t_θ). The hydraulic efficiency of a tank is defined as the ratio of the time taken for 10% of the concentration of a tracer chemical to be detected at the outlet of the tank (t_{10}) to the theoretical contact time if perfect plug flow conditions were present (t_θ). The observed time for 10% of tracer material to pass through a process (t_{10}) was identified by

Teixeira and Siqueira (2008) as being the only hydraulic efficiency indicator examined that gave a statistically robust and fit for purpose short circuiting parameter.

3.8.3 Chlorine decay

In this work a first order decay equation is used, as only decay within the contact tank is considered. A first order equation is used as they are simple and have been applied successfully in previous studies (Powell, 1998, Gang et al., 2002). The chlorine decay model used is based on Brown (2009). In Brown's work, chlorine decay at six WTWs in the West Midlands of the UK was investigated, via co-ordinated sampling campaigns and laboratory tests.

Brown (2009) found that modelling the decay within the contact tank purely as first order decay resulted in under-prediction of the chlorine dose. The implications of this were that when actual initial chlorine doses were used with the relationships identified, overestimates of the free chlorine residuals from contact tanks were predicted. The influence of this undesirable characteristic was reduced by Brown, by the addition of an initial chlorine consumption value, to represent the decay that occurred within the first five minutes of chlorine addition (approximately 20% of total decay observed).

The models and parameters identified in Brown (2009) for modelling chlorine decay are used as the basis for the models described here as the chlorine doses are similar to those used at typical UK operational sites and the model parameters are reported for a range of different source water characteristics and operating conditions. A general purpose model based on the mean of parameters reported by Brown are used here, as although the determination of decay parameters for individual sites is useful, it is expensive and time consuming, making it impractical as a routine operation. The instantaneous demand in this work is modelled using

Equation 3-17. The bulk decay of chlorine in the contact tank, after five minutes of exposure, is modelled using a decay rate parameter calculated using Equation 3-18 in the first order decay Equation 3-19. Representative decay rate parameters are identified from Table 3-6 based on what range of contact times are observed at WTWs. This theory is applied to the dynamic model using CSTRs and directly using Equation 3-19 in the static model.

$$Cl_{5\,min} = Cl_0 \times [A + (a \times Cl_0) + (b \times T) + (c \times TOC) + (d \times Br)] \qquad \text{Equation 3-17}$$

$$K_b = A + (a \times Cl_0) + (b \times T) + (c \times TOC) + (d \times Br) \qquad \text{Equation 3-18}$$

$$Cl = Cl_{5\,min} e^{-K_b t} \qquad \text{Equation 3-19}$$

Where: Cl = residual free chlorine concentration (mg/l); $Cl_{5\,min}$ = free chlorine dose after five minutes (mg/l); Cl_0 = chlorine dose (mg/l); T = temperature (ºC); TOC = total organic carbon (mg/l); Br = Bromide (µg/l); K_b = decay rate parameter (hr^{-1}) and t = contact time (hr).

Table 3-6 Mean parameters for initial five minute decay and bulk decay parameters, adapted from Brown (2009)

Relationship	**A**	**a**	**b**	**c**	**d**
Initial 5 mins factor	0.940	0.042	-0.0037	-0.0470	-0.00043
K_b ~ 5-30 mins	0.336	-0.302	0.0111	0.0964	0.00243
K_b ~ 5-60 mins	0.221	-0.217	0.0086	0.0634	0.00180
K_b ~ 5-90 mins	0.162	-0.168	0.0071	0.0548	0.00127
K_b ~ 5-120 mins	0.104	-0.134	0.0064	0.0504	0.00083

3.8.3.1 *Dynamic modelling of decay*

A representative number of CSTRs can be identified by using an estimate of contact tank hydraulic efficiency (t_{10}:t_θ) (see section 3.8.2), using Equation 3-20 (Michalewicz, 1996). Equation 3-20 is derived in Appendix E. This method was found to be effective by Teefy (1996).

$$F = 1 - e^{-n\frac{t}{\bar{t}}}\left[1 + n\frac{t}{\bar{t}} + \cdots + \left(n\frac{t}{\bar{t}}\right)^{n-1}\frac{1}{(n-1)!}\right] \qquad \text{Equation 3-20}$$

Where: F = fraction of tracer that has passed through after time t; n = representative number of CSTRs; t = time since beginning of tracer test (min) and $\bar{t}$ = mean residence time (min).

Table 3-7 shows representative number of CSTRs for different t_{10}:t_θ values. These values are calculated using Equation 3-20 and Excel's solver function.

Table 3-7 Representative number of CSTRs for different t_{10}:t_θ values

CSTRs	**$t/\bar{t}$ nearest**	**$t/\bar{t}$ range**		
1	0.105	0.000	to	0.186
2	0.266	0.186	to	0.317
3	0.367	0.317	to	0.402
4	0.436	0.402	to	0.461
5	0.487	0.461	to	0.506
6	0.525	0.506	to	0.541
7	0.556	0.541	to	0.569
8	0.582	0.569	to	0.593
9	0.604	0.593	to	0.613
10	0.622	0.613	to	0.630
11	0.638	0.630	to	0.645
12	0.652	0.645	to	0.659
13	0.665	0.659	to	0.671
14	0.676	0.671	to	0.682
15	0.687	0.682	to	0.691
16	0.696	0.691	to	0.700
17	0.704	0.700	to	0.708
18	0.712	0.708	to	0.716
19	0.720	0.716	to	0.723
20	0.726	0.723	to	0.729
21	0.733	0.729	to	0.735
22	0.738	0.735	to	0.741
23	0.744	0.741	to	0.746
24	0.749	0.746	to	0.751
25	0.754	0.751	to	1.000

In order that representative chlorine consumption is calculated for varying chlorine doses, it is necessary to have a set of parallel CSTRs, with no decay modelled, so that residual chlorine concentration can be compared. Where the inlet chlorine is modelled as a consistent concentration this additional set of CSTRs with no decay modelled, is unnecessary.

3.8.4 THM formation

The likelihood of harmful concentrations of disinfection by-products being formed is addressed by using trihalomethanes (THMs) as a reference pollutant.

The kinetics of THM formation are complex and no analytical-mechanistic models exist. The modelling approach taken here is based on the methodology that links the formation of THMs to free chlorine consumption (Equation 3-21) following Clark and Sivaganesan (1998), Hua (2000) and Brown et al. (2010). The practical application of this method at operational sites is dependent on accurate measurement of chlorine consumption.

$$THM = K_{TC}(Cl_0 - Cl) \qquad \text{Equation 3-21}$$

Where: K_{TC} = coefficient of proportionality between TTHM and chlorine consumption (µg/l per mg/l); Cl_0 = chlorine dose (mg/l); Cl = residual chlorine (mg/l).

K_{TC} values reported by Hua (2000) and Brown (2009), for data from three and six WTWs in the West Midlands, were 45 and 34 µg/l per mg/l free chlorine consumed respectively. A conservative value of 45 µg/l per mg/l is used here to reduce the likelihood that THM production is underestimated. The TOC value used in Equation 3-17 and Equation 3-18 represents pre-chlorination concentration taking into account TOC removal due to clarification, filtration and

GAC adsorption. The bromide concentration is taken as the raw water concentration as it is not removed effectively by conventional treatments pre-chlorination (Brown, 2009).

3.8.5 Chlorination alkalinity modelling

The influence of coagulants on alkalinity and pH is discussed in section 3.3.3. It is shown that the addition of coagulants reduces the alkalinity of the water. The addition of free chlorine at the super chlorination stage and some dechlorinating substances also reduces the alkalinity of the water further. In order that the final water entering the distribution network has enough buffering potential to reduce the risk of corrosion, slaked lime is often added to increase the alkalinity. A representative dose of slaked lime that results in the alkalinity of the final water returning to its raw water value is applied in this work.

Whether chemicals increase or decrease the alkalinity is dependent on if the chemicals added are hydrogen donators or acceptors (donators decrease alkalinity). The influence of the individual chemicals on the alkalinity is given in greater detail in Appendix B.

3.9 Summary

This chapter described the models that were produced for processes typically applied to lowland surface water sources in the UK. The models were developed using case study data from Trimpley WTW from July 2011 and January 2012. Models were produced for coagulation, DAF and HBC clarification, RGF, GAC and super chlorination. The models described in this chapter are used to model Trimpley WTW in greater detail (see chapter four) and to perform theoretical optimisations of Trimpley WTW (see chapter five).

Static and dynamic models were produced for each treatment process as modules using MATLAB/Simulink. This was done so that the accuracy of these types of models could be compared. These modules could then be used in parallel or series to model different WTW designs.

The removal of TOC due to the addition of ferric or aluminium salt coagulants was represented using the model developed by Edwards (1997) along with a carbonate model similar to the method described in Najm (2001). A coagulant dosing algorithm was also developed. This algorithm predicted the coagulant concentration required to limit clarified TOC below a designated concentration.

HBC clarification was modelled dynamically, based on the model reported in Head et al. (1997). If the floc blanket within the dynamic model is assumed to remain consistent and the flow though the blanket assumed to be plug flow then the model simplifies to an exponential decay model. This simplified model was used to represent the process statically.

The static DAF model was based on the model reported in Edzwald (2006) but with separation assumed to be perfect. The dynamic model, which was influenced by the model presented in

the OTTER program (WRc, 2002), defined the entire tank as the contact zone and modelled the degree of mixing through the use of multiple CSTRs.

Rapid gravity filtration was modelled using the Bohart & Adams equation (1920), with the dynamic model being enhanced through the addition of running means for clarified turbidity and superficial filtration velocity and backwashes triggered by elevated head loss or filtered turbidity.

Based on a study of TOC removal efficiency of other WTWs in the region (Brown et al., 2011b), a representative proportional reduction in TOC concentration due to filtration and GAC adsorption was applied. Solids removal by GAC was not modelled as this is not the processes primary purpose and solids removal can reduce the efficiency of the overall adsorption process.

The degree of disinfection achieved was specified as the CT value. In order to calculate this, the residual free chlorine concentration and retention time (as t_{10}) had to be determined. Bulk decay rate parameters were developed using a range of relationships reported in Brown (2009) for different ranges of detention time for WTWs in the West Midlands. A relationship also from Brown (2009) for the initial five minute decay was also developed.

Through analysis of the case study chlorination data, some additional mechanisms that could require modelling were identified. The contact tank inlet concentration was seen to vary substantially in the case study data. It was found that modelling the inlet concentration as a representative, consistent value did not reduce the accuracy of the predicted residual concentration greatly (see Figure 3-5 and Figure 3-6). The draw-off from partially treated water for backwashing resulted in the contact tank discharge rate reducing by approximately 10%. This mechanism will need to be considered in future contact tank models.

4 CASE STUDY

The water treatment works (WTW) process models are used to simulate an operational site, in order to test their accuracy, when observed time series and Monte-Carlo operating conditions are applied. This chapter describes the site modelled, the methods that used to adapt the general models (see chapter three) to the specific site, the data used to calibrate and verify the model and the verification results.

4.1 Overview

Trimpley WTW is located in rural Worcestershire, England. The water treated at Trimpley is abstracted from the River Severn on a lowland reach before being impounded in a reservoir. Water abstracted from the reservoir can either be treated on site or transferred to supplement the supply of Frankley WTW, a larger works in Birmingham. Trimpley WTW has a maximum treatment capacity of 2500 m^3/h (60 Ml/d) (Severn Trent, 2011).

4.1.1 Trimpley WTW Description

Figure 4-1 shows a schematic of Trimpley WTW. This figure illustrates what treatment is carried out at the site. The site had an observed abstraction rate of approximately 1570 m^3/h (38 Ml/d) and a discharge of 1350 m^3/h (32 Ml/d) in 2011.

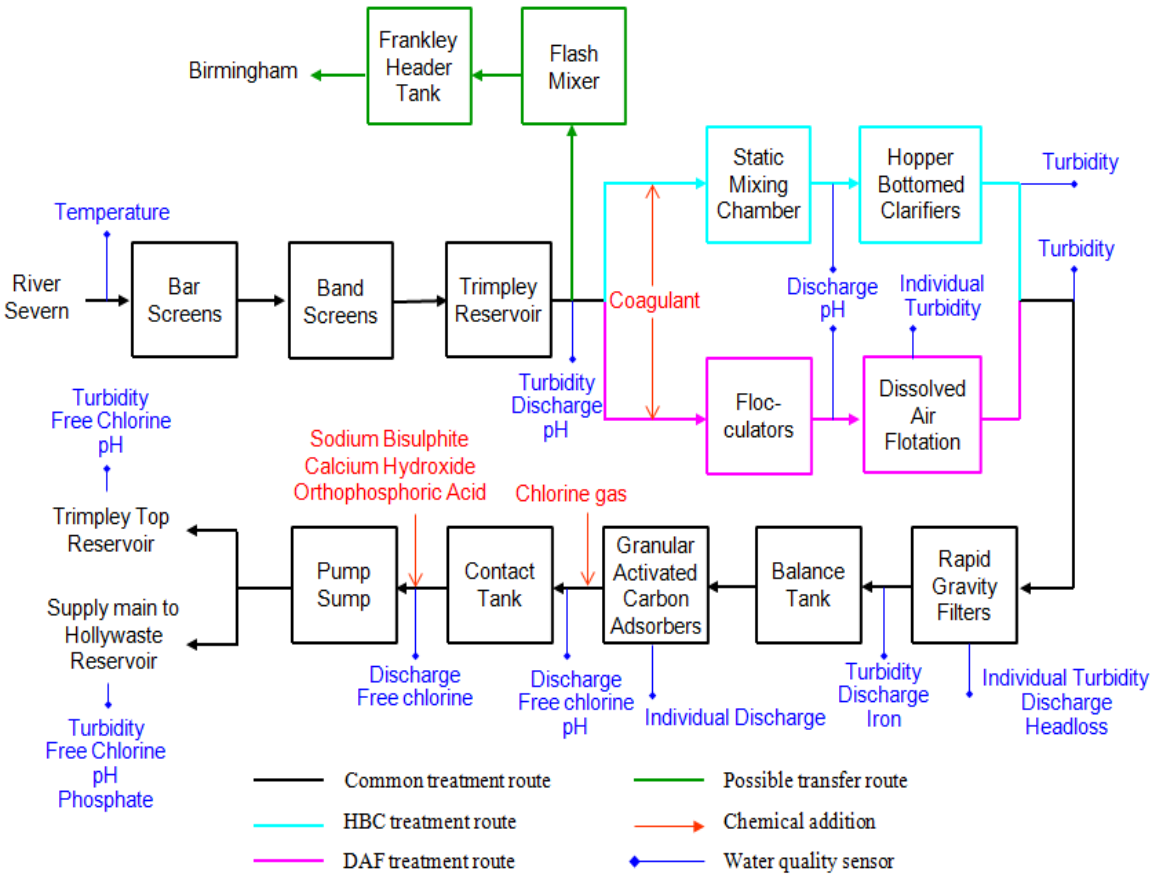

Figure 4-1 Schematic of Trimpley WTW, adapted from Severn Trent (2012b)

Source water is abstracted from the River Severn through bar screens and band screens before being stored in Trimpley Reservoir. This reservoir has a storage capacity of approximately one week and acts as a buffer to variation in river water quality. It also allows abstraction from the river to be stopped if the quality falls below an acceptable level, causing less disruption to supply. Water treated at Trimpley is divided into two treatment streams, one of which has floc blanket, hopper bottomed clarifiers (HBCs) (shown in cyan) and the other dissolved air flotation (DAFs) clarifiers (shown in magenta). In both streams the water has ferric sulphate coagulant added before flocculation and clarification. In the HBC stream a lower coagulant concentration of approximately 15 mg/l (as Fe^{3+}) is dosed before a static mixing chamber leading to multiple HBCs. The DAF stream has a higher coagulant dose of approximately 17 mg/l (as Fe^{3+}) added before the flocculators. Post clarification, the waters are blended together

before being filtered through dual media (anthracite/sand) rapid gravity filters. The water then passes through a balance tank, to reduce the fluctuations in discharge that are caused by the backwashing of the filters, before being treated by granular activated carbon (GAC) adsorbers. Chlorine gas dosed upstream of the contact tank is controlled by a feedback loop that is dependent on the free chlorine concentration entering and exiting the contact tank. Disinfected water has sodium bisulphite added to reduce the free chlorine to a suitable residual concentration for distribution. To help reduce corrosion of the distribution network calcium hydroxide, traditionally called slaked lime, is added to increase the pH and orthophosphoric acid is added to encourage a protective coating to form in the distribution network. The water then enters a mixing tank before being distributed between Trimpley Top Reservoir and a supply main to Hollywaste Reservoir. Water abstracted from Trimpley Reservoir can optionally be diverted from Trimpley to Frankley WTW (shown in green). This transferred water goes to a flash mixer before entering the Frankley header tank, which reduces fluctuations in discharge for pumping to Birmingham.

Throughout the WTW, in-line sensors measure specific water quality parameters at 15 minute intervals. These data are transferred to an electronic supervisory control and data acquisition (eSCADA) system, stored on site, and archived off site remotely by an external agency, CSE Servelec. All of the parameters investigated, as part of this project, are shown on Figure 4-1 in blue.

4.1.2 Treatment process details

All the treatment processes modelled at Trimpley are specified using information from inspection, documentation, eSCADA data and operator knowledge. The specification of the

processes is shown in Table 4-1 and diagrams showing the dimensions of the HBC and DAF clarifiers are shown in Figure 4-2 and Figure 4-3. The dimensions from the site schematics are in agreement with measurements taken onsite to within ± 1 m.

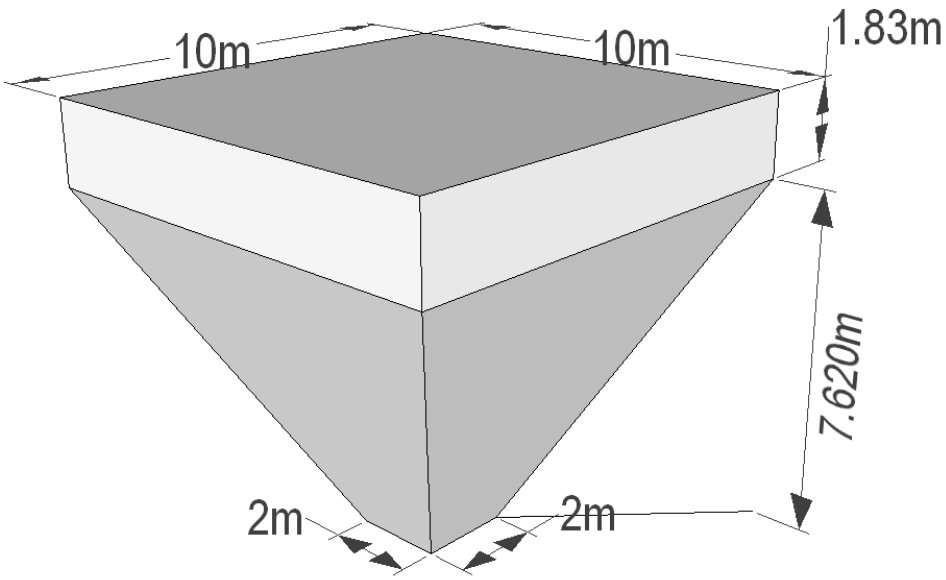

Figure 4-2 HBC tank dimensions

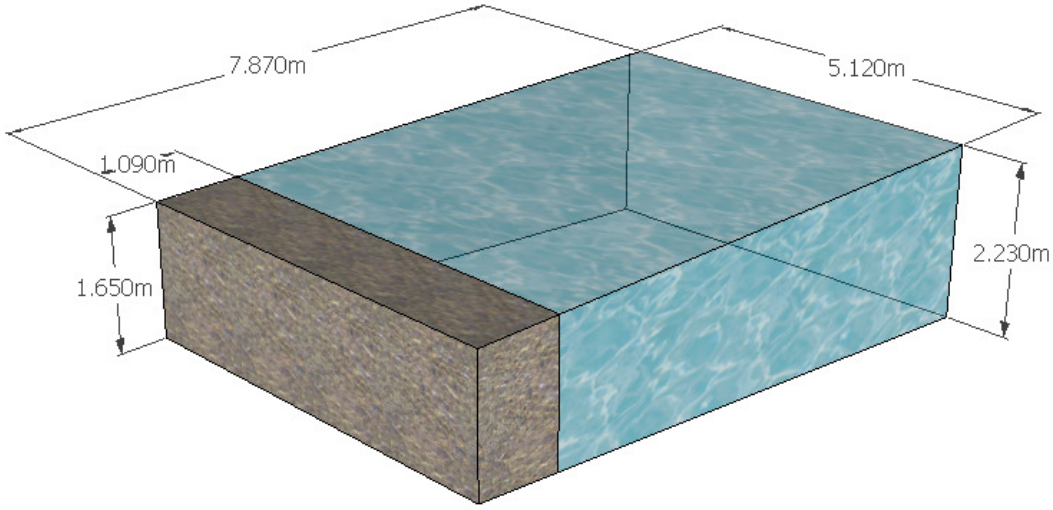

Figure 4-3 DAF tank dimensions

Table 4-1 Treatment process details

Process	**Number of units**	**Dimensions**	**Individual tank discharge and contact time**	**Chemical dose & other operational parameters**
Hopper bottomed clarifiers	10 in continuous use	Surface length: 10.00 m Surface width: 10.00 m Depth top square section: 1.83 m Depth hopper section: 7.62 m Base length: 2.00 m Base width: 2.00 m Volume: 498 m3	Discharge: 65 m3/h Contact time: 7.5 h	Ferric sulphate: 15 mg/l
Dissolved air flotation clarifiers	7 available, brought into service as required	Width: 5.12 m Initial depth: 1.65 m End depth: 2.23 m Contact zone length: 1.09 m Contact zone volume: 9.2 m3 Separation zone length: 6.78 m Total volume: 78 m3	Discharge: 240 m3/h Contact time: 20 min	Ferric sulphate: 17 mg/l Air supply: 7 mg/l Saturator pressure: 4 absolute bar Recycle rate: 10%
Rapid gravity filters	8 in continuous use	Length: 13 m Width: 4.5 m Top anthracite depth: 0.60 m Middle sand depth: 0.80 m Base gravel depth: 0.40 m	Discharge: 180 m3/h Superficial velocity: 3 m/h	Backwash duration: 48 hours Head loss limit: 2 m Turbidity limit: 0.5 NTU
Contact tanks	2 in parallel	Length: 32.18 m Width: 7.5 m Operational depth: 5 m Total volume: 2400 m3	Discharge: 635 m3/h Contact time: 115 min	Free chlorine dose: 1.6 mg/l Residual chlorine: 1.3 mg/l Number of baffles: 2

4.2 Data acquisition

Archived quarter hourly eSCADA and monthly water quality assurance test data were provided by Severn Trent Water for Trimpley WTW initially for July 2011 and January 2012 for development of the WTW models. Further annual data sets from 2011 were then provided for calibration and for the first nine months of 2012 for verification. A data set for the entirety of 2012 is not used due to incomplete data sets for some of the parameters required. The eSCADA data used is described in section 4.2.1. Manual monthly concentrations of alkalinity, bromide, trihalomethane, total organic carbon and measurements of UV_{254} absorbency and pH made by Severn Trent Services for the same period is described in section 4.2.2.

4.2.1 eSCADA data

The specifications of the sensors used is provided in Table 4-2. The turbidity of the water is manually measured for quality assurance at the reservoir intake and after clarification and filtration, and the free chlorine concentration is measured at the contact tank inlet and outlet manually by operators each day to highlight any possible malfunctioning in-line sensors. Sensors are identified as possibly being faulty and needing maintenance if the manual readings differ from in-line measurements by more than specified tolerance limits. The standard deviation between in-line and manual recordings recorded on log sheets at Trimpley works is also shown in Table 4-2.

Table 4-2 Specification of sensors used to calibrate and verify WTW models

Parameter	**Location [SCADA ID]**	**Specification**	**Operators QA (2011)**
Temperature (°C)	Intake from river [E521]	YSI Sonde multi-head unit Resolution 0.01°C Accuracy ± 0.15°C (YSI, 2012)	n/a
Discharge (Ml/d)	Pre HBCs [E23729] Pre DAFs [E4705] Post bank of filters [E4537] Post contact tank [E14635]	Siemens' Magflo 3000 electromagnetic flow meters Accuracy ± 0.25% (Siemens, 1997)	n/a
Turbidity (NTU)	Intake from reservoir [E22883] Post bank of HBCs [E14519] Post individual DAFs [E4525/E4526/E4527/E4531/ E4532/E4533/E4534] Post combined HBC & DAF [E4598] Post Individual filters [E4559/E4561/E4572/E4574/ E4586/E4588/E4600/E4602] Post bank of filters [E4564]	Sigrist AquaScat WTM used throughout WTW except at filters and final waters where Hach 1720D is used Hach 1720D Accuracy ± 2% or ±0.02 NTU (whichever greater) from 0-40 NTU (Hach, 1999) Sigrist AquaScat WTM turbidity meters Resolution 0.001 FNU Accuracy not specified (SIGRIST, n.d.)	Intake from reservoir n = 302 Tolerance = 5 NTU σ = 4.6 NTU Post HBC n = 322 Tolerance = 0.25 σ = 0.08 Post HBC & DAF n = 317 Tolerance = 0.25 σ = 0.13 Post Individual filters n = 2162 Tolerance = 0.1 σ = 0.04
Head loss (m)	Post Individual filters [E4558/E4560/E4571/E4573/ E4585/E4587/E4599/E4601]	Endress + Hauser Deltabar PMD 130 Accuracy ±1% (Endress Hauser, n.d.)	n/a
Free chlorine (mg/l)	Pre contact tank [E18605] Post contact tank [E18606]	Capital Controls Series 1930 Sensitivity 0.004 mg/l Display resolution 0.01 mg/l Accuracy ±0.1 mg/l (Severn Trent Services - Capital Controls, 1993, Trimpley Operators, 2012-2013)	Pre contact tank n = 318 Tolerance = 0.1 mg/l σ = 0.08 mg/l Post contact tank n = 963 Tolerance = 0.1 mg/l σ = 0.06 mg/l

Where: n = number of readings; tolerance = limit of deviation between in-line and manual readings triggering inspection of in-line sensor and σ = Standard deviation between in-line and manual readings.

4.2.2 Water quality sampling

To assess the water quality of the river, reservoir and final waters, additional manual measurements of approximately 200 water quality parameters are measured by Severn Trent Services for Trimpley WTW. Monthly concentrations of alkalinity, bromide, trihalomethane, total organic carbon and measurements of UV_{254} absorbency and pH were made during 2011 and 2012 and were used to characterise water quality. A review of the accuracy of the manual measurements in comparison to Analytical Quality Control (AQC) samples taken from Trimpley is given in Table 4-3 (multiple readings indicate multiple tests of accuracy completed). Except for a single assessment of the precision of the bromide concentration measurement, the bias and precision of the methods is less than 5% and all within the regulatory limits.

Table 4-3 Review of accuracy of measurements taken at Trimpley WTW (Mills, 2013)

Parameter	**Basis of Analytical Procedure**	**Current Bias from Routine AQC (Regulatory Limit)**	**Current Precision from Routine AQC (Regulatory Limit)**
Alkalinity as CaCO3	Acid titration to end point of pH 4.5 using auto-titrator	-0.91% (5%)	2.42% (5%)
Bromide	Ion chromatography with conductimetric detection	0.27%	2.28%
pH	pH electrode	0.027 pH units (0.1 pH) 0.016 pH units (0.1 pH)	-0.02 pH units (0.2 pH) -0.03 pH units (0.2 pH)
Specific Absorbance at 254nm	UV Spectrophotometry	-2.06%	4.01%
TOC	TOC analyser – UV/persulphate digestion of organic carbon and detection of released CO2 by Infra-Red (NDIR)	-0.95% (5%)	2.01% (5%)
THM	Headspace GCMS (Gas Chromatography Mass Spectrometry). Total THM is the sum of four individual compounds: (a) chloroform (b) bromoform (c) bromodichloroform (d) dibromochloroform	(a) -2.27% (12.5%) 1.27% (12.5%)	(a) 4.74% (12.5%) 2.52% (12.5%)
		(b) 1.11% (12.5%) 3.81% (12.5%)	(b) 5.17% (12.5%) 3.61% (12.5%)
		(c) -4.99% (12.5%) -3.34% (12.5%)	(c) 3.27% (12.5%) 3.48% (12.5%)
		(d) 2.71% (12.5%) 3.39% (12.5%)	(d) 3.97% (12.5%) 3.96% (12.5%)

4.2.3 Comparison of operating conditions in 2011 and 2012

4.2.3.1 *Weather*

The weather for the years covered in this research are assessed using data provided by the MET Office website (2014) and unless otherwise stated comparisons are based on means for the period 1981 - 2010. In 2011, the year for which data were used to calibrate the WTW models,

the UK experienced its second warmest year observed since 1910 and central England experienced its second warmest year since 1659. The region of England around Trimpley WTW received less rainfall than usual with under 65% of the mean precipitation observed. In comparison, 2012 was a slightly cooler than average year in the UK (-0.1°C). 2012 was wetter than any other year in the 1981-2010 series and rainfall around Trimpley WTW was more than 125% of the yearly mean. 2011 was generally a warm and dry year and 2012 a cooler and wetter year.

4.2.3.2 *Water quality and operational regime*

A comparison of the operating conditions observed in 2011 and 2012 is shown in Figure 4-4. As would be expected for a cooler year, the mean water temperature in 2012 was substantially lower than in 2011 (-2.5°C). The mean concentration of organic content was greater (+ 0.7 mg/l TOC and +0.03 cm^{-1} UV_{254}) and the mean concentration of bromide also reduced by 21% in 2012 (which is in agreement with the inversely proportional relationship between bromide concentration and river flow, described in Brown (2009) for rivers in the same region). The mean reservoir turbidity was lower and turbidity varied less in 2012. Alkalinity, pH and contact tank inlet chlorine concentration also all varied less (as defined by standard deviation) in 2012. Although there were substantial differences in the weather and water quality observed in 2011 and 2012, overall operational conditions were comparable and considered to be suitable for calibration and verification purposes.

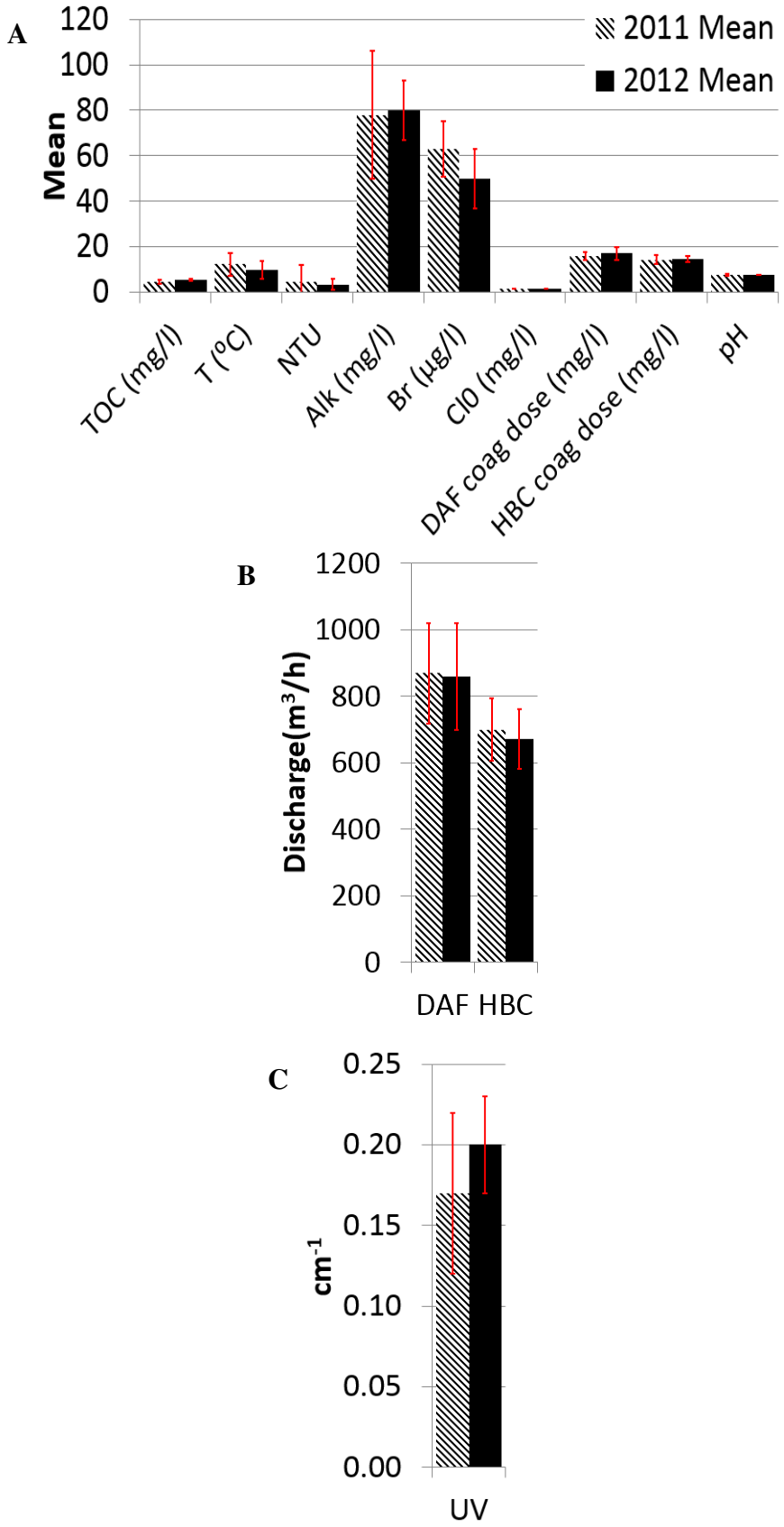

Figure 4-4 Operating conditions 2011 – 2012 (error bars show standard deviation)

4.3 Model description

This section describes the methods used to adapt the general dynamic and static models described in chapter three to the conditions observed at Trimpley WTW. An overview of how the model appeared in Simulink is given in Figure 4-5.

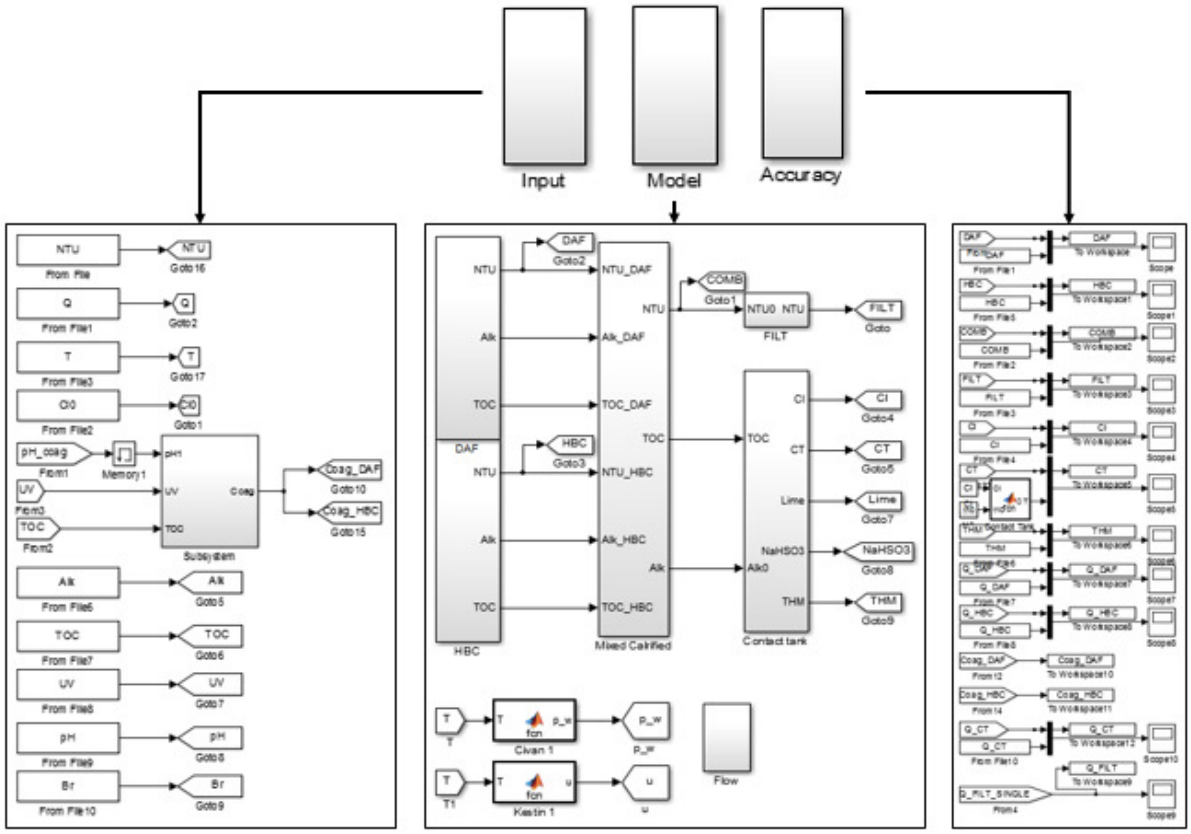

Figure 4-5 MATLAB/Simulink model of Trimpley WTW

4.3.1 Suspended solids removal efficiencies

In order to improve the accuracy of the clarification and filtration models, a cross comparison of mean monthly reservoir water quality parameters (WQPs): temperature, UV_{254}, TOC, SUVA, turbidity, coagulant dose and estimated coagulated suspended solids concentration is made against monthly mean empirical removal efficiency parameters for Trimpley during 2011 (see Table 4-4). Correlations are identified between raw turbidity and most of the empirical removal efficiency parameters (two thirds of relationships had R^2 values greater than 0.5) and

these relationships are used to estimate the removal parameters temporally. The mean R^2 value of these relationships for the dynamic model is 0.63, greater than the 0.50 value achieved for the static model. This "adjustment" of the removal efficiency parameters indicates that the models were otherwise failing to model some mechanisms sufficiently to account for the higher removal rates observed for more turbid raw waters.

Table 4-4 Correlation between WQPs and empirical removal efficiency (R^2)

Parameter	Temperature (°C)	UV_{254} (cm^{-1})	TOC (mg/l)	SUVA (l/mg.cm)	Reservoir turbidity (NTU)	Coagulant dose (mg/l Fe)	Modelled coagulated SS (mg/l)
Dynamic K_f (HBC)	0.03	0.02	0.07	0.01	0.80	0.05	0.66
Dynamic α (DAF)	0.49	0.31	0.41	0.09	0.49	0.37	0.68
Dynamic r (FILT)	0.51	0.00	0.01	0.02	0.61	0.01	0.27
Static k (HBC)	0.10	0.02	0.05	0.00	0.19	0.03	0.31
Static α (DAF)	0.53	0.13	0.18	0.04	0.69	0.13	0.47
Static r (FILT)	0.39	0.04	0.01	0.01	0.61	0.01	0.19
Mean	0.34	0.09	0.12	0.03	0.57	0.10	0.43

The empirical removal parameters used are given in Table 4-5 and the improvement in turbidity prediction for the static and dynamic model using the 2011 calibration data is shown in Table 4-5.

Table 4-5 Empirical removal parameters

Parameter	**Empirical relationship**
Dynamic K_f (HBC)	$0.307*NTU_{Reservoir} + 3.689$ (for 2 CSTRs)
Dynamic α (DAF)	$0.017* NTU_{Reservoir} + 2.05$ (for 1 CSTR)
Dynamic r (FILT)	$0.0003*NTU_{Reservoir} + 0.0038$
Static k (HBC)	$0.016*NTU_{Reservoir} + 0.494$
Static α (DAF)	$0.007*NTU_{Reservoir} + 0.234$
Static r (FILT)	$0.0005*NTU_{Reservoir} + 0.0034$

Table 4-6 Improvement in turbidity prediction for 2011 calibration data

Model	**Outlet Turbidity**	**RMSE (NTU) for efficiency parameter**		**Reduction in RMSE**
		Consistent	**Reservoir water NTU dependent**	
Static model	HBC	0.5453	0.2701	50%
	DAF	0.4224	0.3529	16%
	Combined clarified	0.4481	0.2823	37%
	Filter	0.0691	0.0461	33%
Dynamic model	HBC	0.2718	0.1968	28%
	DAF	0.3450	0.2712	21%
	Combined clarified	0.3021	0.2308	24%
	Filter	0.1362	0.0357	74%

4.3.2 Division of abstraction discharge between HBC and DAF streams

The division of abstracted flows between the treatment streams is analysed using eSCADA data from 2011 (shown in Figure 4-6). Approximately 55% of the treated water passes through the DAF treatment stream, although substantial deviation from this relationship exists.

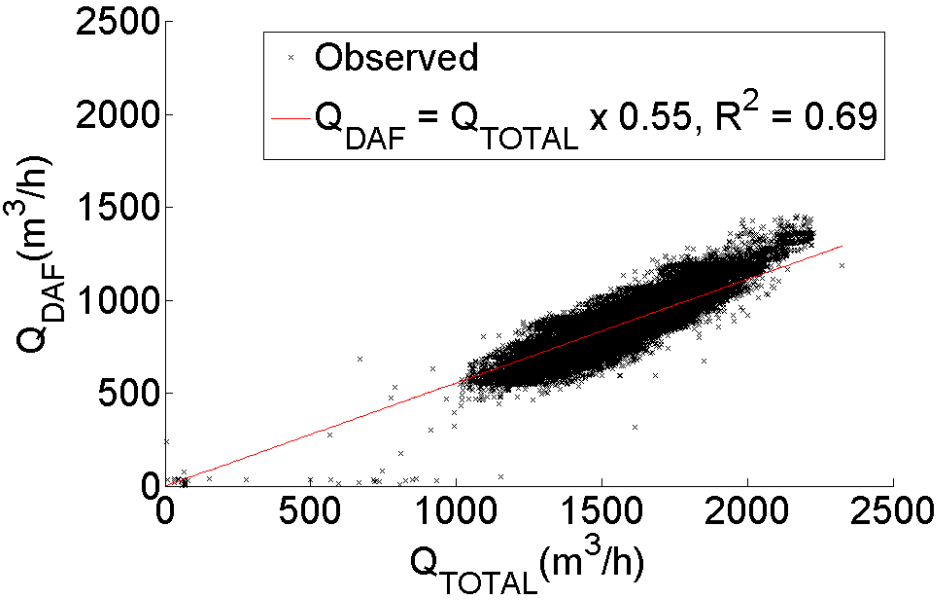

Figure 4-6 DAF stream discharge against abstraction discharge (RMSE 74.7 m^3/h)

4.3.3 Coagulation dosing

The clarification models are calibrated using observed coagulant doses from 2011 and verified using doses from 2012. The coagulant dosing model (described in section 3.3.2.1) is also applied. The coagulant dosing model predicts a minimum coagulant dose to achieve a clarified TOC concentration below 2.5 mg/l. The coagulant dose also has to remain within the dosing range, of 7 to 25 mg/l as Fe^{3+}, which is observed at Trimpley. The clarified TOC limit is set at 2.5 mg/l as this results in a mean coagulant dose most similar to that observed in at Trimpley WTW in 2011 (alternative TOC limits were assessed in 0.5 mg/l increments). For these coagulation conditions, additional solids loading due to TOC removal could be up to approximately 8% of that assumed to occur due to iron hydroxide formation.

4.3.4 Intermittent operation of DAF tanks

The individual DAF tanks at Trimpley have a maximum treatment capacity of 292 m^3/h (7 Ml/d). The discharge through each individual tank is calculated based on the estimated discharge through the DAF bank divided by the minimum number of DAF tanks required to avoid exceeding the individual tank treatment capacity. This mechanism results occasionally in DAF tanks being brought in and out of operation frequently, which causes the discharge for individual tanks to fluctuate unrepresentatively. Operators are able to make strategic decisions to minimise disruption to individual processes, run processes at optimum discharge rates and respond to undesirable process performance. The simple division of discharge modelled, between and within the clarification processes, results in substantially different flow division than was carried out by the operators but is used as replicating the operators control is considered to be prohibitively complex.

4.3.5 Rapid gravity filtration (RGF)

4.3.5.1 *RGF model Bohart and Adams calibration parameters*

Representative scale pilot filters were used, along with clarified water from Trimpley, to estimate the removal parameters of the anthracite and sand media (Omar, 2012, Yegorova, 2013). The values identified by these investigations resulted in predicted removal efficiencies that were significantly greater than those observed in operation (filtered turbidity of approximately 0.001 NTU were predicted). Possible causes of this overestimation of performance include reported inefficient backwashing at Trimpley and uncertainty of the effective size of the sand media used, due to unrepresentative sampling from the surface of the sand supplied by the distributor.

The calibration of the Boharts and Adams parameters is completed using eSCADA data from 2011. This data shows no signs of significant breakthrough, therefore, as described in section 3.6.1.1, a conservative estimate of filter capacity is used (a_0 1000 mg/l).

4.3.5.2 *Clean bed head loss*

A full list of the parameters used to predict the head loss of the filters is given in Table 4-7.

Table 4-7 Parameters for Kozeny-Carman cleanbed headloss equation

Parameter	**Value**
Dynamic viscosity water	1.3x10-3 N.s.m-2
Dynamic viscosity air	1.8x10-3 N.s.m-2
Density of water	1000 kg/m3
Density of air	1.3 kg/m3
Depth of sand	0.8 m
Depth of anthracite	0.6 m
Voidage of sand	0.4
Voidage of anthracite	0.5
Sphericity of sand	0.8
Sphericity of anthracite	0.6
Diameter of sand	0.58 mm
Diameter of anthracite	1.3 mm

The filters show significant differences in head loss profiles. The July 2011 data shows a single broadly distributed band of head loss profile (see Figure 4-7), whereas the head loss observed in January approximately fits into three groups, shown in red, blue and green ellipses in Figure 4-8. The general head loss profile of Trimpley's filters for July 2011 and January 2012 is determined by fitting all of the representative data to a linear equation using MATLAB's polyfit function with clean bed head losses were identified as intercept values. The clean bed head loss is simulated using the Kozeny-Carman equation with eSCADA data from July 2011 and January 2012. The mean clean bed head loss predicted for July 2011 is 0.42m with a standard deviation of 0.05 and for January 2012 the mean is 0.64 m with a standard deviation of 0.08 m. The modelling of clean bed head loss using the Kozeny-Carman equation provides

a representative prediction of observed operation within the range of performance witnessed (mean clean bed head loss under-predicted by 5 cm in July 2011 and over-predicted by 20 cm in January 2012).

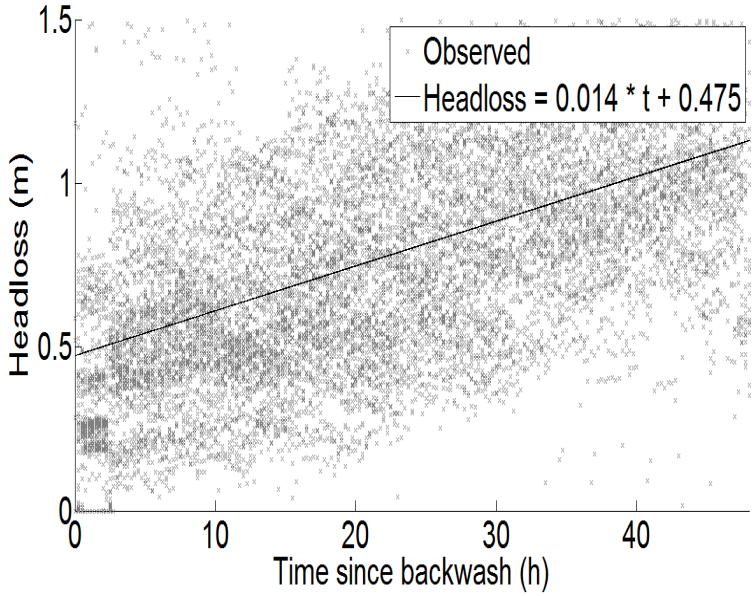

Figure 4-7 Head loss versus time since last backwash from July 2011

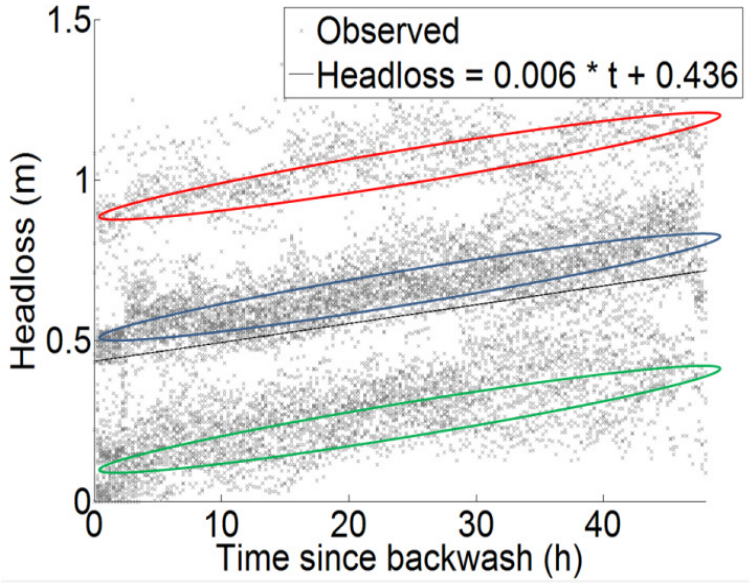

Figure 4-8 Head loss versus time since last backwash from January 2012

4.3.5.3 *Dynamic head loss accumulation calibration*

Due to discrepancies between the performances of the individual filters an empirical method is used to identify a representative head loss coefficient (β). β is varied by factors of ten and applied to the Adin & Rebhun (1977) head loss due to accumulation model. The head loss predicted using this method for July 2011 and January 2012 is shown in Figure 4-9 and Figure 4-10).

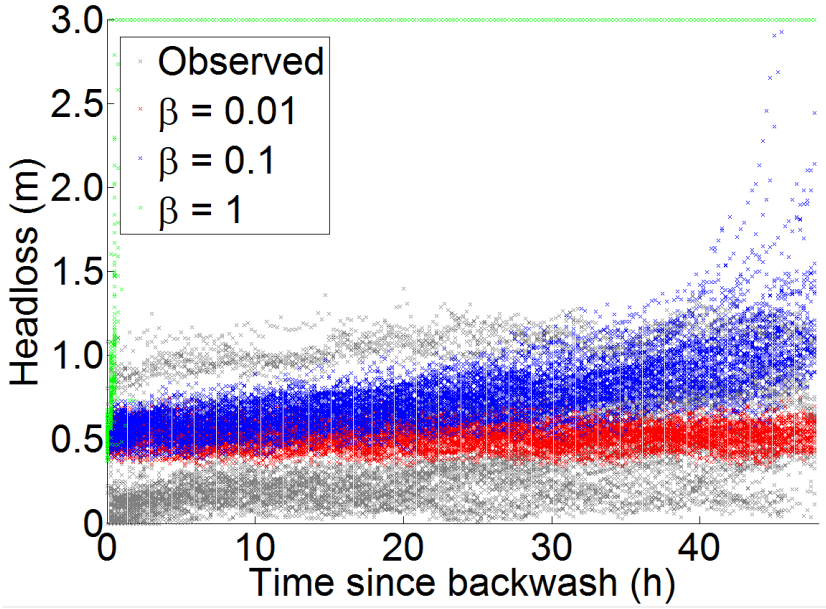

Figure 4-9 Head loss against time since last backwash July 2011

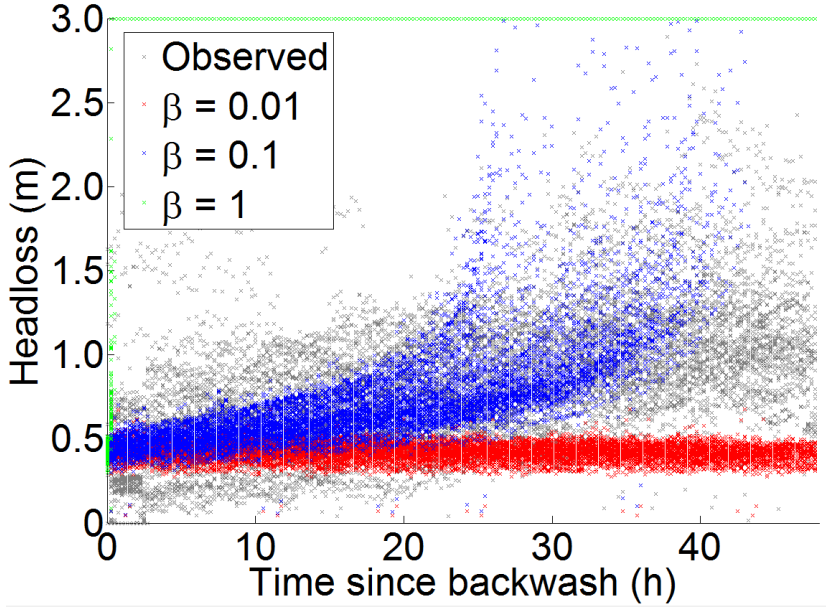

Figure 4-10 Head loss against time since last backwash January 2012

Due to the difference in head loss observed between filters and seasons, a higher β value of 0.1 √(l/mg) is identified as being appropriate, despite having a greater RMSE than a lower 0.01 √(l/mg) value (approximately 0.6 m as opposed to 0.4 m) as it gives a more conservative estimate of when higher head loss (above 1 m) is likely.

4.3.6 TOC removal by filtration and GAC adsorption

The blended turbidity, total organic carbon (TOC) and alkalinity of the clarified water from the HBC and DAF treatment streams is calculated by applying mass balances. TOC concentration is reduced by 25% to take into account removal by filtration and granular activated carbon, as described in section 3.7.1. The accuracy of this assumption is analysed by comparing the modelled and observed final water TOC concentrations (see Figure 4-11). This shows that the concentrations of the modelled and observed final water TOCs are comparable. The modelled final TOC has a RMSE of 0.2 mg/l, which is lower than the RMSE reported for the Edwards general TOC model (Tseng and Edwards, 1999).

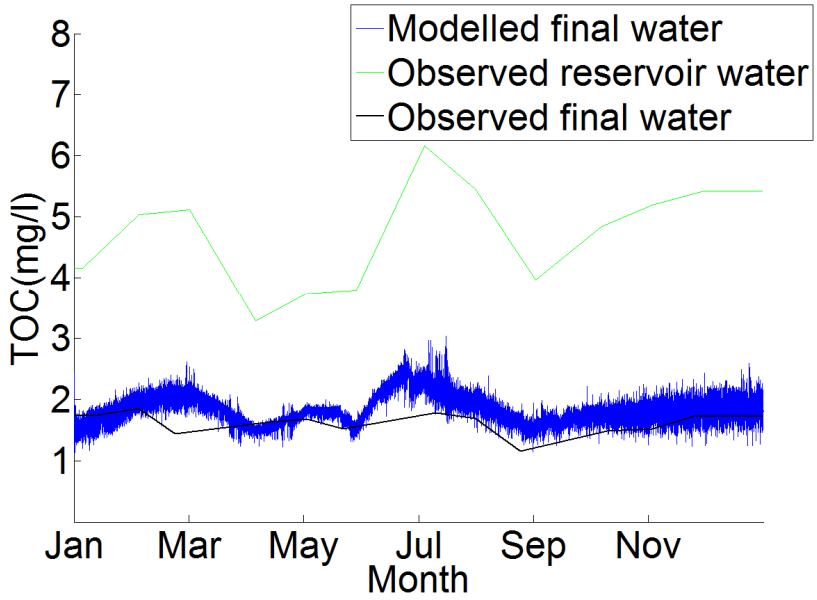

Figure 4-11 Comparison of modelled and observed final water TOC

4.3.7 Chlorination

4.3.7.1 *Contact tank inlet chlorine concentration*

Chlorine is dosed approximately 10 m upstream of the contact tank and the free chlorine decay that occurs before entering the contact tank is assumed to be approximately equivalent to the initial five minute decay that Brown (2009) modelled separately (see section 3.8.3). The contact tank inlet free chlorine concentration has its decay modelled using the 5-120 minute parameters from Table 3-6 as these are most representative of contact times observed at Trimpley WTW.

4.3.7.2 *Contact tank discharge*

An empirical relationship between the time since last backwash of the filters and the reduction in contact tank discharge is investigated, using eSCADA data from January 2012 (see Figure 4-12). It can be seen that the discharge immediately after backwashing is higher than for the majority of the run. This is due to the diversion of flow through the other filters, whilst the backwashed filter discharges its drawdown water. The influence of backwashing is modelled by assigning no reduction in flow for the first hour (to represent draw down effect), a reduction of 20% of abstraction between one to three hours (to represent running to waste and increased backwash water abstraction from post GAC), and for other times a reduction of 10% (to represent water abstraction post GAC). This simple model is also illustrated in Figure 4-12.

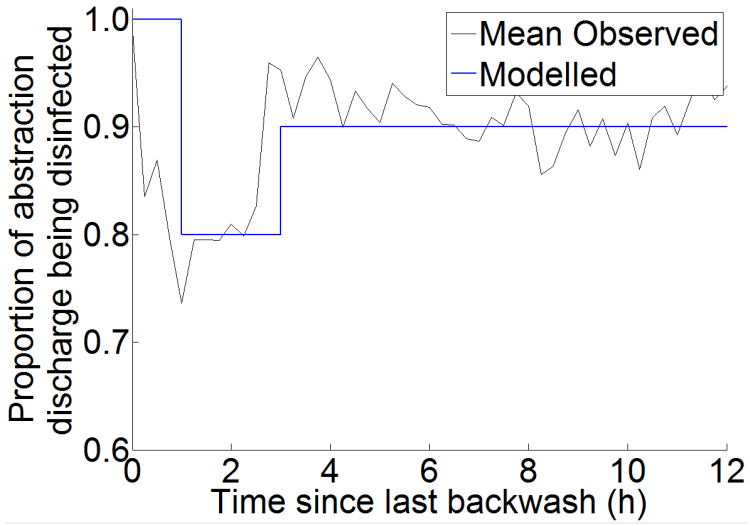

Figure 4-12 Proportion of abstraction discharge disinfected against time since last backwash

4.3.7.3 *Hydraulic efficiency*

The flow regime of the contact tank is defined by a representative number of CSTRs as identified by a previous step change tracer study carried out by Severn Trent Water, which estimated the t_{10}:t_θ efficiency of the tank as 73% (Morse, 2008). A t_{10}:t_θ efficiency of 73% using Table 3-7 results in 21 CSTRs being identified as being representative of the mixing that occurs.

4.3.7.4 *THM formation*

The chlorine consumed in the contact tank and the THM measured in the final water are assessed using eSCADA data from 2011. As can be seen in Figure 4-13, the chlorine consumption fluctuates by approximately 0.5 mg/l due to continual adjustment of the chlorine by the control system and the instantaneous inlet and outlet concentrations being compared. No significant change in chlorine consumption pattern is observed during 2011, however the THM detected in the final water is seen to increase in the summer months. From these data, it is not possible to detect any influence of chlorine consumption on THM formation. To obtain

a representative K_{TC} value for the works during 2011, the mean chlorine consumed within the contact tank is used along with the mean THM concentration detected in the final water to calculate a value of 44 µg/l per mg/l. This indicates that the mean value identified by Hua (2000) of 45 µg/l per mg/l is suitable for modelling THM formation at Trimpley.

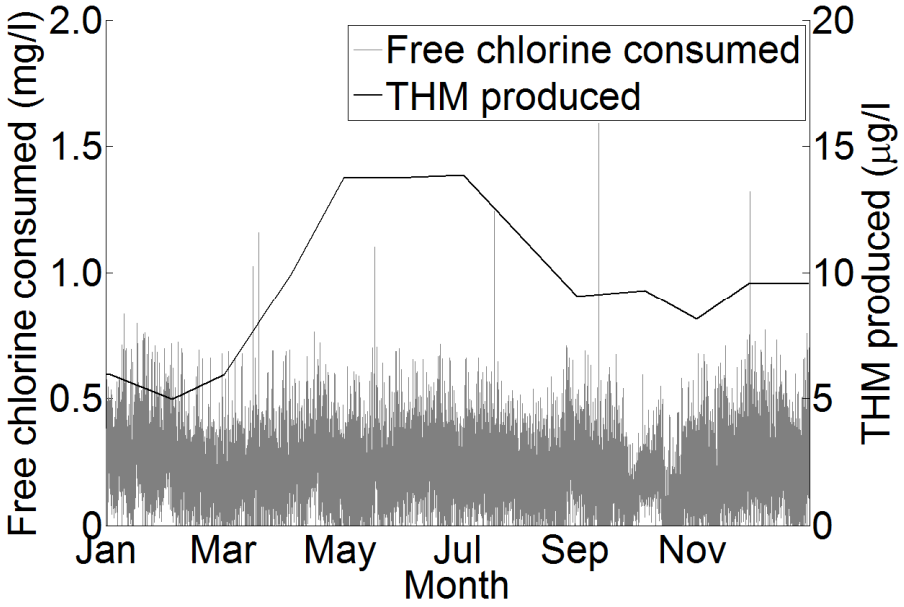

Figure 4-13 Comparison of free chlorine consumption and THM formation observed 2011

4.4 Model verification

The models are calibrated using eSCADA and water quality data from 2011 as described in sections 4.2.1and 4.2.2. The models are verified using data from the first nine months of 2012. The models are tested using observed input time series data to represent the operating conditions and synthetically produced Monte-Carlo time series data produced by random sampling of representative probability distribution functions every simulated day for a simulated year.

4.4.1 Time series simulation

As well as simulating the performance of the works using the input data described above, simulations are also run where the coagulant dose to both clarification streams is specified

using the dosing model described in sections 3.3.2.1 and 4.3.3. The results of these verification simulations follows. The values recorded by the eSCADA system during the verification period are also shown in the results as an 'observed' data set.

Clarification flow rates

The clarification processes' flow rates are modelled using the same method in both the dynamic and the static models. The degree of accuracy achieved is given in Table 4-8. The mean and median values are predicted to within ±5% but the standard deviation of the quantity of water treated by the HBC process was over-predicted by 8% whilst the DAF process standard deviation was under-predicted by 28%. The RMSE of the volumes of water treated by both processes is approximately 10%.

Table 4-8 Accuracy of modelled clarifier inlet flows

Parameter	$\bar{x}$	$\tilde{x}$	**σ**	**RMSE**
Q_{HBC} (m3/h)	671 (+2%)	660 (-0.5%)	98 (+8%)	75 [11%]
Q_{DAF} (m3/h)	842 (-2%)	839 (-3%)	115 (-28%)	73 [9%]

Where: Q = flow to process (m^3/h); $\bar{x}$ = mean; $\tilde{x}$ = median; σ standard deviation; RMSE = root mean square error, ±% = variance with recorded values; and in [] brackets = percentile error.

Clarified turbidity

The dynamic model is more accurate at predicting the clarified turbidity of the HBC, DAF and mixed clarified waters as measured by mean and RMSE values (as shown in Table 4-9 and Table 4-10). The accuracy of the clarification models is worse than that of the QA tests carried out, but of a similar magnitude to the QA tolerance level set by Severn Trent Water (0.25 NTU).

Table 4-9 Dynamic model clarified turbidity accuracy

Parameter	Observed coagulant dose				Modelled coagulant dose				QA RMSE	QA tolerance
	$\bar{x}$	$\tilde{x}$	σ	RMSE	$\bar{x}$	$\tilde{x}$	σ	RMSE		
NTU_{HBC}	0.45 +2%	0.42 ±0%	0.14 -13%	0.18 [41%]	0.53 +20%	0.48 +14%	0.20 +25%	0.22 [50%]	0.11 [25%]	0.25 [56%]
NTU_{DAF}	0.63 -7%	0.62 ±0%	0.10 -63%	0.28 [41%]	0.67 -1%	0.67 +8%	0.12 -56%	0.29 [43%]	n/a	0.25 [37%]
NTU_{COMB}	0.55 -17%	0.54 -13%	0.09 -65%	0.26 [39%]	0.61 -8%	0.60 -3%	0.14 -46%	0.22 [33%]	0.13 [19%]	0.25 [38%]

Table 4-10 Static model clarified turbidity accuracy

Parameter	Observed coagulant doses				Modelled coagulant doses				QA RMSE	QA tolerance
	$\bar{x}$	$\tilde{x}$	σ	RMSE	$\bar{x}$	$\tilde{x}$	σ	RMSE		
NTU_{HBC}	0.33 -25%	0.28 -32%	0.20 +25%	0.26 [59%]	0.40 -9%	0.32 -24%	0.27 +69%	0.26 [59%]	0.11 [25%]	0.25 [56%]
NTU_{DAF}	0.62 -9%	0.59 -5%	0.21 -22%	0.34 [50%]	0.66 -3%	0.64 +3%	0.22 -19%	0.35 [51%]	n/a	0.25 [37%]
NTU_{COMB}	0.49 -26%	0.49 -21%	0.16 -38%	0.32 [48%]	0.54 -18%	0.53 -15%	0.19 -27%	0.28 [42%]	0.13 [19%]	0.25 [38%]

Where: NTU = post process turbidity (NTU); QA RMSE= RMSE of operators quality assurance measurements; QA tolerance = acceptable degree of variance between operators measurements and inline measurements.

The lower degree of variation is also exhibited in the time series plots of clarified turbidity (Figure 4-14 to Figure 4-17) and the probability distributions (Figure 4-18 to Figure 4-21) where the sensitivity of the model in comparison to observed performance is limited.

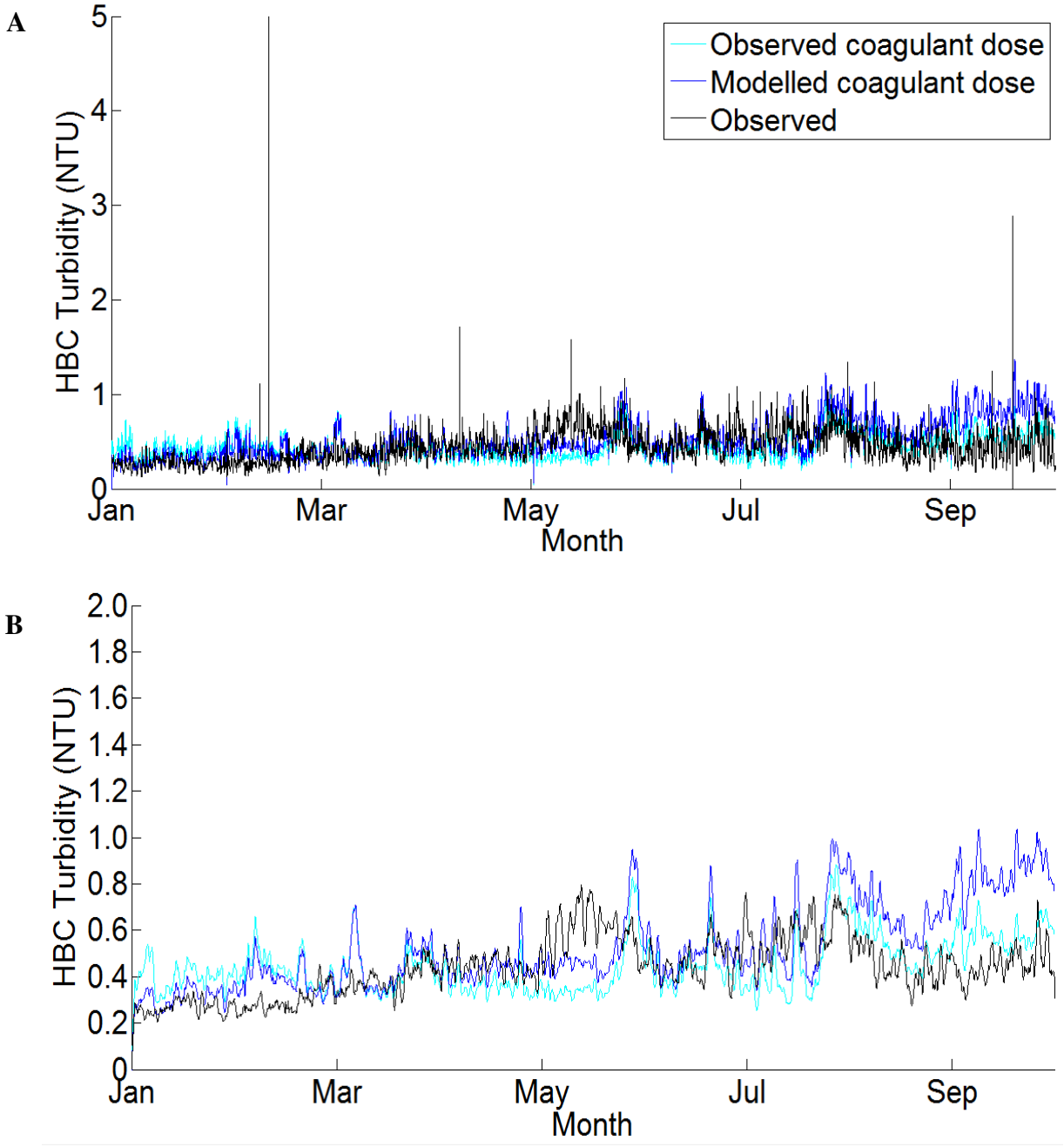

Figure 4-14 Dynamic HBC models performance

(A: 15 minute values, B: daily mean values)

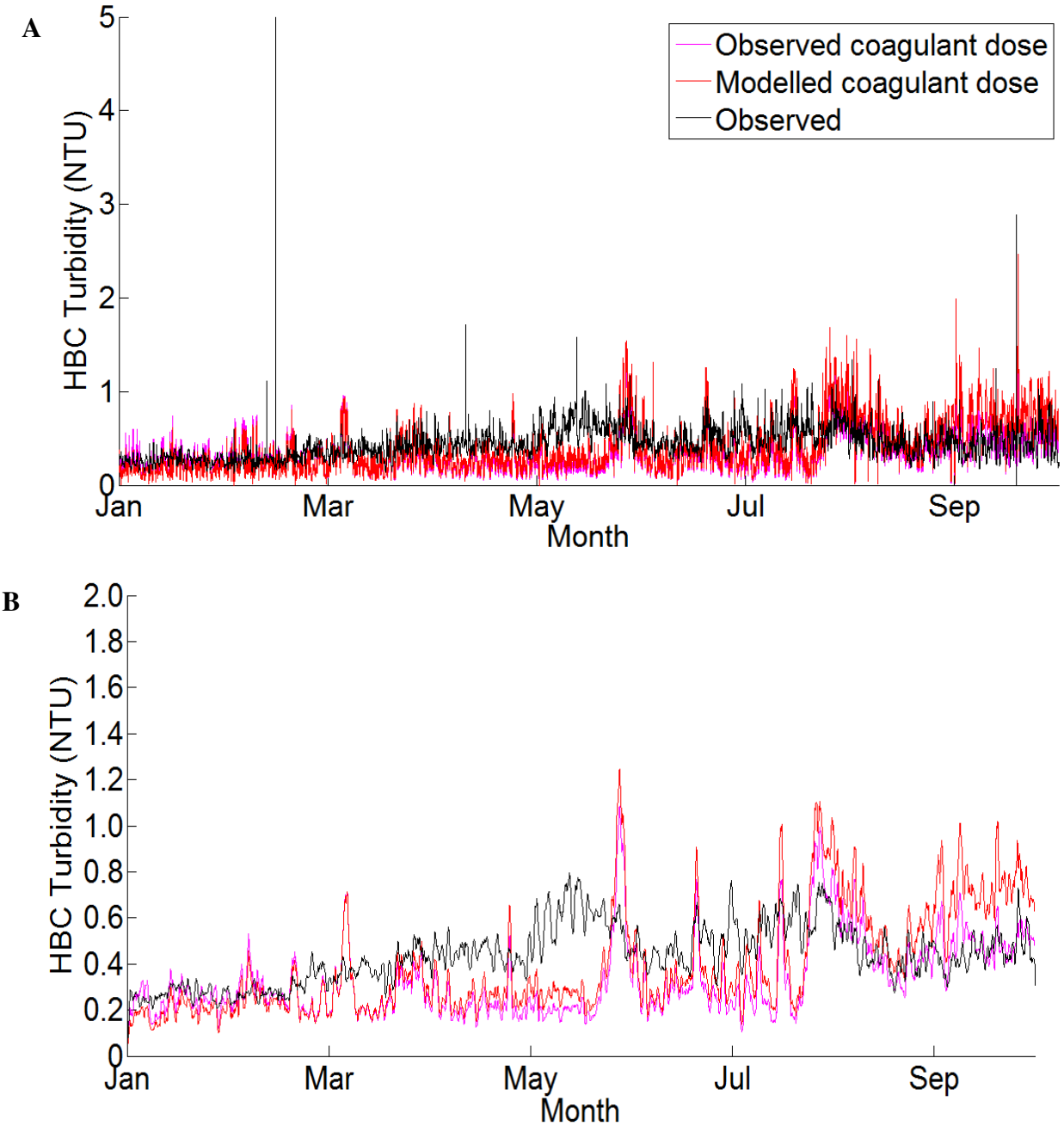

Figure 4-15 Static HBC models performance

(A: 15 minute values, B: daily mean values)

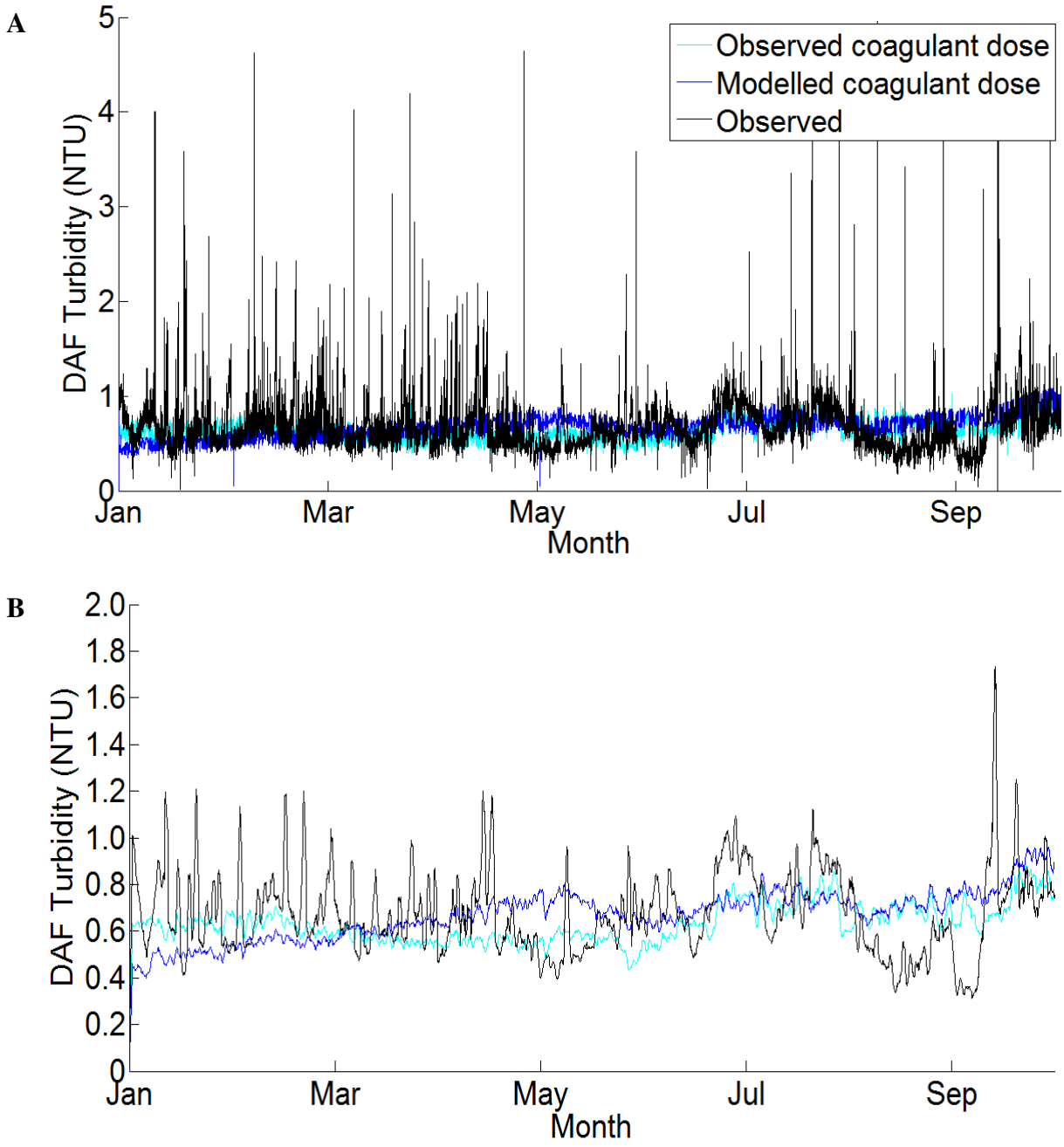

Figure 4-16 Dynamic DAF models performance

(A: 15 minute values, B: daily mean values)

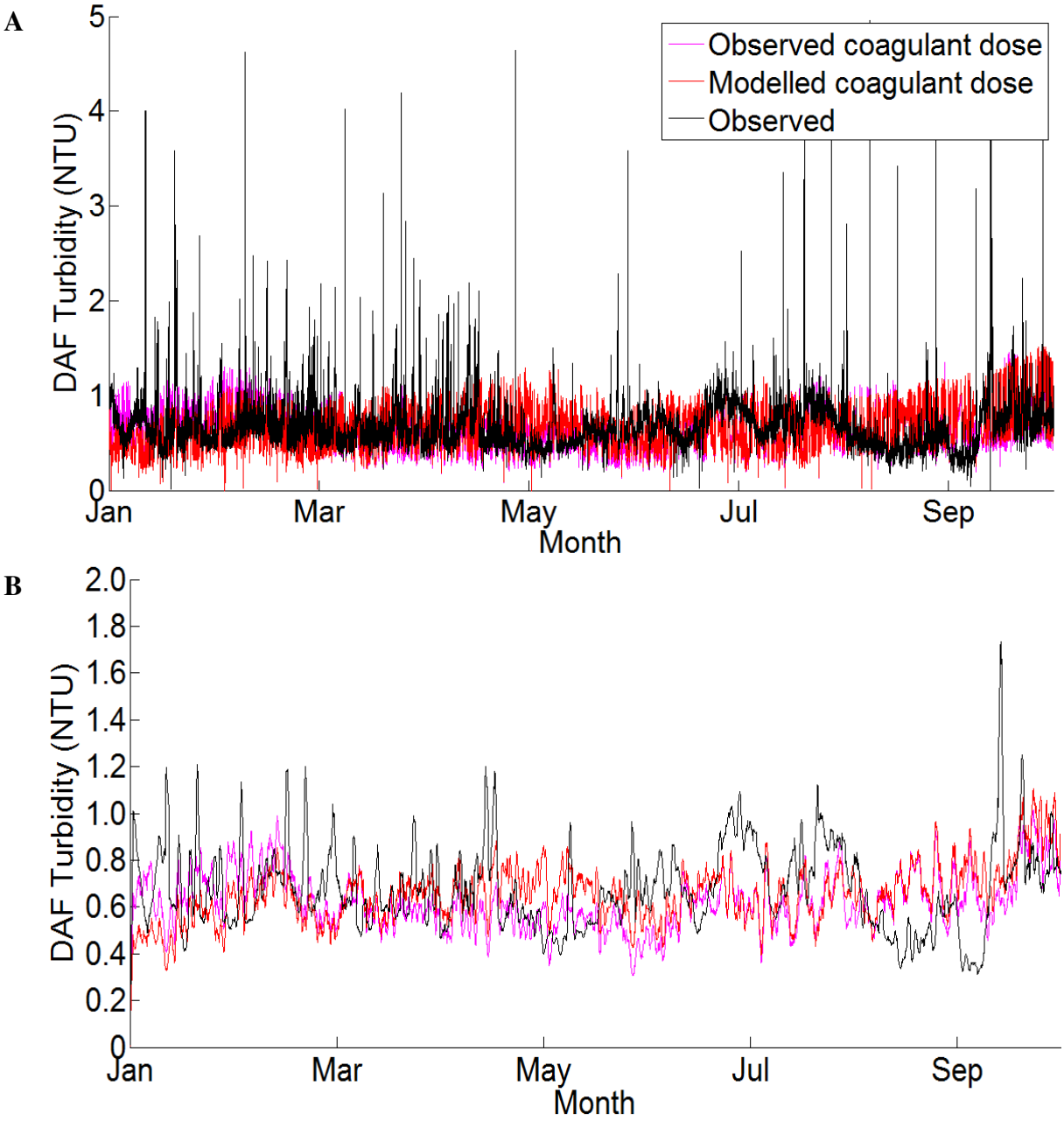

Figure 4-17 Static DAF models performance

(A: 15 minute values, B: daily mean values)

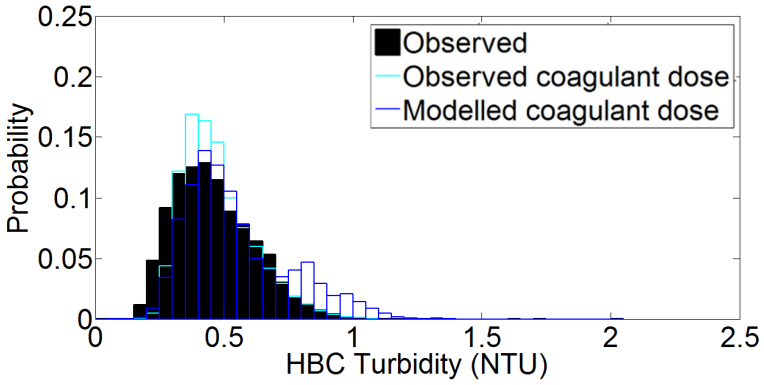

Figure 4-18 Dynamic HBC turbidity PDF

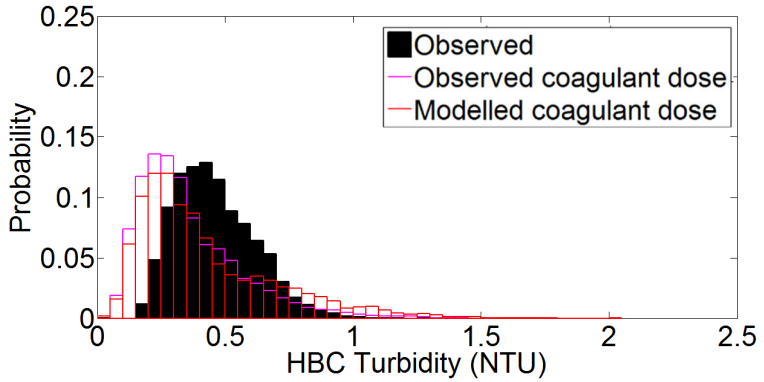

Figure 4-19 Static HBC turbidity PDF

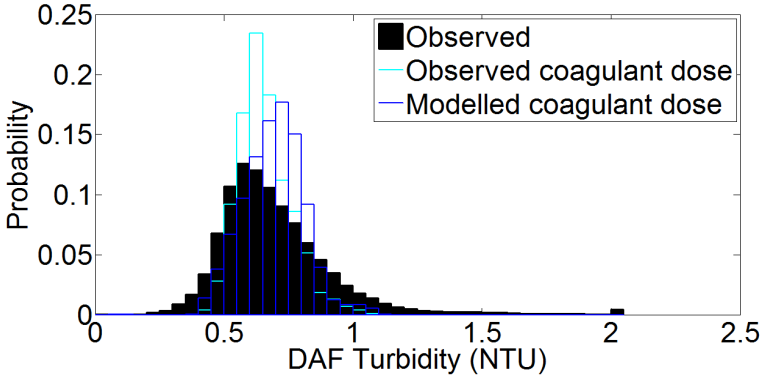

Figure 4-20 Dynamic DAF turbidity PDF

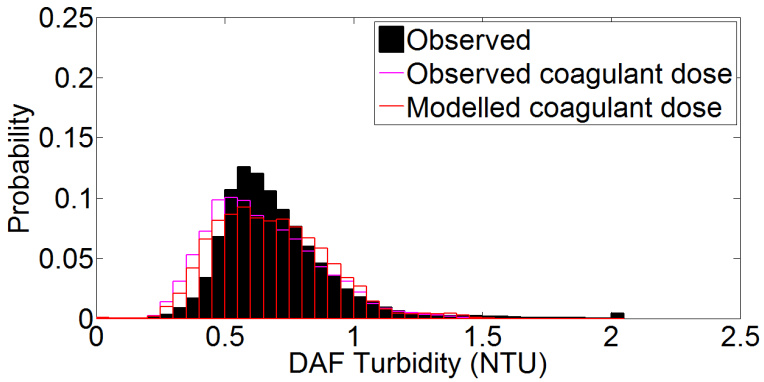

Figure 4-21 Static DAF turbidity PDF

When modelled rather than observed coagulant doses are applied it is found that the mean dose increases from 14.7 mg Fe/l for HBC clarification and 17.1 mg Fe/l for DAF clarification to 17.8 mg Fe/l for both processes. A time series comparison of the coagulant doses is shown in Figure 4-22. As can be seen, the modelled coagulant doses have a similar sensitivity to operating conditions as those prescribed by the operators, particularly in relation to the DAF process.

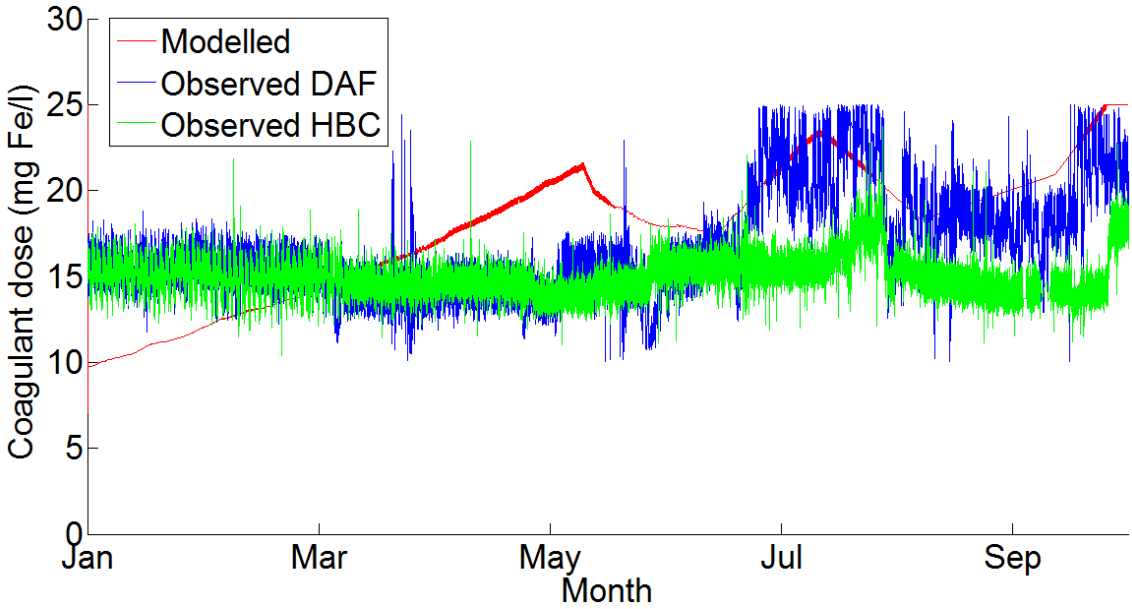

Figure 4-22 Observed and modelled coagulant doses 2012

Filtered turbidity

The accuracy of the dynamic model as measured by the mean, median and the RMSE is lower for the dynamic model than the static model (see Table 4-11). The lower accuracy of the static model is caused by the under-prediction of the mean filtered turbidity to a greater extent than the dynamic model and due to the static model having a substantially greater degree of deviation of filtered turbidity than was observed (σ is greater by approximately 60%).

Table 4-11 Modelled filtered turbidity accuracy

Model	**Observed coagulant dose**				**Modelled coagulant dose**				**QA RMSE**	**QA tolerance**
	$\bar{x}$	$\tilde{x}$	**σ**	**RMSE**	$\bar{x}$	$\tilde{x}$	**σ**	**RMSE**		
Dynamic NTU_{FILT}	0.077 -2%	0.070 -14%	0.032 -6%	0.035 [44%]	0.087 +10%	0.076 -6%	0.043 +26%	0.037 [47%]	0.035 [44%]	0.10 [125%]
Static NTU_{FILT}	0.065 -18%	0.056 -31%	0.042 +24%	0.045 [58%]	0.074 -6%	0.061 -25%	0.053 +56%	0.049 [62%]	0.035 [44%]	0.10 [125%]

It can be seen in Figure 4-23 and Figure 4-24 that both models are more sensitive to short term variations in operating conditions than the observed performance, particularly the static model. This difference between the variance predicted by the models and that observed is also illustrated in Figure 4-25 and Figure 4-26. The RMSE of the dynamic model filtered turbidity is similar to the QA tests carried out by the site operators (both 44%), whereas the static models' RMSE is substantially greater (58%) than the QA tests but still within the QA tolerance limit of 0.1 NTU. Both of the models correctly identify the general seasonality of the filtered turbidity, predicting that it will be greater in the autumn than in the spring (see Figure 4-23 and Figure 4-24).

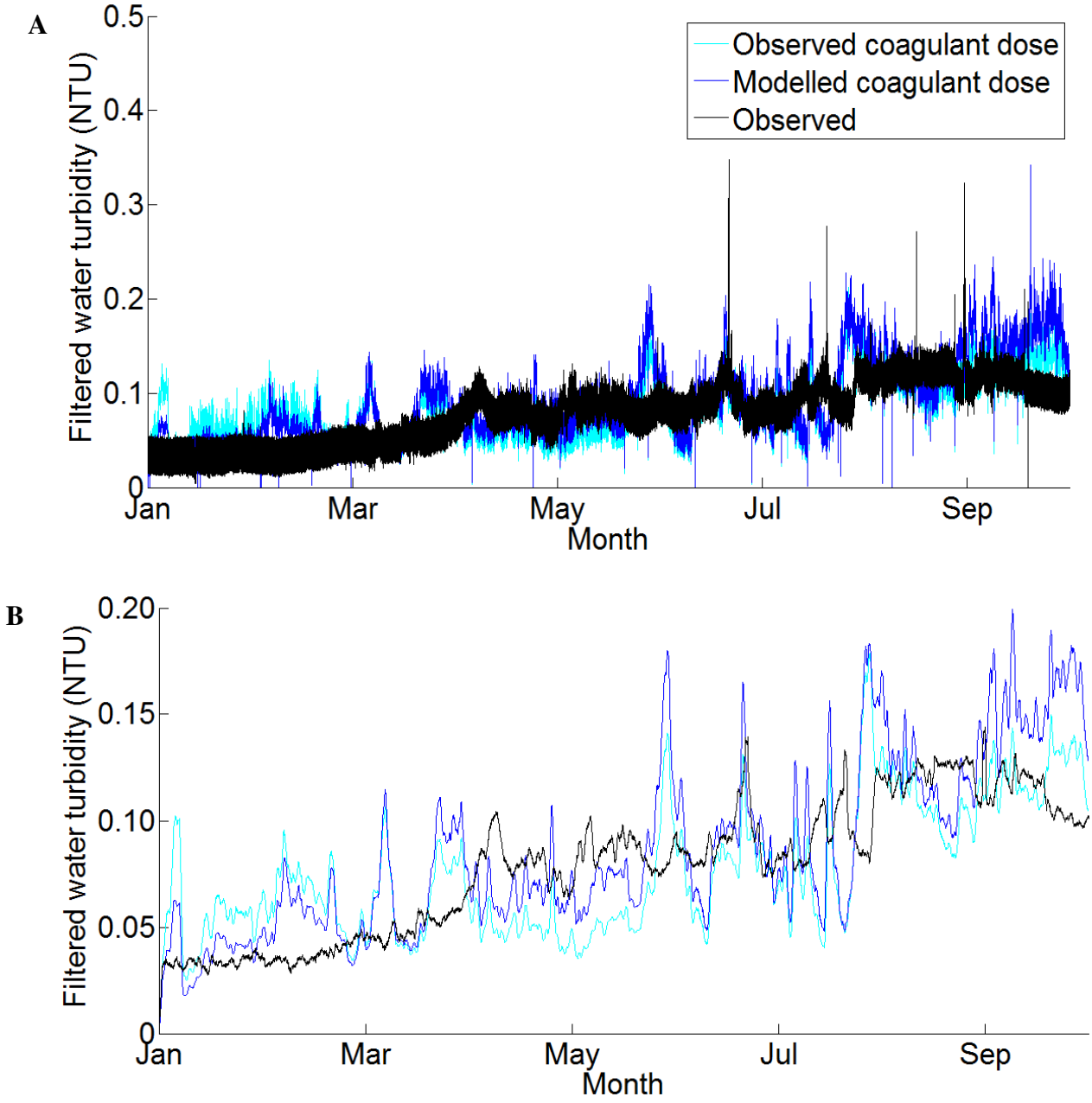

Figure 4-23 Dynamic RGF models performance

(A: 15 minute values, B: daily mean values)

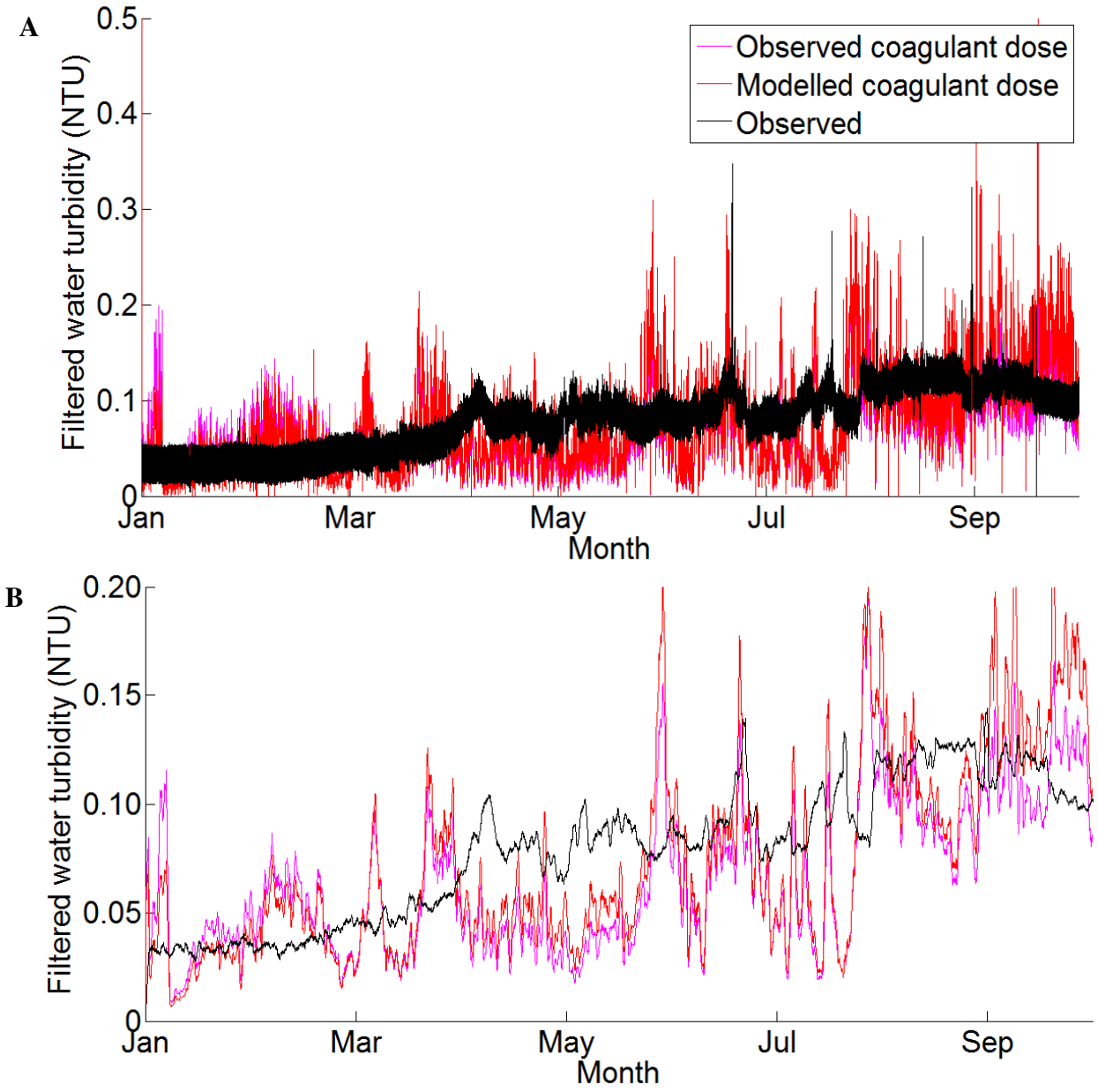

Figure 4-24 Static RGF models performance

(A: 15 minute values, B: daily mean values)

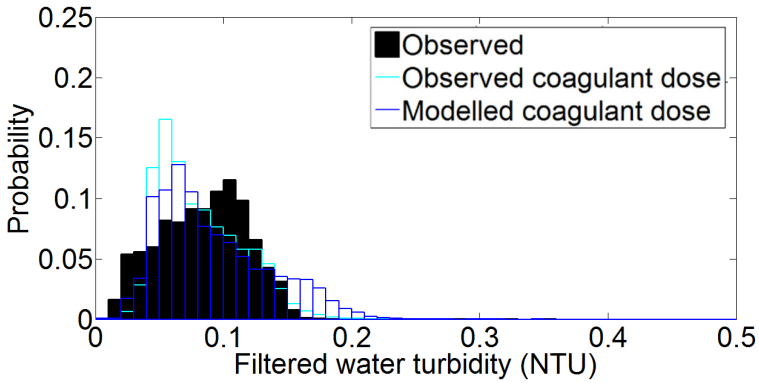

Figure 4-25 Dynamic filtered turbidity PDF

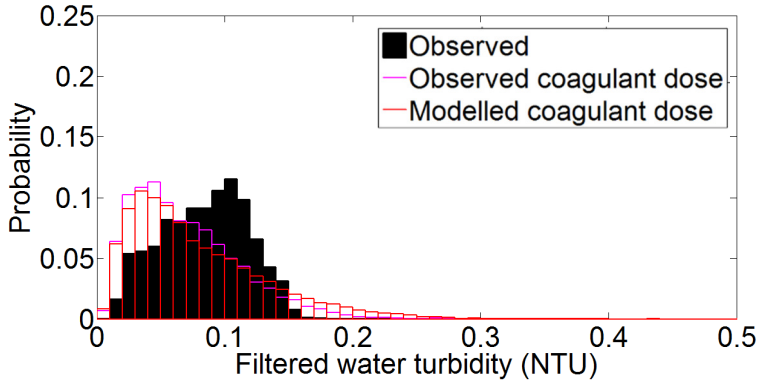

Figure 4-26 Static filtered turbidity PDF

Empirical solids removal efficiency parameters

The use of the empirical solids removal efficiency parameters discussed in section 4.3.1, results in an average reduction in RMSE of approximately 15% when the verification data were applied (see Table 4-12).

Table 4-12 Improvement in turbidity prediction for 2012 verification data

Model	**Outlet Turbidity**	**RMSE (NTU) for efficiency parameter**		**Reduction in RMSE**
		Consistent	**Reservoir water NTU dependent**	
Static	HBC	0.2881	0.2457	15%
	DAF	0.3618	0.3417	6%
	Combined clarified	0.3964	0.3169	20%
	Filter	0.0575	0.0456	21%
Dynamic	HBC	0.207	0.1844	11%
	DAF	0.2972	0.2812	5%
	Combined clarified	0.3265	0.2581	21%
	Filter	0.0436	0.0349	20%

Disinfection

The contact tank residual free chlorine concentration is found to be under-predicted by the static and dynamic models, with mean and median values within -5% of those observed (see Table 4-13 and Table 4-14). The models predict a greater degree of deviation of residual free chlorine concentration, particularly the static model which does not model any degree of mixing within the contact tank. This unrepresentative variation in residual free chlorine concentration causes the RMSE of the models to be greater than both the QA tests and tolerance limits.

Table 4-13 Dynamic model residual free chlorine and CT accuracy

Parameter	Observed coagulant dose				Modelled coagulant dose				QA RMSE	QA tolerance
	$\bar{x}$	$\tilde{x}$	σ	RMSE	$\bar{x}$	$\tilde{x}$	σ	RMSE		
Cl (mg/l)	1.37 +5%	1.36 +5%	0.10 +67%	0.14 [11%]	1.38 +6%	1.38 +7%	0.09 +50%	0.14 [11%]	0.06 [5%]	0.1 [8%]
CT (mg.min/l)	114 +5%	113 +7%	21 ±0%	22 [20%]	114 +5%	114 +8%	20 -5%	22 [20%]	n/a	n/a

Table 4-14 Static model residual free chlorine and CT accuracy

Parameter	Observed coagulant dose				Modelled coagulant dose				QA RMSE	QA tolerance
	$\bar{x}$	$\tilde{x}$	σ	RMSE	$\bar{x}$	$\tilde{x}$	σ	RMSE		
Cl (mg/l)	1.37 +5%	1.36 +5%	0.14 +133%	0.17 [13%]	1.38 +6%	1.37 +6%	0.08 +33%	0.13 [10%]	0.06 [5%]	0.1 [8%]
CT (mg.min/l)	113 +4%	112 +6%	21 ±0%	23 [21%]	113 +4%	113 +7%	18 -14%	21 [19%]	n/a	n/a

Where: Cl = contact tank inlet free chlorine concentration (mg/l); CT = product of Cl and t_{10} contact time (mg.min/l), maximum value specified as 200 mg.min/l.

The static and dynamic models have similar accuracy, with mean values over-predicted by approximately 5% and a degree of variation similar to that observed at the works. The over-prediction of CT is due to the over-prediction in residual chlorine just discussed. The RMSE of the CT values by the models was approximately 20%. Some of this error is attributable to

the relatively high frequency reductions in discharge rates caused by backwashing of the rapid gravity filters and granular activated carbon beds which are triggered as required.

When the influence of the high frequency variation in discharge is smoothed by taking daily averages of values, as shown in Figure 4-27 and Figure 4-28, the models correctly identify periods of lower than and greater than average disinfection. When modelled, rather than observed, coagulant doses are applied to the models, the residual chlorine and CT mean values are similar (±1%). The degree of deviation of these values, however, decreases due to the stabilisation of the TOC concentration entering the contact tank. Figure 4-29 and Figure 4-30 show that the modelled CT distributions are more negatively skewed than that observed.

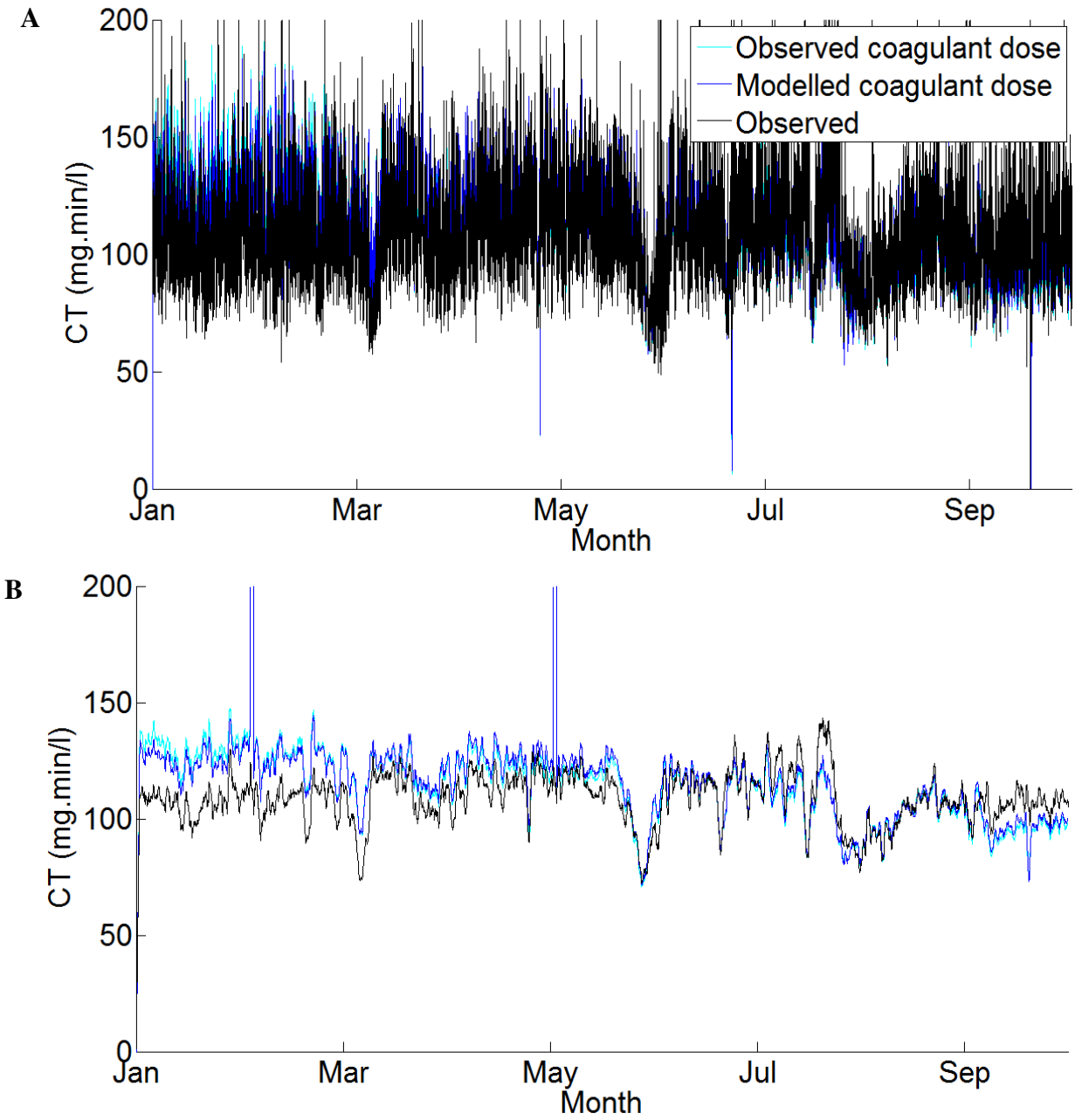

Figure 4-27 Dynamic disinfection models CT performance

(A: 15 minute values, B: daily mean values)

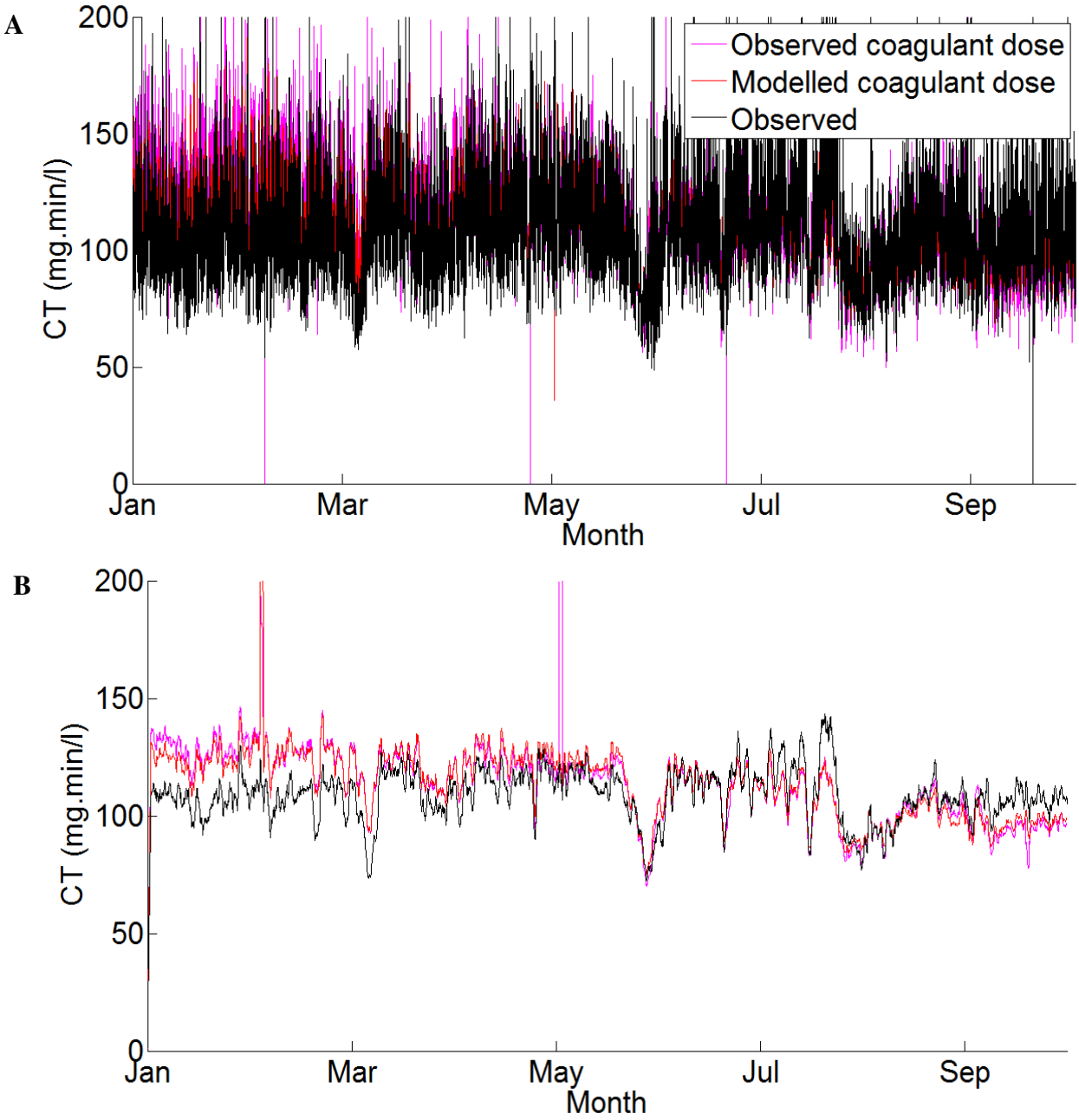

Figure 4-28 Static disinfection models CT performance

(A: 15 minute values, B: daily mean values)

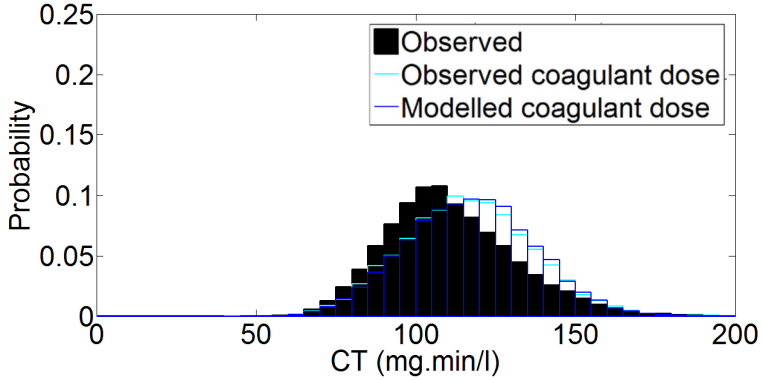

Figure 4-29 Dynamic CT PDF

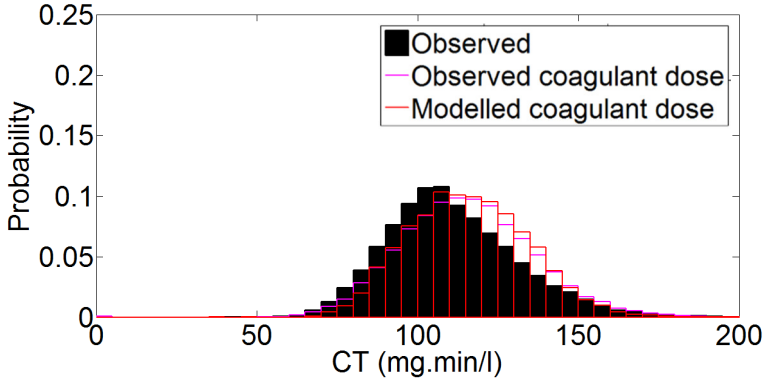

Figure 4-30 Static CT PDF

THM formation

The formation of THMs is under-predicted by the dynamic and static models with the mean predicted by the static model being under-predicted by approximately 20% and the static model under-predicted by approximately 30%. The dynamic model is also found to be more accurate in terms of median values predicted and RMSE value. Both of the models are less accurate than both the QA test and tolerance values set for THM concentrations (see Table 4-3 and Table 4-15). Despite the limited accuracy of the modelled THM concentrations, the seasonal sensitivity of the models is found to be accurate, with higher concentrations predicted in the summer months, as can be seen in Figure 4-31 to Figure 4-32.

Table 4-15 Modelled THM formation accuracy

Model	Observed coagulant dose				Modelled coagulant dose				QA RMSE	QA tolerance
	$\bar{x}$	$\tilde{x}$	σ	RMSE	$\bar{x}$	$\tilde{x}$	σ	RMSE		
Dynamic THM (µg/l)	7.84 -21%	9.07 -9%	4.77 +31%	3.03 [31%]	7.49 -24%	7.24 -27%	3.81 +5%	3.35 [34%]	[5%]	[12.5%]
Static THM (µg/l)	6.99 -29%	8.60 -13%	4.71 +30%	3.39 [34%]	7.19 -27%	7.64 -23%	3.55 -2%	3.47 [35%]	[5%]	[12.5%]

When the coagulant dose is modelled, to maintain a consistent clarified TOC, the standard deviation of THM concentrations reduces from +30% to ±5% of that observed. This, however, is found to have a limited influence on the RMSE accuracy of the model (±5%). Figure 4-33 and Figure 4-34 show the modelled THM production to be more positively skewed than that observed.

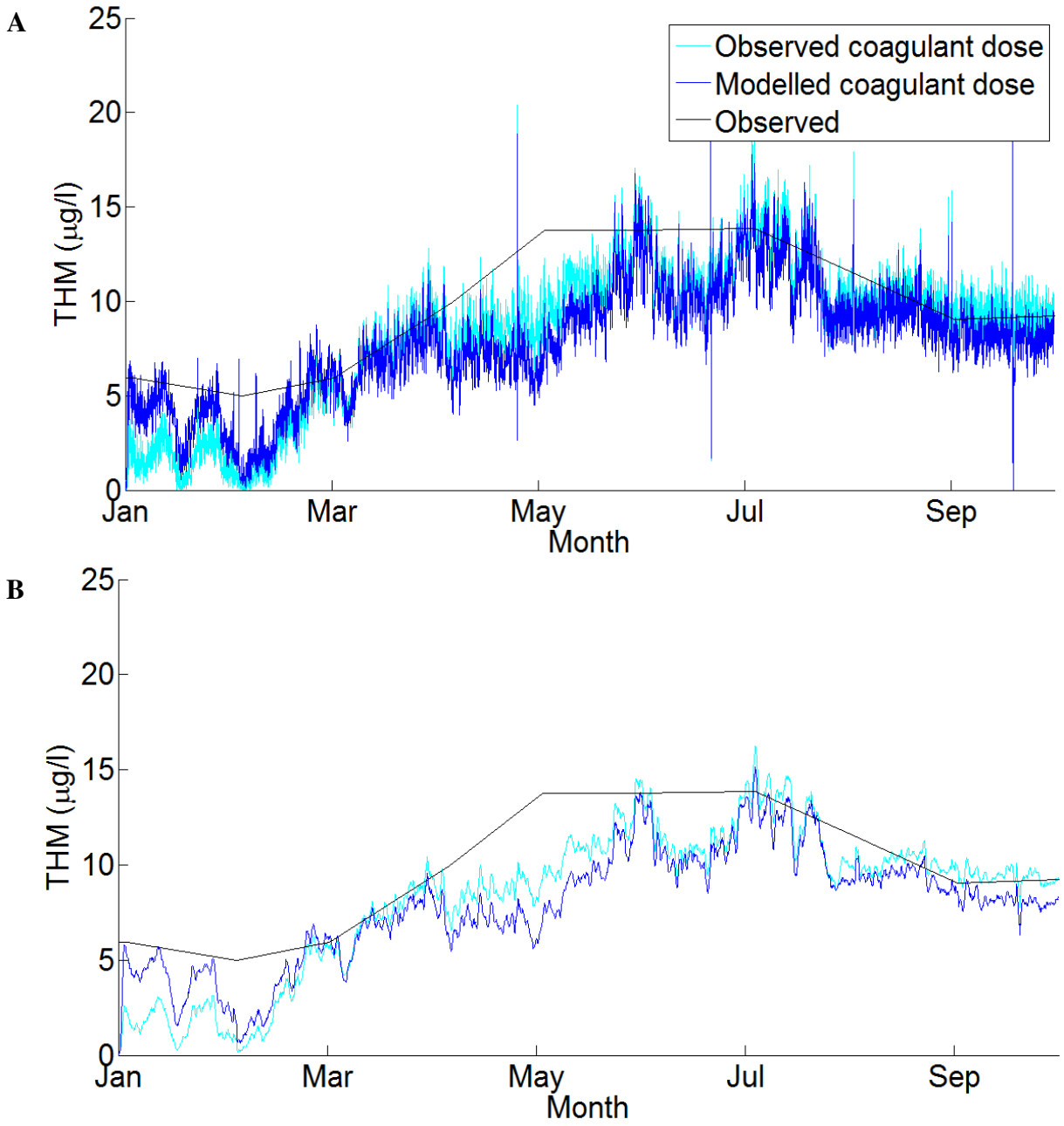

Figure 4-31 Dynamic disinfection models THM performance

(A: 15 minute values, B: daily mean values)

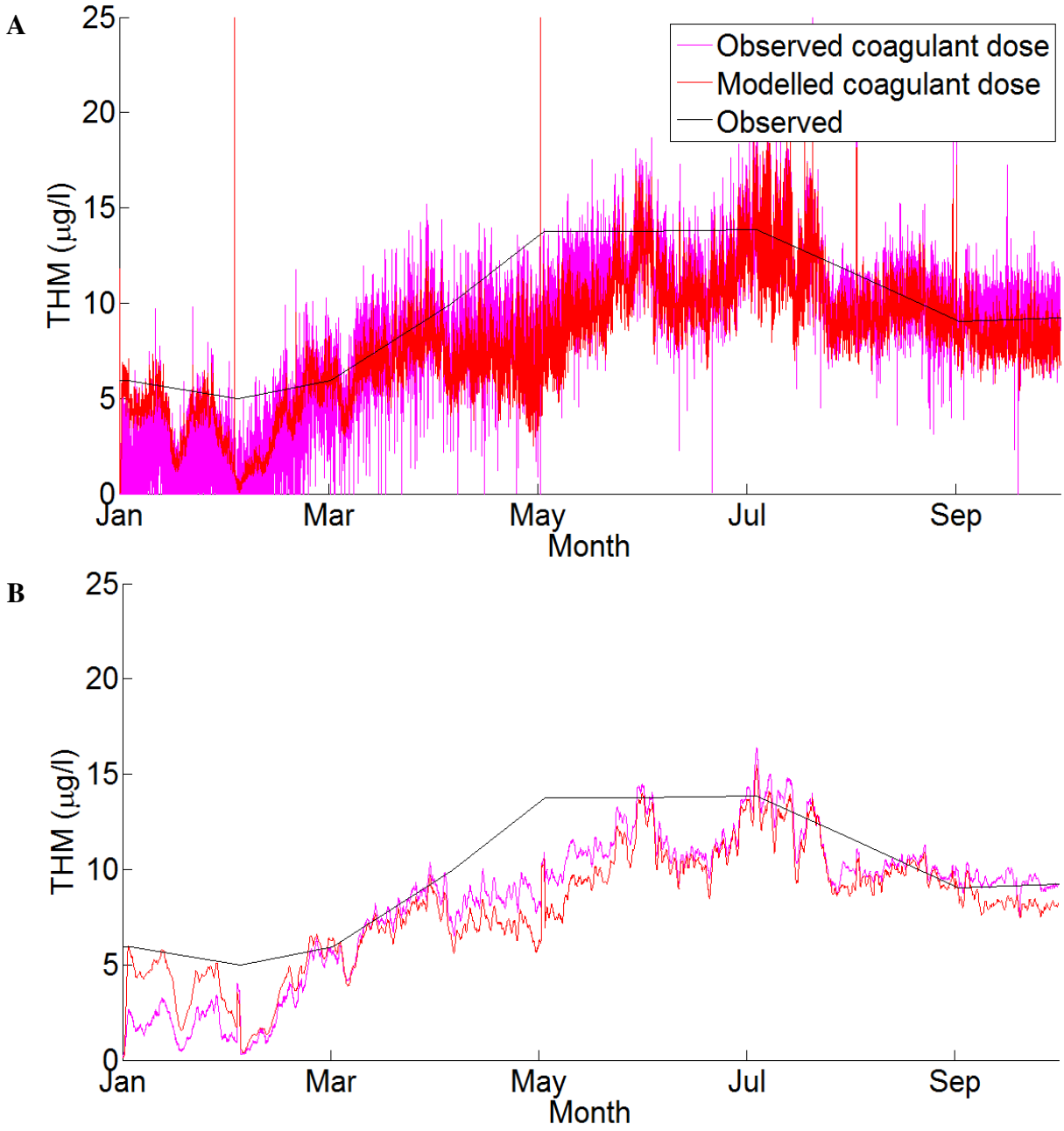

Figure 4-32 Static disinfection models THM performance

(A: 15 minute values, B: daily mean values)

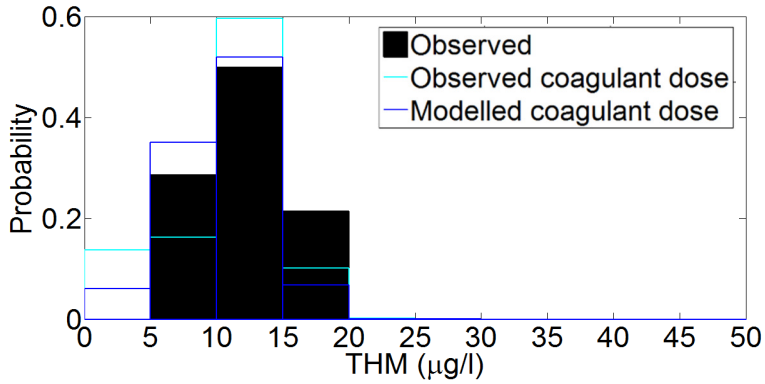

Figure 4-33 Dynamic THM PDF

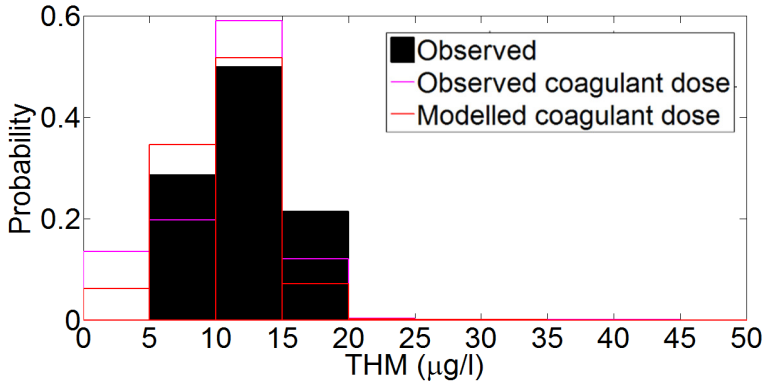

Figure 4-34 Dynamic THM PDF

4.4.2 Monte-Carlo (MC) simulation

In order that the performance of the WTW can be assessed for conditions other than those observed, synthetic time series data are produced using a Monte-Carlo approach. In the Monte-Carlo simulations, the model inputs are varied each simulated day for a simulated year, using randomly produced values from probability distributions that are representative of the conditions observed in 2012. The values are applied alongside coagulant doses calculated using the predictive algorithm. This technique allows an almost infinite combination of operating conditions to be applied to the WTW models.

The eSCADA and QA data collected from Trimpley WTW are assessed to see if they approximate to a selection of 'standard' distributions using the Anderson-Darling test (adtest) function within MATLAB. This test is used as it places greater emphasis on detecting if

outlying values depart from the distributions being assessed. The likelihood of the operating condition parameters coming from 'standard' distributions is shown in Table 4-16. As the operating conditions parameters are found to approximate to different or none of the 'standard' distributions, non-standard distributions (as shown in Figure 4-35 to Figure 4-43) are used to define each to maintain a consistent approach.

Table 4-16 Likelihood of parameters coming from 'standard' distributions

Distribution	**Normal**	**Exponential**	**Extreme value**	**Log normal**	**Weibull**
Alkalinity	✓	×	✓	×	✓
Bromide concentration	×	×	✓	×	×
Turbidity	×	×	×	×	×
pH	✓	×	✓	✓	✓
Abstraction rate	×	×	×	×	×
Water temperature	×	×	×	×	×
TOC concentration	✓	×	×	✓	✓
UV_{254} absorption	✓	×	✓	✓	✓
Contact tank inlet chlorine concentration	×	×	×	×	×

Where: × = null hypothesis that the data are from a population with specified distribution is rejected at the 5% significance level and ✓ null hypothesis is not rejected at the 5% significance level.

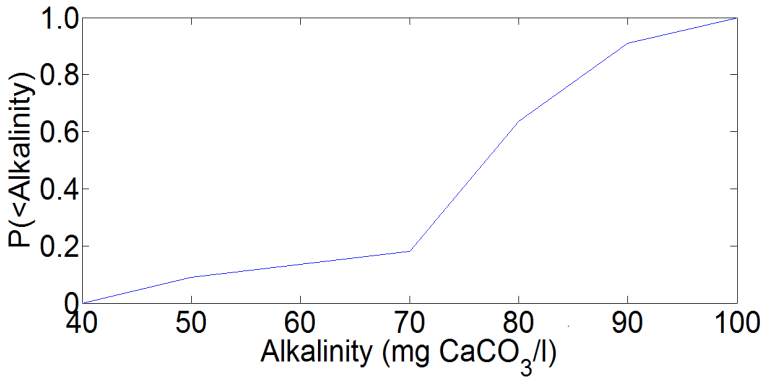

Figure 4-35 Alkalinity CDF

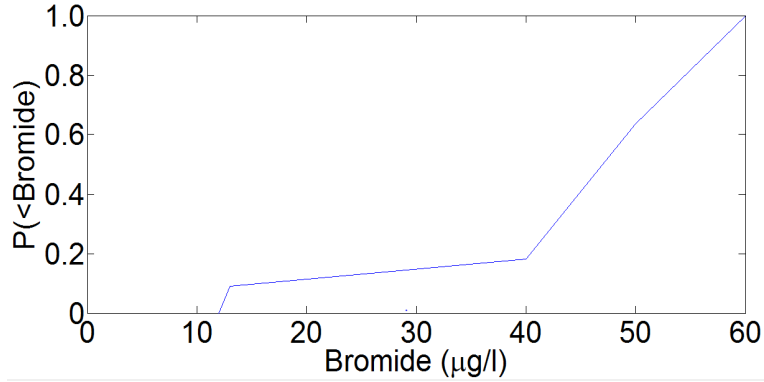

Figure 4-36 Bromide CDF

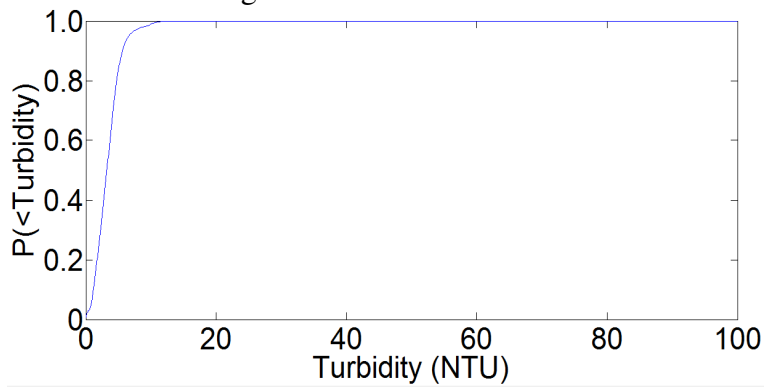

Figure 4-37 Turbidity CDF

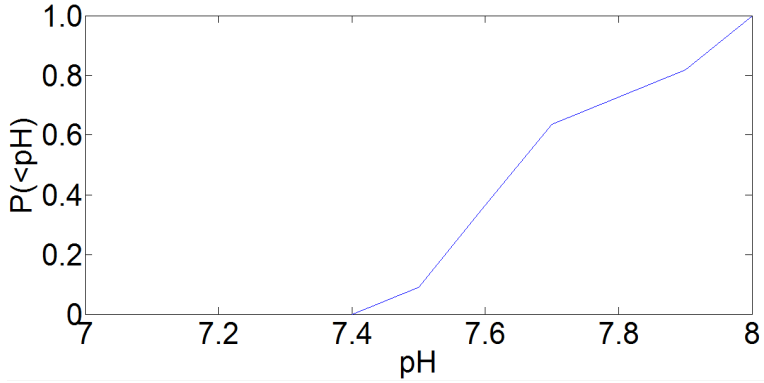

Figure 4-38 pH CDF

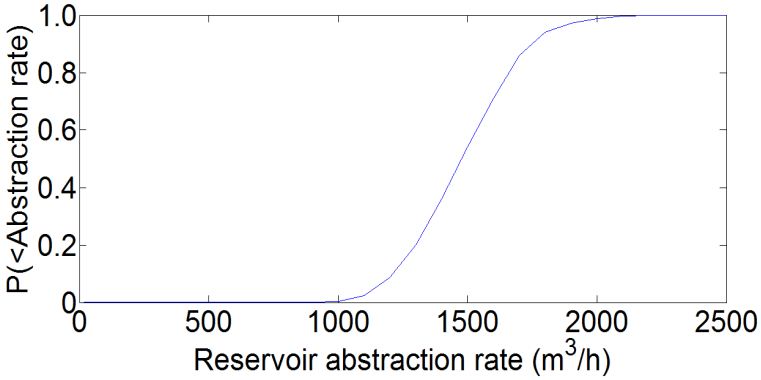

Figure 4-39 Abstraction rate CDF

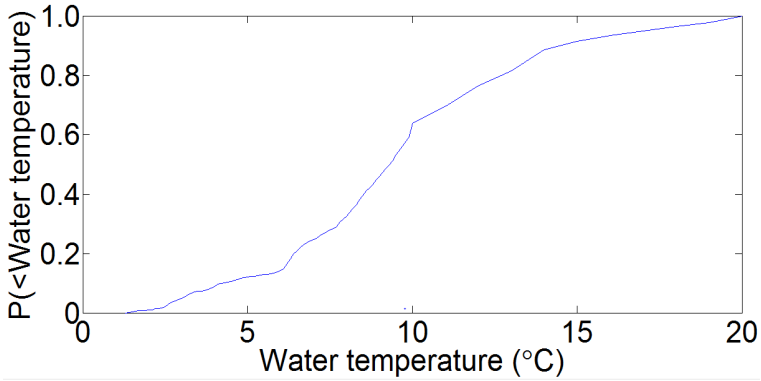

Figure 4-40 Water temperature CDF

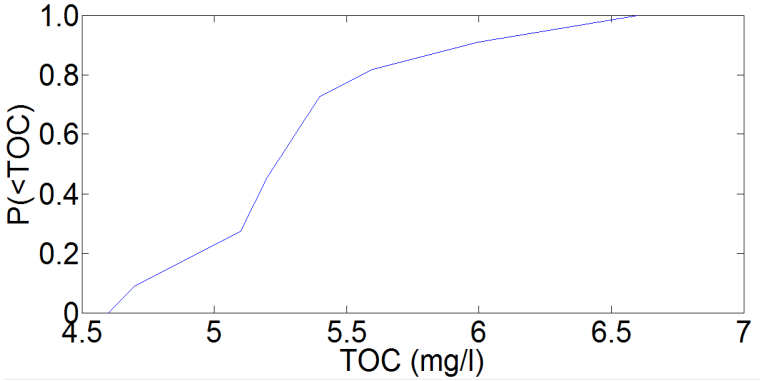

Figure 4-41 TOC CDF

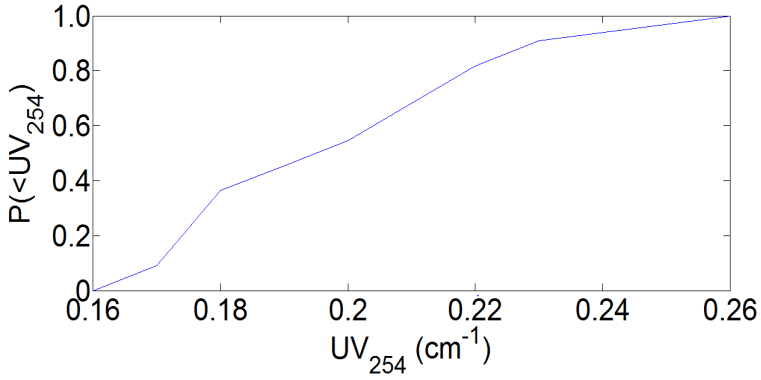

Figure 4-42 UV_{254} CDF

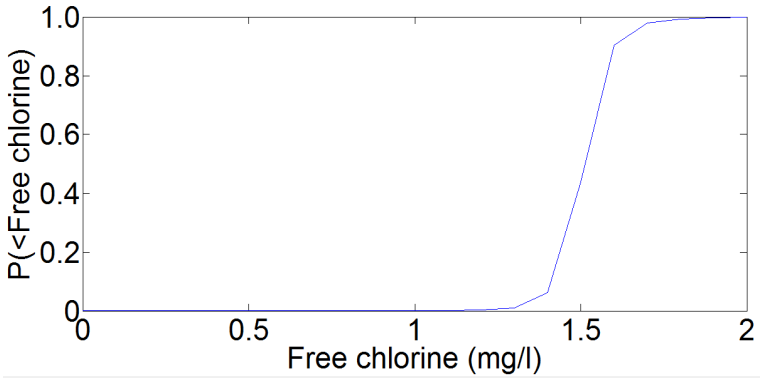

Figure 4-43 Inlet chlorine conc CDF

In the comparison of results which follows, the influence of applying Monte-Carlo conditions to the models is compared to the performance of the models when the time series data were applied along with modelled coagulant dosing (shown in section 4.4.1). This is done so that the influence of applying Monte-Carlo conditions can be observed more clearly.

Clarification flow rates

Under Monte-Carlo conditions, the mean, median and standard deviation of flow treated by each clarification stream is less than predicted under time series conditions (see Table 4-17). The mean flows vary by less than 1%, whilst the standard deviations vary by less than 10% between the three simulations run.

Table 4-17 Accuracy of Monte-Carlo modelled clarifier inlet flows

	Run 1			**Run 2**			**Run 3**			**Variance from time series results**		
Parameter	$\bar{x}$	$\tilde{x}$	**σ**	$\bar{x}$	$\tilde{x}$	**σ**	$\bar{x}$	$\tilde{x}$	**σ**	$\bar{x}$	$\tilde{x}$	**σ**
Q_{HBC} (m^3/h)	645	631	96	644	635	90	648	642	97	-4% to -3%	-4% to -3%	-8% to ±0%
Q_{DAF} (m^3/h)	788	772	118	785	777	110	786	777	118	-7% to -6%	-8% to -7	-4% to +3%

Clarified turbidity

Both the dynamic and static HBC models mean HBC clarified turbidity reduces under Monte-Carlo conditions (by more than 5%). The degree of deviation in HBC clarified turbidity reduces on average, with the most varied simulation having a standard deviation comparable to those predicted when time series data were applied (±5%). The DAF clarification models, in comparison, do not predict significantly reduced clarified turbidity under Monte-Carlo conditions and see a reduction in the deviation of results (see Table 4-18 and Table 4-19).

Table 4-18 Dynamic model Monte-Carlo clarified turbidity accuracy

Parameter	**Run 1**			**Run 2**			**Run 3**			**Variance from time series results**		
	$\bar{x}$	$\tilde{x}$	**σ**	$\bar{x}$	$\tilde{x}$	**σ**	$\bar{x}$	$\tilde{x}$	**σ**	$\bar{x}$	$\bar{x}$	**σ**
NTU_{HBC}	0.48	0.44	0.20	0.48	0.45	0.17	0.49	0.45	0.18	-9% to -8%	-8% to -6%	-15% to ±0%
NTU_{DAF}	0.66	0.64	0.14	0.66	0.65	0.14	0.66	0.64	0.16	-1%	-4% to -3%	+17% to +33%
NTU_{COMB}	0.59	0.57	0.15	0.59	0.57	0.14	0.59	0.56	0.15	-3%	-7% to -5%	±0% to +7%

Table 4-19 Static model Monte-Carlo clarified turbidity accuracy

Parameter	**Run 1**			**Run 2**			**Run 3**			**Variance from time series results**		
	$\bar{x}$	$\tilde{x}$	**σ**	$\bar{x}$	$\tilde{x}$	**σ**	$\bar{x}$	$\tilde{x}$	**σ**	$\bar{x}$	$\bar{x}$	**σ**
NTU_{HBC}	0.34	0.27	0.26	0.33	0.28	0.22	0.33	0.28	0.21	-18% to -15%	-16% to -13%	-22% to -4%
NTU_{DAF}	0.68	0.60	0.27	0.69	0.67	0.25	0.68	0.62	0.31	+3% to +5%	-6% to +5%	+14% to +41%
NTU_{COMB}	0.53	0.48	0.21	0.53	0.51	0.19	0.52	0.48	0.22	-4% to -2%	-9% to -4%	±0% to +16%

Although it is possible to observe substantial variation in the distribution of clarified turbidity between Monte-Carlo simulation runs in Figure 4-44 to Figure 4-47, the general profiles of the distributions are in agreement with those produced when time series data are applied (see Figure 4-18 to Figure 4-21).

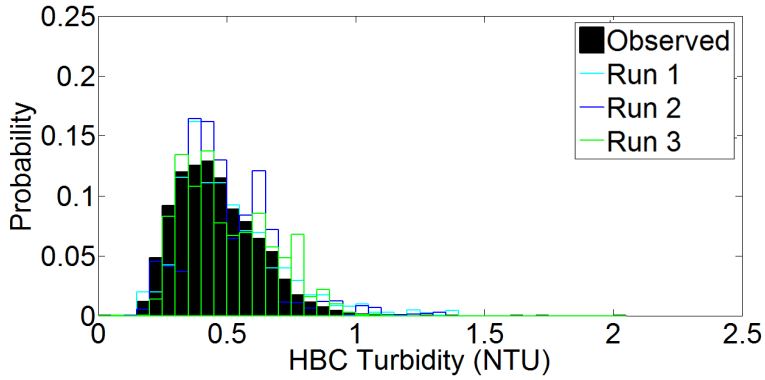

Figure 4-44 MC dynamic HBC turbidity PDF

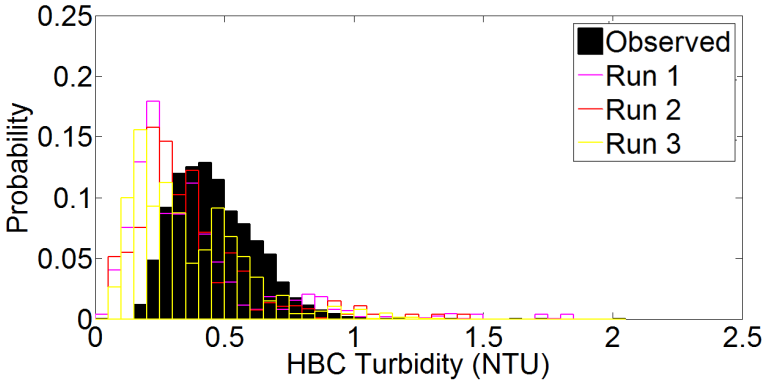

Figure 4-45 MC static HBC turbidity PDF

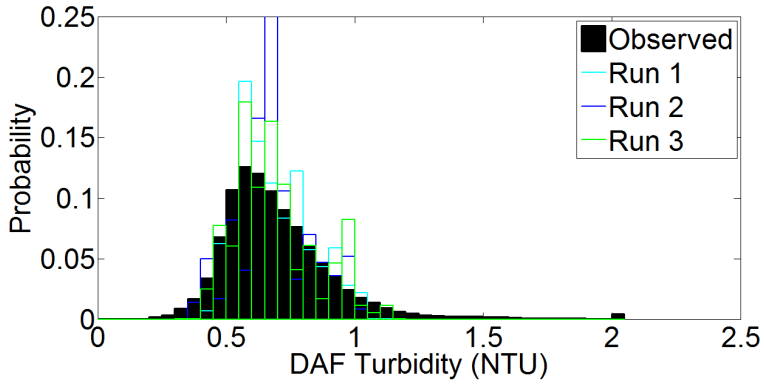

Figure 4-46 MC Dynamic DAF turbidity PDF

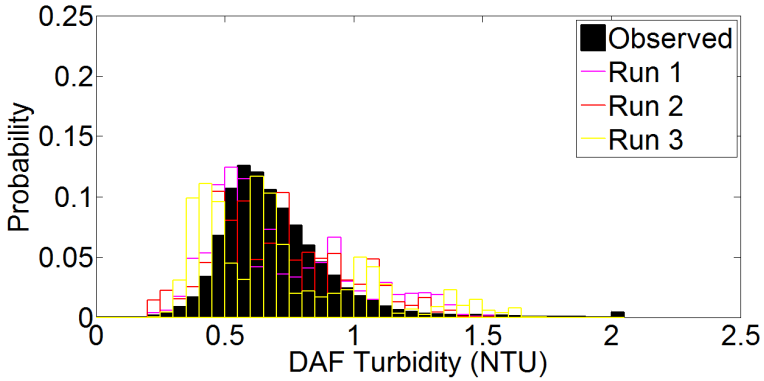

Figure 4-47 MC Static DAF turbidity PDF

Table 4-20 Modelled Monte-Carlo filtered turbidity accuracy

Model	**Run 1**			**Run 2**			**Run 3**			**Variance from time series results**		
	$\bar{x}$	$\tilde{x}$	**σ**	$\bar{x}$	$\tilde{x}$	**σ**	$\bar{x}$	$\tilde{x}$	**σ**	$\bar{x}$	$\bar{x}$	**σ**
Dynamic NTU_{FILT}	0.079	0.069	0.056	0.081	0.073	0.074	0.078	0.072	0.034	-10% to -7%	-9% to -4%	-21% to +72%
Static NTU_{FILT}	0.065	0.052	0.049	0.064	0.054	0.041	0.067	0.057	0.050	-14% to -9%	-15% to -7%	-23% to -6%

Filtered turbidity

The mean filtered turbidity predicted by both models is less than when time series conditions are applied (dynamic model filtered turbidity reduces by as much as 10%, static by 14%). The standard deviation from the dynamic model varies from -20% to +80% whilst the static model exhibits reduced deviation by as much as -20% of that predicted when time series operating conditions were applied (see Table 4-20). The distribution of filtered turbidity under Monte-Carlo conditions is seen to be comparable for the dynamic model but the static model distribution exhibits greater positive skew (see Figure 4-48 and Figure 4-49).

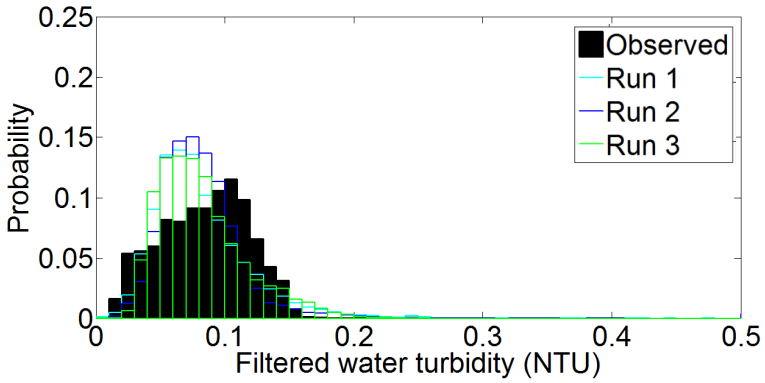

Figure 4-48 MC dynamic filtered turbidity PDF

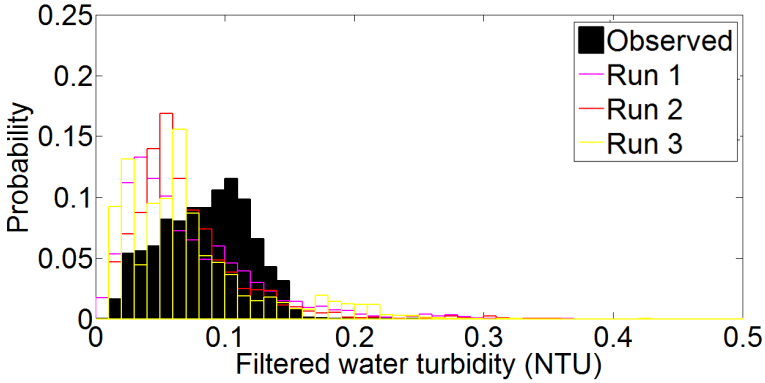

Figure 4-49 MC static filtered turbidity PDF

Disinfection

The mean contact tank residual free chlorine concentration is predicted by both models to increase by 3% under Monte-Carlo conditions, whilst the degree of variation decreases. This contributes towards mean CT values increasing by 7%. The increased CT values have greater absolute standard deviations of +10% to +20%, but have similar relative standard deviations as those observed under time series operating conditions (within +5%) (Table 4-22 and Table 4-21). The distribution of CT under Monte-Carlo conditions is seen to skew negatively in agreement with the increase in mean values observed but otherwise the distribution is similar as for time series conditions (see Figure 4-29, Figure 4-30, Figure 4-50 and Figure 4-51).

Table 4-21 Dynamic model Monte-Carlo residual free chlorine and CT accuracy

Parameter	**Run 1**			**Run 2**			**Run 3**			**Variance from time series results**		
	$\bar{x}$	$\tilde{x}$	**σ**	$\bar{x}$	$\tilde{x}$	**σ**	$\bar{x}$	$\tilde{x}$	**σ**	$\bar{x}$	$\bar{x}$	**σ**
Cl (mg/l)	1.42	1.42	0.05	1.41	1.42	0.07	1.42	1.42	0.07	+2% to +3%	+3%	-44% to -22%
CT (mg.min/l)	122	120	22	121	120	20	121	120	21	+6% to +7%	+5%	±0% to +10%

Table 4-22 Static model Monte-Carlo residual free chlorine and CT accuracy

Parameter	**Run 1**			**Run 2**			**Run 3**			**Variance from time series results**		
	$\bar{x}$	$\tilde{x}$	**σ**	$\bar{x}$	$\tilde{x}$	**σ**	$\bar{x}$	$\tilde{x}$	**σ**	$\bar{x}$	$\bar{x}$	**σ**
Cl (mg/l)	1.42	1.43	0.06	1.41	1.42	0.07	1.42	1.42	0.07	+2% to +3%	+4%	-25% to -13%
CT (mg.min/l)	122	120	22	121	119	20	121	119	19	+7% to +8%	+5% to +6%	+6% to +22%

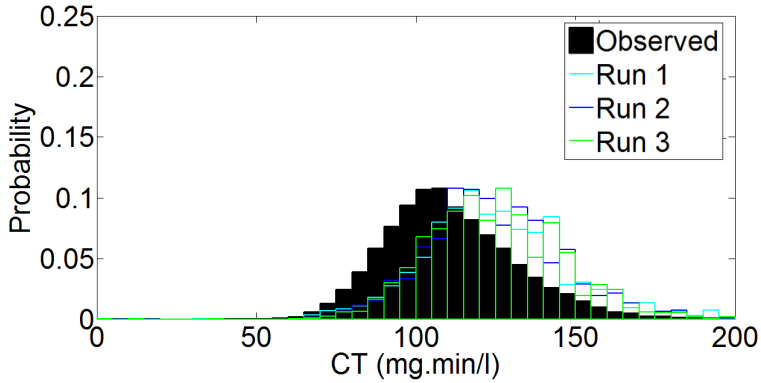

Figure 4-50 MC dynamic CT PDF

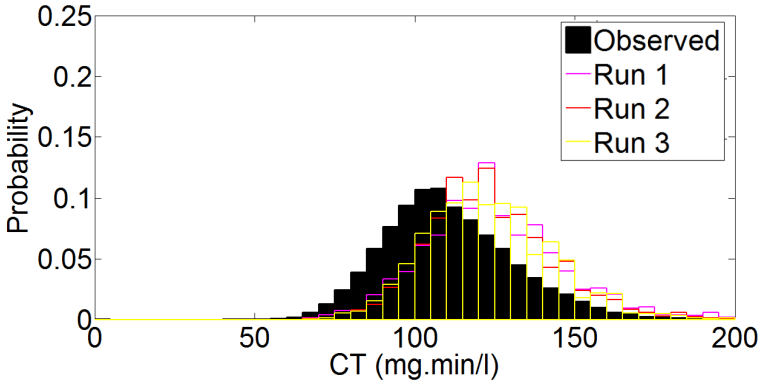

Figure 4-51 MC static CT PDF

THM formation

Due to the reduction in predicted free chlorine consumed under the Monte-Carlo conditions, the mean production of THMs is also predicted to decrease, by up to 14% for the dynamic model and 19% for the static model. The degree of variation in THM production is also found to reduce for both models by approximately 40% (see Table 4-23). This overall reduction in THM production also results in the likelihood that the concentration of THMs will be greater than 15 µg/l decreasing, as seen in Figure 4-33, Figure 4-34, Figure 4-52 and Figure 4-53.

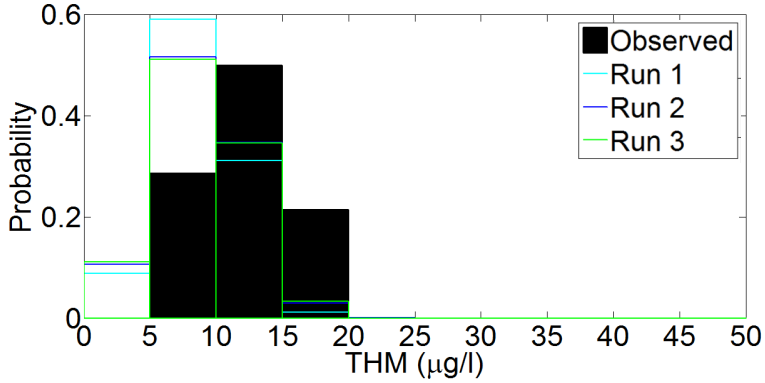

Figure 4-52 MC dynamic THM PDF

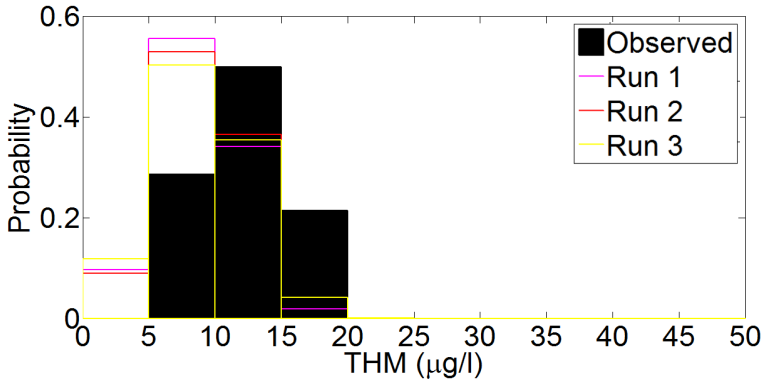

Figure 4-53 MC static THM PDF

Table 4-23 Modelled Monte-Carlo THM formation accuracy

Model	Run 1			Run 2			Run 3			Variance from time series results		
	$\bar{x}$	$\tilde{x}$	σ	$\bar{x}$	$\tilde{x}$	σ	$\bar{x}$	$\tilde{x}$	σ	$\bar{x}$	$\bar{x}$	σ
Dynamic THM (µg/l)	7.06	6.96	2.44	6.44	6.64	3.01	6.65	7.29	2.30	-14% to -6%	-8% to +1%	-40% to -21%
Static THM (µg/l)	6.83	7.62	3.20	5.85	5.75	3.06	6.95	7.59	2.08	-19% to -3%	-25% to ±0%	-41% to -10%

4.4.3 Failure rate analysis

In order to have an indication of how well the models will be able to optimise the design and operation of a water treatment works (WTW) it is important to know how accurately the models predict when a WTW's performance will not meet set performance criteria. The performance criteria selected to represent "good" operation are described in this section followed by an assessment of how well the models managed to predict the likelihood of failing the criteria.

4.4.3.1 *Performance criteria*

In order to perform optimisations using the WTW models, it is necessary to identify "good" performance criteria to be achieved. These criteria are listed in Table 4-24.

Table 4-24 Good operating performance criteria

Failure parameter	Failure condition
Blended clarified turbidity	> 1 NTU
Filtered turbidity	> 0.1 NTU
Free chlorine concentration multiplied by contact time (CT)	< 60 mg.min/l
Trihalomethanes (THM)	> 25 µg/l
Flow through DAF clarification	> 300 m^3/h
Flow through HBC tank	> 200 m^3/h

The blended clarified turbidity target is set as 1 NTU, which is greater than the observed mean value of 0.6 NTU for in 2011. The target turbidity is equivalent to the WTW final water legislative limit (2010), allowing clarification and filtration to act as a multiple barriers for achieving legislative compliance. The filtered turbidity target is set at 0.1 NTU to achieve final water turbidity comparable to the current quality (mean value observed for 2011 is 0.08 NTU). The degree of disinfection required is set as 60 mg.min/l, which is twice the recommended limit for treating reservoir abstracted waters (Cooperative Research Centre for Water Quality Treatment, 2007) and equivalent to the recommended limit for treating water directly abstracted from the river at the site (Morse, 2008). This limit is less than the observed mean degree of disinfection observed, which have a median value of 105 mg.min/l and a 5^{th} percentile value of 79 mg.min/l (the mean value is heavily skewed by a few extremely high values). It is assumed that approximately half of trihalomethanes (THMs) formed due to chlorination are formed in the distribution system, as indicated by Brown (2009). Therefore a WTW final water THM limit of 25 µg/l should result in THM concentrations at customers' taps being kept at approximately half of the legislative limit of 100 µg/l (Water Supply Regulations, 2010). This THM limit is above the mean concentration of 9.4 mg/1 observed in 2011. The maximum discharges of the clarification processes are based on the process specifications for Trimpley WTW (Severn Trent, 2011). The individual DAF tanks have their discharge limited to 292 m^3/h, and the HBC tanks are limited to 200 m^3/h.

4.4.3.2 *Failure rate results*

The likelihood of failing clarified and filtered turbidity, CT and THM performance targets is predicted to within 15% for both models when time series data or Monte-Carlo conditions are applied (see Table 4-25 and Table 4-26 for details).

When the time series operating conditions are applied, with actual and predicted coagulant doses, the static model is more accurate at predicting the likelihood of the DAF clarified turbidity increasing above 1 NTU than the dynamic model. The static model is able to predict the likelihood of failing this criteria within 2% whilst the dynamic model significantly under-predicts this failure rate by more than 5%. Under Monte-Carlo conditions, the likelihood of DAF clarified turbidity exceeding 1 NTU predicted by the dynamic model remains similar whilst the static model's failure rate approximately trebles.

The dynamic model's ability to predict the failure likelihood of the HBC clarified turbidity criteria is good, being within ±0.1% of that observed for time series operating conditions with actual coagulant doses applied. The static model, in comparison, over-predicts the failure rate by 1%. When predicted coagulant dosing is applied to the models, due to the mean increase in dose, the likelihood of failure of the HBC turbidity criteria increases for both models. This failure likelihood reduces by up to 2% when Monte-Carlo condition are applied.

Under time series conditions with actual coagulant doses applied both of the models under-predict the likelihood of the filtered turbidity exceeding 0.1 NTU by approximately half. When predicted coagulant dosing is applied, the predicted failure rate of both of the models increases by more than 5% and when Monte-Carlo conditions are applied the likelihood of exceeding 0.1 NTU reduces by up to 15%.

The likelihood of the degree of disinfection, as measured by CT, falling below 60 mg.min/l is accurately predicted by both models to within 0.1%. However, when Monte-Carlo conditions are applied the likelihood of failure of this criteria falls below the models' detection limits. Exceeding the THM concentration limit is not predicted to occur by the models in agreement with the observed measurements. Any prediction of the THM concentration exceeding 25 µg/l

will therefore be likely to be for conditions beyond the range of conditions observed in the 2012 verification data set.

Table 4-25 Failure likelihood observed and predicted by dynamic WTW model

Parameter	Observed	Modelled with observed coagulant dose	Modelled with TOC dependent coagulant dose	MC run 1	MC run 2	MC run 3
DAF (> 1 NTU)	6.8%	0.2%	1.0%	0.6%	0.3%	2.2%
HBC (> 1 NTU)	0.1%	0.1%	2.4%	2.3%	2.2%	0.2%
COMB (> 1 NTU)	7.5%	0.0%	0.4%	1.2%	0.8%	0.1%
FILT (> 0.1 NTU)	30.7%	18.1%	27.0%	15.2%	10.2%	15.3%
CT (< 60 mg.min/l)	0.1%	0.2%	0.2%	0.0%	0.0%	0.0%
THM (> 25 µg/l)	0.0%	0.0%	0.0%	0.0%	0.0%	0.0%

Table 4-26 Failure likelihood observed and predicted by static WTW model

Parameter	Observed	Modelled with observed coagulant dose	Modelled with TOC dependent coagulant dose	MC run 1	MC run 2	MC run 3
DAF (> 1 NTU)	6.8%	5.0%	5.7%	14.4%	13.7%	18.7%
HBC (> 1 NTU)	0.1%	1.1%	4.0%	2.6%	1.8%	0.8%
COMB (> 1 NTU)	7.5%	0.2%	2.0%	2.1%	1.1%	3.9%
FILT (> 0.1 NTU)	30.7%	14.2%	21.5%	15.9%	10.9%	15.2%
CT (< 60 mg.min/l)	0.1%	0.2%	0.0%	0.0%	0.0%	0.0%
THM (> 25 µg/l)	0.0%	0.0%	0.0%	0.0%	0.0%	0.0%

4.5 Summary

This chapter described the creation of dynamic and static models of Trimpley WTW and their calibration and verification using a mixture of eSCADA and monthly water quality data from 2011 and 2012. The water quality at various stages of treatment was found to be reasonably consistent due to the necessity to provide an acceptable final water quality for consumers. This limited the range of operating conditions that were examined. In order to account for improved solids removal efficiency observed for higher turbidity waters, empirical relationships between reservoir turbidity and treatment efficiency parameters were developed for the solids removal models (clarification and filtration).

Using the static and dynamic models of Trimpley WTW, the following findings were observed:

- The coagulant dosing algorithm predicted similar doses and sensitivity to operating conditions as those applied by the operators at Trimpley (see Figure 4-22).
- The use of the empirical solids removal efficiency parameters resulted in an average reduction in RMSE of approximately 15%. Due to the increased complexity and less conservative predictions of WTW performance that these parameters introduce, the justification for application of similar relationships in future work is limited.
- The modelling of the DAF process was found to be complicated by the operational regime of bringing in additional tanks as they were required. The ability to replicate the DAF clarified turbidity was also limited by the different performance of the individual tanks due to operational setup and maintenance condition.
- The calibration of the filtration model was found to be problematic due to lack of turbidity breakthrough observed in the eSCADA data and an inability to replicate representative filter performance in pilot filter plants. A general, conservative estimate

of filter capacity was eventually applied, along with empirically determined attachment coefficients.

- The dynamic models were found to be more accurate than the static models. When observed time series input data were applied to the models, the RMSE of the dynamic model was found to be at least 5% less for the solids removal models (HBC and DAF clarified and rapid gravity filtered turbidity) and between 1% to 3% less for the disinfection models (residual chlorine concentration, CT and THM formation).
- Clarified and filtered turbidity was predicted with RMSEs less than 50%. Due to this relatively low degree of accuracy over annual periods, it seems that the justification for the complexity of some of the models along with the considerable amounts of calibration data they require is limited for whole works modelling.
- The dynamic filtration model was found to have a RMSE equivalent to that achieved by manual water quality tests made (0.035 NTU) and within the tolerance limit set for filtered turbidity measurements (0.1 NTU). The static filtration model had a slightly greater RMSE (0.045 NTU).
- Decay within the contact tank was modelled using parameters based on those reported by Brown (2009) for decay that occurs between 5 – 120 minutes after dosing. This method was found to under-predict chlorine decay, presumably because some of the initial chemical reactions with fast kinetics (represented by Brown as reactions that occurred in the first five minutes) were still occurring. The RMSE of the residual chlorine concentration using both models was approximately 0.15 mg/l.
- The under-prediction of chlorine consumption resulted in the degree of disinfection achieved (measured as CT) being over-predicted (+5%) and the production of THMs being under-predicted (-20% to 30%).

- The operating condition parameters (reservoir alkalinity, bromide concentration, turbidity, pH, abstraction rate, temperature, TOC, UV254 and contact tank inlet free chlorine concentration) were found to possibly approximate to different or no standard distributions (normal, exponential, extreme value, log normal or weibull) and so were represented by non-standard distributions.
- The pseudo-random sampling of the operating condition parameters each simulated day for a simulated year resulted in the mean values of the performance parameters varying by up to 15% with the dynamic model and up to 20% for the static model, compared with the application of time series operating conditions.
- The likelihood of failing clarified and filtered turbidity, CT and THM performance targets was predicted to within 15% for both models when time series data were applied under Monte-Carlo conditions.

5 OPTIMISATION CASE STUDY

The dynamic and static models developed and calibrated for Trimpley WTW are applied to three optimisation processes which are:

1. The identification of abstraction rates for which the WTW is predicted to operate acceptably for different raw water temperatures and total organic carbon (TOC) concentrations;
2. The application of the models along with a genetic algorithm to identify solutions for minimising footprint area and unacceptable performance;
3. The application of the models along with a genetic algorithm to identify solutions for minimising operating costs and unacceptable performance.

The University of Birmingham's BlueBEAR high powered computing cluster (HPC) is used to complete the optimisations. Optimisations are carried out using multiple 48 hour sessions on a single core of a 64-bit 2.2 GHz Intel Sandy Bridge E5-2660 worker with 32 GB of memory. This chapter describes the methods, results, analysis and conclusions of these optimisations.

5.1 Operating zone identification

As the operating conditions change at a WTW, the range of abstraction rates which result in a final water of an acceptable water quality varies. For instance, for a raw water with a specific water quality, if the abstraction rate was set too high then the solids removal processes would be overloaded and final water would be unacceptably turbid. Alternatively, for the same conditions, if the abstraction rate was set too low then the contact time would be excessively long and the formation of disinfection by-products could be unacceptably great. An "operating zone" defines the range of operating conditions for which a WTW is expected to produce water

of an acceptable water quality. This operating zone could be used by operational and resource planning staff to predict the range of abstraction rates at which WTWs should be operated depending on raw water quality. The use of this information could reduce the frequency at which final water of an unacceptable water quality is produced.

In defining the operating zone for Trimpley WTW, temperature and TOC concentration are selected as variable parameters alongside abstractions rate due to their influence on both the solids removal and disinfection processes. Other water quality, design and operational parameters are assigned set values approximately equivalent to those observed in 2011. Coagulant dose is predicted using the method described in section 4.3.3. The values applied are given in Table 5-1. The water quality is assumed to be of an acceptable quality if the "good" performance criteria (as defined in section 4.4.3.1) are achieved.

Table 5-1 Operating zone parameters used

Parameter	**Value**
HBC units	10
DAF units	7
RGF units	8
Contact tank volume	2400 m3
Filtration run length	48 hours
Proportion of abstracted water	0.55
DAF compressor pressure	400 kPa
Contact tank inlet free Cl	1.6 mg/l (1.56 mg/l observed)
Reservoir turbidity	5 NTU (4.7 NTU observed)
Reservoir alkalinity	80 mg/l as CaCO3 (78 mg/l observed)
Reservoir UV254	0.17 cm-1 (0.173 cm-1 observed)
Reservoir pH	7.7 (7.72 observed)
Reservoir bromide	50 (63 µg/l observed)
Reservoir TOC concentration	1 to 10 mg/l in single unit increments (range 3.3 mg/l to 6.2 mg/l observed)
Reservoir temperature	0 to 30 ^{0}C in single unit increments (range 1.7 ^{0}C to
Abstraction rate	100 to 2500 m3/h in 100 m3/h increments (maximum
Clarified TOC target	2.5 mg/l
Time simulated	50 hours spin up, 50 hours measured

A range of reservoir TOC concentrations and temperatures are applied, beyond but of the same magnitude to those observed in 2011. Abstraction rates vary from a minimum value of 100 m^3/h and increase in 100 m^3/h increments until a complete maximum discharge surface is identified. The clarified TOC target value is selected as being representative of operating conditions at Trimpley, as described in chapter four. As the filtration run length is set at forty eight hours and the minimum abstraction rate is set at 100 m^3/h, the maximum theoretical contact tank retention time is twenty four hours. Fifty hours is therefore reasoned, and found, to be a sufficient simulated time for the models to initialise. The performance of the works is assessed over a subsequent fifty hour period, covering a period just over that taken to complete two complete filtration sequences.

The observed performance of the Trimpley WTW was "good" 67% of the time in 2011. The observed filtered turbidity failed to meet the "good" criteria 31% of the time, blended clarified turbidity 1.6% and disinfection, as measured by CT, 0.16%. The "good" performance criteria has to be met 90% of the time for a solution to be acceptable, an improvement on the performance currently observed but of the same magnitude. The models are simulated for every combination of reservoir TOC concentration, temperature and abstraction rate listed in Table 5-1 (7750 combinations) and operating zones are identified. Surface plots are then produced of the minimum and maximum abstraction rates which achieve the "good" performance criteria (see section 5.1.1).

5.1.1 Operating zone results

The results of the operating zone analysis are shown in Figure 5-1 and Figure 5-2. These graphs show the range of abstraction rates for which acceptable works performance is predicted for varying raw water temperature and TOC concentrations. The maximum abstraction rates for which acceptable works performance is predicted is shown for the static and dynamic models as red and blue surfaces respectively and the minimum abstraction rate for which acceptable works performance is predicted is shown for the static and dynamic models as magenta and cyan surfaces respectively. Abstraction rates between these limits was predicted to result in acceptable works performance. These graphs also show the mean abstraction rates which were observed at Trimpley during 2012 for varying temperature and TOC concentration conditions.

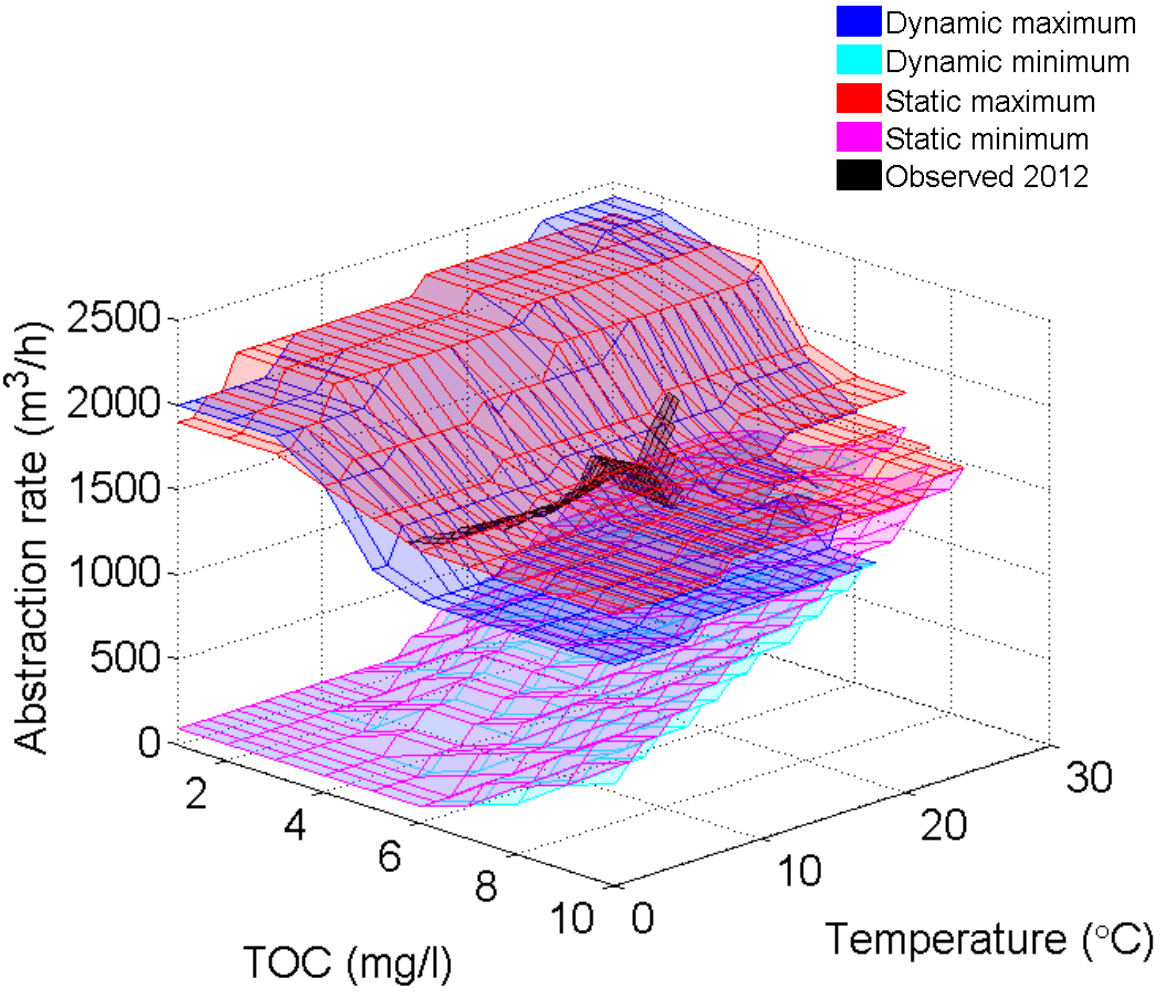

Figure 5-1 Predicted operating zone

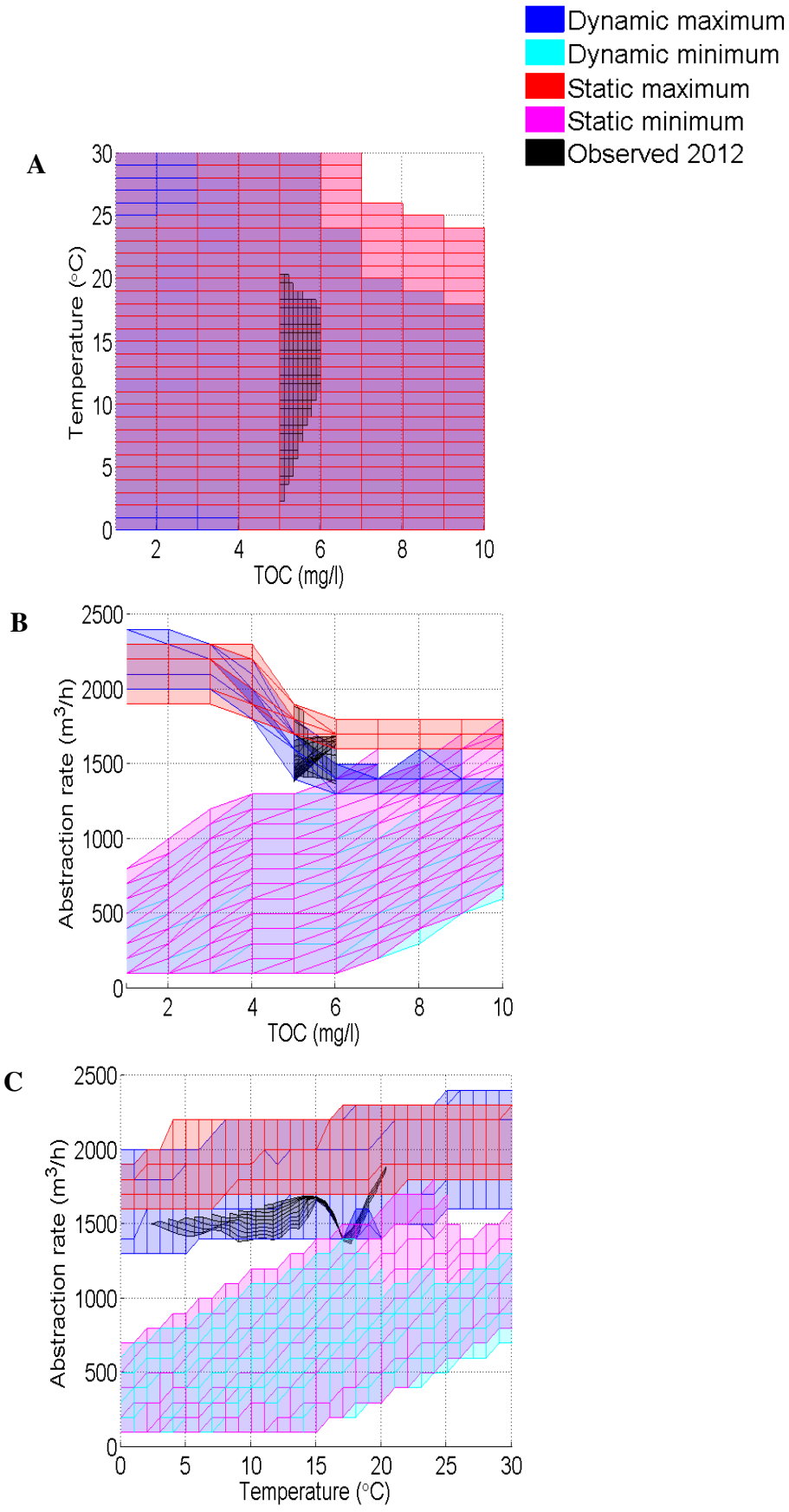

Figure 5-2 Individual relationships between operating zone parameters

5.1.2 Operating zone analysis

The abstraction rates identified using the dynamic and static models have similar minimum and maximum profiles (see Figure 5-1), indicating that the same causes of failure are likely to limit abstraction rates for both models. For raw water TOC concentrations below the clarified TOC target (2.5 mg/l), a minimal dose of coagulant will be added. For these conditions, the maximum abstraction rate is limited by the ability to achieve sufficiently low clarified and filtered turbidity.

Both models predict that for low raw TOC concentrations, the maximum abstraction rate increases by 400 m^3/h (20%), as the temperature increases from 0 ^{0}C to 30 ^{0}C (see Figure 5-2 C). For these low raw TOC concentration conditions, greater maximum abstraction rates are observed for higher temperatures. This is because the faster settling velocities caused by lower viscosities result in more efficient clarification.

For low raw organic compounds concentrations reduced free chlorine decay occurs, making failure due to insufficient disinfection and excessive THM formation unlikely. As the raw TOC concentration increases above the clarified target level, the maximum abstraction rates fall significantly due to the extra solids loading on the clarification and filtration stages (see Figure 5-2 B). This is due to the increased coagulant doses applied.

For waters cooler than 18 ^{0}C and initial TOC concentrations above 6 mg/l (where the maximum coagulant dose would have been applied), both models predict no correlation between the maximum abstraction rate and raw TOC concentration. For these elevated initial TOC concentrations, the clarified water TOC concentration will be above its target concentration. Although elevated TOC concentrations, for cooler waters, are not predicted to produce unacceptable WTW performance, the influence of higher TOC concentrations in the

distribution network could result in increased biological growth. For this reason, it could be desirable to set a target final water TOC concentration for works optimisation.

The vast majority of the reservoir water quality and operating conditions are set to consistent, representative values. Under these conditions, it is found that the dynamic model's maximum abstraction rate is more sensitive to TOC concentration and temperature than the static model's (57% greater range of values observed). The difference can be accounted for by the explicit modelling of water viscosity in the dynamic HBC and filtration models, not present in their static counterparts.

The dynamic model predicts a lower maximum abstraction rate for the majority of the operating zone (see Figure 5-1). The differing performance of the models indicates that, for the conditions set, the static model removes a greater proportion of the suspended solids introduced through coagulant addition than the dynamic model.

The models have comparable maximum abstraction rates when minimum coagulant doses are applied and the dynamic model has significantly lower maximum abstraction rates for higher coagulant doses. The maximum abstraction rates predicted by the two models have disparities of up to ±300 m^3/h for similar conditions.

The dynamic model's predictions of maximum discharges are below the mean operating conditions observed in 2011 for comparable conditions (see Figure 5-2). This indicates that the dynamic model gives a conservative estimate of maximum discharge, whilst the static model's predictions are vice-versa. It should be noted that the relative acceptable abstraction rates identified by both models may be dependent on the specific values used to define the raw water quality and operating conditions.

Acceptable minimal abstraction rates for both models are found to be dependent on reservoir water temperature and TOC concentration (see Figure 5-1). Higher temperatures and initial TOC concentrations result in increased THM formation or reduced disinfection (as measured by CT value). The minimal abstraction rates become more significant at temperatures above 18 ^{0}C and initial TOC concentrations above 6 mg/l. Under these conditions, the maximum and minimum abstraction rates converge, making acceptable treatment unachievable (see Figure 5-2). Under these conditions, abstractions rates are either too high to achieve acceptable solids removal, or too low to achieve low enough THM concentrations or high enough CT values. The lower maximum abstraction rates predicted by the dynamic model result in its "untreatable" zone being larger than that identified by the static model. In practice, under these "untreatable" conditions, the operational regime of the works could be altered to either improve solids removal (i.e. higher DAF compressor pressure) or the chlorine consumption could be reduced temporally, assuming sufficient disinfection could still be achieved. In 2012 these "untreatable" conditions were not observed at Trimpley WTW.

The use of operational zone graphs could assist operators, or automated control systems, in the identification of suitable WTW abstraction rates, dependent on the observed water temperature and TOC concentration. This could result in the instances where a WTW's performance is substandard being reduced. In reality, all of the raw water quality and operational values set as constant values would vary and influence the performance of the works. The degree of variation from the assumed conditions would need to be taken into account when using the operating zone.

5.2 Genetic algorithm optimisations

Two separate optimisations are carried out based on the model developed of Trimpley WTW which was described in chapter four. A design optimisation to minimise the footprint of the works and an operating regime optimisation to minimise the operational costs of the works are carried out. In this section the optimisation problems are defined in greater detail, the optimisation process described and the results of the optimisations presented.

5.2.1 Footprint and failure rate optimisation

A multi-objective optimisation problem is set to minimise the footprint and failure likelihood of WTW designs for operating conditions similar to those observed at Trimpley WTW. Capital costs of WTW processes are traditionally specified by treated volumes independent of quality (McGivney and Kawamura, 2008, Gumerman et al., 1979b, Clark, 1982) rather than constructional considerations, such as volume and pump specifications. This resulted in the design of the works being optimised based on minimising the footprint area. The design options are limited (as shown in Table 5-3) and the failure likelihood is based on the performance criteria described in section 4.4.3.1. The operating regime of the works in terms of the target clarified TOC concentration, DAF compressor pressure, filtration duration and contact tank inlet chlorine concentrations are all set to be representative of those observed at Trimpley (as defined in Table 5-1). The performance of the designs is evaluated over simulated years, with water quality and abstraction rates sampled each simulated day, from probability distributions characteristic of conditions observed in the first nine months of 2012 (see section 4.4.2). The footprint areas of each process are based on the dimensions of the processes observed at the Trimpley site.

Table 5-2 Design options

Parameter	Range	Increments	Footprint
Proportion of water treated by DAF stream	0% to 100%	10%	None
HBC units	0 to 10	1	100 m^2 per unit
DAF units	0 to 10	1	40 m^2 per unit
RGF units	1 to 10	1	60 m^2 per unit
Contact tank volume (m^3)	400 to 4000	400	0.2 m^2/m^3

5.2.2 Operating cost and failure rate optimisation

The second objective function minimisation optimisation problem is carried out using the same method as that used in the footprint area optimisation problem except this time the design of the works is fixed and the operating regime parameters are varied. The problem set is to minimise the operating costs (as calculated in section 5.2.3) and failure likelihoods (as defined in section 4.4.3.1). The operating regimes are limited as shown in Table 5-3. The design of the works in terms of the numbers of clarification and filtration units, and the volume of the contact tank are set to be representative of Trimpley WTW as defined in Table 5-1.

Table 5-3 Operating regime options

Parameter	Range	Increments
Proportion of water treated by DAF stream	0% to 100%	1%
Target clarified TOC concentration (mg/l)	1 to 5	0.1
DAF compressor pressure (kPa)	300 to 700	10
Filtration run duration (hrs)	24 to 96	1
Contact tank inlet chlorine concentration (mg/l)	1 to 5	0.1

5.2.3 Operational costs

In order that different operating regimes can have their comparative costs compared, costing formulas are produced. All costs are calculated at current value (taken as being December 2012) and where historical data are used it was adjusted to current value based on the consumer price indices produced by the Office for National Statistics (2013).

The total annual comparative cost of operating the works are calculated as shown in Equation 5-1. The costing formulas and chemical costs are given in Appendix F.

$$£_{total} = £_{coagulant} + £_{DAF} + £_{backwash} + £_{sludge} + £_{Cl_2} + £_{SBS} + £_{lime} \quad \text{Equation 5-1}$$

Where: $£_{total}$ = total comparative cost (£); $£_{coagulant}$ = cost of coagulant (£); $£_{DAF}$ = cost of DAF clarification (£); $£_{backwash}$ = cost of filter backwashing (£); $£_{sludge}$ = cost of sludge disposal (£); $£_{Cl2}$ = cost of chlorination (£); $£_{SBS}$ = cost of sodium bisulphite (£) and $£_{lime}$ = cost of lime (£).

5.2.4 Identification of a robust parameterisation set for NSGAII

The optimisation of both objective function minimisation problems is carried out using genetic algorithms (GAs) based on the NSGAII method described in section 2.2.4.4. The NSGAII is modified for use in this work by introducing maximum and minimum limits and discrete values for the parameters to be optimised. These adjustments are made due to functional limitations of the models and also to reduce the computational demand, as only distinctly unique solutions are simulated.

In order to identify suitable internal parameters for the NSGAII algorithm, preliminary optimisations were carried out over 12 hours using a control set of parameters (pop = 30, P_c = 0.7, η_c = 20, p_m = 0.1 and η_m = 20) and alternative runs where individual parameters were adjusted. The final generation of solutions identified by the genetic algorithms were used to assess the effectiveness of the optimisations based on: how many unique solutions were identified; how many Pareto optimal solutions were identified (out of the global set) and the summation of the crowding parameter of the unique solutions (as described in section 2.2.3.4). The number of unique solutions along with the summation of the crowding parameter was used to assess the degree of convergence that had occurred and how well the search space had been explored. The crowding values for the failure probability and either the footprint area or

operating cost (depending on the optimisation being completed) were normalised by dividing by the greatest value observed for each value in the whole data set to balance the influence of the objective functions. The summation of the crowding factors did not include infinite values to allow comparison between the solutions. The results of this sensitivity analysis is shown in Table 5-4.

Through examination of the sensitivity analysis results, no clearly optimal set of parameters are identified for use in each optimisation problem but a few conclusions are be made about some of the parameters based on agreement across all of the runs carried out. A lower population of ten, a lower cross-over probability of 50% and a cross-over distribution index of thirty are identified as being more likely to result in premature convergence. They are considered to be more likely to result in premature convergence as their use results in less unique solutions and/or the reduction in the crowding parameter. It is also identified that a lower mutation probability is more likely to result in a greater number of Pareto solutions being identified and that the mutation distribution index has very little influence on the performance of the GA. The inability to clearly identify optimal parameters from this process is possibly due to complex interactions between the parameters (a complete cross comparison between the parameters was not completed due to the prohibitive computation demands of achieving this) and also due to the random nature of the process. The GA internal parameters finally applied (see Table 5-5) are based on the control set of parameters used in the sensitivity analysis with the reduction of the mutation probability down to 5% and the reduction of the cross-over distribution index to ten. The mutation probability is reduced based on the increased number of Pareto solutions identified through its use and the recommendations of De Jong (1975) and Grefenstette (1986). The cross-over distribution index meanwhile is reduced based on the assumption that higher values can result in premature convergence and the finding in Sharifi

(2009) that a value of ten resulted in the identification of a greater proportion of Pareto solutions and higher quality solutions than other values. The suitability of using a hundred generations is assessed by assessing the influence of simulating an additional hundred generations on the performance of the GA (see section 5.2.6.4).

To make the search for near-optimal solutions more thorough, and to reduce the influence of possible premature convergence, each optimisation is carried out three times using different initial random seeding of the Mersenne Twister random number generator (Matsumoto and Nishimura, 1998, Moler, 2008). The loss of Pareto solutions, a known deficiency of the NSGAII process is addressed through the compilation of a secondary population of all parent solutions identified through each population.

Table 5-4 Sensitivity analysis of GA parameters

	Footprint and failure rate optimisation						**Operating cost and failure rate optimisation**					
	Dynamic model			**Static model**			**Dynamic model**			**Static model**		
	Unique Solutions	**Pareto Solutions**	**Crowding**	**Unique Solutions**	**Pareto Solutions**	**Crowding**	**Unique Solutions**	**Pareto Solutions**	**Crowding**	**Unique Solutions**	**Pareto Solutions**	**Crowding**
Control	15	3	2.72	15	1	2.48	10	0	1.02	23	0	1.91
pop = 10	-11	-2	-1.83	-11	+2	-0.25	-9	±0	-1.02	-14	±0	-0.43
pop = 50	+17	-3	+0.02	±0	+4	-0.14	±0	±0	-0.05	-7	+1	-0.14
P_c = 0.5	±0	+3	+0.15	-5	+5	+0.22	-4	±0	-0.55	±0	+5	-0.41
P_c = 0.9	+9	-3	-0.48	-1	±0	+0.48	+7	+8	-0.20	-18	±0	+0.51
η_c =10	-1	-3	-0.24	-4	+1	+0.01	-2	+4	-0.21	+5	+3	+0.09
η_c =30	-1	-2	-0.83	-3	+8	-0.02	-2	±0	-0.15	-4	±0	+0.43
P_m = 0.05	-8	±0	-0.67	-4	+2	+0.20	+13	+20	-0.25	±0	+4	+0.16
P_m = 0.15	+1	-3	-0.42	-3	+5	-0.26	-5	±0	+0.06	±0	+13	-0.38
η_m =10	±0	±0	±0.00	-4	±0	-0.59	±0	±0	±0.00	-1	+7	+0.23
η_m =30	±0	±0	±0.00	-2	±0	-0.15	+7	±0	-0.20	-2	±0	+0.94

Table 5-5 NSGAII parameters used

pop	**P_c**	**η_c**	**P_m**	**η_m**	**Generations**
30	0.7	10	0.05	20	100

Where: pop = population; P_c = probability of cross-over; η_c = cross-over distribution index; P_m = probability of mutation and η_m = mutation distribution index.

5.2.5 Computational demand

The mean computational time required to simulate generations of solutions using the dynamic model is found to be between twice (for the operational cost optimisation) and eight times as long (for the footprint area optimisation) as that required by the static model (see Figure 5-3 and Figure 5-4). The relative simulation time of the dynamic model for single solutions is even greater, as the use of the static model results in more unique solutions typically having to be simulated each generation (see Table 5-6 and Table 5-7). The computational time required by the dynamic model, in both optimisations, is more dependent on the solutions simulated, with less optimised solutions in earlier generations taking considerably longer to simulate than later generations and considerable difference in simulation speed between the different runs due to the random nature of the solutions identified (see Figure 5-3 and Figure 5-4). In the operating zone identification (section 5.1), the dynamic model is observed to take considerably longer to simulate conditions where the reservoir TOC concentration is similar to the clarified target value. This indicates that the computational resources required to optimise the dynamic model are dependent on the solutions and conditions modelled and that greater restriction of the possible solution parameters could result in reduced demands. Overall, the static model is found to simulate generations of solutions more quickly and more reliably than the dynamic model.

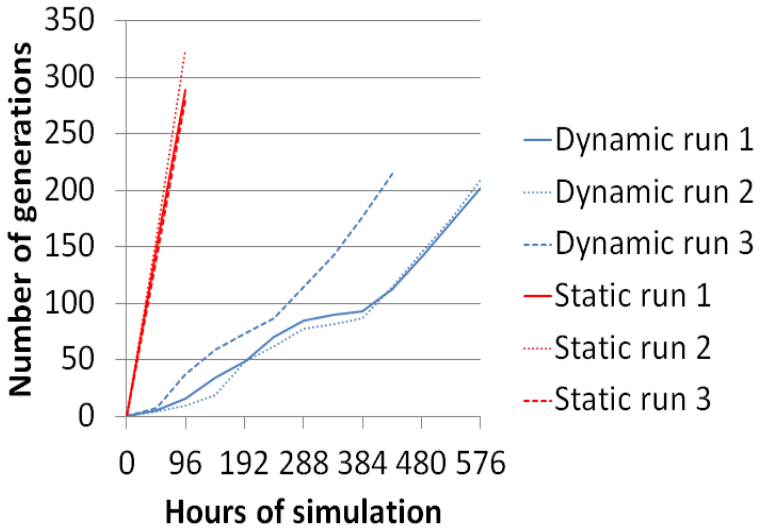

Figure 5-3 Simulation speed of footprint area optimisation

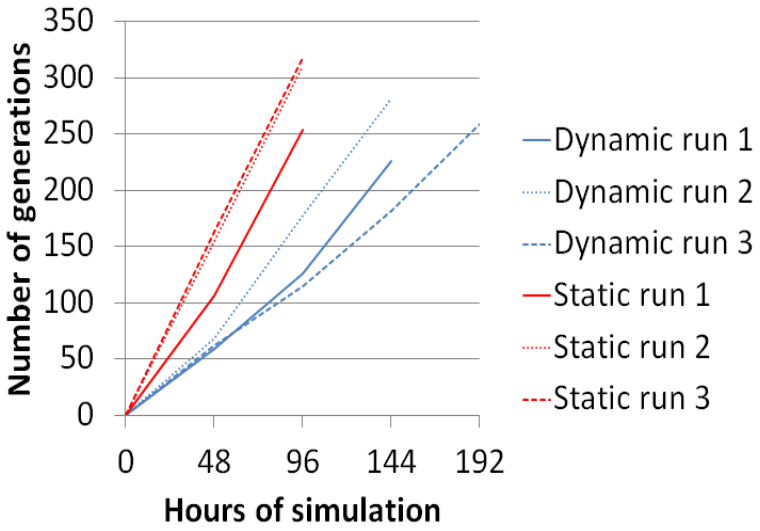

Figure 5-4 Simulation speed of operational cost optimisation

5.2.6 Degree of optimisation achieved

In order to compare the solutions identified by the dynamic and static models, it is necessary to determine whether the solutions can be considered near-optimal. Without assessing the performance of every possible combination of solution parameters, it is not possible to be certain that the solutions identified by a GA are true Pareto solutions or that all possible true Pareto solutions have been identified. It is therefore advantageous to measure how the solutions identified vary generationally to assess how likely it is that considerably fitter solutions are still likely to be found.

The degree of optimisation achieved by the GA is assessed by observing the variance of four optimisation metrics. These metrics assess how the objective functions, non-dominated fraction and convergence of the solution population vary generationally. A greater degree of optimisation is assumed if these metrics are found to stabilise, indicating that the solution set is not evolving significantly towards fitter solutions. In order to give greater confidence in the degree of optimisation achieved after an initial hundred generations, an additional hundred generations is simulated for comparison.

The objective functions are assessed using the mean value from the Pareto optimal solutions for each optimisation run's population. The non-dominated fraction is calculated on the basis of the number of designs which are found to be in the first Pareto front of the solution space. The convergence metric (developed by Deb & Jain, 2002 as described in Shi & Reitz, 2010) is a measure of how the Pareto solutions identified in any generation compare with the Pareto solutions from the preceding generation. The convergence metric is calculated as described in Shi & Reitz (2010). Higher convergence metric values indicate a greater degree of variance between two generations, whereas a convergence metric value of zero indicates that all

solutions had counterparts with identical objective function scores in the previous generation. Unlike their application in Shi & Reitz (2010), the convergence metric values are not normalised to allow more direct comparison between different runs of the optimisation processes. Optimal solutions, using each model, are defined as being the Pareto optimal solutions of all the solutions simulated in the initial one hundred generations of three runs of the genetic algorithm.

5.2.6.1 *Footprint and failure rate optimisation metrics*

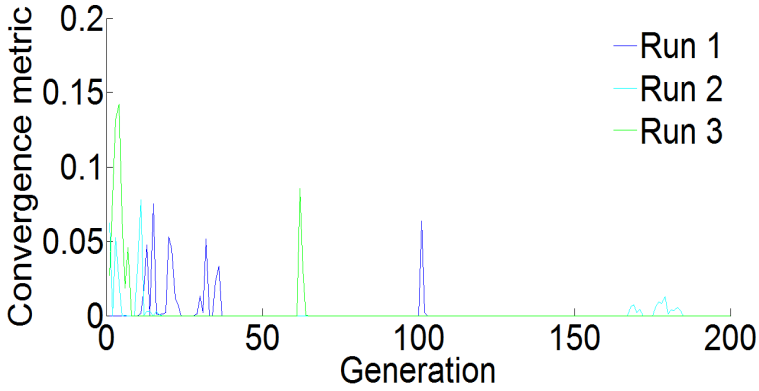

Figure 5-5 Convergence metric - footprint - dynamic

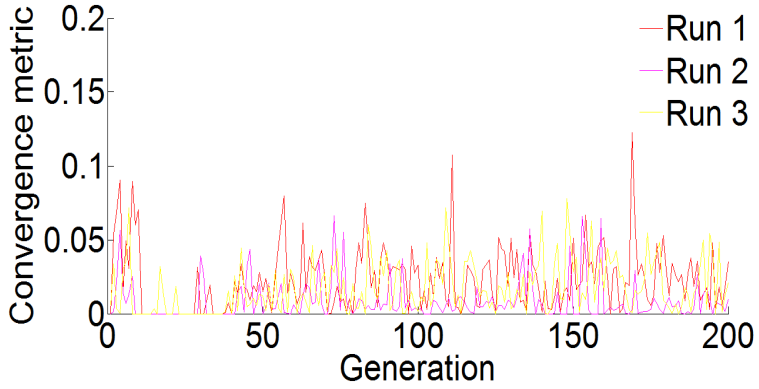

Figure 5-6 Convergence metric - footprint - static

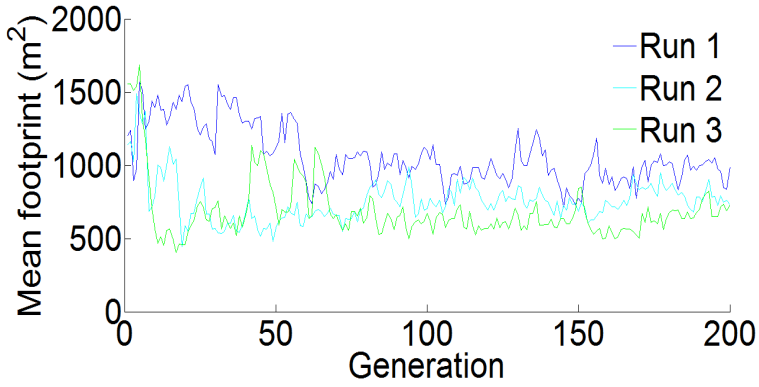

Figure 5-7 Mean footprint - footprint - dynamic

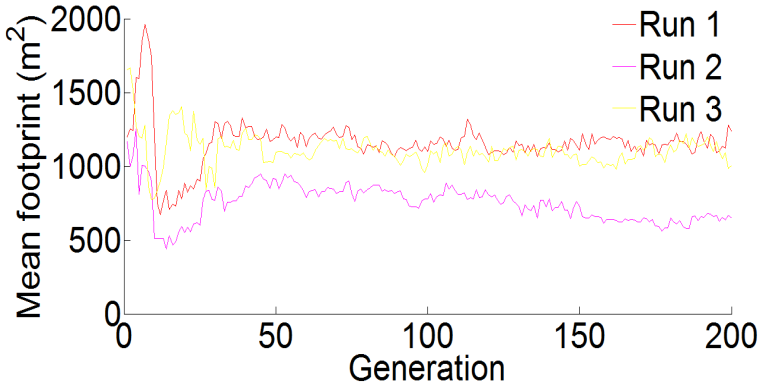

Figure 5-8 Mean foot print - footprint - static

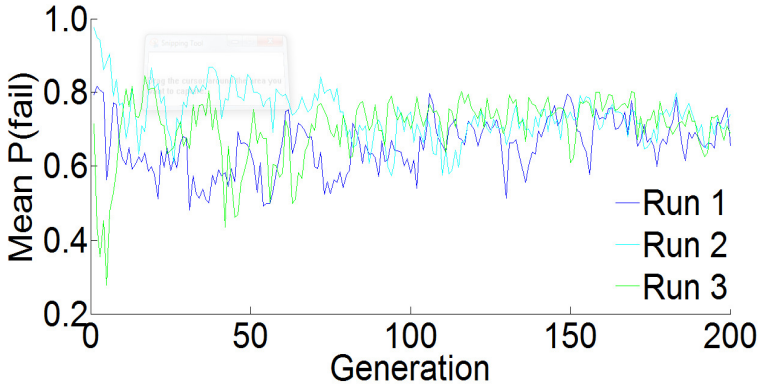

Figure 5-9 Mean P(fail) - footprint - dynamic

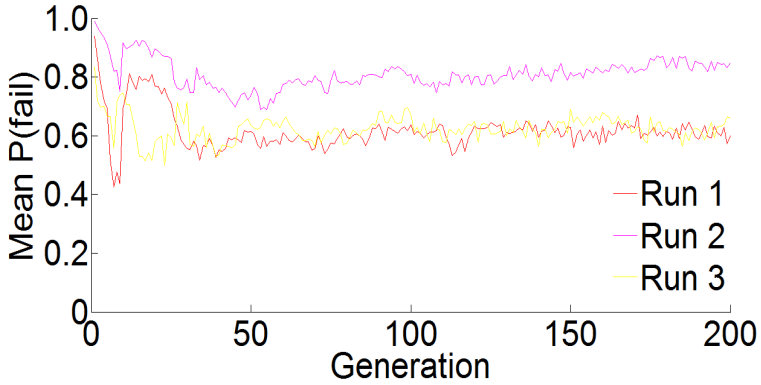

Figure 5-10 Mean P(fail) - footprint - static

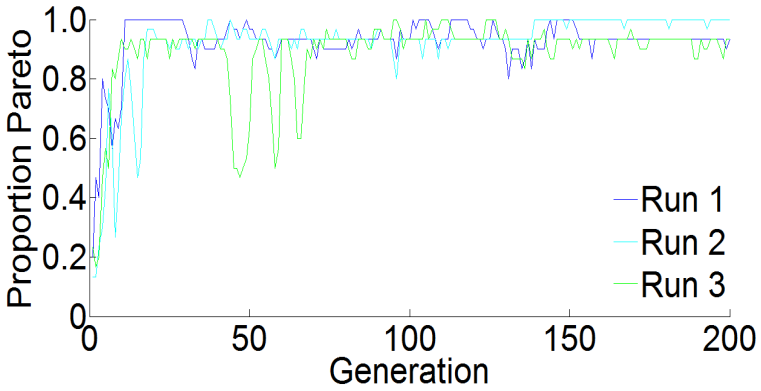

Figure 5-11 Proportion of Pareto - footprint - dynamic

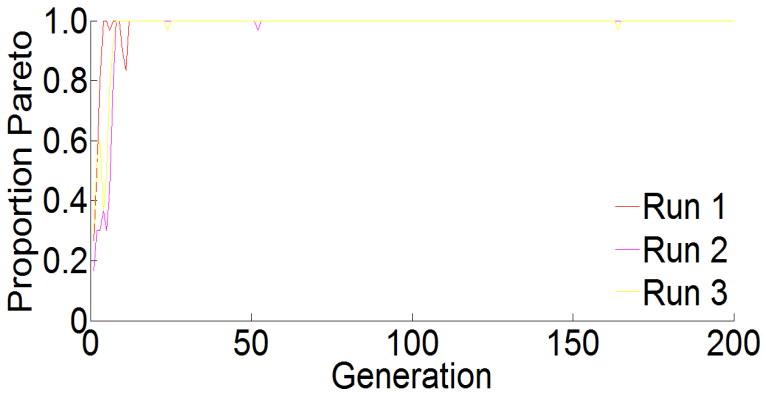

Figure 5-12 Proportion of Pareto - footprint - static

5.2.6.2 *Operating cost and failure rate optimisation metrics*

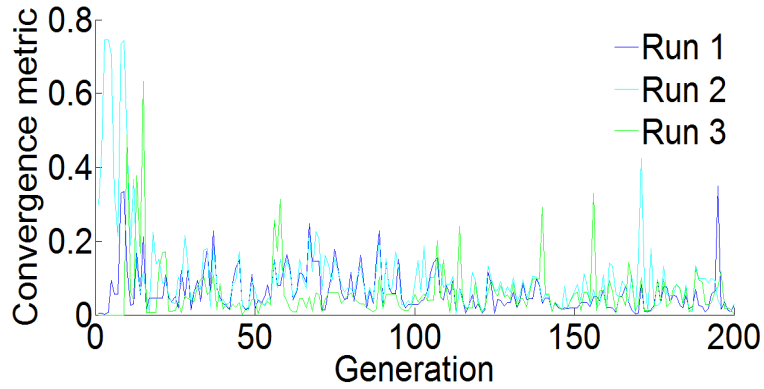

Figure 5-13 Convergence metric - operating cost – dynamic

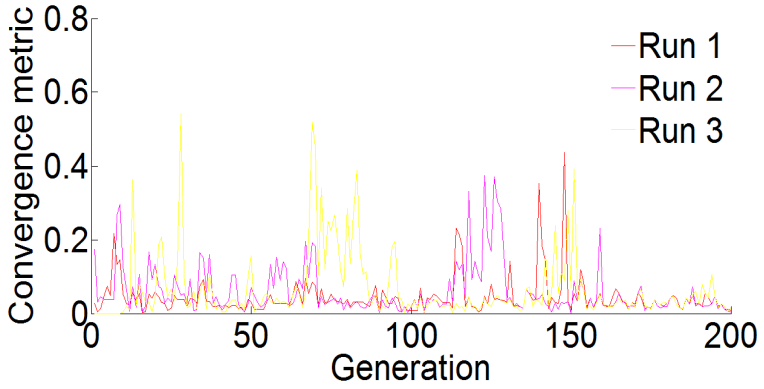

Figure 5-14 Convergence metric - operating cost - static

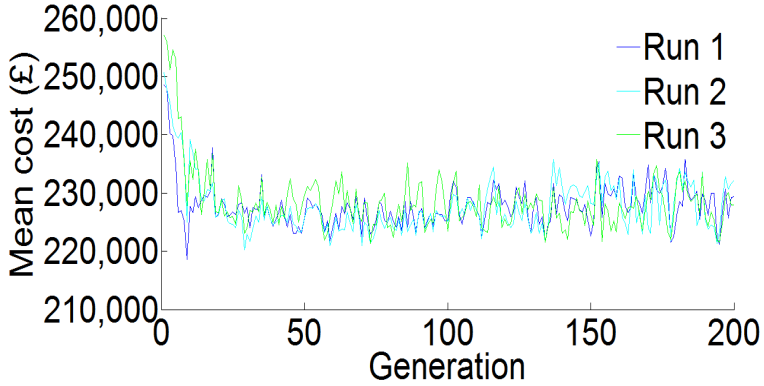

Figure 5-15 Mean cost - operating cost - dynamic

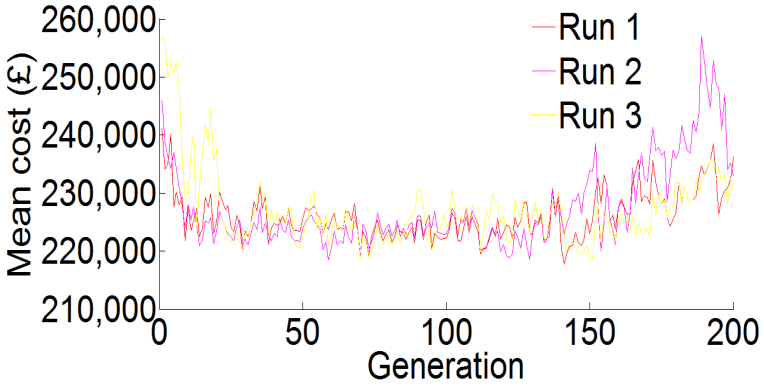

Figure 5-16 Mean cost - operating cost - static

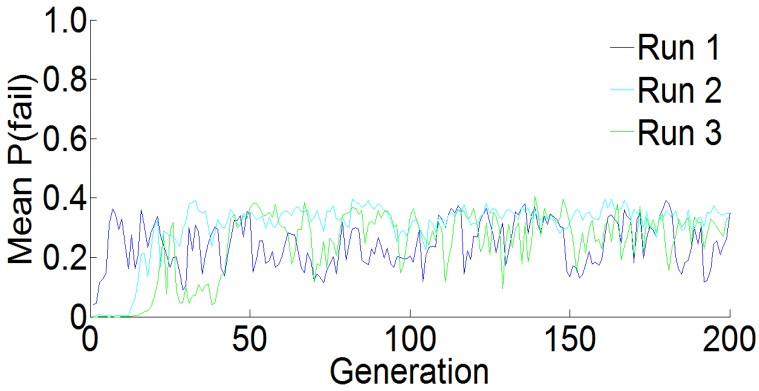

Figure 5-17 Mean P(fail) - operating cost - dynamic

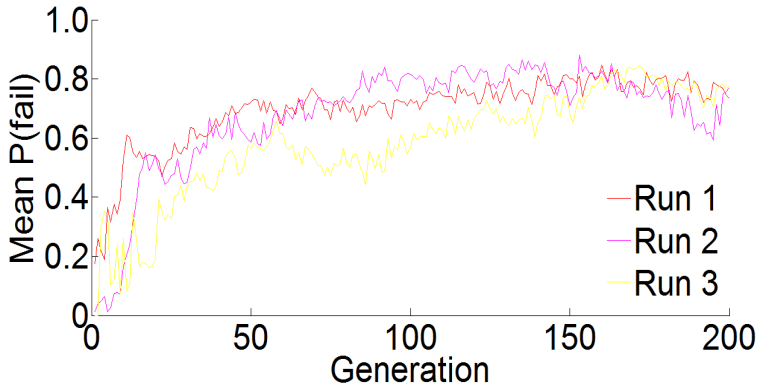

Figure 5-18 Mean P(fail) - operating cost - static

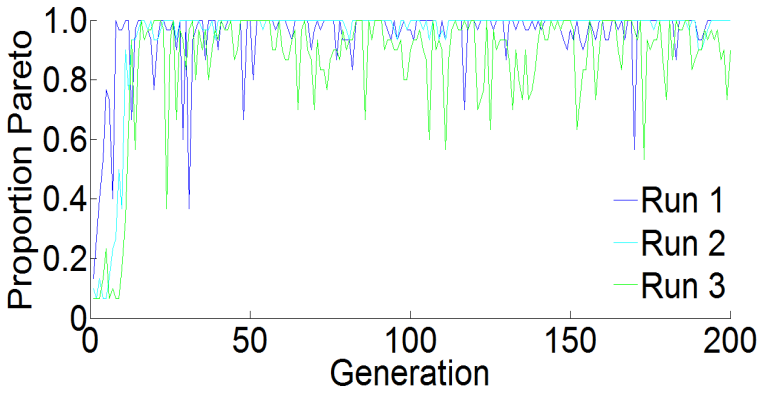

Figure 5-19 Proportion of Pareto - operating cost - dynamic

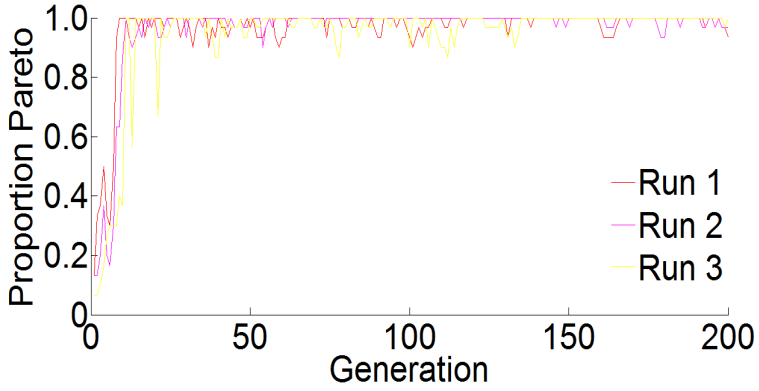

Figure 5-20 Proportion of Pareto - operating cost - static

5.2.6.3 *Pareto solutions after 100 and 200 generations*

Table 5-6 Comparison of Pareto solutions – footprint and failure rate optimisation

Model	**Unique Pareto solutions identified after**	
	100 generations	**200 generations**
Dynamic model	34	41 (4 solutions from 100th generation dominated and 11 new solutions identified)
Static model	37	45 (2 solutions from 100th generation dominated and 10 new solutions identified)

Table 5-7 Comparison of Pareto solutions – operating cost and failure rate optimisation

Model	**Unique Pareto solutions identified after**	
	100 generations	**200 generations**
Dynamic model	18	19 (2 solutions from initial 100 generations dominated and 3 new solutions identified)
Static model	32	32 (2 solutions from initial 100 generations dominated and 2 new solutions identified)

5.2.6.4 *Degree of optimisation analysis*

Based on visual assessment of the optimisation metrics (convergence metric, mean cost function, mean failure rate and proportion of Pareto solutions) over 200 generations, near optimal solutions are predicted to have been achieved after 100 generations for both optimisation problems. This judgement is made on the basis of similar optimisation metric behaviour after 100 and 200 generations (see Figure 5-5 to Figure 5-20). There are some exceptions: a decreasing trend for the mean footprint identified in run two of the footprint optimisation using the static model (Figure 5-8); an increasing trend for the mean operating cost identified in all runs of the cost optimisation using the static model (Figure 5-16) and mean

failure rate peaking after 100 generations in all runs of the cost optimisation using the static model (Figure 5-18).

Pareto fronts for each optimisation problem are plotted for the non-dominated solutions identified after 100 and 200 generations (Figure 5-23 and Figure 5-24). In the footprint optimisation, the performance of the new non-dominated solutions, identified using both models, are seen to be different enough to be clearly visible in the functional space. The majority of the new solutions identified fit approximately on the existing Pareto front, representing only a diversification of solutions rather than improvement in solutions. Exceptions to this are circled in Figure 5-23, where a clear improvement in the Pareto front can be observed. For the cost optimisation, the Pareto fronts identified using both models are not significantly different enough between the 100^{th} and 200^{th} generations to be visible in the functional space (seen in Figure 5-24). From these observations, it is concluded that the solutions from the footprint optimisation undergo a greater degree of additional optimisation than the cost optimisation beyond the 100^{th} generation, and for the footprint area optimisation, solutions using the static model undergo greater additional optimisation than from using the dynamic model. The general profile of the Pareto fronts, for both optimisation problems, using both models, does not change considerably beyond the 100^{th} generation in comparison to the significantly different results identified using the two different models. Therefore, for the purposes of comparing solutions identified using the dynamic and static models, the Pareto solutions identified after simulating 100 generations are considered to be representative.

The optimisation metrics discussed in this section are examined primarily to assess the degree of optimisation achieved but they also provided information that is used to identify characteristic differences in optimisation processes using the dynamic and static models. The

optimisations using the dynamic model has solution populations which are less diverse, both in terms of the numbers of unique solutions identified and the dispersion of solutions across the failure range. This lower diversity in the solution population coincides with a lower mean proportion of solutions being Pareto optimal each generation. The lower proportion of Pareto solutions is due to the less diverse solution population being less able to respond to generational variability in the stochastic conditions.

5.2.7 Reliability distribution of solutions

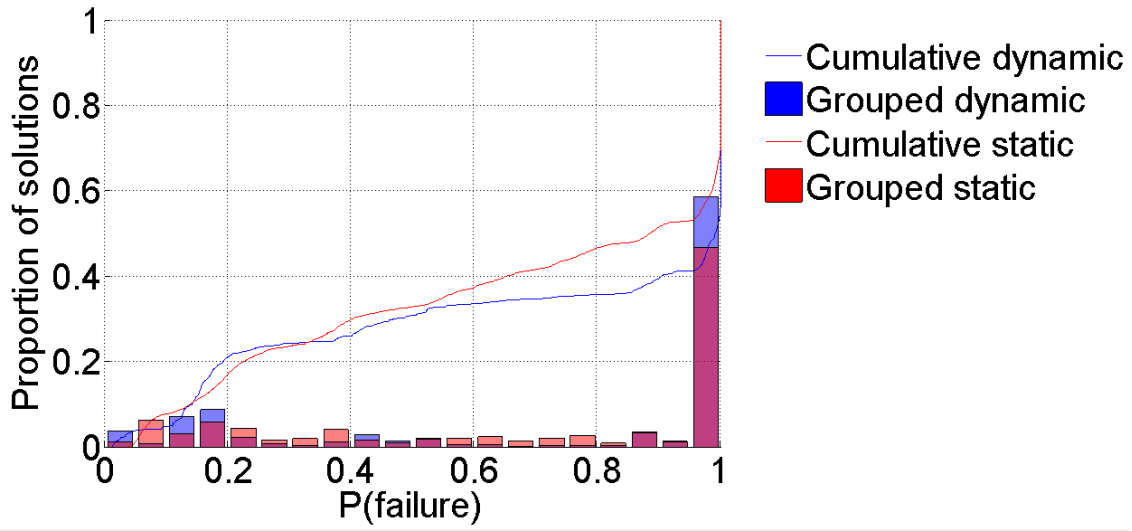

Figure 5-21 Distribution of footprint and failure rate solutions

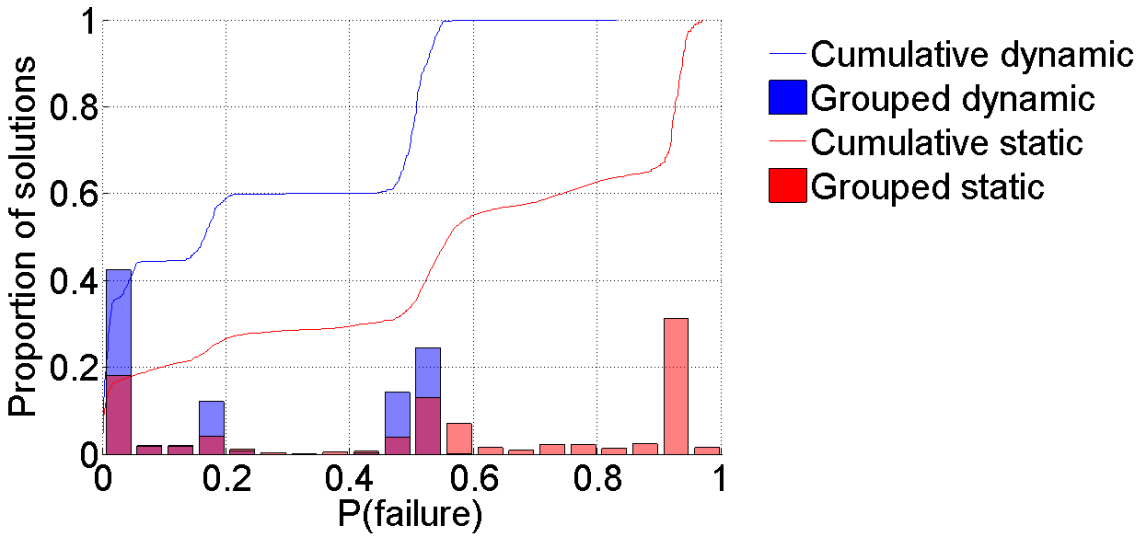

Figure 5-22 Distribution of operating cost and failure rate solutions

For most of the optimisations examined, the majority of the Pareto optimal solutions identified after 100 generations have failure rates greater than 50% (see Figure 5-21 and Figure 5-22). The exception being operational cost optimisation using the dynamic model. Reliable solutions, with failure rates less than 5%, in all cases account for a minority of solutions (1.4% to 42.6%). This indicates that the use of the NSGAII, without the application of constraints or penalty functions explicitly favouring high reliability solutions, is not an efficient method of identifying reliable WTW designs and operating solutions. The optimisation of solutions with higher failure rates reduces the computational resources dedicated to identifying high reliability solutions. The optimisation method also results in solutions from the two models being difficult to compare, due to the differing reliabilities of the solutions identified.

5.2.8 *Pareto fronts*

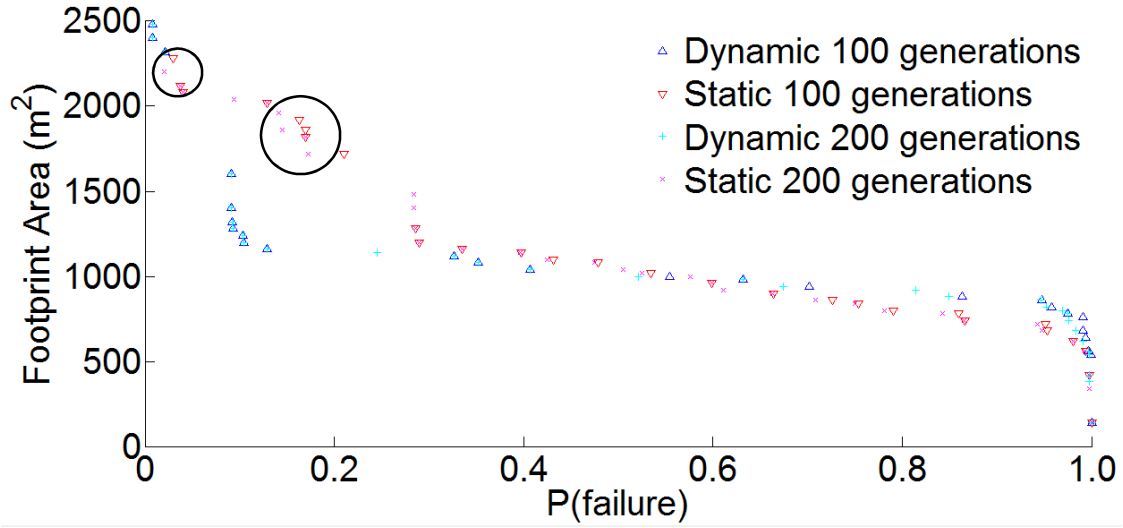

Figure 5-23 Footprint area vs. failure rate of Pareto optimal solutions

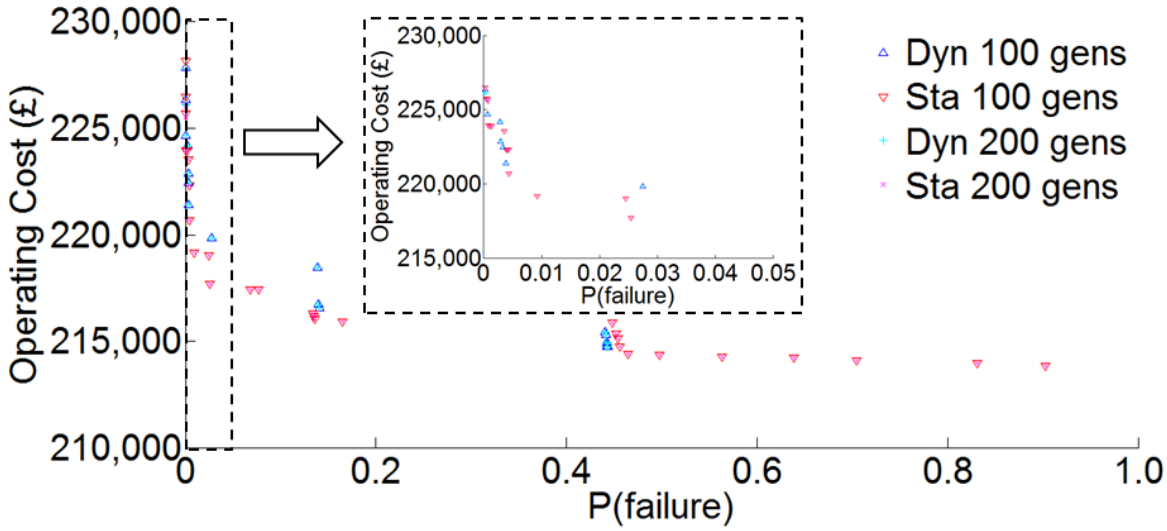

Figure 5-24 Comparative cost vs. failure rate of Pareto optimal solutions

For both optimisations, the gradients of the Pareto fronts tends to be inversely proportional to the failure rate, with some other notable points of interest, such as the rapidly decreasing footprint areas of WTW designs as failure rates approach 100%, or the sharp reduction in operating costs for operating regimes with failure rates between 40% and 50%. The correlation between failure rate and cost function is most pronounced for operational cost optimised solutions with failure rates below 5%. For the majority of near-optimal solutions identified, the additional resources required to achieve incremental improvements in reliability are

proportional to the existing reliability of the solutions. This is due to the increasingly high incremental costs required to operate the WTW at a "good" performance level for rarer and increasingly severe operating conditions.

The footprint areas rapidly reduce towards minimum sized solutions for near-optimal designs with failure rates approaching 100%. This effect is observed because considerably greater resources are required to provide a solution which fails the performance criteria most of the time compared to one which fails them all of the time. The same effect is not observed in the cost optimisation, as even the minimal cost solutions do not predict failure rates of 100%. This again shows that the operational cost optimisation parameters are more restricted to values representative of those found at operational sites than in the footprint area optimisation.

The application of dynamic or static models is not found to consistently identify more optimistic or conservative solutions to optimisation problems. The relative costs of the solutions identified are dependent on the multi-objective problems set and the reliability of the solutions identified.

5.2.9 Solutions identified

5.2.9.1 *Solution analysis*

This section compares the individual solution parameters, identified using both models, for each optimisation problem.

Coagulation

Optimal target clarified TOC concentrations of between 4 to 5 mg/l are identified using both models, approximately double the current predicted concentration. The target TOC concentrations predicted using both models are similar; with their Pareto optimal solutions both having mean values of 4.9 mg/l and standard deviations of 0.2 mg/l (see Figure 5-34). The higher target clarified TOC concentrations result in lower coagulant doses, subsequently reduced: (i) coagulant; (ii) pH/alkalinity adjusting chemical; and (iii) sludge disposal costs. Lower solids loading of the clarification and filtration stages is also achieved. However, higher TOC concentrations could result in increased THM formation and biological growth in the distribution system.

Operational cost optimised solutions, which predict no failure events, have maximum target clarified TOC concentrations (5.0 mg/l) along with contact tank inlet chlorine concentrations comparable to those currently observed (1.8 mg/l using the dynamic model, 1.5 mg/l using the static model and 1.6 mg/l observed). This indicates that either the site has the potential to remove significantly less TOC without increasing THM concentrations beyond the target limit of 25 µg/l (observed THM concentrations were less than 15 µg/l) or that THM formation is under-predicted by the models.

Clarification

In the footprint area optimisations, it is found that a lower proportion of treatment by the DAF stream, along with a greater number of DAF and HBC clarification tanks, results in improved reliability. For solutions with failure rates of 100%, a wide range of proportions of water treated by DAF clarification are observed. For these solutions, the division between the clarification processes does not affect WTW performance, as no clarification took place.

Solutions with failure rates above 30% have greater proportions of their water treated by DAF clarification, due to the process's ability to treat higher volumes of water to the required standard, per footprint area. For solutions with lower failure rates, both models identify complete treatment by DAF clarification. The more reliable solutions have a more comparable split of treatment between the two clarification processes.

The number of DAF tanks in operation is limited, with additional tanks, if available, being brought into service for every 293 m^3/h of water being treated. As the potential number of DAF tanks provided a greater treatment capacity than is required, additional HBC clarification tanks are identified for achieving the highest reliability solutions because treatment by additional HBC units provide more reliable clarified turbidity performance than is possible by additional DAF units. This is because all HBC tanks present are always in operation, meaning that additional tanks always result in lower superficial velocities and greater solids removal rates.

The use of the dynamic model results in a higher proportion of water being treated by the DAF stream for higher reliability Pareto solutions and a greater dependency on DAF clarification than found using the static model (see Figure 5-25 to Figure 5-27). For comparable solutions with failure rates greater than 30%, which are only treated by DAF clarification, the number of DAF units identified using both models are similar (see Figure 5-27). This suggests that the

relative reliability of the DAF treatment process, in comparison to the HBC clarification process, is greater in the dynamic model than in the static model. As greater dependence on DAF clarification results in reduced footprint area, greater dependency on DAF clarification indicates that the dynamic DAF model predicts performance failure events less often than the static model, for comparable solutions, in the size optimisation problem.

Greater proportions of water being treated by DAF clarification is found to result in improved reliability of solutions in the operating cost optimisations (see Figure 5-30). This indicates that DAF clarification more reliably meets the performance criteria than HBC clarification, for the typically lower coagulant doses and increased DAF compressor pressures identified in the operating cost optimisation. When the static model is used it is found that, for lower reliability solutions where the probability of failure is greater than approximately 45%, the proportion of DAF treatment is the dominant factor in determining the failure rate of solutions. This is concluded from the stronger degree of correlation between proportion of DAF treatment and failure rate than seen for the other solution parameters (see Figure 5-30 to Figure 5-34).

The DAF compressor pressure appears to be weakly optimised as there is little correlation between compressor pressure and the reliability of solutions (see Figure 5-31). This is because DAF air compression costs are underestimated, making cost savings due to compressor pressure optimisation more difficult to identify (maximum annual costs are approximately £500, comparable to the random variation in total operating costs due to the stochastic conditions).

For the most reliable Pareto solutions identified (those with failure rates less than 5%) it is found that using the dynamic model solutions have larger mean proportions of DAF treatment (90.2% vs. 72.2%) and greater mean DAF compressor pressures (649 kPa vs. 458 kPa) than those identified using the static model. The greater degree of DAF clarification, again identified

by the dynamic model, is another indicator that the relative reliability of the DAF treatment process, in comparison to the HBC clarification process, is greater in the dynamic model than in the static model.

Filtration

In the footprint area optimisation, reliable solutions, with failure rates less than 35%, are found to identify the maximum number of filters, ten, as near-optimal (see Figure 5-28). This indicates that these solution's failure rates are strongly influenced by filtered turbidity exceeding its limit. At present, eight rapid gravity filters are installed at Trimpley WTW which operate at the relatively low filtration rates of approximately 3 m/h. The results from this optimisation suggests that to ensure a highly reliable supply of filtered turbidity below 0.1 NTU even lower filtration overflow rates could be required. The dynamic and static models both identify a similar number of filters as near-optimal across their Pareto fronts.

The near-optimal filtration run lengths identified in the operational cost optimisation are in the region of the maximum value of 96 hours (see Figure 5-32), with low standard deviations and negligible correlation with failure rate (dynamic model mean 95.3 ± 2.7 hours, static model mean 95.1 ± 3.7 hours). The models therefore predict that filtration run durations could be increased significantly beyond their current interval of 48 hours, without reducing the reliability of the works. As solutions identified using the static model frequently predict these extended durations, frequent unscheduled backwashes are not required to achieve this performance and therefore disruption to operational routine is predicted to be minimal.

The similarities between the number of filters and filtration durations identified as optimal using both models indicates that the extra complexity and associated additional computational resources of the dynamic model is not justified for this application. This conclusion is based on

the assumption that, for both models, the solids loading on the filters was comparable. This is assumed because the clarified turbidity in both models is limited to the same extent by the clarified turbidity limit (1 NTU) influencing the performance of the optimised solutions.

Chlorination

In the footprint area optimisations, the volume of the contact tank correlates with the reliability of the solutions. This is because larger contact tanks improve the probability that the required degree of disinfection, as measured by CT, is achieved. Maximum contact tank volume could have been limited by smaller tanks achieving no failure events and by larger contact tanks possibly producing THM concentrations greater than their target limit.

Use of both models results in the near-optimal contact tank volume reducing for solutions with failure rates below 5%. This is due to the volume of the contact tank being optimised for two separate groups of solutions whose failure rates are predominantly due to clarified and filtered turbidity limits being exceeded. This results in the contact tank volume forming two separate correlations with failure rate: one for failure rates below 5% and another for solutions with failure rates above 10% (see Figure 5-29).

For solutions with failure rates of approximately 10% to 20%, the contact tank volume identified using the static model is considerably greater than that using the dynamic model. The higher contact tank volumes identified using the static model indicate that the static model predicts failure due to insufficient disinfection, as measured by CT, more often than the dynamic model for some solutions. This could be due to chlorine consumption in the static model being more influenced by fluctuating conditions or due to contact tank discharge being reduced in the dynamic model by unscheduled backwashes. The contact tank volumes in the solutions identified using the dynamic model, with failure rates less than 20%, show greater

correlation with failure rate. This could be due to the static model's limitations in optimising contact tank volume.

In the operating cost optimisation, the correlation between inlet contact tank chlorine concentration and failure rate are comparable between solutions from both models (see Figure 5-33). Solutions with failure rates less than 40% are found to require greater than 1 mg/l of free chlorine and the maximum dose identified using the dynamic model was 1.8 mg/l in comparison to 1.5 mg/l using the static model. The lower maximum chlorine concentration identified by the static model could be due to higher reliability solutions with greater chlorine concentrations not having evolved. It can be seen that a significantly greater number of solutions with failure rates under 5% are identified using the dynamic model (see Figure 5-22). These results indicate that for the observed operating conditions, the current inlet concentration of 1.6 mg/l appears to ensure that the required degree of disinfection is provided reliably without significant risk of exceeding the final water THM concentration limit set.

5.2.9.2 *Footprint and failure rate optimisation solutions*

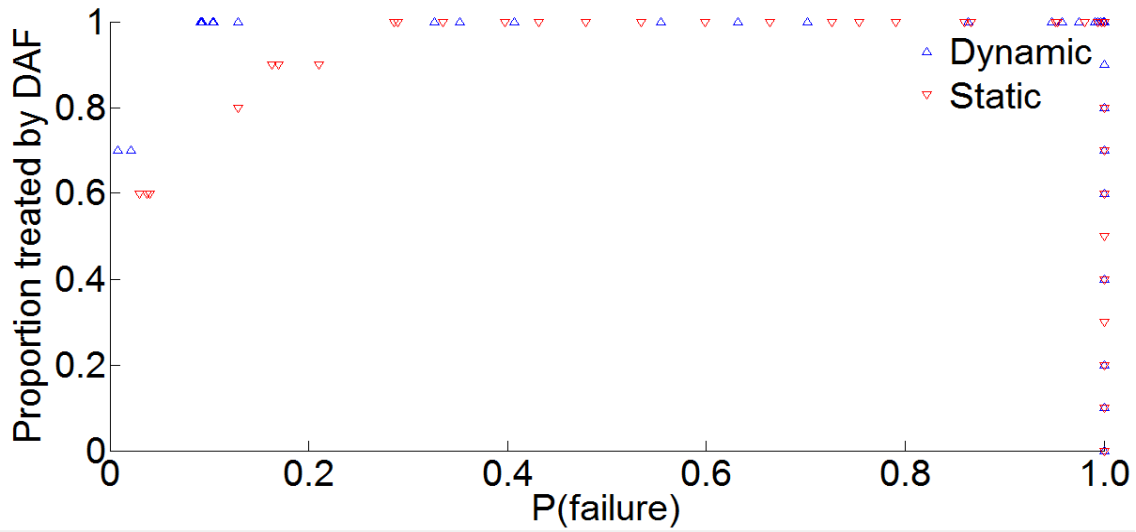

Figure 5-25 Proportion treated by DAF vs. failure rate of Pareto optimal solutions

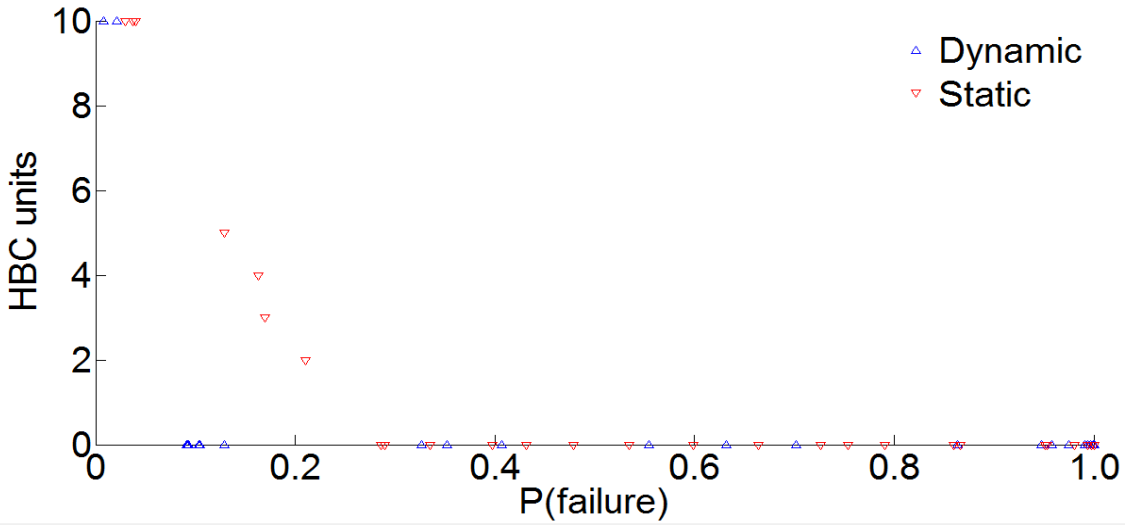

Figure 5-26 Number of HBC units vs. failure rate of Pareto optimal solutions

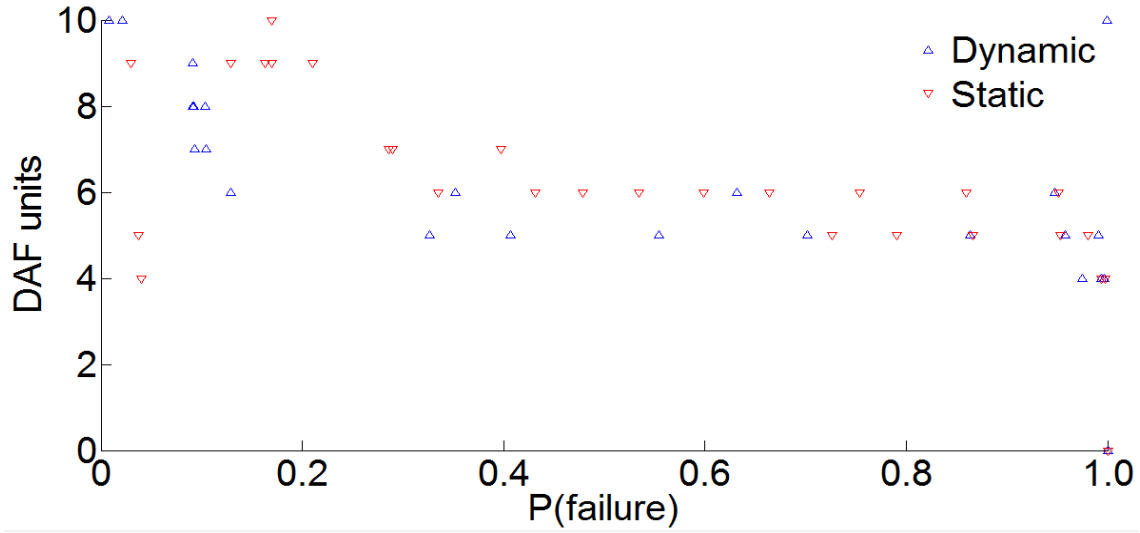

Figure 5-27 Number of DAF units vs. failure rate of Pareto optimal solutions

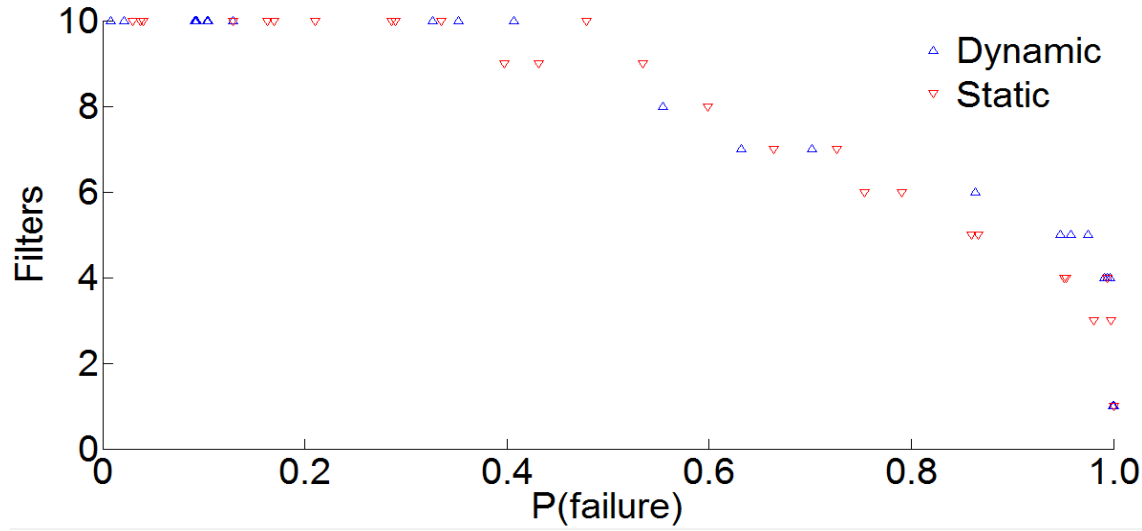

Figure 5-28 Number of filters vs. failure rate of Pareto optimal solutions

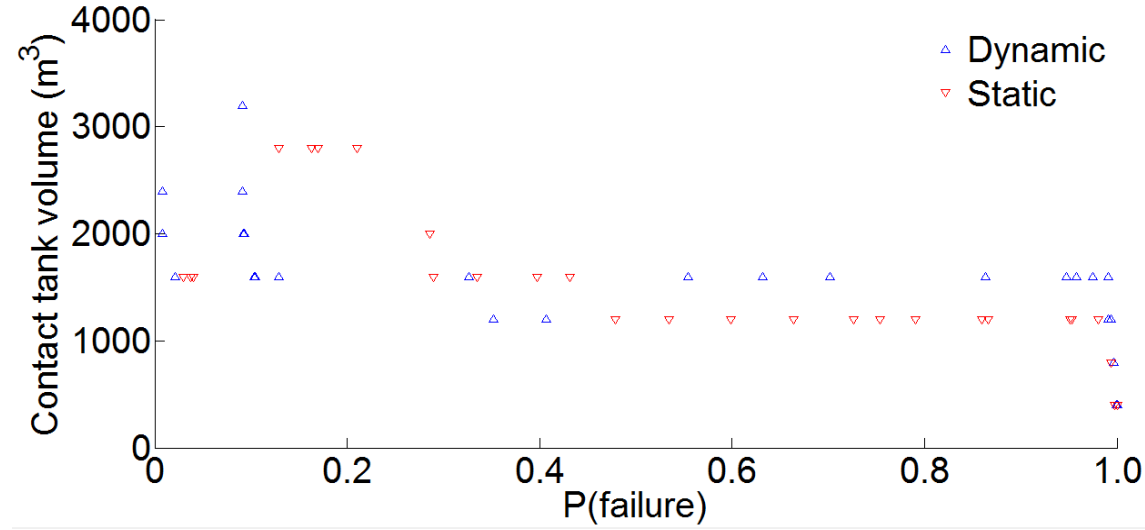

Figure 5-29 Contact tank volume vs. failure rate of Pareto optimal solutions

5.2.9.3 *Operating cost and failure rate solutions*

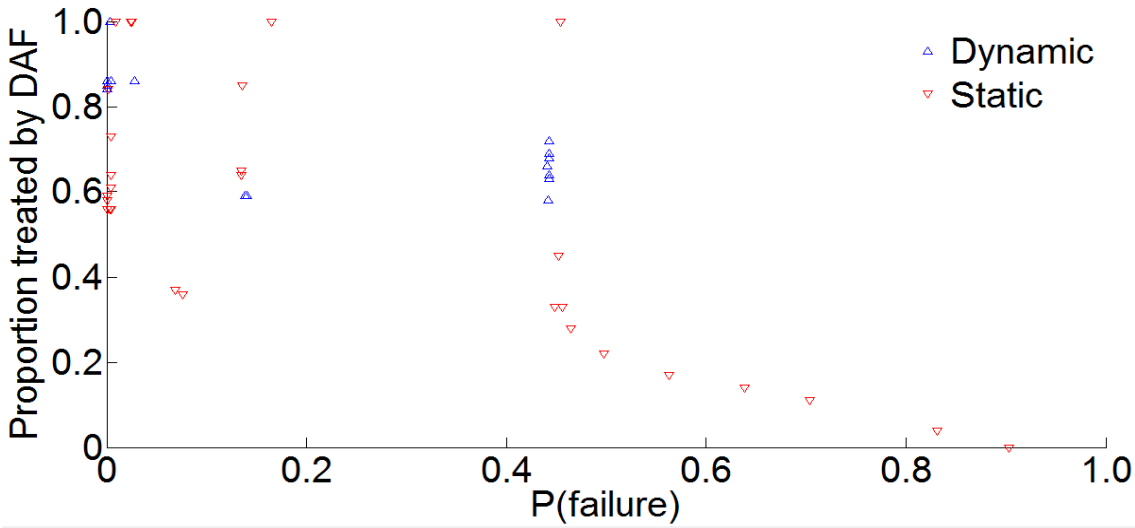

Figure 5-30 Proportion treated by DAF vs. failure rate of Pareto optimal solutions

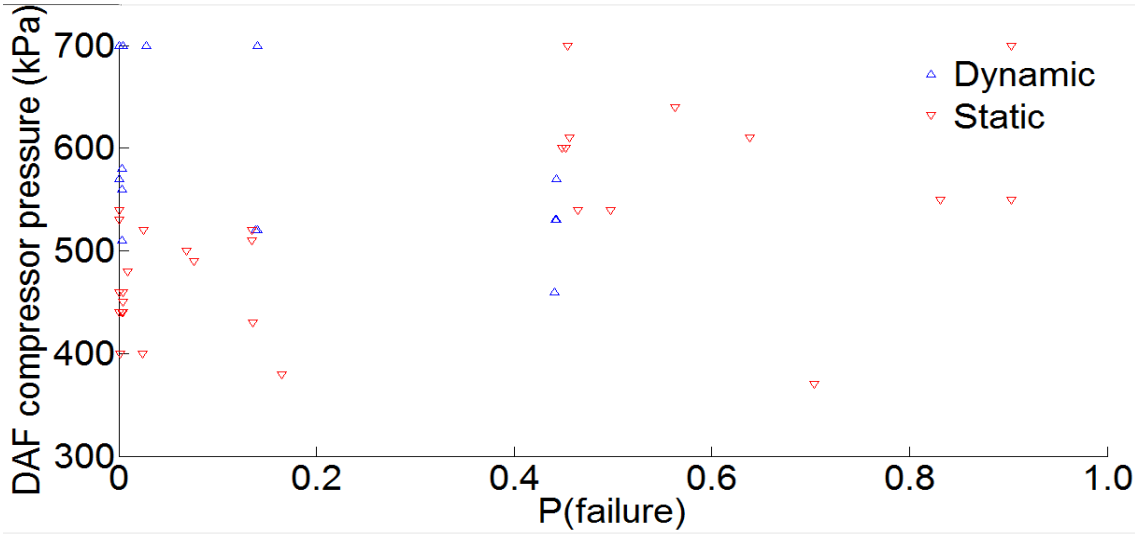

Figure 5-31 Compressor pressure vs. failure rate of Pareto optimal solutions

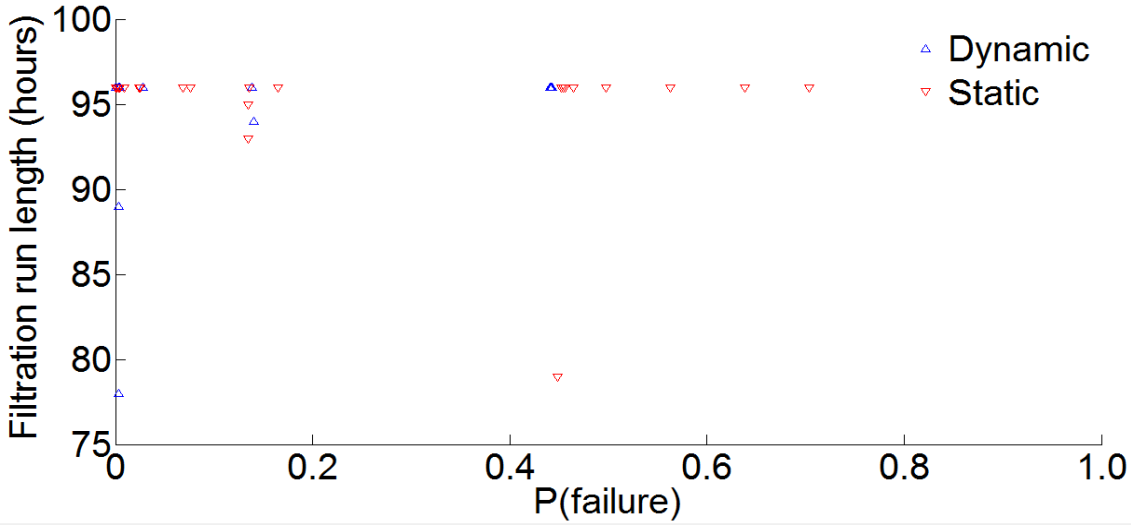

Figure 5-32 Filtration run length vs. failure rate of Pareto optimal solutions

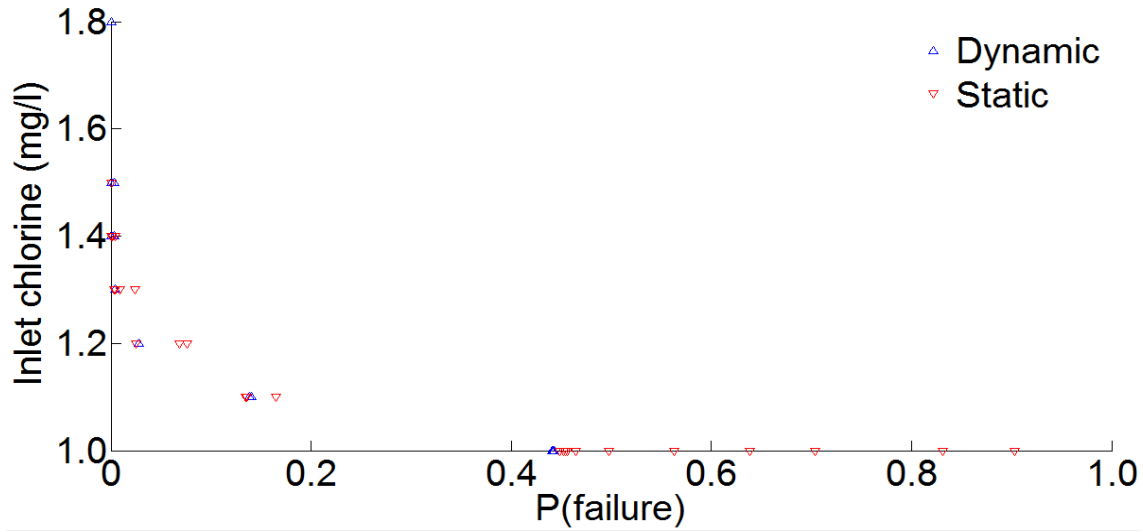

Figure 5-33 Contact tank chlorine concentration vs. failure rate of Pareto optimal solutions

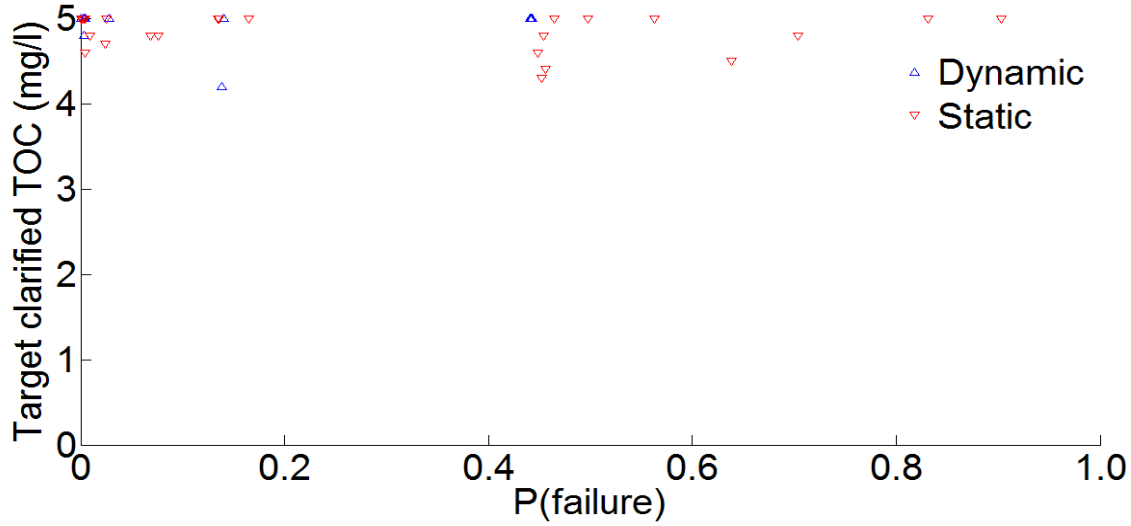

Figure 5-34 Target clarified TOC vs. failure rate of Pareto optimal solutions

5.3 Summary

In this chapter, abstraction rates predicted to result in "good" performance at an operational WTW were investigated. This investigation was completed separately using both dynamic and static computational models. Simulated water temperature and total organic carbon (TOC) concentrations were adjusted and the range of abstraction of rates for which "good" performance was predicted was identified. The following key observations were made:

- Both models identified similar relationships between raw water temperature, TOC concentration and abstraction rates, indicating that the same causes of failure were likely to be limiting their operating zones (see Figure 5-1).
- For raw waters with temperatures below 18 °C and TOC concentrations below 6 mg/l, the predominant limiting factor of maximum abstraction rate was the achievement of a sufficiently low clarified and filtered turbidity.
- The minimum abstraction rate was limited by achieving sufficient residual free chlorine concentration and limiting THM production.
- The maximum abstraction rate was found to increase at higher temperatures due to increased solids removal by clarification.
- The maximum abstraction rate was found to be strongly dependent on the raw TOC concentration, due to the additional solids loading caused by increased coagulant doses.
- For the operational conditions simulated, the use of the dynamic model resulted in a greater range of and, for the vast majority of raw water conditions examined, lower maximum abstraction rates.

- The maximum abstraction rates predicted using the dynamic model were lower than observed abstraction rates for similar conditions in 2012, indicating that these predicted maximum abstraction rates gave conservative estimates.
- The maximum abstraction rates predicted using the static model were greater than the observed abstraction rates for similar conditions in 2012.
- For warmer raw waters with elevated TOC concentrations, it was found that "good" performance could not be achieved purely through abstraction rate control, due to either clarified / filtered turbidity or THM production being too great or insufficient disinfection (measured as CT) being achieved.
- Due to the similar predictions made by the different models it is concluded that the use of a static WTW model would be sufficient for this type of analysis in future as a result of its lower complexity and computational demands.

Two multi-objective optimisations of the WTW were completed using genetic algorithms based on the NSGAII. The first optimisation identified WTW designs that minimised footprint area and failure rate, with a fixed WTW operating regime. The second optimisation identified operating regimes that minimised the operational cost and failure rate, with a fixed WTW design. Near-optimal solutions were identified as being the Pareto solutions from all the simulated generations. The following conclusions were drawn from the results of these optimisations:

- During an attempted calibration of the GA internal parameters, variation of most of the parameters identified solution populations with comparable fitness in terms of the number of Pareto solutions they identified and degree of diversity achieved. It was concluded that future investigations which are concerned with using GAs, rather than

developing them, should apply appropriate values based on the state-of-the-art guidance rather than calibrate them to the individual problem.

- For the purposes of comparing the dynamic and static model solutions, 100 generations was identified as achieving an acceptable degree of optimisation because Pareto fronts changed very little after simulating an additional 100 generations.
- Reliable solutions (those with P(fail) < 5%), in all cases, accounted for a minority of solutions identified (1.4% to 42.6%). It was found that the operational cost optimisation produced a higher proportion of reliable solutions than the footprint area optimisation. This was due to the parameters in the operational cost optimisation being more constrained.
- The dynamic model identified solutions with failure rates greater than approximately 50% as non-optimal due to the additional backwash costs associated with less intensive clarification treatment.
- Allowing increased clarified TOC to approximately twice their current predicted concentrations was identified as near-optimal. This was due to predicted reduced coagulant costs and low likelihood of substantially increased THM production.
- DAF compressor pressures were poorly optimised due to the underestimation of compressor costs, making savings due to optimisation more difficult to identify.
- Greater proportions of DAF clarification were identified using the dynamic model. It was therefore concluded that the relative reliability of the DAF process, in comparison to the HBC process, was greater than that found using the static model.
- Filtration run durations of 96 hours (twice as long as those currently applied) were identified as being able to achieve “good” WTW performance for conditions with reduced coagulant doses without the need for frequent unscheduled backwashing.

- The mean computational time required to simulate generations of solutions using the dynamic model was found to be between twice (for the operational cost optimisation) and eight times as long as that required by the static model (for the footprint area optimisation).
- The computational time required by the dynamic model, in both optimisations, was more dependent on the solutions simulated and could be reduced by restricting solution parameters further.
- The application of dynamic or static models was not found to consistently identify more optimistic or conservative solutions to optimisation problems. The relative costs of the solutions identified were dependent on the multi-objective problems set and the reliability of the solutions identified.

6 DISCUSSION

6.1 Introduction

The use of computational models to optimise the performance of water treatment works (WTWs) is examined in this thesis. Generic, static and dynamic WTW models are used, developed from state of the art process models. These models are programmed in the MATLAB/Simulink block diagram environment. Trimpley WTW is modelled by applying these generic models to specific site conditions. The accuracy of static and dynamic WTW models is for the first time assessed over annual periods using separate calibration and verification data from an operational WTW.

The models apply both observed coagulant doses and those predicted by a coagulant dosing algorithm. The dosing algorithm applies a coagulant concentration that is predicted to maintain the clarified total organic carbon (TOC) concentration below a specified limit. It is necessary to predict coagulant dose as operators vary it substantially over the year. Coagulant dose prediction allows future or stochastic conditions to be modelled more representatively.

The verified models of Trimpley WTW are used to identify a range of abstraction rates for which performance criteria are expected to be achieved for varying reservoir water quality. The operating conditions for which acceptable performance is expected are identified as the WTW's "operating zone". The performance criteria include turbidity, disinfection, disinfection by-product and surface loading limits for individual processes and the reservoir water quality is varied in terms of temperature and TOC concentration.

The performance of a WTW for theoretical adjusted designs of operating regimes can also be predicted by computational models. These assessments can be carried out with no risk posed to operational performance or consumer health and at potentially lower cost than alternative pilot plant studies. Due to the complex, multiple, non-linear relationships between raw water quality, WTW design, operating regime, final water quality and operating costs, optimisation of WTWs poses difficult problems for which the application of Monte-Carlo techniques and genetic algorithms are suitable. Solutions identified through these methods may not be intuitively identified through conventional methods due to the complex interactions present. The solutions found by Monte-Carlo techniques also have the advantage that they have a predicted likelihood of failure, which is not provided for solutions identified using deterministic conditions.

A Monte-Carlo technique is applied here using stochastic data sampled every simulated day, from representative probability distributions, for a simulated year. The predicted performance of the WTW under Monte-Carlo conditions is then compared to its time series performance. The models in this work are also applied under Monte-Carlo conditions with NSGAII inspired algorithms to identify near-optimal designs and operating regimes. These optimisations are multi-objective with both a cost function and a reliability criteria to minimise. The multiple-objectives result in Pareto sets of solutions being identified, which cover a range of failure rates and costs but which are not superior to each other in both respects.

The discussion in this section focuses on the development and application of static and dynamic water treatment models to replicate the performance of an operational works and the application of optimisation techniques to suggest efficient design and operational regime solutions for this

site. Practical applications of findings made from the observed data, modelling and optimisation are also discussed. The key findings are:

- Dynamic WTW models are more accurate than static models at predicting the water quality at an operational site but the RMSE of static models is within 5% of the dynamic models for all of the performance criteria assessed.
- When genetic algorithms are applied alongside dynamic and static WTW models to design and operational regime optimisation problems, they identify substantially different solutions from each other.
- Overall, static models are identified as being more suitable for whole works optimisation purposes.

6.2 WTW operation and modelling

6.2.1 Need to assess solids removal and disinfection performance

Previous attempts to predict the performance of WTWs has focused on either solids removal, such as the optimisation work carried out by Gupta and Shrivastava (2006, 2008, 2010), or disinfection, such as the climate change work of Clark et al (2011). It is predicted in this thesis that increased coagulant doses added at a WTW in response to increased source water TOC concentration can reduce the maximum abstraction rate due to increased solids loading (see section 5.1). Owing to the inter-relationships between these two facets of water treatment, it is considered important to consider them together.

6.2.2 Division of flow between DAF and HBC clarifiers

At Trimpley WTW, it is observed that the HBC process produces lower and more consistent clarified turbidity than the DAF process (0.44 NTU vs. 0.68 NTU). The DAF process is also known to be more energy demanding and therefore it is recommended that a greater proportion of water be processed by the HBC tanks. It makes economic sense that the proportion of water treated by the HBC process should be increased until its clarified turbidity is at least as high as the more operationally costly DAF process.

6.2.3 Coagulation and flocculation

It is, perhaps, surprising that the models used in this research do not attempt to predict the influence of coagulant on floc formation potential and instead are limited to predicting the reduction in TOC and increase in suspended solids concentration. Floc formation is not modelled in this research due to the lack of appropriate models. In some previous whole WTW modelling programs such as WATPRO and Stimela, floc size was not modelled. In OTTER, flocs were assumed to have a diameter of 5 microns after coagulation and to have a maximum flocculated floc size predicted by Parker et al's (1972) equation. The maximum floc size was then adjusted in OTTER based on an unreferenced relationship to give a representative flocculated floc size. The models in this research are applied on the assumption that the application of enhanced coagulation doses and flocculation results in flocs which can be efficiently removed by the solids removal processes. If this assumption is not accurate, the models can be expected to over-predict the efficiencies of the solids removal processes.

The models take into account the potential formation of metal hydroxide precipitates caused by the addition of certain coagulants. Ensuring an efficient balance between achieving sufficient

TOC removal and minimising additional suspended solids content is addressed in two ways in this research: the application of a coagulant dosing algorithm that attempts to achieve a specified clarified TOC concentration and the identification of an optimal clarified TOC concentration for minimising the fraction of the time that a works is not achieving its water quality goals.

The TOC dosing algorithm is found to show some correlation with operator specified doses (see Figure 4-22). It is suggested by the modelling and optimisations carried out here that raw water TOC concentrations could be used to specify coagulant doses using the Edwards (1997) TOC adsorption isotherm (as described in section 3.3.2.1). This application would be similar to the empirical methods developed by van Leeuwen et al. (2003, 2009). If this type of coagulant dosing was applied at the Trimpley WTW (which would require in-line TOC monitoring to be installed), it is possible that coagulant could be dosed more efficiently. This would result in more consistent chlorine demand and THM production, due to a more stable organic content. The use of the coagulation dosing model is found to alter predicted mean THM concentrations by less than ±0.5 µg/l and reduce the standard deviation by 20% for the dynamic model and 25% for the static model (see Table 4-15). The use of the dosing model in the operating cost optimisations results in a reduced mean coagulant dose without predicting prohibitively high concentrations of THMs. Lower mean doses would result in reduced coagulant and sludge treatment costs. These predictions are based on the coagulation and flocculation at the works still being able to produce flocs which are equally easily removed by the solids removal processes with lower coagulant doses. If the minimal coagulant dose of 7 mg/l as Fe is applied, as identified as acceptable by the operational regime genetic algorithm, then the coagulation and sludge disposal costs are predicted to approximately half. This reduction would equate to a

predicted saving in coagulant costs of approximately £250,000 per year and sludge disposal costs of approximately £19,000 per year (based on a reduction of coagulant dose from 16 mg/l, a mean abstraction rate observed in 2011 of 38Ml/d and costs given in Appendix F). The identified optimal clarified TOC concentrations are likely to be too great as: i) the identified TOC removal efficiencies are less and the final water TOC concentrations greater than those of other WTWs in the region (Brown, 2009); ii) a strong correlation between TOC concentration and THM formation has previously been identified (Powell et al., 2000, Golfinopoulos and Arhonditsis, 2002) and iii) iron based coagulant doses (as Fe) less than initial TOC concentrations have been found to result in poor floc formation (Jarvis et al., 2005b).

6.2.4 Solids removal

6.2.4.1 *General*

Suspended solids will not all be removed equally easily. Individual particles' physical and chemical properties and their interactions with process chemicals and processes will influence their propensity to be removed. When the removal efficiency parameters for the models are calculated for monthly periods, they are found to vary with a standard deviation of 9% to 32% in 2011. This variation in clarification performance was not reported by Head et al. (1997) for the dynamic HBC model or by Edzwald (2006) for the static DAF model. Substantial variation in removal efficiency may not have been observed in these previous studies because they were tested over shorter periods. This variation in mean monthly removal efficiency is possibly due to a variation in the average properties of the particles each month. It is found that by introducing removal efficiency relationships dependent on initial turbidity, a mean reduction of predicted turbidity RMSE of 35% is achieved for the calibration data. This improvement is

found to reduce to 15% when the verification data is applied, implying some degree of correlation rather than causation in the relationship. With the lower RMSE improvement identified for independent data sets, the increased complexity and less conservative predictions of WTW performance, the justification for application of similar relationships in future work is limited.

The accuracy to which WTW solids removal can be modelled is limited to some extent by the variation in performance of different units of the same process. The individual DAF tanks mean clarified turbidity for January 2012 is found to vary with a standard deviation of 36% and the mean filtered turbidity for July 2011 and January 2012 is found to vary with a standard deviation of 13% to 38% between filters. This variation in performance indicates that process control at WTWs could be a considerable limitation in the accuracy of WTW models. Previous documentation of the models that are developed here do not disclose their predictive accuracy and restrict themselves to application using bench scale or pilot plants for periods of time of less than a week (Edzwald et al., 1992, Adin and Rebhun, 1977, Saatci and Oulman, 1980), occasionally using operational works for periods of time less than a month (Head et al., 1997). It is found that clarified and filtered turbidity can be predicted with RMSEs under 50%. Due to the relatively low degree of accuracy when replicating the performances over annual periods, it seems that the justification for the complexity of some of the models, along with the considerable amounts of calibration data they require, is limited for whole works modelling. The application of simpler models calibrated using limited process and telemetry data could be more suitable, providing that conservative estimates of performance and caution over the reliability of results is used.

Unlike the method applied in Gupta and Shrivastava (2006, 2008, 2010), where only final water solids content was assessed, acceptable water treatment is judged to only occur in this work if solids content after clarification and filtration meet set criteria. These dual criteria for solids removal are set because reducing the solids content below target concentrations does not guarantee microbiological quality but merely indicates that processes are operating effectively (Allen et al., 2000). It is important that clarification and filtration are both operating effectively in order minimise the likelihood of pathogens passing through to the disinfection stage. A second reason for setting a separate clarified solids content limit is that, when applied alongside an optimisation process, it acts to promote solutions that have similar clarified turbidity as that used to calibrate the filter models originally, increasing the reliability of the predictions made.

Although the models in the operational zone analysis (section 5.1) predict that warmer water would result in an increase in the maximum possible abstraction rate, this does not indicate that climate change, resulting in possibly warmer mean temperature, will be likely to result in lower turbidity final waters. Climate change could also influence other water properties such as alkalinity, hardness, TOC and ammonia concentrations. Clark et al. (2011) reported that for a river they investigated, TOC was predicted to increase in the future (by 0.03 mg/l per annum) and that TOC was identified as being the dominant parameter in determining disinfection by-product concentrations. It is shown in Section 5.1 that controlling TOC concentrations using enhanced coagulation could reduce the maximum abstraction rate of a WTW considerably and so there is uncertainty in the influence of climate change on the operation of WTWs.

6.2.4.2 *Hopper Bottomed Clarification (HBC)*

Two different approaches are taken to modelling Hopper Bottomed Clarifiers. In the static model, exponential decay of solids content is applied and in the dynamic model a more complex CSTR approach is taken, based on the model described in Head et al. (1997). The more complex model takes into account additional mechanisms such as the influence of sludge blanket thickness on removal rate and the potential for the sludge blanket to overtop. Head et al. tested the dynamic HBC model using separate calibration and verification data over approximately a month and reported accuracy of a similar degree to that achieved in this work, which Head et al. described as "good". Head et al. also observed peaks in clarified turbidity due to line flushing (two of which can be seen in Figure 6-1).

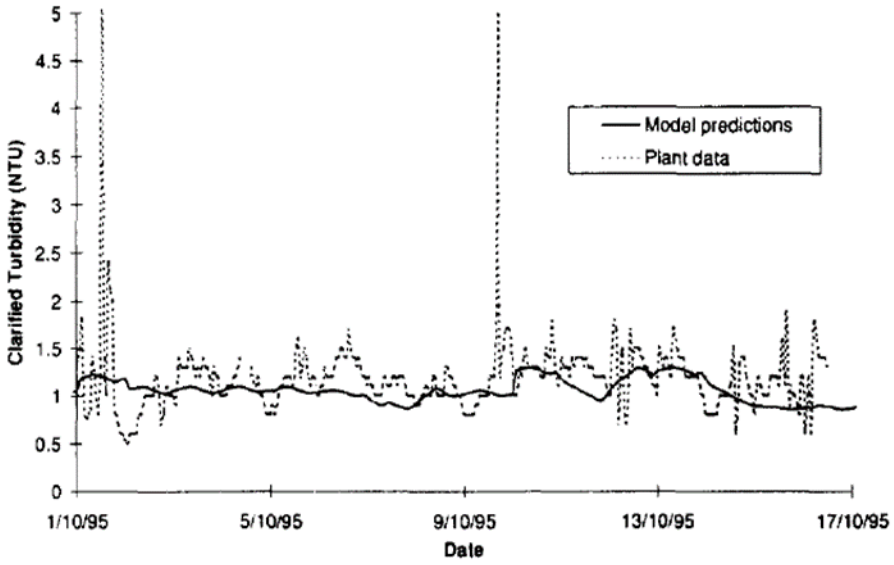

Figure 6-1 Performance of dynamic model as applied in Head et al. (1997)

The RMSE of the more complex dynamic model is less than that of the static model, but of a similar magnitude (RMSE ± 0.1 NTU). In light of this, the use of static decay equations to model solids removal by HBC clarifiers is recommended, with conservative limitations placed on surface loading rates in order to reduce the likelihood of loss of the sludge blanket.

Although it is found that the improvement in accuracy of predicting HBC clarified turbidity using a dynamic model, in comparison to using a simpler exponential decay model, is limited, some insight into applying the dynamic model for whole works reliability studies is gained. It is found that: (i) the settlement of primary particles does not require modelling; (ii) setting an initial sludge blanket concentration reduces initialisation time; (iii) the accuracy of the model is insensitive to the number of continuously stirred tank reactors (CSTRs) used; (iv) the application of non-works specific hindered settling parameters can result in unrepresentative sludge concentrations being predicted and (v) the model is capable of predicting clarified turbidity to a reasonable accuracy when general, non-works specific calibration parameters are applied.

The modelling of primary particles is found not to be necessary, as under low surface loading rates, which are the only conditions where this mechanism is likely to have a substantial influence, sludge blanket removal is likely to result in sufficient solids removal. The use of general Barnea and Mizrahi (1973) hindered settling parameters from Head et al's (1997) previous study in the dynamic HBC model is found to result in a greater than expected volumetric blanket concentration (approximately 60% as opposed to an expected concentration below 30%). It is possible, however, that the low overflow rate of the HBCs at Trimpley WTW could develop a thicker than average blanket.

6.2.4.3 *Dissolved air flotation (DAF) clarification*

A lower degree of accuracy is achieved in predicting DAF clarified turbidity than HBC clarified turbidity using static and dynamic models. The lower degree of accuracy achieved is partly due to individual tanks being brought in and out of service and them appearing to have substantially

different removal efficiencies (mean turbidity of different tanks is found to have a standard deviation of 34%). The difference in turbidity removal efficiency between the DAF tanks could be due to their maintenance condition or small differences in their setup. The DAF clarified turbidity is also found to spike more often (see Figure 4-16 and Figure 4-17) and have a greater standard deviation than HBC clarified turbidity (0.27 NTU vs. 0.16 NTU). The greater degree of variation in solids removal performance by the DAF process indicates possible operational deficiencies such as floc carry over or streaming which is not replicated by the models.

The static and dynamic models that were both based on the attachment model described in Edzwald (2006) are found to have comparable accuracy in predicting clarified turbidity, with the dynamic model having a RMSE 0.06 NTU lower than the static model. Due to the difficulties identified for predicting DAF solids removal efficiency, it is possible that simpler static decay rate equations could be used to predict the performance of the process for whole works modelling to a sufficient degree of accuracy.

6.2.4.4 *Filtration*

Due to the lack of turbidity breakthrough observed at Trimpley WTW, it is possible that increasing the durations of filtration runs may result in: the mean filtered turbidity reducing (due to filter ripening occurring less often), a reduction in backwashing energy use, less loss of partially treated water and less disruption of disinfection discharge. For these reasons, it is recommended that increasing the duration of filtration runs at Trimpley is investigated further.

Turbidity breakthrough of the filters is not observed at Trimpley WTW and two individual pilot plant studies failed to accurately identify filtration parameters (Omar, 2012, Yegorova, 2013). The pilot plant studies identified parameters which substantially over-predicted the solids

removal ability of Trimpley WTW's rapid gravity filters, despite using water sourced from upstream of the operational filters, using representative filter media and depths. Some of the difficulty in identifying representative parameters for the filtration model may be due to the filters at Trimpley WTW not sufficiently representing ideal filters. Evidence that some filters were not operating optimally is identified in the variance in mean filtered turbidity and head loss between filters (measured over month long periods). This variation in performance is defined by mean filtered turbidity standard deviations of 13% to 38% and mean head loss standard deviations of 51% to 66% between filters, for data collected in July 2011 and January 2012. Due to the difficulties identified in defining the performance of the filters, the Bohart & Adam equation is adopted due to its lower computational requirements and the necessity to only subjectively identify a single removal efficiency parameter.

The accuracy of the dynamic filter model is better than the static model, with RMSEs of 0.035 NTU and 0.045 NTU respectively. Some of the additional error of the static filtration model comes from the tendency of its predicted filtered turbidity to fluctuate to a greater extent than is observed in reality. This fluctuation is due to the static model not having a mechanism to dampen the influence of short term fluctuations in operating conditions. As the RMSEs of the two models are similar (± 0.01 NTU) and the likelihoods of exceeding the target filtrated turbidity of 0.1 NTU are also similar (± 5%), this indicates that the additional complexity of the dynamic model may not be justified for whole works modelling.

The use of a filter ripening mechanism results in filtered turbidity within the initial six hours after backwashing being predicted with a RMSE of 0.025 mg/l. The influence of the ripening process is reduced at operational sites by running initial flows after backwashing to waste until

filtered water turbidity reduces below a prescribed value (0.5 NTU at Trimpley). If it is assumed that this degree of temporary increase in filtered turbidity is acceptable, as at Trimpley, and that the energy costs of backwashing and the chemical costs of passing previously coagulated water to waste are sufficient to identify longer filtration durations then it may be acceptable not to model ripening for WTW optimisation purposes.

It is shown in this discussion that the certainty in the modelled filter performance is limited, due to performance variation between filters in the same bank and difficulty in identifying robust process parameters. It is also found that applying dynamic aspects to the nominally static logistic curve approximation of filter performance improves predictive ability marginally and that the influence of ripening could be considered negligible for whole works optimisation purposes. If it is also assumed that the influence of backwashing on contact tank discharge (discussed further in section 6.2.6) is not modelled and that a conservative approach is required to predicting filter performance, then a very simple filter model could be appropriate. It is possible that the Bohart & Adam equation could be applied statically to represent the mean performance of a bank of filters with the time since last backwash parameter consistently set as being the filter run duration. This simple solids removal model could be applied alongside a head loss model which limits clean head loss to a fraction of the maximum head loss permissible.

6.2.5 Adsorption

When modelling of TOC removal by GAC was attempted at Trimpley WTW, it was found that sufficient data were not available to model the temporal variation of performance, as only monthly reservoir and final water TOC concentrations were routinely recorded. This resulted

in a decision to model TOC removal due to GAC and filtration together, using a fractional reduction typical for WTWs in the surrounding area. This method resulted in representative final TOC concentrations being predicted.

6.2.6 Chlorine disinfection and disinfection by-product formation

In this work, some empirical, general site, very fast free chlorine concentration consumption (occurring within the first five minutes) and fast first order decay chlorine parameters (for five minutes to two hours) are used to predict chlorine consumption. These relationships are developed from the site specific relationships reported by Brown (2009) for WTW in the West Midlands, UK. Contact tank inlet free chlorine concentration data are available for this site and the accuracy of applying the first order decay equations to a static plug flow and a dynamic multiple CSTR model are assessed. The decay occurring in the initial five minutes is assumed to occur between the dosing point and the contact tank. The contact times at Trimpley are found to exceed two hours approximately a third of the time, which is longer than any of the durations investigated in the decay relationships reported by Brown (2009). Free chlorine consumption is found to be under-predicted by approximately 5% in the models used. This indicates that either the non-site specific relationship used to predict chlorine decay is too conservative or that a substantial amount of fast initial chlorine decay reactions are still occurring as the chlorinated water enters the contact tank. It is likely that free chlorine decay could be modelled more accurately if initial dose data was available. THM formation is predicted based on a direct correlation with free chlorine consumption, as applied by Hua (2000) and Brown et al. (2010), due to its simplicity and basis on rational theory.

In assessing the performance of Trimpley WTW, the contact tank inlet and outlet free chlorine concentrations are found to vary with a standard deviation of approximately 0.1 mg/l. This variation is thought to be due to varying initial water quality and the presence of chlorine dosing feedback control. The backwashing of filters and adsorption beds is also found to influence the volumetric discharge of contact tanks as a result of irregular draw-off of partially treated water for backwashing purposes. The influence of this draw-off is seen to include a temporary increase in discharge when treatment beds are drawn down. This additional variance of contact tank discharge rate is likely to affect disinfection and the production of disinfection by-products.

No clear correlation between free chlorine consumption within the contact tank and THM formation is observed, although the frequency of THM concentration readings is low (once a month). If the recorded data are representative of THM formation, then it is possible that the formation of THMs is strongly dependent on the initial chlorine consumption that took place before the contact tank that is not measured. Despite this, THM formation prediction based on predicted chlorine consumption is found to have a RMSE less than 5 µg/l. This indicates that the chlorine consumption / THM formation correlation applied may not have a strong causal relationship.

The dynamic model's RMSEs for predicting CT, THM formation and residual free chlorine concentration are found to be lower than those predicted using the static model, but of the same magnitude (±3%). The accuracy of the models for predicting CT, THM formation and residual free chlorine concentration is approximately ±10%, ±20% and ±30% respectively. Overall, for whole works modelling, the marginal improvement in predictive ability is not sufficient to

justify the increase in complexity and computational resources required to model disinfection dynamically.

The majority of the error observed in the THM models is caused by a general under-prediction of THM production (mean concentrations are 21% to 29% lower than observed). Chlorine consumption between the dosing point and the contact tank inlet not being calculated and under-prediction of chlorine consumption within the contact tank (residuals approximately 5% greater than observed) would have contributed towards this under-prediction of THM formation. If free chlorine consumption before the contact tank had been predicted accurately, and included in the total consumption, then an improved estimate of THM formation could have been made.

When Monte-Carlo conditions are applied to the models, despite a marginal decrease in mean abstraction rates, it is found that the models predict lower chlorine consumption and THM formation than when time series data are applied. A possible reason for this is that under Monte-Carlo conditions, correlations between water quality parameters are not represented, such as between TOC or bromine concentration with UV_{254} absorption. These correlations, which have been shown to exist elsewhere by Clark et al. (2011), may be accountable for the higher mean THM concentration predicted for time series conditions.

6.3 Accuracy of static and dynamic WTW models

6.3.1 Calibration and verification data

The data used to calibrate the models comes from a warmer drier year whereas the data used to verify the models comes from a cooler wetter year. According to previous research, the change in conditions between the calibration and verification years should have resulted in: (i) mean

TOC concentration and solubility reducing but with greater concentration flux; (ii) a reduction in coagulation efficiency; (iii) reduced THM formation and (iv) reduced reservoir residence time leading to larger more easily removed organic matter reaching the WTW (Ritson et al., 2014). It is actually observed, in contradiction to the findings reported in Ritson et al. (2014), that the mean TOC concentration increased whilst its standard deviation reduced and the production of THMs increased. The mean dose of coagulant and clarified turbidity did, however, increase during the verification period, supporting the prediction that the coagulation efficiency should reduce. These results provide an indication of the uncertainty of the implications of climate change on the performance of WTWs. This variation in the weather and water quality between the calibration and verification data are also likely to have reduced the accuracy of the models. Both of the years examined also had cool summers, limiting the peak reservoir water temperature. This is likely to have limited the THM production observed in both years. The water temperature used in the modelling is from the river abstraction point, which is likely to fluctuate more than the reservoir that would have acted as a thermal store. This means that the model is likely to have exhibited greater extremes of water temperature than are actually experienced at the WTW.

As the data used to calibrate and verify the model come from an operational WTW, the range of performance observed is limited, due to the operators striving to provide a satisfactory water quality for consumers. In particular, the inability to observe clearly the breakthrough characteristics of the rapid gravity filters has limited the ability to model filtration to a high degree of certainty. This means that when unsatisfactory performance is predicted (as defined in section 4.4.3.1), the model is likely to be operating at, or beyond, the range of the calibration and verification data. The considerable uncertainty in modelled failure prediction could result

in substantial operational savings not being identified for the sake of minimal reductions in the likelihood of WTWs not achieving their operational goals.

6.3.2 Time series performance

The RMSE achieved in replicating key performance criteria are shown in Table 6-1.

Table 6-1 RMSE of models

Parameter	**Static model**	**Dynamic model**
HBC clarified turbidity (NTU)	0.26	0.18
DAF clarified turbidity (NTU)	0.28	0.34
Rapid gravity filtered turbidity (NTU)	0.045	0.035
Residual free chlorine concentration (mg/l)	0.17	0.14
Product of residual free chlorine concentration and t_{10} contact time (mg.min/l)	23	22
THM production (µg/l)	3.0	3.4

The RMSE accuracy of the static and dynamic models is comparable to the quality assurance targets set for measurements taken from Trimpley WTW by Severn Trent Water. The RMSE of the THM predictive models is greater than the operators' quality assurance limit but the RMSE of the readings is within 5 µg/l and is compared to infrequent (monthly) measurements. The dynamic models were found to be more accurate than the static models, with the RMSE of the dynamic model at least 5% less than that of the static model for the solids removal processes (HBC and DAF clarified and rapid gravity filtered turbidity) and between 1% to 3% less for the disinfection models (residual chlorine concentration, CT and THM formation). For Trimpley WTW, the RMSE of the clarification models used is greater than the difference in mean clarified turbidity from the HBC and DAF processes. The accuracy of any optimisation process which attempts to compare the performance of these two clarification processes is, therefore, likely to be minimal (see Table 4-9 and Table 4-10).

When the models are used to predict the fraction of time that key water quality goals could be met, an accuracy of ±15% is achieved. For observed time series conditions, the static model is found to be more likely to predict elevated clarified turbidity (NTU > 1) whilst the dynamic model is found to predict elevated filtered turbidity (NTU > 0.1) more often. Both models predict similar likelihoods of achieving insufficient disinfection (CT < 60 mg.min/l) or elevated THM concentration (THM > 25 µg/l) (±3%) (Table 4-25 and Table 4-26). The dynamic model predicts a higher likelihood of filtered turbidity exceeding 0.1 NTU due to interventional backwashes, which cause filter ripening to occur. Although the filtered turbidity is higher than usual during filter ripening, it can be ensured that filtered water is run to waste until a specified turbidity is achieved. Assuming this is acceptable, the static models are likely to identify more robust, conservative, solutions than the dynamic models when applied to optimisation processes.

6.3.3 Monte-Carlo Analysis

In order to assess the performance of the examined WTW stochastically, it is necessary to define the probability distributions of the observed water quality parameters. The likelihood that the probability distributions of the water quality parameters could be approximated to a selection of standard distributions is assessed to a 5% significance level using the Anderson-Darling test (see Table 4-16). However, for a consistency of approach, non-standard distributions are used to represent the operating conditions in this thesis. Operating conditions are sampled, each simulated day, over a simulated year, in each Monte-Carlo run.

The synthetically produced time series data used in the Monte-Carlo analysis will not be completely representative of the conditions observed at the works. The non-standard

distributions, which are used to represent the operating conditions observed at Trimpley, are produced by interpolating between the lower boundary values of the cumulative frequency bins used to segment the recorded data. This procedure results in a slight under-estimation of the operating condition parameters used in the Monte-Carlo analysis. The independent simulated daily sampling of all of the operating conditions also results in conditions that differ from observed time series data as the recorded data's parameters are seen to vary in magnitude over different time frames. Any correlations between the operating conditions, which were identified by Clark et al. (2011) to exist at another WTW are also not represented.

When Monte-Carlo conditions are applied, the mean of the key performance parameters adjusted by up to 15% for the dynamic model and up to 20% for the static model, in comparison with the application of time series data (see Table 4-18 to Table 4-23). This variation in performance is likely to be caused by the random nature of the Monte-Carlo process, inexact representation of operating conditions and the lack of correlation between operating conditions modelled. Some of the variation in performance, under Monte-Carlo conditions, could be reduced through the use of greater sampling of operating conditions for each simulation. This would act to reduce the performance variation between independent runs. The range of mean key performance values, produced from three separate Monte-Carlo runs, is found to be less than 5%, except THM production. The high degree of variation predicted for THM production indicates that predicted chlorine consumption is sensitive to particular combinations of operating condition parameters, and therefore requires a greater number of operating condition samples to be made, to achieve more consistent performance.

Both models, for time series and Monte-Carlo conditions, are found to predict the likelihood of failing the specified water quality goals to within 15% of that observed operationally (see Table 4-25 and Table 4-26). The application of the Monte-Carlo techniques is found to vary failure rates by less than 5%, except for filtered turbidity for both models and DAF clarified turbidity for the static model. The static model's DAF clarified turbidity exceeds 1 NTU significantly more often under Monte-Carlo conditions (+10%) and this is possibly due to the loss of some correlation between operating conditions. The decrease in the fraction of time that filtered turbidity is predicted to exceed 0.1 NTU under Monte-Carlo conditions (-10%) could partially be caused by the mean abstraction rate applied being slightly lower than that observed. Application of Monte-Carlo conditions to the WTW models results in: the predicted likelihood of the performance criteria not being met differing from those made using time series data (by up to approximately 10%), with a precision of ±5% and an accuracy of ±15%. The static WTW models are able to predict the likelihood of the performance criteria not being met to a similar degree of accuracy as the more complex dynamic models and so are more suitable for whole works modelling.

6.4 Water treatment works optimisation

6.4.1 Operating zone analysis

Computational models of WTWs are not commonly used for day to day operational guidance. This is because there are multiple, complex relations between the operating conditions and the process found at WTWs. It is therefore difficult to make simple recommendations based on a manageable number of water quality parameters. A novel method to address this issue is applied. The majority of operating conditions are set to values typical of those observed at

Trimpley WTW and the source water temperature and TOC concentration are varied in multiple simulations. For each set of conditions, the minimum and maximum abstraction rate for which the WTW is expected to meet its performance targets is predicted using both the static and the dynamic models. The results from this analysis is graphically presented in a 3D "operating zone". This diagram could be used by operators to give guidance as to what range of abstraction rates should result in acceptable WTW performance, dependent on water temperature and TOC concentration.

It is found that the static and dynamic models identified similar "operating zones", indicating that the same failure mechanisms are likely to be limiting their range of abstraction rates. For raw waters with temperatures below 18 °C and TOC concentrations below 6 mg/l, the predominant limiting factor of maximum abstraction rate is the achievement of a sufficiently low clarified and filtered turbidity. As raw water TOC concentration increases, the maximum abstraction rate reduces due to extra solids loading caused by the need for additional coagulant. This relationship is not observed for conditions where higher raw water TOC concentrations require the specified maximum coagulant dose. For raw waters warmer than approximately 18°C, with TOC concentrations above approximately 6mg/l, it is found that "good" performance could not be achieved purely through abstraction rate control. This is because either the clarified or filtered turbidity is too great or because of excessive THM production. For the operational conditions simulated, the use of the dynamic model results in a greater range of and lower maximum abstraction rates, for the vast majority of conditions examined. The greatest difference in the acceptable maximum abstraction rate predicted by the models is 300 m^3/h.

Due to the similar predictions made by the different models, it is concluded that the use of a static WTW model would be sufficient for this type of analysis in future as a result of its lower complexity and computational demands. The simulation results indicate that the maximum abstraction rate of a WTW is highly dependent on the raw water temperature and TOC concentration (if coagulant is being dosed to limit its clarified concentration). The plateauing of maximum abstraction rates for TOC values above 6 mg/l and subsequent analysis of the coagulant dosing algorithm suggests that if reservoir TOC concentrations rise substantially above their current mean concentrations of 5.4 mg/l, the current maximum dosing of coagulant at Trimpley would be insufficient to maintain current, predicted, clarified TOC concentrations. Perhaps most importantly, the operating zone analysis predicts that for warm waters with high TOC concentrations, it may not be possible to meet the specified operating criteria under the current operating regime. If the reservoir water is warmer with elevated TOC concentrations, relatively frequently because of changes in climate or catchment management, then the operating regime or capital infrastructure may need to be adjusted in the future.

6.4.2 Application of genetic algorithms (GAs) to WTW optimisation problems

6.4.2.1 *Optimisation problems and techniques*

The design of the works is optimised by minimising the footprint area and a separate optimisation is carried out for operational costs. In both optimisation problems, the fraction of the time that performance targets are not achieved is also minimised. As each optimisation has two objectives, multiple Pareto optimal solutions are identified (see section 2.2.4.2). Each of the optimisation problems set has five decision variables, for which a range and a precision is specified. The range and precision of the variables is limited so that the computation demand

of the optimisation process is reduced. As a result of these limits, the number of possible solutions reduces from being infinite to approximately one hundred thousand and seven hundred million solutions for the design and operating regime problems respectively.

The NSGAII algorithm is applied to both of the optimisation problems and found to identify sufficiently converged solution populations after a hundred generations, to represent a pseudo-Pareto set. The failure rate of the solutions is unconstrained and the majority of Pareto solutions identified have failure likelihoods greater than 50%. As unreliable solutions are of less interest, the use of some mechanism to limit the failure likelihood could have resulted in more efficient use of computational resources, although premature convergence could be a concern. Another problem with not constraining the failure rate of solutions is that the optimal solutions identified by the static and dynamic models are difficult to compare, as they inhabit different regions of the reliability search space. The use of constrained or pseudo-constrained acceptable failure rates, as carried out by Gupta and Shrivastava (2006, 2008, 2010), would have allowed easier comparison of solutions identified through the use of the different models. Constraining the precision of solutions and simulating only unique solutions improves the efficiency of the search process but solutions identified in previous generations require their reliability to be reassessing each generation. This is necessary because of the variance in conditions between runs (found to result in approximately a 5% variance in failure rate during model verification). This continual assessment of reliability does have the advantage that over multiple generations, the solution population is assessed against an increasingly diverse set of conditions, resulting in a more robust population evolving. If the sampling of the conditions is increased so that the variance in performance of the model is negligible between runs, then it could be possible that only newly identified solutions would need their reliability evaluated. For computationally

demanding models this could improve the reliability of results (as a greater combination of conditions could be assessed) and reduce the computational demand (as individual solutions would only be assessed once).

6.4.2.2 *Identification of suitable genetic algorithm internal parameters*

The influence of using a lower, intermediate and higher values for each internal parameter is investigated, as in Sharifi (2009). Owing to the higher computational resources required by the models in this work, a full cross comparison of different combinations of parameters is not carried out. Instead, a control set of intermediate parameter values is identified and then the influence of applying higher and lower values to each parameter is investigated. The variation of most of the internal parameters identified solutions populations with comparable fitness in terms of the number of Pareto solutions identified and the degree of diversity exhibited (see Table 5-4). Although this method does not identify a clear set of optimal GA internal parameters, it does identify a few parameter values as being either preferable or unsuitable. The difficulty in identifying optimal internal parameters is due to the complex interactions between them and the inherent randomness of the GA process. The GA internal parameters are not optimised for each combination of model type (static or dynamic) and optimisation problem (design or operating regime), as it is preferable to assess the optimal solutions identified by the models using identical GAs. Using guidance from the internal parameters sensitivity analysis, along with recommendations from previous research (see section 2.2.3.8), a set of reasonable GA internal parameters is identified. The values applied are considered to be appropriate based on previous findings that a range of settings can result in good performance (Grefenstette, 1986) and that the same solutions can be found using GAs with either general or optimised internal

parameters (Franchini and Galeati, 1997). The influence of possible premature convergence or loss of Pareto solutions is addressed through the application of multiple independent runs of the GAs and the compilation of a secondary population of all Pareto solutions identified. The use of the NSGAII inspired genetic algorithm with: (i) a population of thirty, (ii) cross-over probability of 70% and distribution index of ten along with (iii) a mutation probability of 5% and distribution index of twenty is found to result in sufficiently converged solution populations after a hundred generations. It is concluded that future investigations that are concerned with using GAs, rather than developing them, should in many instances identify appropriate values based on state-of-the-art guidance rather than calibrate them to individual problems.

6.4.2.3 *Solutions identified*

In this work, for the first time, designs and operating regimes, identified by genetic algorithms from performance criteria assessed by static and dynamic WTW models, are compared. This work is also novel in the application of whole works optimisation techniques to case study data from an operational works. The models used are calibrated and verified to observed performance and both solids removal and disinfection performance criteria are assessed. This is unlike past studies, which have tended to focus on one or the other (Gupta and Shrivastava, 2008, Clark et al., 2011).

Despite the similarity in predictive ability of the static and dynamic models in terms of their RMSE (±5%) and likelihood of failing the performance targets (±5%), the designs and operating regimes identified through the use of a genetic algorithm are substantially different. This is particularly prominent in the weighting placed on the alternative clarification processes. It is found that the use of the dynamic model results in a greater emphasis being placed on DAF

clarification. From this, it is concluded that the relative reliability of the DAF process, in comparison to the HBC process, is greater in the dynamic rather than static model (see Figure 5-25 and Figure 5-27). Despite the differences in solutions identified using the static and dynamic models, it is found that neither model results in the identification of consistently more costly or reliable solutions. The relative costs of the solutions identified by the models is dependent on the multi-objective problem set and the reliability of the solutions identified.

The observed difference in mean clarified turbidity between the HBC and DAF processes at Trimpley WTW (±0.24 NTU) is comparable to the RMSE of the clarification models produced (0.18 NTU to 0.34 NTU). This indicates that the accuracy of the clarification models is insufficient to reliably differentiate between the two processes. For future WTW optimisation studies using computational models, it is recommended that alternative treatments are not investigated until the potential to successfully optimise a simple linear treatment chain has been substantiated.

The optimisations identify maximum contact tank volumes and inlet chlorine concentrations comparable to those currently used in operation at Trimpley WTW. The observed contact tank inlet free chlorine concentration (1.6 mg/l) lies between the maximum identified by the static model (1.5 mg/l) and the maximum identified by the dynamic model (1.8 mg/l). Although this shows that the process is able to identify contact tank inlet free chlorine concentrations similar to those applied in reality, in future it could be more useful to optimise contact tank outlet concentrations. The maximum contact tank volumes identified as optimal are larger than those observed at the site (2400 m^3), with the static model identifying a maximum volume of 3200 m^3 and the dynamic model identifying a maximum volume of 2800 m^3. This indicates that the

contact tank at Trimpley may be under-sized for the conditions it operates under. This conclusion is supported by the observed CT value at Trimpley WTW being seen to fall to almost 60 mg.min/l in the summer months. A relatively high target clarified TOC concentration (approximately 5 mg/l) is identified as being optimal due to the lower doses of coagulant required. Although this is predicted to not result in excessive free chlorine consumption or disinfection by-product formation, application of this operating regime may not be suitable, as insufficient destabilisation of colloids or excessive organic growth in the distribution network could result. Longer duration filtration runs are also identified as being preferable at Trimpley. This is in agreement with the observed performance, where excessive head loss or turbidity breakthrough are rarely observed. As the identified optimal filtration duration (96 hours) is considerably outside the calibration conditions observed, limited confidence should be placed in this estimate but it is believed that the application of long filtration runs should be considered at Trimpley WTW.

6.5 Benefits of static models for optimisation

It is found that static models are more suitable for whole WTW modelling than dynamic models. Static models, in comparison to dynamic models, are shown to be able to predict more conservative estimates of the likelihood of WTW failing performance criteria, whilst having similar RMSE accuracies and predicting comparable cost solutions when used to solve optimisation problems. The use of static models reduces the computational requirements of carrying out optimisations (the optimisations using the dynamic models are found to take two to eight times the computational resources of the static models), allowing a greater number of operating conditions to be considered and/or generations to be simulated. Static models also

have no requirement for the sampling frequency of operating condition parameters be defined. Static models, due to their lack of necessity for differential equations, are faster to simulate and more consistent in their computational requirements. When applied along with genetic algorithms, it is possible to more accurately estimate the computational resources and time required to complete an optimisation process.

7 CONCLUSIONS

This thesis investigates the development of a software tool to: identify operating conditions under which water treatment works (WTWs) are expected to produce water of an acceptable water quality and to minimise WTW design and operational costs, using genetic algorithms and Monte Carlo methods. A summary of the conclusions of this research are outlined below in further detail with the aims and objectives they relate to shown in square brackets.

7.1 WTW Modelling

1. Dynamic WTW models are found to be more accurate than static models at predicting the performance of an operational site over a nine month period. The RMSE of the dynamic model is found to be at least 5% less than the static model for the solids removal processes and 1% to 3% less for the disinfection and disinfection by-product formation processes [A1, O2].
2. Clarified and filtered turbidity are predicted to a RMSE of under 50% [A1, O2].
3. The use of the empirical solids removal efficiency parameters (dependent on initial turbidity) results in an average reduction in RMSE of approximately 15% [A1, O1, O2].
4. The backwashing of filters and adsorption beds can influence the volumetric discharge of contact tanks [O1].
5. No correlation between chlorine consumption within the contact tank and THM formation is observed at the examined site [O1].

7.2 Use of Monte-Carlo analysis for analysing WTW performance

6. The likelihood that the probability distributions of a range of key operating conditions could come from a selection of standard distributions is assessed to a 5% significance level using the Anderson-Darling test (see Table 4-16) [A3, O5].
7. The application of stochastic operating conditions to the WTW models is found to vary mean performance parameters by approximately 15% [A1, O6].
8. "Good" WTW performance, defined by taking into account legislative limits and observed operational performance, is defined (as shown in Table 4-24) [A2, A3, O3].
9. The likelihood of failure to achieve specified water quality goals is predicted to within 15% (see Table 4-25 and Table 4-26) [A1, O6].

7.3 Operating zone analysis

10. Static and dynamic models identified similar relationships between raw water temperature, TOC concentration and acceptable abstraction rates [A2, O4].
11. Maximum abstraction rate is found to be inversely correlated with initial TOC concentrations below 6 mg/l [A2, O4].
12. For raw waters warmer than approximately 18 °C with TOC concentrations above approximately 6mg/l, it is predicted that "good" performance cannot be achieved purely through abstraction rate control, due to either clarified / filtered turbidity or THM production being too great or insufficient disinfection [A2, O4].

7.4 Optimisation of WTW design and operating regime using genetic algorithms

13. The optimisation process is found to be relatively insensitive to the internal parameters applied. Use of typical values from state-of-the-art guidance is found to be effective [A3, O7].
14. The application of dynamic or static models is not found to consistently identify more optimistic or conservative solutions to optimisation problems [A3, O7].

7.5 Benefits of static models for optimisation purposes

15. The static models used are faster to simulate and more consistent in their computational requirements than the dynamic models [A3, O7].
16. Static models are found to be more suitable for whole WTW optimisation modelling. Static models are shown to predict failure of water quality goals more often for existing conditions at an observed site whilst having a similar RMSE accuracy and predicting solutions of comparable cost when applied to optimisation problems [A1, A3, O7].

8 RECOMMENDATIONS FOR FURTHER WORK

8.1 Introduction

This thesis presents the modelling of a water treatment works (WTW) and the application of optimisation techniques including: the identification of operational conditions for which "good" water quality could be expected; and the use of genetic algorithms to identify near-optimal works designs and operating conditions. This chapter suggests recommendations for future work.

8.2 Modelling

8.2.1 General

- Future WTW optimisation studies should initially be applied to operational sites which do not have alternative processes or that the dependence on each alternative process is not attempted to be optimised (as current models appear to not be capable of accurately modelling their relative performance). WTWs which exhibit signs of turbidity breakthrough at the end of filtration cycles should also be examined. Alternatively, the construction of a pilot plant which replicates whole works treatment could be used to examine water treatment optimisation. This would enable greater control of operating conditions and of water quality measurement.
- The application of control systems for determining the division of flows between alternative treatment streams dependent on raw and treated water quality measurements could be examined to improve operational efficiency.

8.2.2 Coagulation & flocculation

- The dosing algorithm described in this work could be applied to operational as its sensitivity to changing operational conditions is found to approximately correlate with those applied by operational staff for the DAF stream at the examined site. If successful, this algorithm could have the potential to respond to changing water quality more rapidly than operators and could also enable greater automation of process control. The dosing of coagulant could even take into account predicted chlorine decay and trihalomethane production to optimise coagulant dose further.
- The potential to control the dose of coagulant and pH to achieve optimal TOC adsorption could be examined. This could predict the magnitude of cost savings of reducing the quantities of coagulants applied whilst also examining the influence of disinfection. At present the influence of water quality, coagulant dose and flocculation on the solids removal efficiencies of clarification and filtration process is not understood sufficiently to enable accurate modelling and could be examined further.

8.2.3 Solids removal

- Due to the difficulty in predicting the solids removal efficiency of clarification and filtration processes for varying initial turbidity water, it would be interesting to see how much of this variation can be explained by non-linearity of the turbidity suspended solids relationship and/or the variation in the distribution of particle size with turbidity. The variation in these relationships between WTWs and seasons would also be of interest and of potential benefit to the modelling process.

8.2.4 Disinfection

- The potential for incorporating free chlorine decay relationships, dependent on the contact tank inlet water quality, into control systems to maintain target residual concentrations could be investigated.
- As no strong correlation is identified between free chlorine consumption within the contact tank and THM formation at the WTW examined but previous studies have found there to be a correlation between total free chlorine consumption and THM formation, the relationship between the fast initial decay reactions of free chlorine and the formation of THMs should be examined in greater detail.

8.3 Optimisation

- As the accuracy of the static and dynamic water treatment works models are found to be comparable for whole works optimisation, it would be prudent to research the potential for simplifying the modelling process further and identify the influence on optimisations carried out. The relative accuracy of models where each process is represented by a single unit with its depth and total footprint area defined should be examined. These models would not take into account the influence of intermittent or cyclical individual process units (such as DAF tanks and filters) which would reduce their complexity substantially as well as allowing greater precision in the optimised solutions identified.
- The WTW construction costing equations which exist (McGivney and Kawamura, 2008, Clark, 1982, Gumerman et al., 1979b) are approximate and are not suitable for optimisation work. As the building of WTWs is a fairly infrequent event and their costing commercially sensitive, it is unlikely that sufficiently accurate costing models

are going to be available in the foreseeable future. It is therefore recommended that future WTW optimisation study focuses on operational costs. Also, due to an insufficient degree of certainty in solids removal modelling, optimisation should focus on the coagulation and disinfection stages with solids removal purely modelled to assess whether solids loading originating from coagulant addition is likely to be acceptable.

- For the further assessment of the use of Monte-Carlo methods for WTW optimisation, the consequences of approximating operating conditions to standard distributions (such as normal etc.) and/or applying observed correlations between raw water quality parameters, as identified in Clark et al. (2011), could be examined.

REFERENCES

ADIN, A. & REBHUN, M. 1977. MODEL TO PREDICT CONCENTRATION AND HEAD LOSS PROFILES IN FILTRATION. *Journal American Water Works Association,* 69**,** 444-453.

ADLAN, M. 1998. *A STUDY OF DISSOLVED AIR FLOTATION TANK DESIGN VARIABLES AND SEPARATION ZONE PERFORMANCE.* PhD, THE UNIVERSITY OF NEWCASTLE UPON TYNE.

ALLEN, M. J., CLANCY, J. L. & RICE, E. W. 2000. The plain, hard truth about pathogen monitoring. *Journal American Water Works Association,* 92**,** 64-76.

BARNEA, E. & MIZRAHI, J. 1973. A generalized approach to the fluid dynamics of particulate systems : Part 1. General correlation for fluidization and sedimentation in solid multiparticle systems. *The Chemical Engineering Journal,* 5**,** 171-189.

BILOTTA, G. S. & BRAZIER, R. E. 2008. Understanding the influence of suspended solids on water quality and aquatic biota. *Water Research,* 42**,** 2849-2861.

BINNIE, KIMBER & SMETHURST 2006. *Basic Water Treatment*, Royal Society of Chemistry.

BLACK & VEATCH CORPORATION 2010. White's Handbook of Chlorination and Alternative Disinfectants (5th Edition). John Wiley & Sons.

BOHART, G. S. & ADAMS, E. Q. 1920. Some aspects of the behavior of charcoal with respect to chlorine. *Journal of the American Chemical Society,* 42**,** 523-544.

BOUCHIER 1998. Cryptosporidium in Water Supplies. DEFRA.

BRAND, N. & OSTFELD, A. 2011. Optimal Design of Regional Wastewater Pipelines and Treatment Plant Systems. *Water Environment Research,* 83**,** 53-64.

BRENNTAG. 2013. *RE: Official Quotation.*

BROWN, D. 2009. *THE MANAGEMENT OF TRIHALOMETHANES IN WATER SUPPLY SYSTEMS.* University of Birmingham.

BROWN, D., BRIDGEMAN, J. & WEST, J. R. 2011a. Predicting chlorine decay and THM formation in water supply systems. *Reviews in Environmental Science and Bio-Technology,* 10**,** 79-99.

BROWN, D., BRIDGEMAN, J. & WEST, J. R. 2011b. Understanding data requirements for trihalomethane formation modelling in water supply systems. *Urban Water Journal,* 8**,** 41-56.

BROWN, D., WEST, J. R., COURTIS, B. J. & BRIDGEMAN, J. 2010. Modelling THMs in water treatment and distribution systems. *Proceedings of the Institution of Civil Engineers-Water Management,* 163**,** 165-174.

BURLINGAME, G. A., PICKEL, M. J. & ROMAN, J. T. 1998. Practical applications of turbidity monitoring. *Journal American Water Works Association,* 90**,** 57-69.

CHEN, P. H., JENQ, C. H. & CHEN, K. M. 1996. Evaluation of granular activated carbon for removal of trace organic compounds in drinking water. *Environment International,* 22**,** 343-359.

CHICK, H. 1908. An investigation of the laws of disinfection. *Journal of Hygiene,* 8**,** 92-158.

CIKUREL, H., REBHUN, M., AMIRTHARAJAH, A. & ADIN, A. 1996. Wastewater effluent reuse by in-line flocculation filtration process. *Water Science and Technology,* 33**,** 203-211.

CIVAN, F. 2007. Critical modification to the Vogel-Tammann-Fulcher equation for temperature effect on the density of water. *Industrial and Engineering Chemistry Research,* 46**,** 5810-5814.

CLARK, R. M. 1982. COST ESTIMATING FOR CONVENTIONAL WATER-TREATMENT. *Journal of the Environmental Engineering Division-Asce,* 108**,** 819-834.

CLARK, R. M., LI, Z. W. & BUCHBERGER, S. G. 2011. Adapting water treatment design and operations to the impacts of global climate change. *Frontiers of Earth Science,* 5**,** 363-370.

CLARK, R. M. & SIVAGANESAN, M. 1998. Predicting chlorine residuals and formation of TTHMs in drinking water. *Journal of Environmental Engineering,* 124**,** 1203-1210.

CLEMENTS, M. & HAARHOFF, J. 2004. Practical experiences with granular activated carbon (GAC) at the Rietvlei Water Treatment Plant. *Water Sa,* 30**,** 89-95.

COLEY, D. A. 1999. *An Introduction to Genetic Algorithms for Scientists and Engineers*, World Scientific Publ.

COOPERATIVE RESEARCH CENTRE FOR WATER QUALITY TREATMENT 2007. *Modelling Coagulation to Maximise Removal of Organic Matter: A Pilot Plant and Laboratory Based Study: Chemical Dose Prediction*, CRC for Water Quality and Treatment.

COURTIS, B. J. 2003. *Water Quality Chlorine Management.* PhD, University of Birmingham.

CRITTENDEN, J., TRUSSELL, HAND, HOWE, TCHOBANOGLOUS & HARZA, M. W. 2005. *Water treatment: principles and design*, John Wiley.

CUNNINGHAM, R. 1999. The Bouchier Report - a recommendation too far? *Journal of Hospital Infection,* 41**,** 261-262.

DALY, R., VAN LEEUWEN, J. & HOLMES, M. 2007. Modelling Coagulation to Maximise Removal of Organic Matter. CRC.

DARBY, J. L. & LAWLER, D. F. 1990. Ripening in depth filtration: effect of particle size on removal and head loss. *Environmental Science & Technology,* 24**,** 1069-1079.

DAVIS, L. 1991. *Handbook of genetic algorithms*, Van Nostrand Reinhold.

DE JONG, K. A. 1975. *Analysis of the behavior of a class of genetic adaptive systems,*. Ph.D. thesis, Univ. of Michigan

DEB, K. 2000. An efficient constraint handling method for genetic algorithms. *Computer Methods in Applied Mechanics and Engineering,* 186**,** 311-338.

DEB, K., JAIN, P., GUPTA, N. K. & MAJI, H. K. 2004. Multiobjective placement of electronic components using evolutionary algorithms. *Ieee Transactions on Components and Packaging Technologies,* 27**,** 480-492.

DEB, K., PRATAP, A., AGARWAL, S. & MEYARIVAN, T. 2002. A fast and elitist multiobjective genetic algorithm: NSGA-II. *Ieee Transactions on Evolutionary Computation,* 6**,** 182-197.

DEPARTMENT OF ENERGY & CLIMATE CHANGE 2012. Comparisons of industrial and domestic energy prices: quarterly figures.

DES MOINES WATER WORKS 2012. 2012 Water Treatment Chemicals – Analysis of Bids and Authorize Execution of Contract.

DHARMAPPA, H. B., FUJIWARA, O., VERINK, J. & VIGNESWARAN, S. 1994a. WATER-TREATMENT SYSTEM-DESIGN FOR TURBIDITY REMOVAL .2. OPTIMIZATION. *Journal of Environmental Engineering-Asce,* 120**,** 921-942.

DHARMAPPA, H. B., VIGNESWARAN, S., VERINK, J. & FUJIWARA, O. 1994b. WATER-TREATMENT SYSTEM-DESIGN FOR TURBIDITY REMOVAL .1. SIMULATION. *Journal of Environmental Engineering-Asce,* 120**,** 900-920.

DHARMARAJAH, A. H. & CLEASBY, J. L. 1986. PREDICTING THE EXPANSION BEHAVIOR OF FILTER MEDIA. *Journal American Water Works Association,* 78**,** 66-76.

DUDLEY, J., DILLON, G. & RIETVELD, L. C. 2008. Water treatment simulators. *Journal of Water Supply Research and Technology-Aqua,* 57**,** 13-21.

DWI. 2010. *Drinking water standards / regulations* [Online]. Available: http://dwi.defra.gov.uk/consumers/advice-leaflets/standards.pdf [Accessed 24/08/2011].

ECKART, Z., MARCO, L. & LOTHAR, T. 2001. SPEA2: Improving the Strength Pareto Evolutionary Algorithm. Computer Engineering and Networks Laboratory (TIK)

Swiss Federal Institute of Technology (ETH) Zurich.

EDWARDS, M. 1997. Predicting DOC removal during enhanced coagulation. *Journal / American Water Works Association,* 89**,** 78-89.

EDZWALD, J. K. 2006. Chapter 6: Dissolved air flotation in drinking water treatment. *In:* NEWCOMBE, G. & DIXON, D. (eds.) *Interface science in drinking water treatment: theory and applications.* Elsevier.

EDZWALD, J. K., WALSH, J. P., KAMINSKI, G. S. & DUNN, H. J. 1992. FLOCCULATION AND AIR REQUIREMENTS FOR DISSOLVED AIR FLOTATION. *Journal American Water Works Association,* 84**,** 92-100.

ENDRESS HAUSER n.d. Technical Information: Differential Pressure Transmitter.

FOGEL, D. B. 1994. An introduction to simulated evolutionary optimization. *Neural Networks, IEEE Transactions on,* 5**,** 3-14.

FONSECA, C. M. & FLEMING, P. J. 1998. Multiobjective optimization and multiple constraint handling with evolutionary algorithms - Part I: A unified formulation. *Ieee Transactions on Systems Man and Cybernetics Part a-Systems and Humans,* 28**,** 26-37.

FOUNDATION FOR WATER RESEARCH 2011. Cryptosporidium in Water Supplies. 3rd Edition ed.

FRANCHINI, M. & GALEATI, G. 1997. Comparing several genetic algorithm schemes for the calibration of conceptual rainfall-runoff models. *Hydrological Sciences Journal-Journal Des Sciences Hydrologiques,* 42**,** 357-379.

GANG, D. D., SEGAR JR, R. L., CLEVENGER, T. E. & BANERJI, S. K. 2002. Using chlorine demand to predict TTHM and HAA9 formation. *Journal / American Water Works Association,* 94**,** 76-86.

GEANKOPLIS, C. J. 1993. *Transport processes and unit operations*, Allyn and Bacon.

GOLFINOPOULOS, S. K. & ARHONDITSIS, G. B. 2002. Multiple regression models: A methodology for evaluating trihalomethane concentrations in drinking water from raw water characteristics. *Chemosphere,* 47**,** 1007-1018.

GREFENSTETTE, J. J. 1986. Optimization of Control Parameters for Genetic Algorithms. *Systems, Man and Cybernetics, IEEE Transactions on,* 16**,** 122-128.

GUMERMAN, R. C., CULP, R. L. & CLARK, R. M. 1979a. COST OF GRANULAR ACTIVATED CARBON ADSORPTION TREATMENT IN THE UNITED-STATES. *Journal American Water Works Association,* 71**,** 690-696.

GUMERMAN, R. C., CULP, R. L., HANSEN, S. P., LINECK, T. S., LABORATORY, M. E. R. & CULP/WESNER/CULP 1979b. *Estimating Water Treatment Costs*, Environmental Protection Agency, Office of Research and Development, Municipal Environmental Research Laboratory.

GUPTA, A. K. & SHRIVASTAVA, R. K. 2006. Uncertainty analysis of conventional water treatment plant design for suspended solids removal. *Journal of Environmental Engineering-Asce,* 132**,** 1413-1421.

GUPTA, A. K. & SHRIVASTAVA, R. K. 2008. Optimal design of water treatment plant under uncertainty using genetic algorithm. *Environmental Progress,* 27**,** 91-97.

GUPTA, A. K. & SHRIVASTAVA, R. K. 2010. Reliability-Constrained Optimization of Water Treatment Plant Design Using Genetic Algorithm. *Journal of Environmental Engineering-Asce,* 136**,** 326-334.

HACH. 1999. *1720D Low Range Process Turbidimeter* [Online]. Available: http://www.pertechinc.com/manuals/Hach1720D-Turbidity-Analyizer-O&M-Manual.pdf [Accessed 18/10/2012].

HEAD, R., HART, J. & GRAHAM, N. Simulating the effect of blanket characteristics on the floc blanket clarification process. Proceedings of the 1996 IAWQ/IWSA Joint Group on Particle Separation, 4th International Conference on the Role of Particle Characteristics in Separation Processes, October 28, 1996 - October 30, 1996, 1997 Jerusalem, Isr. Elsevier Science Ltd, 77-84.

HIRSCHEN, K. & SCHAFER, M. 2006. A study on evolutionary multi-objective optimization for flow geometry design. *Computational Mechanics,* 37**,** 131-141.

HORN, J. 1997. Multi-criterion decision making. *In:* BAECK, T., FOGEL, D. B. & MICHALEWICZ, Z. (eds.) *Handbook of Evolutionary Computation.* Taylor & Francis.

HUA. 2000. *THE EFFECTS OF WATER TREATMENT WORKS ON CHLORINE DECAY AND THM FORMATION.* PhD, University of Birmingham.

HUA, F., WEST, J. R., BARKER, R. A. & FORSTER, C. F. 1999. Modelling of chlorine decay in municipal water supplies. *Water Research,* 33**,** 2735-2746.

HYDROMANTIS 2009. WATPRO Version 3 Users' Manual.

ICIS 2006. Indicative chemical prices A-Z.

ICIS 2013. CHLOROE - End user cost of chlorine Thomson Reuters Datastream.

INAMDAR, S. V., GUPTA, S. K. & SARAF, D. N. 2004. Multi-objective optimization of an industrial crude distillation unit using the elitist non-dominated sorting genetic algorithm. *Chemical Engineering Research & Design,* 82**,** 611-623.

IZQUIERDO, J., PEREZ, R. & IGLESIAS, P. L. 2004. Mathematical models and methods in the water industry. *Mathematical and Computer Modelling,* 39**,** 1353-1374.

JAIN, N. K., JAIN, V. K. & DEB, K. 2007. Optimization of process parameters of mechanical type advanced machining processes using genetic algorithms. *International Journal of Machine Tools & Manufacture,* 47**,** 900-919.

JARVIS, P., BUCKINGHAM, P., HOLDEN, B. & JEFFERSON, B. 2009. Low energy ballasted flotation. *Water Research,* 43**,** 3427-3434.

JARVIS, P., JEFFERSON, B., GREGORY, J. & PARSONS, S. A. 2005a. A review of floc strength and breakage. *Water Research,* 39**,** 3121-3137.

JARVIS, P., JEFFERSON, B. & PARSONS, S. A. 2005b. How the natural organic matter to coagulant ratio impacts on floc structural properties. *Environmental Science & Technology,* 39**,** 8919-8924.

JIANG, J. Q., ZHOU, Z. & SHARMA, V. K. 2013. Occurrence, transportation, monitoring and treatment of emerging micro-pollutants in waste water - A review from global views. *Microchemical Journal,* 110**,** 292-300.

KADU, M. S., GUPTA, R. & BHAVE, P. R. 2008. Optimal design of water networks using a modified genetic algorithm with reduction in search space. *Journal of Water Resources Planning and Management-Asce,* 134**,** 147-160.

KAINI, P., ARTITA, K. & NICKLOW, J. W. 2012. Optimizing Structural Best Management Practices Using SWAT and Genetic Algorithm to Improve Water Quality Goals. *Water Resources Management,* 26**,** 1827-1845.

KAPELAN, Z. S., SAVIC, D. A. & WALTERS, G. A. 2005. Multiobjective design of water distribution systems under uncertainty. *Water Resources Research,* 41.

KEELEY, J., JARVIS, P. & JUDD, S. J. 2012. An economic assessment of coagulant recovery from water treatment residuals. *Desalination,* 287**,** 132-137.

KEMIRA. 2013. *RE: FW: Cost Estimates.* Type to AUTHOR.

KESTIN, J., SOKOLOV, M. & WAKEHAM, W. A. 1978. Viscosity of liquid water in range 8°C to 150°C. *Journal of Physical and Chemical Reference Data,* 7**,** 941-948.

LAUMANNS, M., THIELE, L., DEB, K. & ZITZLER, E. 2002. Combining convergence and diversity in evolutionary multiobjective optimization. *Evolutionary Computation,* 10**,** 263-282.

LEMONT 2010. USEPA WTP v2.1. Modeling Summary. AECOM.

LETTERMAN, R. D. & ASSOCIATION, A. W. W. 1999. *Water quality and treatment: a handbook of community water supplies*, McGraw-Hill.

LOVE, T. & SYMONS, M. 1978. Operational aspects of granular activated carbon adsorption treatment. US EPA.

LYKINS, B. W., CLARK, R. M. & ADAMS, J. Q. 1988. GRANULAR ACTIVATED CARBON FOR CONTROLLING THMS. *Journal American Water Works Association,* 80**,** 85-92.

MÄLZER & DING, W. 2006. Recent Activities in Mechanistic, CFD and Neuronal Network Modelling at the IWW.

MAN, K. F., TANG, K. S. & KWONG, S. 1996. Genetic algorithms: Concepts and applications. *IEEE Transactions on Industrial Electronics,* 43**,** 519-534.

MATSUMOTO, M. & NISHIMURA, T. 1998. Mersenne twister: a 623-dimensionally equidistributed uniform pseudo-random number generator. *ACM Trans. Model. Comput. Simul.,* 8**,** 3-30.

MCGIVNEY, W. & KAWAMURA, S. 2008. Cost Estimating Manual for Water Treatment Facilities. John Wiley & Sons.

MET OFFICE. 2014. *Weather summaries* [Online]. Available: http://www.metoffice.gov.uk/climate/uk/summaries [Accessed 21/05/2014 2014].

MHAISALKAR, V. A., BASSIN, J. K., PARAMASIVAM, R. & KHANNA, P. 1993. DYNAMIC-PROGRAMMING OPTIMIZATION OF WATER-TREATMENT-PLANT DESIGN. *Journal of Environmental Engineering-Asce,* 119**,** 1158-1175.

MICHALEWICZ, Z. 1996. *Genetic algorithms+ data structures= evolution programs*, springer.

MILLS, G. 1/5/13 2013. *RE: Statement Regarding Performance of Selected Chemistry Procedures.* Type to SWAN, R.

MOLAK, V. 1997. *Fundamentals of Risk Analysis and Risk Management*, Lewis Publ.

MOLER, C. B. 2008. *Numerical Computing with MATLAB*, Society for Industrial and Applied Mathematics (SIAM, 3600 Market Street, Floor 6, Philadelphia, PA 19104).

MORSE, A. 2008. Trimpley WTW contact tank retention study. Severn Trent.

NAJM, I. 2001. User-friendly carbonate chemistry charts. *Journal American Water Works Association,* 93**,** 86-93.

NAZEMI, A., YAO, X., CHAN, A. H. & IEEE 2006. *Extracting a set of robust pareto-optimal parameters for hydrologic models using NSGA-II and SCEM*.

NELSON, P. R., COFFIN, M. & COPELAND, K. A. F. 2003. Introductory statistics for engineering experimentation.

NICKLOW, J., REED, P., SAVIC, D., DESSALEGNE, T., HARRELL, L., CHAN-HILTON, A., KARAMOUZ, M., MINSKER, B., OSTFELD, A., SINGH, A., ZECHMAN, E. & EVOLUTIONARY, A. T. C. 2010. State of the Art for Genetic Algorithms and Beyond in Water Resources Planning and Management. *Journal of Water Resources Planning and Management-Asce,* 136**,** 412-432.

NIEMINSKI, E. C., BELLAMY, W. D. & MOSS, L. R. 2000. Using surrogates to improve plant performance. *Journal American Water Works Association,* 92**,** 67-+.

OFFICE FOR NATIONAL STATISTICS 2013. Consumer Price Indices - Composite Price Index and annual change 1800 to 2011: Jan 1974=100. 15 January 2013 ed.

OMAR, K. 2012. *An experimental analysis of water treatment filtration.* MSc, University of Birmingham.

OWEN, D. M., AMY, G. L., CHOWDHURY, Z. K., PAODE, R., MCCOY, G. & VISCOSIL, K. 1995. NOM - CHARACTERIZATION AND TREATABILITY. *Journal American Water Works Association,* 87**,** 46-63.

PACKHAM, R. F. 1990. Cryptosporidium and Water Supplies - the Badenoch Report. *Water and Environment Journal,* 4**,** 578-580.

PERRY, R. H., GREEN, D. W. & MALONEY, J. O. 1998. *Perry's chemical engineers' handbook*, McGraw-Hill.

PHILLIPS, H., SAHLSTEDT, K., FRANK, K., BRATBY, J., BRENNAN, W., ROGOWSKI, S., PIER, D., ANDERSON, W., MULAS, M., COPP, J. & SHIRODKAR, N. 2009. Wastewater treatment modelling in practice: a collaborative discussion of the state of the art. *Water Science & Technology,* 59.

POWELL, J. C. 1998. *Modelling Chlorine in Water Distribution Networks.* University of Birmingham.

POWELL, J. C., HALLAM, N. B., WEST, J. R., FORSTER, C. F. & SIMMS, J. 2000. Factors which control bulk chlorine decay rates. *Water Research,* 34**,** 117-126.

PURCELL, P. J. 2005. Milestones in the development of municipal water treatment science and technology in the 19th and early 20th centuries: Part II. *Water and Environment Journal,* 19**,** 404-409.

RIETVELD & DUDLEY 2006. D5.4.1 Models for drinking water: state of the art. Techneau.

RIETVELD, VAN SCHAGEN, K. & VAN DIJK, J. C. INFORMATION TECHNOLOGY FOR LINKING RESEARCH TO EDUCATION AND TRAINING IN DRINKING WATER TREATMENT. Proceedings of the 2004 Water Institute of Southern Africa (WISA) Biennial Conference, 2004 Cape Town, South Africa.

RIETVELD, L. C. & DE VET, W. W. J. M. 2009. Dynamic Modeling of Bentazon Removal by Pseudo-Moving-Bed Granular Activated Carbon Filtration Applied to Full-Scale Water Treatment. *Journal of Environmental Engineering-Asce,* 135**,** 243-249.

RIETVELD, L. C., VAN DER HELM, A. W. C., VAN SCHAGEN, K. M. & VAN DER AA, L. T. J. 2010. Good modelling practice in drinking water treatment, applied to Weesperkarspel plant of Waternet. *Environmental Modelling & Software,* 25**,** 661-669.

RITSON, J. P., GRAHAM, N. J. D., TEMPLETON, M. R., CLARK, J. M., GOUGH, R. & FREEMAN, C. 2014. The impact of climate change on the treatability of dissolved organic matter (DOM) in upland water supplies: A UK perspective. *Science of the Total Environment,* 473**,** 714-730.

SAATCI, A. M. 1989. HARMONIC MEAN CONDUCTIVITY IN DECLINING RATE FILTERS. *Journal of Environmental Engineering-Asce,* 115**,** 462-466.

SAATCI, A. M. 1990. APPLICATION OF DECLINING RATE FILTRATION THEORY - CONTINUOUS OPERATION. *Journal of Environmental Engineering-Asce,* 116**,** 87-106.

SAATCI, A. M. & HALILSOY, M. 1987. A NEW SOLUTION OF THE DEEP BED FILTER EQUATIONS. *Chemical Engineering Journal and the Biochemical Engineering Journal,* 34**,** 147-150.

SAATCI, A. M. & OULMAN, C. S. 1980. THE BED DEPTH SERVICE TIME DESIGN METHOD FOR DEEP BED FILTRATION. *Journal American Water Works Association,* 72**,** 524-528.

SARKAR, D. & MODAK, J. M. 2006. Optimal design of multiproduct batch chemical plant using NSGA-II. *Asia-Pacific Journal of Chemical Engineering,* 1**,** 13-20.

SEVERN TRENT 2011. Trimpley Data Sheet.

SEVERN TRENT 2012a. Trimpley archive data.

SEVERN TRENT 2012b. Trimpley WTW schematic.

SEVERN TRENT SERVICES - CAPITAL CONTROLS 1993. Model 1930 Triplication controller operating and maintenance manual.

SEVERN TRENT SERVICES - CAPITAL CONTROLS 2000. Comparison of costs - chlorine gas versus hypochlorites.

SHARIFI, S. 2009. *Application of evolutionary computation to open channel flow modelling.* PhD, University of Birmingham.

SHI, Y. & REITZ, R. D. 2010. Assessment of Multiobjective Genetic Algorithms With Different Niching Strategies and Regression Methods for Engine Optimization and

Design. *Journal of Engineering for Gas Turbines and Power-Transactions of the Asme,* 132.

SIEMENS. 1997. *SITRANS F M MAGFLO Product Manual* [Online]. Available: http://cache.automation.siemens.com/dnl/zMxNTkzAAAA_17616325_HB/ls27v202_s.pdf [Accessed 18/10/2012].

SIGRIST. n.d. *On-line turbidimeter Aquascat [Manual]* [Online]. Available: http://www.photometer.com/en/products/details/documentdetail.html?RevId=8393 [Accessed 21/01/2013].

SIRIWARDENE, N. R. & PERERA, B. J. C. 2006. Selection of genetic algorithm operators for urban drainage model parameter optimisation. *Mathematical and Computer Modelling,* 44**,** 415-429.

SNOEYINK, V. L. & JENKINS, D. 1980a. *Water chemistry*, Wiley.

SNOEYINK, V. L. & JENKINS, D. 1980b. *Water Chemistry, Laboratory Manual*, Wiley.

STIMELA. 2011. *Introduction in Stimela* [Online]. Delft University. Available: http://www.stimela.nl/ [Accessed 29 March 2011].

STUMM, W. & MORGAN, J. J. 1970. *Aquatic chemistry: an introduction emphasizing chemical equilibria in natural waters*, Wiley-Interscience.

TAMPA BAY WATER 2011. Sodium Bisulphite Supply Services - Award Contract No. 2012-019 to the lowest, responsive, responsible bidder - Allied Universal Corporation - Approve.

TANG, Y., REED, P. & WAGENER, T. 2006. How effective and efficient are multiobjective evolutionary algorithms at hydrologic model calibration? *Hydrology and Earth System Sciences,* 10**,** 289-307.

TEBBUTT, T. H. Y. 1992. *Principles of water quality control*, Elsevier Science Limited.

TEEFY, S. 1996. *Tracer studies in water treatment facilities: a protocol and case studies*, AWWA Research Foundation and American Water Works Association.

TEIXEIRA, E. C. & SIQUEIRA, R. D. 2008. Performance assessment of hydraulic efficiency indexes. *Journal of Environmental Engineering-Asce,* 134**,** 851-859.

THE WATER SUPPLY REGULATIONS 2010.

TRIMPLEY OPERATORS. 2012-2013. *RE: Telephone correspondance.* Type to AUTHOR.

TSENG, T. & EDWARDS, M. 1999. Predicting full-scale TOC removal. *Journal / American Water Works Association,* 91**,** 159-170.

TUDOR, R. & LAVRIC, V. 2010. Optimization of Total Networks of Water-Using and Treatment Units by Genetic Algorithms. *Industrial & Engineering Chemistry Research,* 49**,** 3715-3731.

UKWIR 1999. Recyling of water treatment works sludges.

USEPA 1992. Water Treatment Plant Simulation Program v1.53 User Manual v1.21.

VAN LEEUWEN, J., HOLMES, M., HEIDENRICH, C., DALY, R., FISHER, I., KASTL, G., SATHASIVAN, A. & BURSILL, D. 2003. Modelling the application of iorganic coagulants and pH control reagents for removal of organic matter from drinking waters. *International Congress on Modelling and Simulation (Modsim), Townsville, Australia.* .

VAN LEEUWEN, J., HOLMES, M., KAEDING, U., DALY, R. & BURSILL, D. 2009. Development and implementation of the software mEnCo (c) to predict coagulant doses for DOC removal at full-scale WTPs in South Australia. *Journal of Water Supply Research and Technology-Aqua,* 58**,** 291-298.

VAN VELDHUIZEN, D. A. & LAMONT, G. B. 2000. Multiobjective Evolutionary Algorithms: Analyzing the State-of-the-Art. *Evolutionary Computation,* 8**,** 125-147.

VASCONCELOS, J. J. & BOULOS, P. F. 1996. *Characterization and Modeling of Chlorine Decay in Distribution Systems*, Amer Water Works Assn.

WANG, D., LI, S. & ZHOU, X. 2013. Control-Oriented Modeling and Real-Time Control for the Ozone Dosing Process of Drinking Water Treatment. *Environmental Science & Technology,* 47**,** 2197-2203.

WATSON, H. E. 1908. A note on the variation of the rate of disinfection with change in the concentration of the disinfectant. *Journal of Hygiene,* 8**,** 536-542.

WONG, G. S. K. & EMBLETON, T. F. W. 1984. VARIATION OF SPECIFIC-HEATS AND OF SPECIFIC-HEAT RATIO IN AIR WITH HUMIDITY. *Journal of the Acoustical Society of America,* 76**,** 555-559.

WRC 2002. *WRc OTTER Version 2.1.3 User Documentation*.

YEGOROVA, D. 2013. *An experimental analysis of filtration breakthrough.* MSc, University of Birmingham.

YSI. 2012. *Multiparameter Sonde specifications* [Online]. Available: http://www.ysi.com/products.php [Accessed 18/10/2012].

Appendix A NSGAII algorithm details

NSGAII Procedure

The NSGAII operation procedure outlined here (see Figure A-A) is based on the description provided in Deb et al. (2002). Initially, a random parent population is produced (P_t) and an offspring population is generated (Q_t) using simulated binary crossover (SBX) and polynomial mutation. The combined population (R_t) is then graded by Pareto rank (F_1, F_2, F_3 etc.) and sub-graded by crowding parameter in either the genetic or objective space (Deb et al., 2002). Using this grading system, the subsequent parent population (P_{t+1}) is filled with the fittest solutions.

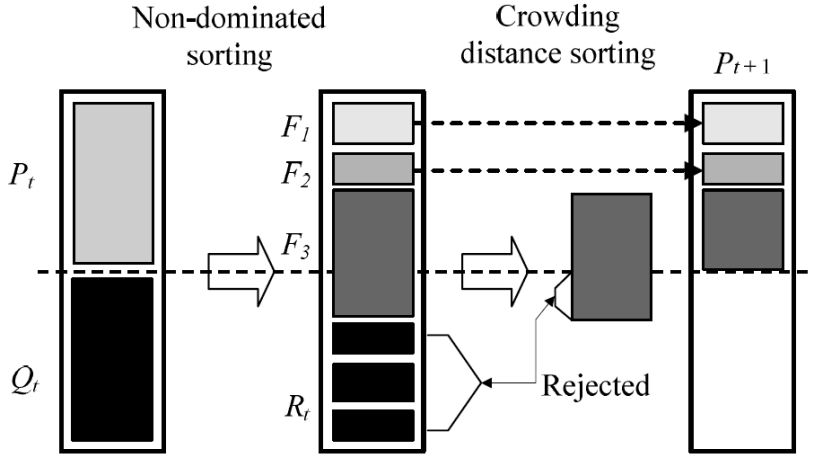

Where: P_t = parent population; Q_t = offspring population; R_t = combined population; F_1 = Pareto optimal set; F_2 = second Pareto rank; F_3 = third Pareto rank and P_{t+1} = subsequent parent population.

Figure A-A NSGAII procedure (Deb et al., 2002)

Simulated binary crossover (SBX)

The SBX operator can imitate sexual reproduction, creating offspring chromosomes based on the genes of parents. Two parent solutions are selected at random and a random number between zero and one is generated in order to ascertain whether cross-over occurs. If this random number is less than the specified cross-over probability then sexual reproduction takes place. If they do not sexually reproduce then asexual reproduction occurs. The SBX process calculates the value

of each gene of offspring solutions X and Y, based on the genes of the parents A and B, using the following method outlined in Deb (2000):

1. Randomly generate a number u between zero and one
2. Calculate spread factor parameter β using a polynomial distribution described by Equation A-A, where η_c is the cross-over distribution index which can take any positive value. Smaller values of η_c make it more likely that solutions dissimilar to the parent solutions are predicted.

$$if\ u \leq 0.5, \qquad \beta = (2u)^{\frac{1}{\eta_c+1}} \qquad \text{Equation A-A}$$

$$else, \qquad \beta = \left[\frac{1}{2(1-u)}\right]^{\frac{1}{\eta_c+1}}$$

3. Calculate the offspring genes' values using Equation A-B and Equation A-C

$$X = 0.5[(A+B) - \beta|B-A|] \qquad \text{Equation A-B}$$

$$Y = 0.5[(A+B) + \beta|B-A|] \qquad \text{Equation A-C}$$

Polynomial mutation

All offspring solutions genes have a possibility of undergoing mutation. If a randomly generated number between zero and one is less than the specified mutation probability then mutation occurs. Polynomial mutation is performed as described in Deb (2000):

1. Randomly generate a number *u* between zero and one
2. Calculate spread factor parameter δ using polynomial distribution described by Equation A-D, where η_m is the mutation distribution index which can take any positive value. Smaller values of η_m make it more likely that genes will vary significantly.

$$if\ u \leq 0.5, \qquad \delta = (2u)^{\frac{1}{\eta_m+1}} - 1 \qquad \text{Equation A-D}$$

$$else, \qquad \delta = 1 - [2(1-u)]^{\frac{1}{\eta_m+1}}$$

3. Calculate the offspring gene value X using Equation A-E, where A is the original value of the gene and Δ_{max} is the maximum variation allowed in the parent solution (i.e. the difference between the maximum and minimum value specified for a gene).

$$X = A + \delta(\Delta_{max}) \qquad \text{Equation A-E}$$

Pareto ranking of solutions

The ordering into Pareto rank can be accomplished by selecting two random solutions and placing them into a preliminary first Pareto set (F_1). If either of these solutions is dominated by the other then it is removed from the preliminary first Pareto set. All of the other solutions are then randomly entered into the preliminary first Pareto set and compared to the existing

members; again any dominated solutions are removed. Once this process is completed, the members of the first Pareto set are defined and removed from the combined population (R_t) before the process is repeated to find subsequent Pareto sets.

Crowding parameter

The crowding parameter measures how dissimilar a particular solution is in comparison with the rest of the population. It can be calculated in either the genetic or objective space. The method is performed as described in Deb et al. (2002):

1. The solutions are ranked by the first parameter to be compared.
2. The difference between the parameter value of the solutions just larger and smaller than the solution of interest is recorded. Solutions which have maximum or minimum parameter values are given a crowding value of infinity.
3. The solutions are then ranked and the crowding values calculated for any additional parameters to be compared.
4. The final crowding parameter is calculated by summing the crowding values of all the parameters compared.

The calculation of the crowding parameter is shown in Figure A-B. In this situation, variance in two parameters is measured for a solution (k) by summing the horizontal and vertical distance between k-1 and k+1. Solutions which are less crowded are favoured in order to promote diversity.

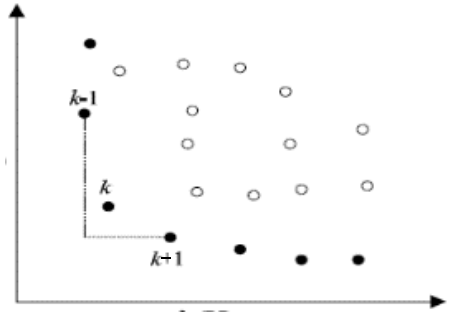

Figure A-B Crowding parameter calculation (Deb et al., 2002)

Appendix B Carbonate chemistry model

Alkalinity adjustment due to coagulant addition

Aluminium sulphate ($Al_2(SO_4)_3.xH_2O$), aluminium chloride ($AlCl_3$), ferric sulphate ($Fe_2(SO_{4)3}$) and ferric chloride ($FeCl_3$) are all common coagulants used in water treatment. When they are added to water they dissociate to form trivalent metals ions of either Fe^{3+} or Al^{3+}, hereon referred to as Me^{3+} ions. Each mole of Me^{3+} ion added to the water will produce a mole of metal hydroxide ($Me(OH)_3$) and three moles of hydrogen ions, and consume three moles of alkalinity, as shown in Equation B-A (Crittenden et al., 2005, Tseng and Edwards, 1999). This is approximately true if TOC-coagulant precipitates are negligible, coagulant doses are greater than 1 mg/l as Me^{3+} and solubility of the coagulant metal is low, which it is at pH 5.5-8.0 for alum and 4.0-8.0 for ferric coagulants (Tseng and Edwards, 1999). The alkalinity reduction due to the addition of coagulant is shown in Equation B-B where $eqM(CaCO_3)$ is the equivalent molar mass of calcium carbonate and $M(Me^{3+})$ is the molar mass of the metal ion.

$$Me^{3+} + 3H_2O \Leftrightarrow Al(OH)_{3(am)} + 3H^+ \qquad \text{Equation B-A}$$

$$Alkalinity_{Me^{3+}} = -3Me^{3+} \times \frac{eqM(CaCO_3)}{M(Me^{3+})} \qquad \text{Equation B-B}$$

Chlorine

When gaseous chlorine is used to chlorinate water, due to its low concentration, it behaves as a strong acid. This results in the equilibrium shown in Equation 2-1 being forced to the far right donating a mole of hydrogen ions. Further dissociation of the hypochlorous acid (HOCl) as shown in Equation 2-2 donates further hydrogen but the extent of this dissociation is dependent on the pH and temperature (Black & Veatch Corporation, 2010).

Further hydrogen donation may occur as the chlorine reacts with other chemicals in the water (such as arsenic, carbon, cyanide, hydrogen sulphide, iron, manganese, or nitrites) and as the exact composition of the water is rarely known, a good estimate of hydrogen production can be made by assuming that each mole of molecular chlorine (Cl_2) produces two moles of hydrogen ions (Black & Veatch Corporation, 2010) which consume two moles of alkalinity. The alkalinity reduction as $CaCO_3$ due to the addition of a chlorine gas is shown in Equation B-C.

$$Alkalinity_{Cl_2} = -Cl_2 \frac{eqM(CaCO_3)}{eqM(Cl_2)} \qquad \text{Equation B-C}$$

Where: $Alkalinity_{Cl2}$ = Alkalinity alteration due to addition of free chlorine (mg/l $CaCO_3$); Cl_2 = concentration of chlorine added (mg/l); $eqM(CaCO_3)$ = equivalent molar mass of calcium carbonate (50 g/mol) and $eqM(Cl_2)$ = equivalent molar mass of chlorine (35.5 g/mol).

Sodium bisulphite

Dechlorination is carried out to reduce the residual free chlorine concentration from the contact tank, after super chlorination, so that it is suitable for distribution. Although sulphur dioxide (SO_2) is more commonly used, sodium bisulphite ($NaHSO_3$) is sometimes used where feed rates of SO_2 would be too low to be practical or where SO_2 storage is considered too hazardous.

The reaction between sodium bisulphite and chlorine is shown in Equation B-D. Each mole of sodium bisulphite donates two moles of hydrogen ions (Black & Veatch Corporation, 2010) which consume two moles of alkalinity. The dose of sodium bisulphite required to reduce the concentration down to a specified distribution concentration is shown in Equation B-E. The alkalinity reduction as $CaCO_3$ due to the addition of a sodium bisulphite is shown in Equation B-F.

$$NaHSO_3 + Cl_2 + H_2O \rightarrow NaHSO_4 + 2H^+ + 2Cl^- \qquad \text{Equation B-D}$$

$$NaHSO_3 = \frac{eqM(NaHSO_3)}{eqM(Cl_2)} \times (Cl_{2res} - Cl_{2dis}) \qquad \text{Equation B-E}$$

$$Alkalinity_{NaHSO_3} = -NaHSO_3 \frac{eqM(CaCO_3)}{eqM(NaHSO_3)} \qquad \text{Equation B-F}$$

Where: $NaHSO_3$ = concentration of sodium bisulphite; $eqM(NaHSO_3)$ = equivalent molar mass sodium bisulphite (52 g/mol); Cl_{2res} = residual contact tank free chlorine; Cl_{2dis} = target distribution network free chlorine (mg/l) and $Alkalinity_{NaHSO3}$ = Alkalinity alteration due to addition of sodium bisulphite (mg/l $CaCO_3$).

The dose of sodium bisulphite required at any time was calculate as the dose necessary to reduce the contact tank residual chlorine concentration to 0.6 mg/l of free chlorine.

Slaked lime

Slaked lime, also known as hydrated lime or calcium hydroxide ($Ca(OH)_2$), can be added to the water to increase the alkalinity. As calcium hydroxide is a strong base and almost completely dissociates in water, each mole of calcium hydroxide accepts two moles of hydrogen ions from solution (Equation B-G) and increases the alkalinity by two moles (Equation B-H).

$$Ca(OH)_2 + 2H^+ \rightarrow Ca^{2+} + 2H_2O \qquad \text{Equation B-G}$$

$$Alkalinity_{Ca(OH)_2} = +Ca(OH)_2 \frac{eqM(CaCO_3)}{eqM(Ca(OH)_2)} \qquad \text{Equation B-H}$$

Where: $Alkalinity_{Ca(OH)2}$ = Alkalinity alteration due to addition of slaked lime (mg/l CaCO3); $Ca(OH)_2$ = concentration of slaked lime (mg/l) and $eqM(Ca(OH)_2)$ = equivalent molar mass slaked lime (37g/mol).

Total carbonate concentration (C_T)

Considering only the carbonate species, the alkalinity of a solution is described by Equation B-I to Equation B-O (Stumm and Morgan, 1970, Snoeyink and Jenkins, 1980b).

$$[Alk] = [HCO_3^-] + 2[CO_3^{2-}] + [OH^-] - [H^+] \qquad \text{Equation B-I}$$

$$[HCO_3^-] = C_T \alpha_1 \qquad \text{Equation B-J}$$

$$[CO_3^{2-}] = C_T \alpha_2 \qquad \text{Equation B-K}$$

$$\alpha_1 = \frac{1}{\frac{[H^+]}{K_1} + 1 + \frac{K_2}{[H^+]}} \qquad \text{Equation B-L}$$

$$\alpha_2 = \frac{1}{\frac{[H^+]^2}{K_1 K_2} + \frac{[H^+]}{K_2} + 1} \qquad \text{Equation B-M}$$

$$\frac{[H^+][HCO_3^-]}{[H_2CO_3^*]} = K_1 \qquad \text{Equation B-N}$$

$$\frac{[H^+][CO_3^{2-}]}{[HCO_3^-]} = K_2 \qquad \text{Equation B-O}$$

Where: C_T = total carbonic species concentration (mol/l), K_1 = acidity constants for carbonic acid (dimensionless), K_2 = acidity constants for bicarbonate ion (dimensionless) and $[H_2CO_3^{*}]$ = molar concentration of H_2CO_3 and $CO_{2(aq)}$.

The equilibrium constants for carbonic acid (K_1) and the bicarbonate ion (K_2) are reported as being $10^{-6.3}$ and $10^{-10.3}$ respectively at 25 °C (Stumm and Morgan, 1970, Snoeyink and Jenkins, 1980b). It is assumed that K_1 and K_2 are temperature dependent and by applying Arrhenius' equation as shown in Equation B-P, along with the reported standard enthalpy changes for both reactions as in the Water Treatment Plant Simulation Program Manual (USEPA, 1992), Equation B-Q and Equation B-R can be used to give a temperature-dependent estimate of K_1 and K_2.

$$K = exp\left\{\left[\frac{\Delta H_{25^oC}}{R}\left(\frac{1}{T_{25^oC}} - \frac{1}{T}\right] - lnK_{25^oC}\right\} \qquad \text{Equation B-P}$$

$$K_1 = exp\left\{\left[\frac{7700J/mol}{8.314J/mol.^o K}\left(\frac{1}{298.15^o K} - \frac{1}{T}\right] - 14.5\right\} \qquad \text{Equation B-Q}$$

$$K_2 = exp\left\{\left[\frac{14900J/mol}{8.314J/mol.^o K}\left(\frac{1}{298.15^o K} - \frac{1}{T}\right] - 23.7\right\} \qquad \text{Equation B-R}$$

Combining Equation B-I and Equation B-M yields Equation B-S, which can be used to estimate the total carbonic species concentration (C_T) using the initial water alkalinity and pH.

$$[C_T] = \frac{[Alk] - [OH^-] + [H^+]}{\frac{1}{\frac{[H^+]}{K_1} + 1 + \frac{K_2}{[H^+]}} + 2\frac{1}{\frac{[H^+]^2}{K_1K_2} + \frac{[H^+]}{K_2} + 1}} \qquad \text{Equation B-S}$$

Coagulated pH calculation

Using the total carbonic species concentration (C_T) of the initial water, it is possible to estimate the hydrogen ion concentration (and therefore pH) after any alkalinity alteration due to coagulation (Equation B-T; simply a rearrangement of Equation B-S). This technique is similar to the graphical method described in Snoeyink and Jenkins (1980b).

$$[H^+] = [C_T]\left(\frac{1}{\frac{[H^+]_0}{K_1}+1+\frac{K_2}{[H^+]_0}} + \frac{2}{\frac{{[H^+]_0}^2}{K_1K_2}+\frac{[H^+]_0}{K_2}+1}\right) + \frac{k_w}{[H^+]_0} - [Alk] \qquad \text{Equation B-T}$$

As $[H^+]$ appears on both sides of the equation, it is necessary to use an iterative method to identify a suitable concentration of hydrogen ions. When Equation B-T was applied, in this work, using a direct iterative method it was found to be unstable, resulting in the solution moving to maxima or minima positions. The Newton-Raphson method was used to solve this iterative equation, as described in Equation B-U where $[H^+]_0$ is the previous estimate of $[H^+]$, $f([H^+]_0)$ is the current estimate of $[H^+]$ using Equation B-T, and $f'([H^+]_0)$ is the product of the derivative of $f([H^+]_0)$, as shown in Equation B-V.

$$[H^+] = [H^+]_0 - \frac{f([H^+]_0)}{f'([H^+]_0)} \qquad \text{Equation B-U}$$

$$\frac{d[H^+]}{d[H^+]_0} = [C_T]\left\{\frac{K_1\left(K_1K_2 - {[H^+]_0}^2\right)}{\langle K_1(K_2 + [H^+]_0) + {[H^+]_0}^2\rangle^2} - \frac{2K_1K_2(K_1 + 2[H^+]_0)}{\langle K_1(K_2 + [H^+]_0) + {[H^+]_0}^2\rangle^2}\right\} - \frac{k_w}{[H^+]^2}$$

Equation B-V

In order to stabilise the performance of the pH predictive model, the rate of change of the pH was set as 6 pH unit/h. The rate limit was identified as being the highest rate (to the nearest 0.5 pH unit/h) that did not result in the pH fluctuating on occasion to maxima or minima positions.

Appendix C Derivation of Bohart & Adams Equation

The capacity of the filter media to remove substances from a solution decreases in proportion to the current capacity and the concentration of the incoming substances.

$$\frac{\partial a}{\partial t} = -kac \qquad \text{Equation C-A}$$

Where: a = residual capacity; c = concentration at distance x from start and k = rate parameter.

$$\frac{\partial a}{\partial t} \times \frac{\boldsymbol{\partial t}}{\boldsymbol{\partial x}} = -kac \times \frac{\boldsymbol{\partial t}}{\boldsymbol{\partial x}} \rightarrow \frac{\partial a}{\partial x} = \frac{-kac}{v} \qquad \text{Equation C-B}$$

Rate of capacity reduction = rate of removal of substances

$$\frac{\partial c}{\partial x} = \frac{-kac}{v} \qquad \text{Equation C-C}$$

From Equation C-A

$$\frac{\partial \frac{a}{\boldsymbol{a_0}}}{\partial t \boldsymbol{k c_0}} = -\boldsymbol{k}\frac{a}{\boldsymbol{a_0}}\frac{c}{\boldsymbol{c_0}} \qquad \text{Equation C-D}$$

From Equation C-C

$$\frac{\partial \frac{c}{\boldsymbol{c_0}}}{\partial x \frac{\boldsymbol{k a_0}}{\boldsymbol{v}}} = \frac{-\boldsymbol{k}\frac{a}{\boldsymbol{a_0}}\frac{c}{\boldsymbol{c_0}}}{\boldsymbol{v}} \qquad \text{Equation C-E}$$

If $a' = a/a_0$; $c' = c/c_0$; $t' = tkc_0$; $x' = xka_0/v$; then

$$\frac{\partial a'}{\partial t'} = -a'c' \qquad \text{Equation C-F}$$

$$\frac{\partial c'}{\partial x'} = -a'c' \qquad \text{Equation C-G}$$

From Equation C-F

$$\frac{\partial a'}{\partial t'}\frac{1}{a'} = -\cancel{a'}c' \rightarrow\rightarrow \ln a' = -c't' \qquad \text{Equation C-H}$$

$$\frac{\partial \ln a'}{\partial t'} = \frac{-dc't'}{dt'} \rightarrow \frac{\partial \ln a'}{\partial t'} = -c' \qquad \text{Equation C-I}$$

From Equation C-G

$$\frac{\partial c'}{\partial x'}\frac{\mathbf{1}}{\boldsymbol{c'}} = -a'\cancel{\boldsymbol{c'}} \qquad \text{Equation C-J}$$

$$\int \frac{1}{c'}\partial c' = \int -a'\,\partial x' \qquad \text{Equation C-K}$$

$$\ln c' = -a'x' \qquad \text{Equation C-L}$$

$$\int \frac{1}{a'}\partial a' = \int -c'\,\partial t' \qquad \text{Equation C-M}$$

$$\frac{\partial \ln c'}{\partial x'} = \frac{-da'x'}{dx'} \qquad \text{Equation C-N}$$

$$\frac{\partial \ln c'}{\partial x'} = -a' \qquad \text{Equation C-O}$$

From Equation C-H

$$\int \frac{\partial \ln a'}{\boldsymbol{\partial t'}} = \int -c' \boldsymbol{\partial t'} \qquad \text{Equation C-P}$$

When x’ = 0, c’ = 1

$$\ln a' = -t \rightarrow a' = e^{-t\prime} \qquad \text{Equation C-Q}$$

From Equation C-O

$$\int \frac{\partial \ln c'}{\boldsymbol{\partial x'}} = \int -a' \boldsymbol{\partial x'} \qquad \text{Equation C-R}$$

When t’ = 0, a’ = 1

$$\ln c' = -x \rightarrow c' = e^{-x\prime} \qquad \text{Equation C-S}$$

From Equation B-Q and Equation C-S

$$\frac{a'}{c'} = \frac{e^{-t\prime}}{e^{-x\prime}} \rightarrow e^{x\prime - t\prime} \qquad \text{Equation C-T}$$

$$\frac{c'}{a'} = \frac{e^{-x\prime}}{e^{-t\prime}} \rightarrow e^{t\prime - x\prime} \qquad \text{Equation C-U}$$

From Equation C-F

$$\frac{\partial a'}{\partial t' \boldsymbol{a'^2}} = \frac{-a'c'}{\boldsymbol{a'^2}} \rightarrow -\frac{c'}{a'} \qquad \text{Equation C-V}$$

From Equation B-U

$$-\frac{c'}{a'} = -e^{t'-x'}$$ Equation C-W

$$\int \frac{1}{a'^2}\partial a' = \int -e^{t'-x'}\,\partial t$$ Equation C-X

$$-\frac{1}{a} = -e^{t\prime-x\prime} - k$$ Equation C-Y

When t' = 0, a' = 1

$$\frac{1}{1} = e^{-x'} + k$$ Equation C-Z

$$k = 1 - e^{-x'}$$ Equation C-AA

$$\frac{1}{a'} = e^{t\prime-x\prime} - e^{-x'} + 1$$ Equation C-BB

$$a' = \frac{1}{e^{t'-x'} - e^{-x'} + 1} = \frac{e^{x\prime}}{e^{t\prime} + e^{x\prime} - 1}$$ Equation C-CC

As -1 is negligible except for very small values of t' and x'

$$a' = \frac{e^{x\prime}}{e^{t\prime} + e^{x\prime}} = \frac{1}{e^{t'-x'} + 1}$$ Equation C-DD

From Equation C-G

$$\frac{\partial c'}{\partial x'\boldsymbol{c'^2}} = \frac{-a'c'}{\boldsymbol{c'^2}}$$ Equation C-EE

From Equation B-Q

$$-\frac{a'}{c'} = -e^{x'-t'}$$ Equation C-FF

$$\int \frac{1}{c'^2}\partial c' = \int -e^{x'-t'}\,\partial x$$ Equation C-GG

$$-\frac{1}{c} = -e^{x\prime-t\prime} - k$$ Equation C-HH

When x’ = 0, c’ = 1

$$\frac{1}{1} = e^{-t'} + k$$ Equation C-II

$$k = 1 - e^{-t'}$$ Equation C-JJ

$$\frac{1}{c'} = e^{x\prime-t\prime} - e^{-t'} + 1$$ Equation C-KK

$$c' = \frac{1}{e^{x'-t'} - e^{-t'} + 1} = \frac{e^{t\prime}}{e^{t\prime} + e^{x\prime} - 1}$$ Equation C-LL

As -1 is negligible except for very small values of t’ and x’

$$c' = \frac{e^{t\prime}}{e^{t\prime} + e^{x\prime}} = \frac{1}{e^{x'-t'} + 1}$$ *Equation* C-MM

$$\frac{a}{a_0} = \frac{1}{e^{\mathrm{tkc_0 - xka_0/v}} + 1}$$ Equation C-NN

$$\frac{c}{c_0} = \frac{1}{e^{\mathrm{xka_0/v - tkc_0}} + 1}$$ Equation C-OO

As a’+ c’ = 1

$$\frac{a}{a_0} = 1 - \frac{c}{c_0}$$ Equation C-PP

Appendix D Derivation of head loss due to solids accumulation equation

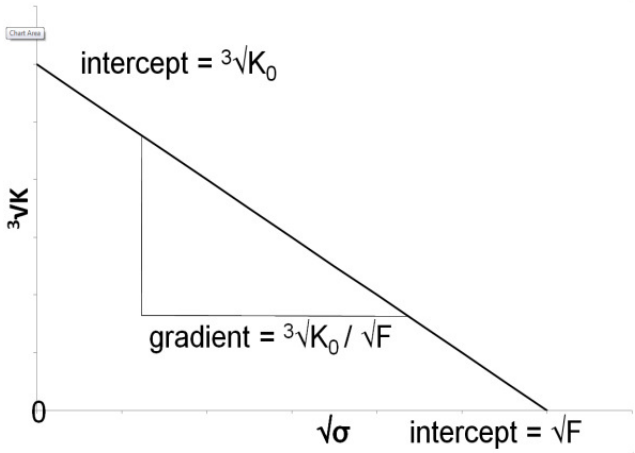

Figure D-A Hydraulic conductivity, solids accumulation relationship

Where: K = hydraulic conductivity (m/h); K_0 = clean bed hydraulic conductivity (m/h); σ = accumulated solids concentration (mg/l) and F = accumulated solids concentration capacity (mg/l).

$$\sqrt[3]{K} = \sqrt[3]{K_0} - \frac{\sqrt[3]{K_0}}{\sqrt{F}}\sqrt{\sigma} \qquad \text{Equation D-A}$$

Divide through by $^3\sqrt{K_0}$

$$\frac{\sqrt[3]{K}}{\sqrt[3]{K_0}} = 1 - \frac{\sqrt{\sigma}}{\sqrt{F}} \qquad \text{Equation D-B}$$

Cube

$$\frac{K}{K_0} = \left(1 - \frac{\sqrt{\sigma}}{\sqrt{F}}\right)^3 \qquad \text{Equation D-C}$$

$K/K_0 = H_0/H$ where H is head loss

$$\frac{H_0}{H} = \left(1 - \frac{\sqrt{\sigma}}{\sqrt{F}}\right)^3$$ Equation D-D

$$H = \frac{H_0}{\left(1 - \frac{\sqrt{\sigma}}{\sqrt{F}}\right)^3}$$ Equation D-E

$$\frac{1}{\sqrt{F}} = \beta$$ Equation D-F

$$H = \frac{H_0}{\left(1 - \beta\sqrt{\sigma}\right)^3}$$ Equation D-G

Appendix E Derivation of representative number of CSTRs from t10 value

A contact tank is represented by four tanks in series as shown in Figure E-A which are perfectly mixed then the concentration in each tank is equal to the concentration leaving each tank.

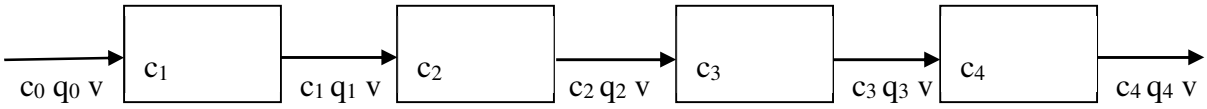

Figure E-A Representation of a contact tank as four CSTRs

Where: c = concentration of tracer; q = mass of tracer transferring between sections; v = flow rate and V_0 = volume of each section.

A plug tracer test is performed and during a portion of time dt a quantity of tracer, $q_0 = v\ dt$, enters the first tank. At t = dt the concentration in the first tank $c_1 = q_0/V_o$ and the rate of outflow is vq_1/V_0. No new tracer enters the first tank and no decay is assumed to occur. This is represented in Equation E-A and Equation E-B.

$$\frac{dq_1}{dt} = \frac{-vq_1}{V_0} \qquad \text{Equation E-A}$$

$$q_1 = q_0 e^{\frac{-vt}{V_0}} \qquad \text{Equation E-B}$$

For the second tank the mass balance can be described as shown in Equation E-C.

$$\frac{dq_2}{dt} = \frac{vq_1}{V_0} - \frac{vq_2}{V_0} \qquad \text{Equation E-C}$$

Substitution q_1 from Equation E-A into Equation E-C gives Equation E-D.

$$\frac{dq_2}{dt} + \frac{vq_2}{V_0} = \frac{v}{V_0} q_0 e^{\frac{-vt}{V_0}}$$ Equation E-D

Using integrating factors as described in Stroud and Booth (2000) Equation E-E, Equation E-F and Equation E-G.

$$\frac{dy}{dx} + Py = Q$$ Equation E-E

$$Integrating\ factor = e^{\int P dx}$$ Equation E-F

$$\frac{d}{dx}\left(ye^{\int P dx}\right) = Qe^{\int P dx}$$ Equation E-G

Equation E-D can be solved as shown in Equation E-H, Equation E-I and Equation E-J.

$$\frac{d}{dt}\left(q_2 e^{\frac{vt}{V_0}}\right) = \frac{v}{V_0} q_0$$ Equation E-H

$$q_2 e^{\frac{vt}{V_0}} = \int \frac{v}{V_0} q_0 dt = \frac{v}{V_0} q_0 t$$ Equation E-I

$$q_2 = \frac{v}{V_0} q_0 t e^{\frac{-vt}{V_0}}$$ Equation E-J

The mass balance for the third tank can be calculated using the same method.

$$\frac{dq_3}{dt} = \frac{vq_2}{V_0} - \frac{vq_3}{V_0}$$ Equation E-K

Substitution q_2 from Equation E-J to Equation E-K

$$\frac{dq_3}{dt} + \frac{vq_3}{V_0} = \left(\frac{v}{V_0}\right)^2 q_0 t e^{\frac{-vt}{V_0}}$$ Equation E-L

Using integrating factors.

$$\frac{d}{dt}\left(q_3 e^{\frac{vt}{V_0}}\right) = \left(\frac{v}{V_0}\right)^2 q_0 t$$ Equation E-M

$$q_3 e^{\frac{vt}{V_0}} = \int \left(\frac{v}{V_0}\right)^2 q_0 t dt = \left(\frac{vt}{V_0}\right)^2 \frac{q_0}{2}$$ Equation E-N

$$q_3 = \left(\frac{vt}{V_0}\right)^2 \frac{q_0 e^{\frac{-vt}{V_0}}}{2}$$ Equation E-O

The mass balance for the fourth tank can be calculated using the same method.

$$\frac{dq_4}{dt} = \frac{vq_3}{V_0} - \frac{vq_4}{V_0}$$ Equation E-P

Substitution in q_3 from Equation E-O to Equation E-P.

$$\frac{dq_4}{dt} + \frac{vq_4}{V_0} = \left(\frac{v}{V_0}\right)^3 \frac{q_0 t^2 e^{\frac{-vt}{V_0}}}{2}$$ Equation E-Q

Using integrating factors

$$\frac{d}{dt}\left(q_4 e^{\frac{vt}{V_0}}\right) = \left(\frac{v}{V_0}\right)^3 \frac{q_0 t^2}{2}$$ Equation E-R

$$q_4 e^{\frac{vt}{V_0}} = \int \left(\frac{v}{V_0}\right)^3 \frac{q_0 t^2}{2} dt = \left(\frac{vt}{V_0}\right)^3 \frac{q_0}{6}$$ Equation E-S

$$q_4 = \left(\frac{vt}{V_0}\right)^3 \frac{q_0 e^{\frac{-vt}{V_0}}}{6}$$ Equation E-T

B general pattern follows that for the n^{th} tank the quantity of tracer can be calculated as:

$$q_n = \left(\frac{vt}{V_0}\right)^{n-1} \frac{q_0 e^{\frac{-vt}{V_0}}}{(n-1)!}$$ Equation E-U

The fraction of tracer that has left the n^{th} tank can be calculated as:

$$F = \frac{q_0 - (q_1 + q_2 + \cdots + q_n)}{q_0}$$ Equation E-V

Substitute Equation E-B, Equation E-J and Equation E-U into Equation E-V.

$$F = \frac{q_0 - (q_0 e^{\frac{-vt}{V_0}} + \frac{v}{V_0} q_0 t e^{\frac{-vt}{V_0}} + \cdots + \left(\frac{vt}{V_0}\right)^{n-1} \frac{q_0 e^{\frac{-vt}{V_0}}}{(n-1)!})}{q_0}$$ Equation E-W

Factorise.

$$F = 1 - e^{\frac{-vt}{V_0}} \left[1 + \frac{vt}{V_0} + \cdots + \left(\frac{vt}{V_0}\right)^{n-1} \frac{1}{(n-1)!}\right]$$ Equation E-X

The mean residence time is calculated as shown in Equation E-YEquation E-Y

$$\bar{t} = \frac{nV_0}{v}$$ Equation E-Y

Applying this to Equation E-X results in the more useful form:

$$F = 1 - e^{-n\frac{t}{\bar{t}}} \left[1 + n\frac{t}{\bar{t}} + \cdots + \left(n\frac{t}{\bar{t}}\right)^{n-1} \frac{1}{(n-1)!}\right]$$ Equation E-Z

Appendix F Operational costs

Chemical, sludge disposal and energy costs

In order to calculate the operating costs of the different processes it was necessary to have estimates of the costs to purchase chemicals, dispose of sludge and power processes. The values used are shown in Table F-A.

All the suspended solid removed at the clarification and filtration stage, including those introduced through the addition of coagulant are assumed to contribute to the total mass of sludge that needs disposing. Total costs of chemicals used (ferric sulphate, chlorine, sodium bisulphite and lime) and sludge requiring disposal were calculated based on cumulative mass over the simulation period converted to an annual cost.

Table F-A Chemical, sludge and energy costs

Item	**Cost**
Ferric sulphate	£2000 per tonne as Fe
Chlorine	£400 per tonne
Sodium bisulphite	£600 per tonne
Slaked lime	£70 per tonne
Sludge disposal	£80 per tonne
Electricity	£0.08 per kWh

Operating costs were calculated per annum. Costs were converted to annual estimates. All costs were at current value (December 2012) and where historical data is used it is adjusted to current values based on the consumer price indices produced by the Office for National Statistics (2013).

Ferric sulphate

Table F-B Costs of ferric sulphate

Source	Iron concentration (%)	Cost per tonne (£)	Cost per tonne Fe (£)
Trimpley, Severn Trent (2012b)	12.5	n/a	n/a
Kemira (2013)*	12.5	140	1120
Brenntag (2013)**	12.6	199	1579
Keeley et al. (2012)***	4.34	85	2004

*Value based on location of WTW, long term supply, 28 tonne tanker delivery to on site tank, WTW quality product PIX112 as used at Trimpley.

** Based on 8 tonne bulk tanker deliveries.

*** Values provided by UK water utilities and chemical suppliers. Costs based on 200 MLD WTW which is larger than Trimpley (60 MLD). Cost per tonne would be expected to be lower for a larger WTW due to economies of scale. Cost liable to market fluctuations.

Estimated cost of coagulant taken as £2000 per tonne based on more diverse range of sources investigated by Keeley et al. (see Table F-B).

Chlorine gas

Table F-C Costs of chlorine gas

Source	Daily consumption (kg/d)	Cost per tonne (£)
Trimpley, Severn Trent (2012b)	49	n/a
ICIS (2006)*	n/a	161-276
ICIS (2013)**	n/a	200
Capital Controls (2000)***	8	795
Capital Controls (2000)***	45	398
Capital Controls (2000)***	189	297

*Indicative prices, S Gulf, domestic, quarter contract.

**Time series of end user costs, given in cents per pound for 2013.

***Based on theoretical scenarios, given in cents per pound. Costs are approximate and caution is recommended for their use based on regional factors including freight, contracts and volumes.

Estimated cost of chlorine taken as £400 per tonne based on consumption rate and application specificity of Capital Controls' estimates (Table F-C), and market fluctuation as indicated in the ICIS data and time series (Figure F-A).

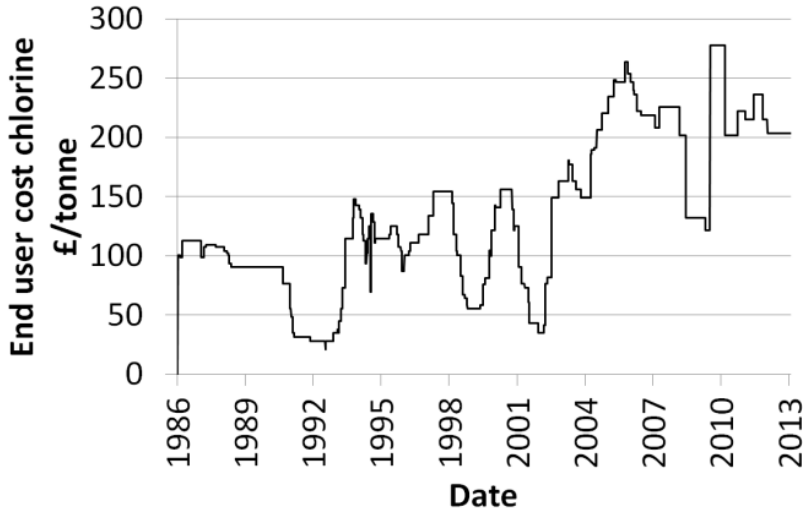

Figure F-A End user cost of chlorine (ICIS, 2013)

Sodium bisulphite

Table F-D Costs of sodium bisulphite

Source	**Sodium bisulphite solution concentration (%)**	**Costs per tonne (£)**	**Costs per tonne Sodium bisulphite (£)**
Trimpley, Severn Trent (2012b)	20	n/a	n/a
Brenntag (2013)	37	282	762
ICIS (2006)**	38	406, 509	1069, 1338
Tampa Bay Water (2011)***	40	179, 173, 228	448, 432, 569

* 8000 litre delivery 23% as SO_2.

**Price based on per 100 lb.

***From water companies awarded contracts, concentration stated for first contract price and for others assumed to be the same.

Estimated cost of sodium bisulphite taken as £600 per tonne based on Tampa Bay Water's specific application to water treatment (see Table F-D).

Slaked lime

Table F-E Costs of slaked lime

Source	**Costs per tonne (£)**
Trimpley, Severn Trent	n/a
Brenntag (2013)*	£215
ICIS (2006)**	£55-62
Keeley et al. (2012)***	£70
Des Moines Water Works (2012)****	£48, £59

*Hydrated, Ultralime 40 x 25kg bags

**Hydrated, bulk, f.o.b. works

*** Values provided by UK water utilities and chemical suppliers. Costs based on 200 MLD WTW which is larger than Trimpley (60 MLD). Cost per tonne would be expected to be lower for a larger WTW due to economies of scale. Cost liable to market fluctuations.

****Based on contracts awarded by company for quick lime which is assumed to be pure

Estimated cost of slaked lime taken as £70 per tonne based on UK basis of Keeley et al. approximation which is of same magnitude as ICIS and Des Moines Water Works values (see Table F-E).

Sludge disposal

The mass of sludge produced from the WTW was based on the removal rate of solids from the clarification and filtration stages. These solids are stored at sludge lagoon at Trimpley WTW which requires occasional dredging. When the lagoon is dredged its sludge requires disposal. As the opportunities for different disposal options in the future are unknown and based on the majority of sludge going to landfill in the UK, disposal by landfill after storage at lagoon was assumed to be £80 per tonne. The costs for this treatment alongside alternative management strategies are presented in Table F-F.

Table F-F Disposal costs of sludge, adapted from UKWIR (1999)

Disposal method	**Mean cost (£ per tonne dry solids)**	**Proportion of sludge (%)**
Landfill	81	57.7
Foul sewer to Waste WTW	Not internally charged	24.6
Transport to Waste WTW	243	4.2
Lagoon	0.6	2.0
Water environment	22	2.3
Land spreading	46	8.7
Construction materials	63	0.5

Electricity

The cost of electricity fluctuates with market forces. Recent price fluctuation is shown in Figure F-B for extra-large industrial users inclusive of tax (Department of Energy & Climate Change, 2012). Based on recent market conditions an estimated cost of electricity was taken as eight pence per kWh.

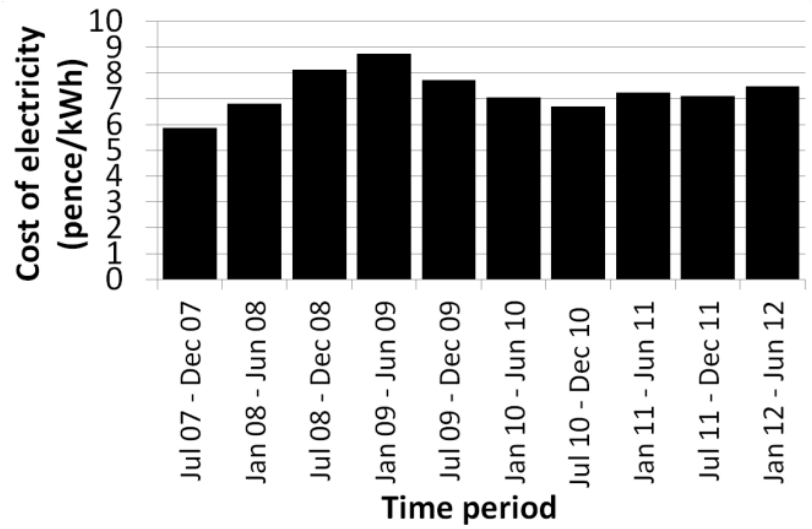

Figure F-B Fluctuation in electricity

DAF operating costs

Due to a lack of DAF energy requirement data also identified by others (Jarvis et al., 2009) DAF aeration costs were calculated from fundamental principles. The actual DAF compressors are operated intermittently to maintain a sufficient pressure. The approximation of the energy consumption assumes continual compression is less efficient. The power required by the DAF compressors was calculated using Equation F-A (Geankoplis, 1993) for adiabatic compression which is what most compressors approximate to (Perry et al., 1998).

$$P = \frac{k}{k-1}\frac{RT_1 m}{M}\left[\left(\frac{p_2}{p_1}\right)^{\frac{k-1}{k}} - 1\right] \qquad \text{Equation F-A}$$

Where: P = useful power (W); k = ratio of specific heat at constant pressure to that at constant volume (1.4 dimensionless) (Wong and Embleton, 1984); R = gas constant (8314 J/kg.K); T_1 = inlet gas temperature (K); m mass flow rate (kg/s); M molar mass (air 29 g/mol) p_1 = inlet pressure (N/m^2) and p_2 = discharge pressure (N/m^2).

The volumetric flow rate can be calculated based on the volumetric concentration of air entering the DAF tank (ϕ), the discharge rate of the process and adiabatic relationship shown in Equation F-B (Perry et al., 1998).

$$Q_{air\ in\ compressor} = \left(\frac{p_2}{p_1}\right)^{\frac{1}{k}} \phi Q_{water\ in\ DAF} \qquad \text{Equation F-B}$$

Where: $Q_{\text{air entering compressor}}$ = volumetric flow entering compressor (m^3/s); p_1 = inlet pressure (N/m^2); p_2 = discharge pressure (N/m^2); k = ratio of specific heat at constant pressure to that at constant volume (1.4 dimensionless) (Wong and Embleton, 1984); ϕ = DAF bubble volume concentration (dimensionless) and $Q_{\text{water in DAF}}$ = DAF discharge (m^3/s).

The mass flow rate is calculated from the volumetric flow rate and the density of air from the ideal gas law (Equation F-C).

$$\rho = \frac{pM}{RT} \qquad \text{Equation F-C}$$

Where: ρ = density (kg/m^3); p = pressure (N/m^2); M molar mass (air 29 g/mol); R = gas constant (8314 J/kg.K) and T = temperature (K).

Combining Equation F-A, Equation F-B and Equation F-C gives compressor power Equation F-D

$$P = \frac{k}{k-1}\left(\frac{p_2}{p_1}\right)^{\frac{1}{k}} \frac{p_1 \phi Q_{water\ in\ DAF}}{\eta}\left[\left(\frac{p_2}{p_1}\right)^{\frac{k-1}{k}} - 1\right] \qquad \text{Equation F-D}$$

Where: P = power required (W); k = ratio of specific heat at constant pressure to that at constant volume (1.4 dimensionless) (Wong and Embleton, 1984); p_1 = inlet pressure (N/m^2); p_2 = discharge pressure (N/m^2); ϕ = DAF bubble volume concentration (dimensionless); $Q_{water\ in\ DAF}$ = DAF discharge (m^3/s) and η = overall efficiency of compressor.

Total cost of DAF aeration was based on the cumulative energy consumption and the cost of electricity. For a typical DAF discharge of 800 m^3/h, saturator pressure of four bar, bubble volume concentration of 0.007 and compressor efficiency of 50% equates to power output of 0.14 kW and a daily cost of £0.27. This appears to be an under estimation of compression costs.

Filtration backwashing costs

Due to a lack of backwashing energy data, costs were calculated from fundamental principles. The energy requirement of the backwash was calculated based on the increase in head of fluid through the filter and an estimation of the head loss through the filter. The head loss through the filter was estimated using the Kozeny-Carmen equation for clean-bed head loss for each stage of the backwash which is then doubled to take into account the effect of solids retained in

the filter. This is in agreement with head loss observed at Trimpley prior to backwash being approximately double that at the start of a filter run for treated water.

The water that is used for backwashing, abstracted post GAC, and water that is run to waste at the start of a filter run are discharged to the sludge lagoon. This water will have been coagulated and a proportion of it will have been aerated. The costs of treating additional water is calculated based on the volume of water sent to the lagoon per backwash (556 m^3), the mean dose of coagulant, the mean cost of DAF treatment and the proportion of water being treated by DAF.

The cost per backwash for coagulant doses observed (15 mg/l) is approximately £16.50 and the cost of additional DAF treatment is approximately £0.01.

Table F-G Predicted energy requirements of backwashing

Backwash stage	**Velocity (m/h)**	**Clean bed headloss (m)**	**Required head (m)**	**Volume (m3)**	**Energy required (J)**
Air	65.0	104.9	211.3	433.6	1,195,191
Air/Water – Air	65.0	104.9	211.3	316.9	853,708
Air/Water – Water	9.4	1.4	4.2	45.8	1,888,411
Water	37.6	5.7	12.8	183.3	23,020,381
Total useful energy (J)					26,957,691
Total useful energy (kWh)					7.5
Total energy consumption assuming 50% pump efficiency (kWh)					15.0
Cost per backwash @ 0.08 £/kWh (£)					1.20